LNGS/EXP-07/03
April 2003

ANNUAL REPORT 2002

INFN

Laboratori Nazionali del Gran Sasso

Annual Report 2002

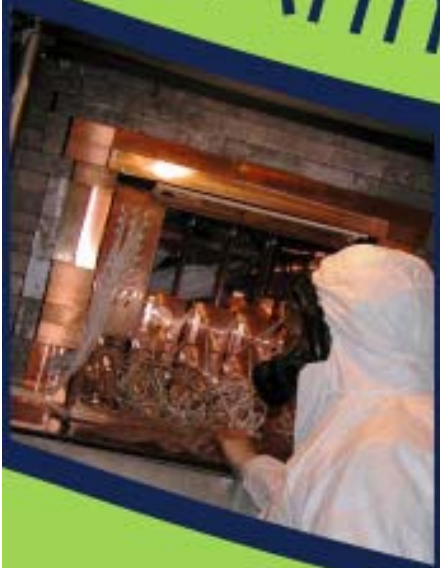

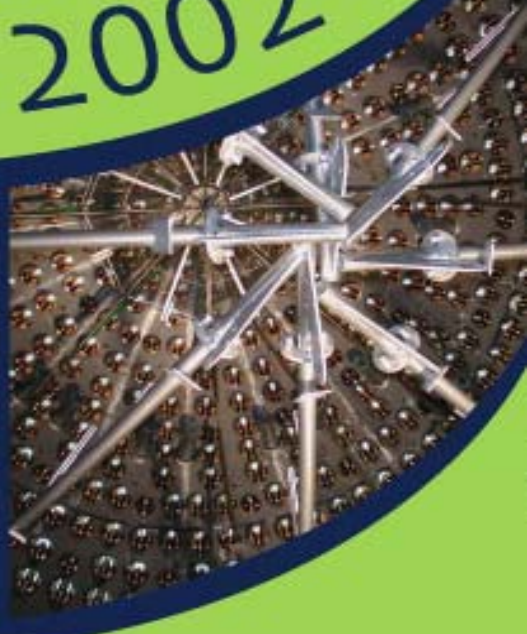

The Gran Sasso National Laboratory

The Gran Sasso National Laboratory (LNGS) is one of four INFN national laboratories. It is the largest underground laboratory in the world for experiments in particle and nuclear astrophysics. It is used as a worldwide facility by scientists (presently 750 in number) from 22 countries.
Its location is between the towns of L'Aquila and Teramo, about 120 km from Rome. The underground facilities are located on a side of the ten kilometres long freeway tunnel crossing the Gran Sasso Mountain. They consist of three large experimental halls, each about 100 m long, 20 m wide and 15 m high and service tunnels for a total volume of about 180,000 cubic metres.
The average 1400 m rock coverage gives a reduction factor of one million in the cosmic ray flux; moreover, the neutron flux is thousand times less than on the surface, thanks to the smallness of the Uranium and Thorium content of the dolomite rocks of the mountain.
The headquarters and the support facilities including the general electric and safety service, library and meeting halls, canteen, computing and networking services, mechanical, electronic and chemical shops, low activity service, assembly halls, offices and administration department are located on the surface (see fig. 1). The mission of the Laboratory is to host experiments that require a low background environment in the field of astroparticle physics and nuclear astrophysics and other disciplines that can profit of its characteristics and of its infrastructures.
Main research topics of the present programme are: neutrino physics with neutrinos naturally produced in the Sun and in Supernova explosion and neutrino oscillations with a beam from CERN (CNGS program), search for neutrino mass in neutrino less double beta decays, dark matter search, nuclear reactions of astrophysical interest.
Solar neutrino physics is one of the main research sectors of the laboratory. The GALLEX experiment, completed in 1997, has given fundamental results in particle physics and astrophysics, showing a relevant deficit in the solar electron neutrino flux at low energy, an observation that contributed to the discovery of neutrino oscillations. This phenomenon implies that neutrinos have non-zero masses and that leptonic charges are not always conserved. For the first time we have evidence of new physics, beyond the standard model.
GNO, the successor of GALLEX, with improved technique continues the measurement, gradually improving the resolution. At the end of 2002 GNO had collected 1578 days of live time pushing the systematic uncertainty to 4.2%. Borexino is dedicated mainly to the measure of the Be line component of the solar neutrino spectrum. In the year 2002 the construction of the main detector and of its ancillary facilities has been almost completed, the test facility CTF has been used for a series of tests.
LENS is a proposal for a real time, flavour sensitive experiment sensitive down to the

fusion neutrinos, aiming to a final clarification of the solar neutrino problem and to the measurement of the oscillation parameters. A series of R&D studies have been performed. The solar models are based on data and extrapolations; in particular the thermonuclear cross sections of the involved reactions are not measured in the relevant energy range but rather extrapolated from higher energies.
The direct measurements are made very difficult by the very low values of the cross sections. Using the new 400 kV accelerator, LUNA measured the cross section of the reaction ^{14}N $(p,\gamma)^{15}$O down to the energy of the nucleosynthesis in the stars. This is the slowest reaction in the CNO cycle and, as such determines the contribution of this cycle to solar burning and neutrino production. Elementary particles are different from their antiparticles because their charges - not only the electric one, but all of them - are opposite. The standard model assumes that neutrinos have only one charge, the lepton number. But, if this charge is not conserved, neutrinos and antineutrinos can be two states of the same particle. In this case well-specified nuclides would decay through the neutrino-less double beta channel. The Laboratory hosts experiments searching for these very rare decays, employing different and complementary techniques.
The Heidelberg-Moscow experiment with a sensitive mass of 11 kg of enriched ^{76}Ge is the most sensitive experiment in the world have accumulated data for a 75 kg y exposure. It took regularly data during 2002.
The second most sensitive experiment on a different isotope in the world is MIBETA that employs an array of 20 thermal detectors, based on TeO_2 crystals (340 g natural tellurium each). The experiment was completed in 2002 with a total exposure of 0.98 kg yr of ^{130}Te. Its place has been taken by CUORICINO, which employs larger TeO_2 bolometers (750 g natural tellurium each). In depth study of the backgrounds continued in 2002, completing the installation of the detectors by the end of the year.
From astronomical observations, we know that about 80% of the matter in the Universe is not made of nuclei and electrons as normal matter. It is called dark matter, because it does not emit light, and its nature is unknown. Probably, its constituents are not yet discovered elementary particles that interact only very weakly with the rest (they are called WIMPs). They are around us, invisible, waiting to be discovered. The search for WIMPs is very difficult and requires a very low background environment and the development of advanced background reduction techniques. The search is going on in many experiments worldwide. At Gran Sasso several experiments, using different techniques, are active.
DAMA employs NaI crystals to detect the WIMPs by means of the flash of light produced in the detector by an Iodine nucleus recoiling after having been hit by a WIMP, a very rare phenomenon. To distinguish these events from the background, DAMA searches for an annual modulation of the rate, a behaviour that has several aspects that are peculiar of the searched effect and not of the main backgrounds. With its about 100 kg sensitive mass DAMA is the only experiment world wide sensitive to the annual modulation signature. The experiment collected data for a further three-year period, after the already published results, and was concluded in the summer 2002. The set up was the dismounted and the set-up LIBRA with 250 kg sensitive mass was installed.
CRESST searches for WIMPs with a cryogenic technique, looking for a, very tiny, temperature increase in the detector, due to the energy deposited by nuclei hit by the WIMPs. Progress toward the final design of the CRESST2 $CaWO_2$ detector has been constant

during 2002, allowing its installation foreseen for the beginning of 2003.
The GENIUS project proposes the use of one ton enriched Germanium with a strong reduction of the background for dark matter searches, double beta decay and other searches. A small test facility GENIUS-TF has been approved so far, with 40 kg of natural Germanium operated in liquid Nitrogen. Its installation has been completed by the end of the year.
One of the major commitments of the Gran Sasso laboratory in the next decennium will be the search of tau neutrino, and possibly electron neutrino, appearance on an artificial neutrino beam being built at CERN in Geneva, the CERN Neutrinos to Gran Sasso (CNGS) project. The beam will be directed through the Earth crust to two detector located in Gran Sasso at 732 km distance. Beam and experiments are foreseen to be ready in 2006.
ICARUS is a general-purpose detector, with a broad physics programme, not limited to the CNGS project. It was proposed in 1985 based on the novel concept of the liquid Argon time-projection chamber. A first 300 t semi-module had been successfully operated on the surface in Pavia in the summer 2001. In 2002 the Collaboration completed the assembly of the second semi-module, developed the analysis of the cosmic ray events collected in 2001 and undertook the development of the "definitive project" and of the risk analysis needed for the installation in the LNGS.
The OPERA experiment is designed for the direct observation of tau neutrinos resulting from oscillations of the muon neutrino of the beam. This search requires both micrometer scale resolution, obtained with modern emulsion techniques and large sensitive mass (1800 t) obtained with Pb sheets interleaved by emulsion layers. In 2002 the design of the apparatus with two super-modules was finalised, optimising the detection rate and the background suppression. The sensitivity to electron neutrino appearance was also studied. The design of all the components of the experiment has been completed and the productions have started.
GIGS is a laser interferometer for geophysical purposes operating since 1994. Strain data have been collected continuously in 2002 and a very-broad-band seismometer has been installed in October.
PULEX-2 was designed to investigate the effects of background radiation on metabolism and responses to external agents on cultured mammelian cells. The results suggest that background radiation can act as a priming dose capable of triggering an adaptive response.
The main activity of the theory group, staff and visitor scientists, has been focussed on astroparticle physics, including solar and Supernova neutrinos, massive neutrinos, ultra high energy cosmic rays, topological defects and relativistic astrophysics. Important activity took place also in particle phenomenology and computer simulations of Lattice Field Theories.
During 2001 the Gran Sasso laboratory became one of the large European infrastructures as a "Low background facility for Particle Physics, Astrophysics, Nuclear Physics and Biology" (HPRI - CT- 2001-00149) in the action "Access to Research Infrastructures". This EU activity aims to maximise the impact of research infrastructures, facilities that provide essential services to Europe's research community in industry and academia.
Another European contract (HPRP-CT-2001-00018), prepared and run in collaboration with the large European particle laboratories, CERN and DESY, aims to evaluate the

effectiveness of their outreach actions.
The geographical location (inside the National Park of Gran Sasso - Monti della Laga) and the special operating conditions (underground, near a highway tunnel and in close proximity to water basins) demand that special attention is paid to the safety and environmental aspects of their activities.
We have introduced also an Environmental Management System (EMS) complying with the UNI - EN - ISO 14001 standard, in order to make the organisation more modern and efficient, to assure the conformity to current laws, and to achieve a continuous improvement of the environment performance.
The system is verified by an independent auditing authority, which constantly checks the conformity to the standard, in order to assure the management, and all the various involved parties (local authorities, citizens, members of the staff, collaborators and research institutes) of the adequacy of the Environmental Policy, the operating conditions, procedures, and checks.

Gran Sasso, April 2003.

The Director of the Laboratory
Prof. Alessandro Bettini

Contents

BOREXINO. Solar Neutrino Physics

Borexino collaboration

H. Back[n], M. Balata[b], A. de Bari[e], T. Beau[o], A. de Bellefon[o], G. Bellini[a1], J. Benziger[c], S. Bonetti[a], A. Brigatti[a], C. Buck[j], B. Caccianiga[a], L. Cadonati[d], F.P. Calaprice[d], G. Cecchet,[e], M. Chen,[q], O. Dadoun[o], D. D'Angelo[h], A. Derbin[m], M. Deutsch[f], A. Di Credico[b], G. Di Pietro[a], F. Elisei[g], A. Etenko[r], F. von Feilitzsch[h], R. Fernholz[d], R. Ford[b], D. Franco[a], B. Freudiger[j], C. Galbiati[d], F. Gatti[i], S. Gazzana[b], M.G. Giammarchi[a], D. Giugni[a], A. Goretti[b], C. Grieb[h], E. de Haas[d], C. Hagner[n], W. Hampel[j], B. Harding[d], F.X. Hartmann[j], R. Hentig[h], G. Heusser[j], A. Ianni,[b], A.M. Ianni[d], L. Ioannucci[b], H. de Kerret[o], S. Kidner[d], J. Kiko[j], T. Kirsten[j], G. Korga[a], Y. Kozlov[r], G. Korschinek[h], D. Kryn[o], V. Lagomarsino[i], M. Laubenstein[b], C. Lendvai[h], M. Leung[d], E. Litvinovich[r], P. Lombardi[a], I. Machulin[r], S. Malvezzi[a], I. Manno[k], J. Maneira[q], D. Manuzio[i], G. Manuzio[i], A. Martemianov[b], F. Masetti[g], U. Mazzucato[g], K. McCarty[d], E. Meroni[a], L. Miramonti[a], M.E. Monzani[a], P. Musico[i], M. Neff[h], A. Nelson[d], L. Niedermeier[h], S. Nisi[b], L. Oberauer[h], M. Obolensky[o], M. Orsini[b], F. Ortica[g], M. Pallavicini[i], L. Papp[a], S. Parmeggiano[a], P.Peiffer [j], L. Perasso[a], A. Perotti[e], A. Pocar[d], R.S. Raghavan[l], G. Ranucci[a], A. Razeto[i], A. Sabelnikov[a], P. Saggese[a], C. Salvo,[i], R. Scardaoni[h], S. Schönert[j], H. Seidl[h], T. Shutt[d], M. Skorokhvatov[r], H. Simgen[j], O. Smirnov[m], A. Sonnenschein[d], A. Sotnikov[m], S. Sukhotin[r], V. Tarasenkov[r], R. Tartaglia,[b], G. Testera[i], D. Vignaud[o], B. Vogelaar[n], V. Vyrodov[r], W. Wojcik[p], O. Zaimidoroga[m], G. Zuzel[p]

[a]Dip. di Fisica dell'Università and Infn Milano - Italy
[b]Laboratori Nazionali del Gras Sasso, Assergi (Aq) - Italy
[c]Dep.t of Chemical Engineering, Princeton University - NJ USA
[d]Dep.t of Physics, Princeton University - NJ USA
[e]Dip. di Fisica dell'Università and Infn Pavia - Italy
[f]Dep.t of Physics, Massachusetts Institute of Technology - MA USA
[g]Dip. di Chimica dell'Università and Infn Perugia - Italy
[h]Technische Universität München - Germany
[i]Dip. di Fisica dell'Università and Infn Genova - Italy
[j]Max Planck Inst. für Kernphysik, Heidelberg - Germany
[k]KFKI-RMKI Research Institute for Particle & Nuclear Physics, Budapest - Hungary
[l]Bell Laboratories, Lucent Technologies, Murray Hill - NJ USA
[m]J.I.N.R. Dubna - Russia
[n]Dep.t of Physics, Virginia Polytechnic Institute - VA USA
[o]Laboratoire de Physique Corpusculaire et Cosmologie, Paris - France
[p]Institute of Physics, Jagellonian University, Kracov - Poland
[q]Dept. of Physics, Queen's University, Ontario - Canada
[r]RRC Kurchatov Institute, Moscow - Russia

[1]Spokesperson

Abstract

The construction of the Borexino experiment is getting at its final stage. The active volume consists of 300 ton ultrapure liquid scintillator, contained in a 100μm thick nylon Inner Vessel, viewed by 2200 photomultipliers mounted on a Stainless Steel Sphere. A Nylon shroud is interposed between the Inner Vessel and the PMTs to reduce radon diffusion. The outer water shield (2400 tons) is instrumented with 200 outward-pointing photomultipliers serving as muon veto. During this year, the final vessel has been shipped to Gran Sasso and is ready to be mounted; tests of its installation have been successfully performed. The total amount of scintillator (PC) for the Inner Vessel has been procured; auxiliary plants for the scintillator mixture preparation and water purification have been completed. The CTF (a prototype detector) has been running for testing the purification plants in the final configuration for Borexino and verifying the purity level of the scintillator batches. A complete test of the detector response (PMTs, DAQ, electronics and calibration systems) in air has been carried out with lasers and a Rn-spiked radioactive source.

1 The experiment: goals and achievements

The nowadays experimental challenge of the solar neutrino research is to make accurate measurements of the neutrinos with energy less than 1 MeV. We need to know the main properties of solar neutrinos, i.e. the total flux, the flavor content and the time dependence of the ^{7}Be neutrinos (energy of 0.86 MeV) and the total flux, flavor content, energy spectrum and time dependence of the fundamental $p-p$ neutrinos (energy less than 0.43 MeV). More than 98% of the calculated standard model solar neutrino flux lies, indeed, below 1 MeV. In contrast, the ^{8}B neutrino flux, the only solar neutrino source which has been experimentally measured in real time, represents only a fraction of less than 10^{-4} of the total solar neutrino flux. Borexino is the first experiment planned to measure in real time the reactions induced by the low energy solar neutrinos. The main goal is to study the monoenergetic 0.862 MeV ^{7}Be solar neutrino, which accounts for ~ 7 % of the total standard model flux, through the detection of the ν-e scattering in a liquid scintillator.

The measurement of the event rate induced by neutrinos originated by this source will provide a direct test of the Standard Solar Model and an improvement in our understanding of the neutrino properties. During this year the SNO and Kamland results have strongly affected our comprehension of the long-standing solar neutrino problem; still we need redundancy and accuracy on the crucial measured parameters to further extend our knowledge on the neutrino fundamental physics.

The electron recoil signal in Borexino from the ^{7}Be- ν occurs in the energy window 0-0.66 MeV at a rate of 0.1 -0.5 events d^{-1} ton^{-1} of target material. Observation of such rare low energy events has never been attempted in real time because of the large background of the detector medium itself, arising from ubiquitous natural radioactive contaminants such as ^{238}U and ^{232}Th. While it was suggested that liquid scintillator might be purifiable, no measured data precluded or promised the radiopurity level of 10^{-16}g/g U and Th necessary to reach a signal/noise ratio of ~ 1.

As a consequence an intense R&D program has been carried out in the last ten years to develop methods for selecting very low radioactivity materials or purify them. An effort

in this field has matched an equally hard research in the field of the detection systems and measurements of ultralow radioactivity levels. Borexino has played a pioneering role in developing a new technology for observing low energy solar neutrinos in real time [1].

Various developments have been attained in the purification methods of liquid aromatic compounds, such as distillation, water extraction, stripping with ultrapure N_2, solid gel column adsorption (Si gel, Al gel). A multi-ton prototype detector, the Counting Test Facility (CTF), has been constructed on purpose and installed in the underground Laboratory at Gran Sasso to verify the Borexino feasibility. The CTF, operative since 1995, has been an important bench mark for testing and studying various solutions for the Borexino detector [2] [3] [4] [5]. In this year a third campaign of measurements has been carried out in CTF, in parallel to the Borexino construction, essentially to test the purification plants in their final configuration for Borexino itself.

2 The Detector

Borexino (Fig.1) is an unsegmented liquid detector featuring 300 tons of shielded ultrapure scintillator viewed by 2200 photomultipliers . The detector core is a transparent spherical vessel (Nylon inner vessel, 100μm thick), 8.5 m of diameter, filled with 300 tons of liquid scintillator and surrounded by 1000 tons of high-purity buffer liquid. The scintillator mixture is PC (1-2-4,Trimethylbenzene) and PPO (2,5 diphenyl oxazole, 1.5g/l) as a fluor, the buffer liquid is pure PC (with the addition of the light quencher DMP). The photomultipliers are supported by the stainless steel sphere (SSS), which also separates the inner part of the detector from the external shielding, provided by 2400 tons of pure water (water buffer). An additional containment vessel (Nylon film radon barrier) is interposed between the scintillator Nylon sphere and the photomultipliers, with the goal of reducing radon diffusion towards the internal part of the detector.

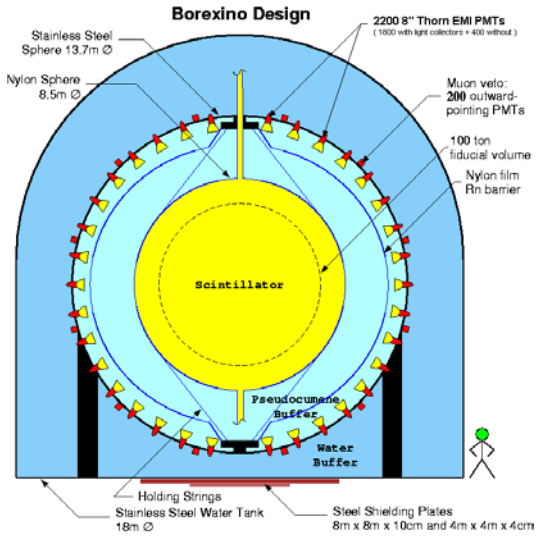

Figure 1: Schematic view of the Borexino detector.

The outer water shield, contained in the Water Tank (WT) is instrumented with 200 outward-pointing photomultipliers serving as a veto for penetrating muons, the only significant remaining cosmic ray background at the Gran Sasso depth (about 3500 meters of water equivalent). Inside the stainless steel sphere , 1800 photomultipliers are equipped with light concentrators so that they can see light coming only from the Nylon Sphere region, while the remaining 400 PMT's are sensitive to light originated in the whole volume of the SSS. This design greatly increases the capability of the system to identify muons crossing the PC buffer but not the scintillator. The Borexino design is based on the concept of a graded shield of progressively lower intrinsic radioactivity as one approaches the sensitive volume of the detector; this culminates in the use of 200 tons of the low background scintillator to shield the 100 tons innermost Fiducial Volume. In these conditions, the ultimate background will be dominated by the intrinsic contamination of the scintillator, while all backgrounds from the construction materials and external shields are almost negligible compared to the signal. Borexino also features several external systems and plants conceived to purify water, nitrogen and scintillator, and clean rooms to keep clean conditions during the installation of the detector.

3 Status of the Experiment: the principal achievements of the year 2002

The completion of Borexino is now reaching its final stage. The installation of the structural part of the detector (water tank, stainless-steel sphere) has been completed , and service systems (as air control in the sphere, clean-rooms, etc.) have been running in standard conditions since last year. The next paragraphs will summarize the principal achievements of this year.

3.1 PMT, DAQ, Electronics and Calibrations

The phototubes (produced by ETL with a special glass of low radioactivity) have been completely assembled , sealed, coupled with the optical concentrators, installed on the SSS, and finally tested (Fig.2); the installation of about 95% of them has been performed at the expected rate of 300 PMTs/month : for technical reasons, the last 5%will be mounted on the SSS after the Nylon vessels insertion. All cables have been positioned from the PMTs to the electronics Front-End (Fig.3).

Full test of main electronics and trigger system using electronic pulses, laser pulses and radon source ("Air Runs") have been carried out in the whole Borexino detector in 5 different short periods (February, April, June, August and December). The HV voltage system has been debugged and tested, all trigger conditions have been studied using laser pulses and radon sources and the entire DAQ system (the analyzer code, the Data Base structure and a graphical command interface) has been tested successfully recording events on disk.

The optical calibration systems have been tested as well in the Air Run periods. The PMT time-equalization system, Fig.4.a, consisting of consecutive optical bundles, Fig.4.b, which split at the various detector interfaces, has been operated by conveying light from a

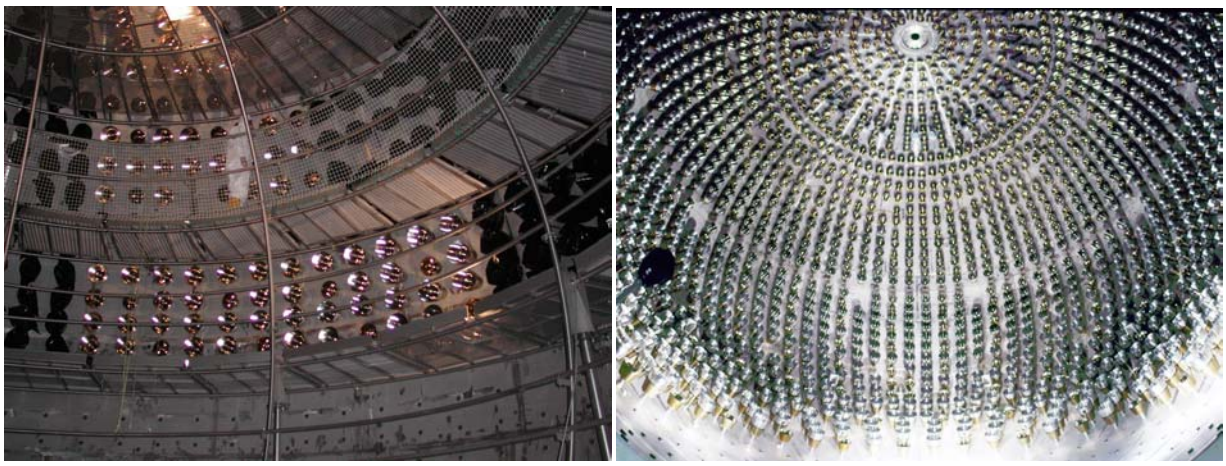

Figure 2: The inside of the Stainless Steel Sphere.

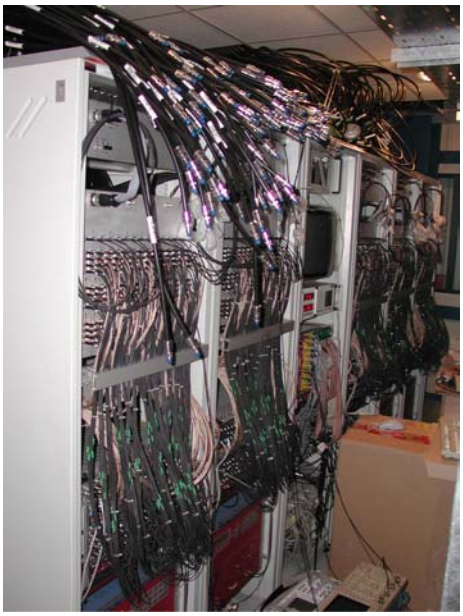

Figure 3: The electronics room.

common laser source (λ=394 nm) to each PMT through the multiplexed system of optical fibers.

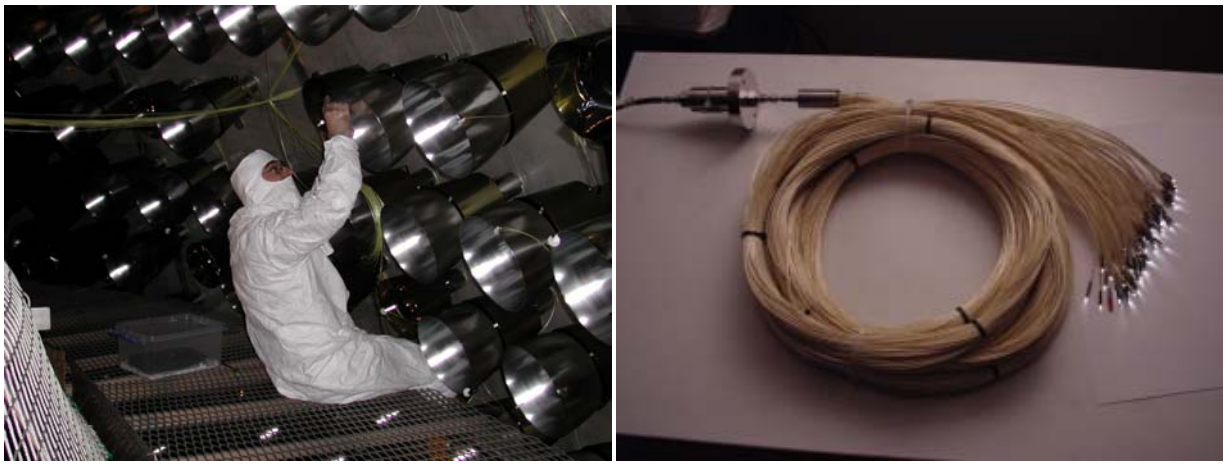

Figure 4: a.)Mounting of the fiber system for the PMT time equalization; b)a bundle of optical fibers.

The stability monitoring system, foreseen to keep under control the optical properties of the fluids in the detector by shooting light of different wavelengths(λ=355 nm and λ=394 nm), from outside through the scintillator, has been run in both final configurations: radial and oblique, the first aimed at the simultaneous illumination of the active volume and buffer, the second at the illumination of the buffer fluid alone. Three oblique feedthroughts on the SSS point at the CCD positioning cameras on the opposite side of the detector. The CCD cameras have been operated during the same debugging runs.

3.2 Nylon Vessels

Prototype vessels were already installed and inflated in a gymnasium at Princeton last year. In this spring, a scaffolding and tower system for installation of the vessels was constructed in the SSS and associated clean room. A preliminary installation test in May was followed by a final test. The final test uses the actual vessel end plumbing, and a mock-up of the vessel made of spare panels from the vessel construction. The vessel system for this test has the same weight, dimensions and handling of the actual vessels in their deflated state. This final test has thus successfully checked all aspects for installation except inflation, which was already realistically tested one year ago. The final vessel for Borexino was shipped to Gran Sasso in August and is ready to be installed.

3.3 Outer Muon Detector

The OD is a water cherenkov detector equipped with 208 encapsulated PMTs, diffuse reflecting Tyvek foil, an OD data acquisition system and an optical calibration system. Highlights within this reporting period are mounting of part of the OD-PMTs, final testing and start of the QTC front-end electronics, the installations of optical calibration fibers and the development of a new VME-LED calibration system.

3.4 Plants

3.4.1 The PPO Plant

The PPO plant of Borexino is meant to be used for the preparation of the Master Solution (MS). The MS is a concentrated solution of PPO in PC with PPO at 200g/l. The MS will be diluted in PC in order to prepare the scintillator for Borexino with the PPO at 1.5g/l. Given the volume of the Inner Vessel, the amount of MS for Borexino is of about 2.400L (7.5l of MS per ton of PC). In order to produce the MS a dedicated plant has been installed. The PPO plant consists of three vessels properly equipped according to their operational function. The PPO plant is connected with the other Borexino plants through the Mod0 system. The PPO plant is now ready to operate.

3.4.2 The DMP plant

DMP (DimethylPhtalate) is a liquid that will be mixed (with a concentration of about 5 g/l) to the Borexino buffer to quench the pure Pseudocumene scintillation light. The small amount of scintillation light produced by pure PC (the absolute yield is about five times lower than that of PC+PPO and is shifted towards the ultraviolet region) could in fact produces some background events. The DMP has been stored in Gran Sasso since June 2002 in a stainless vessel blanketed with High Purity (HP) Nitrogen. The final connection to the Hall-C HP Nitrogen system is still to be completed.

3.4.3 Borexino water loop

The Borexino water purification loop is intended to maintain the purity of the water shield for the experiment. While marginally important in terms of radiopurity, it is needed to keep the water transparent to the Cerenkov light generated by cosmic muons. The system treats 2400 m^3 of water at a recirculation rate of about 5 m^3/hr. The first step of the treatment is a modest filtration. Then the water gets deionized by a mixed-resin bed deionizer. Finally, a 0.1 micron filtering is performed. During the operation of the system it is assumed that the water is already brought in at a high purity level by the main production system. In addition, the system has the possibility of performing a temperature control either in cooling mode or in heating mode. The system has been completed.

3.4.4 PC procurement for the scintillator

The Borexino scintillator features Pseudocumene as a solvent. PC is produced by POLIMERI EUROPA (formerly Enichem) at Sarroch, Sardinia. The total amount of PC needed for the experiment is 1250 tonnes. This amount can be conceptually divided between the Inner Vessel Inventory (280 tonnes) and the remaining part to be used for the Buffer. The Inner Vessel Inventory can be purchased and stored underground in the Hall C Storage Area - with storage capability of 280 tonnes - while the Buffer inventory must be procured during the filling of Borexino goes directly into the detector. The total amount of PC transported to Gran Sasso is now 270 tonnes, thus completing (modulo a minor refill) the Inner Vessel Inventory.

3.5 CTF tests

The CTF (Counting Test Facility) is a prototype detector for Borexino, built to demonstrate the possibility to reach the very high level of radiopurity required by the full scale experiment.

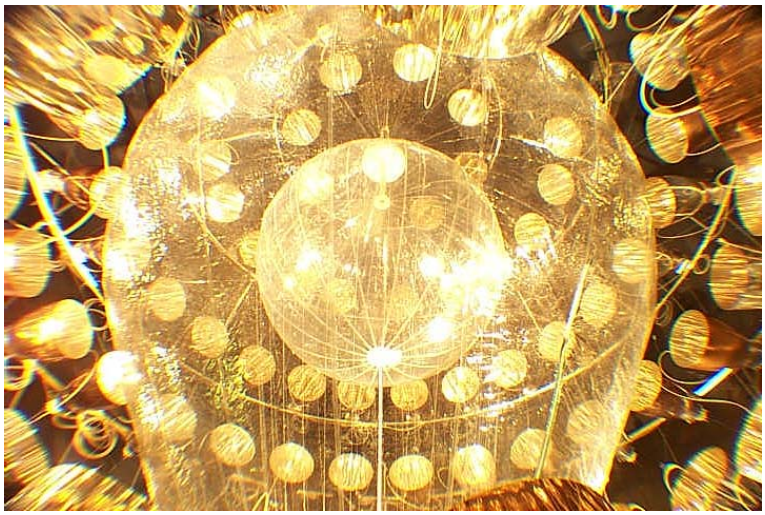

Figure 5: Inside CTF: the Inner Vessel radius is 1.

The detector has been already active in two campaigns, an early one using PC and PPO as scintillator (1995-1997), and a second one using PXE in (2000). During the year 2002 it has been operating as a final test facility for the scintillator (PC/PPO) which will be loaded in Borexino as soon as the vessels are ready for filling (Fig.5).

In this third phase, the first load of scintillator was completed in November 2001. Before filling with scintillator, the CTF water tank and both vessels had been filled with ultrapure water. Then the CTF Inner Vessel has been loaded with scintillator through 'volumetric exchange' of the water contained therein. This technique has proved to work very well and with large margins of safety, allowing the collaboration to decide on the procedure to follow for the Borexino vessels filling. A series of measurements of the ^{14}C content of the PC have followed, making possible a constant monitoring of the scintillator features over the whole procurement campaign (November 2001 - June 2002). The values of $^{14}C/^{12}C$ in the different PC batches varied between 1.3 and 4.7 $\times 10^{-18}$, well within the specifications set by the collaboration. In the first six months of 2002, CTF has allowed a careful check of the plants that will be then extensively used for Borexino: the Unloading Station and the Storage Area (while procuring the PC and transferring it to the other plants for purification), the Mod0 (through both a SiGel column online and batch test), and the US Skids (during the water extraction and nitrogen stripping online tests). Moreover, it has allowed to assess the overall efficiency of the Water Plant (during filling and in the internal loop operations), and the quality of the water produced by the plant itself. In the next months more tests will follow, in order to optimize the purification procedure to be then used for the Borexino IV scintillator.

3.5.1 Module 0

Module 0, besides being a key equipment for the CTF loading-unloading operations, is also a tool for purifying the scintillator through the silica gel column method. A test has been performed, both in loop and batch mode, with a column prototype containing 2.4 kg of silica gel in order to reproduce the same Borexino ratio between silica gel and scintillator. In loop mode the scintillator flows through a close path formed by the the CTF Inner Vessel, the silica gel column itself and a pump assuring a flow rate of 190 kg/h. Since in this condition the purified scintillator is continuously put in contact with the not purified one, it could be shown that the resulting overall purification should amount roughly to a factor e after each complete cycle. The purification capability is however limited by the so-called "breakthrough" of the silica gel, which is reached when impurities in the gel reach an amount that can not be hold any more and are thus released back into the purified scintillator. The expected purification factor was calculated to be between 3 and 4 within infinite purification time, concerning ^{210}Po. Furthermore, it should be noted that the silicagel purification did not affect the PPO-content of the scintillator in a detectable way, and that by counting the Rn events a limit on the silica gel emanation was set of about 0.90 mBq/kg, in agreement with previous estimates of 1.11 mBq/kg. In the batch test the purified scintillator is never in contact with the unpurified one, a condition which is accomplished by separating the following three steps: scintillator unloading from CTF Inner Vessel, silica gel purification and scintillator loading. It has to be pointed out that freshly new silica gel was used for this test, taken however from the same batch of the gel used for the loop test. According to theory, the single-pass purification factor should be much bigger in this batch mode. It was crucial to have enough silica gel not to reach the "breakthrough"-point after the given volume of 4.2 m^3 of scintillator: theoretically for 2.4 kg of silica gel the breakthrough was calculated to happen at 10 m^3. Actually, a comparison with the loop test seems to indicates that the breakthrough was not reached even after 24 m^3 of scintillator.

3.5.2 Purification Skids

The Borexino purification skids (the skids) are a modular construction solvent purification plant, consisting of vacuum distillation, liquid/liquid (water) extraction, and nitrogen gas stripping processes. The skids have been operational since April 2002. This followed careful on-site assembly, cleaning and passivation. During March and April 2002 the water extraction and stripping systems were tuned, tested and conditioned in loop mode with the output flow returned to the input. The water extraction column is a liquid/liquid extraction where water flows counter-current to PC in a tall packed column. The process efficiently removes impurities with a higher solubility in the aqueous phase, including potassium and most heavy metals in the U, Th chains. The large surface area of the packing provides 2 to 3 equilibrium stages, and the water is distilled in a closed loop to maintain purity. The nitrogen stripper is also a tall packed column, with PC falling through the column and high purity nitrogen entering the bottom of the column and venting at the top. The nitrogen stripping has not been well tested yet, since the CTF had no significant radon contamination when the campaign began. However, the radon that was introduced during the looping is consistent with the small known sources following

the stripper column (pump, filter, heat exchanger and lines), indicating that the system is radon tight. It is planned to also directly measure the efficiency of the column for noble gas reduction using a Xenon gas tracer method. However, other investigations of the nitrogen purity for Ar and Kr have shown that probably the N2 stripping cannot be sufficiently effective for these noble gases. A new effort has been undergone by the collaboration to achieve the required levels; the results obtained so far are promising. The present activity is to prepare a test in the CTF of the distillation plant. Here a new batch of PC is distilled, then mixed with new PPO solution (purified in the CTF skid), then the CTF inner vessel is unloaded (replaced with water) then reloaded with the new scintillator. Prior to this test, the module-0 tanks and the interconnection lines have been extensively recleaned and passivated to address some of the contamination possibilities. Following the results of the distillation test, the water extraction will be further tested.

3.5.3 The main Results of the CTF test

The main results, obtained exploiting the energy and position distributions of the events, along with the particle identification capability of the detector, can be summarized as follows:

- Scintillator photon yield: it was found to be in the range of 380 photoelectrons/MeV, corresponding to the expected energy and position resolution of 10% and 13 cm respectively at 1 MeV.
- ^{14}C content: the ratio of $^{14}C/^{12}C$ atoms measured in the four batches of PC under test was respectively $(1.34 \pm 0.01) \times 10^{-18}, (2.6 \pm 0.2) \times 10^{-18}, (4.4 \pm 0.2) \times 10^{-18}$ and $(4.4 \pm 0.4) \times 10^{-18}$.
- ^{238}Ucontent: it is estimated by detecting the $^{214}Bi -^{214} Po$ coincidence events and assuming secular equilibrium. In the first batch of scintillator and before any purification was applied the constant contribution to the count rate was found to be $(14.25 \pm 3.44) \times 10^{-16}$ g/g. After purification with water extraction and Si-Gel column the contamination was reduced to $(6.56 \pm 1.70) \times 10^{-16}$ g/g.
- ^{232}Th content: it is estimated by detecting the $^{212}Bi -^{212} Po$ coincidence events and assuming secular equilibrium. The initial contamination was measured to be $(6.2 \pm 0.8) \times 10^{-15}$ g/g. After purification with the Si-gel column, the contamination has decreased to the level of $(2.6 \pm 0.5) \times 10^{-15}$ g/g and could not be reduced any further by other purification techniques (water extraction and a new Si-Gel purification campaign). There is an indication, though, that the residual $^{212}Bi -^{212} Po$ counts could be due, at least in part, to surface contamination of the Inner Vessel and not to bulk contamination of the scintillator: the spectrum of the residual ^{212}Po events after the column purification is in fact shifted at energy lower than expected and the radial analysis indicates a clustering of the events in the outer part of the IV volume. We do not know yet how much of the previous quoted level, which actually has to be considered only as an upper limit, is to be attributed to such a contamination.

- ^{85}Kr content: it is estimated by detecting its beta decay to 85mRb which is well-tagged since it is followed (t=1.46 msec) by a γ of 514 keV (branching ratio=0.434%) Initially, before any purification, the detected counts in the 85mRb channel were (1.07 ± 0.25) events/day corresponding to a total ^{85}Kr activity of (250 ± 0.60) events/day. Nitrogen stripping performed together with the water extraction seemed to be effective in reducing this contamination to (46 ± 23) events/day. This number should be taken as an upper limit for the ^{85}Kr contamination since the surface contamination which probably affects the Thorium analysis, is likely to also cause an overestimation of the presumed Kr counts by an unpredictable factor.

- single rate: The "radial analysis" (i.e, the study of the event position distribution) for the events in the neutrino window (250-800 keV) indicates a very small contribution from external background (events originating outside the Inner Vessel, like those due to radon in the water, now strongly suppressed, with respect to previous CTF phases, by the outer shroud while revealing the presence of a strong surface contamination, which has remained approximately constant throughout the entire CTF run. The total rate due to this contamination is approximately 1000 counts/day, equally divided between alpha and beta type particles. The spectral shape analysis of these events is complicated since the reconstructed energy for surface events is affected by complex border effects. Nevertheless the results of this analysis are in general compatible with the hypothesis of a contamination due to ^{210}Pb in equilibrium with its daughters ^{210}Bi and ^{210}Po. The radial analysis also indicates an internal contamination. This contamination, at the original level of 1700 events/day, is peaked at $\sim$ 350 keV and better satisfies the alpha-type hypothesis. Several purification schemes have been applied to try and remove it. The first method used, the Si-Gel column purification in loop mode, seemed to be effective in removing approximately half of the alphas, bringing them down to the level of 800 events/day. The water extraction method applied soon after, further reduced the alphas of a factor 4-5. The level of roughly 100 residual events/d obtained at this stage, the lowest throughout the whole testing period, could have been plausibly limited by a number of factors which are now under study. Attempts to apply again these two purification methods didn't give any appreciable results; on the contrary, the last purification with the Si-Gel column "in batch" seemed to increase the alpha count rate, indicating a possible contamination of pipes or/and tanks used in the procedure.

  The position of the energy peak of this internal contamination is compatible with that of the quenched ^{210}Po alphas, while its lifetime seems to be too short: ^{210}Po lifetime is 200 days, while especially the lifetime detected after the last column test is definitely shorter. It is also noticeable that, unlike the surface contamination, the internal one is practically consistent of α-like particles only, which makes it impossible to interpret it in term of ^{210} Pb (^{210}Bi, the predecessor of ^{210}Po, should in fact be present if equilibrium holds). It should be also mentioned that investigations of α- emitting nuclide different from ^{210}Po as origin of the internal contamination, failed to identify an element able to fit all the characteristics of the actual events.

3.5.4 Interpretation and strategy for the future tests.

The results obtained in the two campaigns with the silica gel column need further investigations. In the loop test, after 6 volume cycles, a purification factor for the alphas was achieved in the expected range, namely about 2.5; on the contrary after the batch test, in principle much more effective, the alpha activity surprisingly increased. A plausible explanation could be recontamination due to the wash-off of impurities from the surfaces of two tanks used in the batch mode (and not in the loop one) which were also used at the time of the first scintillator loading; Polonium presents indeed a well known plating properties on metallic surfaces. The whole Module-0 tubing as well as the two tanks have been then thoroughly cleaned with detergent and diluted nitric acid. In the second round of CTF tests it will be important to repeat the batch test.

In the first 3 days (5 cycles) of water extraction running, the purification was very effective, reducing the internal activity (alphas plus betas) from about 750 c/d down to 120 c/d. However, further purification seemed to be quite ineffective, with the final activity left at about 100 c/d. While the purification efficiency seemed very good, the result is not since a purification "plateau " seems to be reached, which is well above the required purity level required for Borexino. In addition this residual activity is well above that previously obtained in CTF 1. While the purification concept seems valid, a recontamination effect in the plants or a not proper mixing seem rather plausible. It is now known from fluid dynamic simulations that, due to the fairly high flow rates , there will be a large zone of the IV volume that does not mix during circulation. Thus there could have been a significant volume that was not at all processed through the purification system, and was only very slowly mixing. We attempted to address this possibility by varying the input temperature and flow rates, but with the testing done so far we are not able to rule out this possibility. The new PC batches or the new PPO may contain Polonium contamination that is complexed with or substituted in organic molecules, and hence is not effectively extracted with water. This last possibility is presently being researched in the context of the known chemistry of Polonium.

After the thorough re-cleaning of the Module 0 pipes and tanks needed to load CTF performed in July, the next step of the testing program is to apply the distillation method. The planned procedure contemplates on one side the batch distillation of 4 tons of PC alone, and on the other the preparation and purification of the required amount of concentrated PPO solution. The two scintillator components will be mixed in the module 0 and then transferred to the CTF vessel. The distillation test will complete the first stage of the CTF program. After that, a further round of testing will be started concerning both the column and the water extraction methods. The new test program will be devoted to gain further insight in the properties and performances of the purification plants. The above-mentioned explanations of the results will be checked, in order to achieve a global comprehension of the purification issue in which all the collected data and hypothesis conceived are put together in a unique coherent picture. In prospect the CTF program will be considered completed with the assessment of the overall purification strategy to be followed to get the ultimate background level required for Borexino.

4 Solar neutrino physics: the Borexino potentiality

The evidence for an active, non-electronic ν component in the samples of the solar neutrino reactions, detected both by SKamiokande and SNO experiments, and the combination of all the results obtained until mid 2002, had already restricted the allowed regions for the $\tan^2\omega$ and δm^2 parameter of the solar ν-oscillation model only to two solutions. The favored regions were the LMA (Large Mixing Angle) and LOW (Low probability, Low mass).

The recent Kamland result, the first obtained with a terrestrial beam exploring the neutrino oscillation parameters relevant for the solar neutrino oscillation, further constrained the allowed solutions. The LMA solution is now the only allowed solution at more than 3 σ level. The LOW, Vacuum, and SMA solutions are now disfavored at 4.7 σ, 4.8 σ and 6.1 σ respectively.

The rates expected in Borexino are respectively 30 counts/day in the LMA solution, and 23 events/day in the LOW solution, to be compared to an expected background of roughly 15 events/day . These values refer to the energy of electron scattered by ^{7}Be ν ranging from 0.25 to 0.8 MeV, which is the experimental range where the neutrinos coming from ^{7}Be source are detectable in Borexino, and to the 100 ton Fiducial Volume. The good capability of Borexino of detecting seasonal variations is overall important to tag the solar origin of the detected neutrinos : their flux variation due to the eccentricity of the Earth orbit is about 7%, with a typical $1/R^2$ behavior (the Borexino sensitivity to this effect is 5 σ of C.L. in 3 years of data taking).

Moreover, an additional seasonal variation should be dramatically exhibited by Borexino in the Vacuum Oscillation hypothesis: the lack of this effect should strengthen the cancellation of this solution, as it is now disfavored.

Borexino will offer a very good sensitivity to the Day/Nigth difference in the event rates, effect which is enhanced in the LOW solution just in the ^{7}Be ν energy region.

Finally, the direct measurement of the reactions induced by neutrinos arisen in the ^{7}Be source inside the Sun will be the an important experimental proof to test the Standard Solar Model.

5 List of papers published in year 2002

1. H.O.Back et al. *Search for electron decay mode $e \to \gamma + \nu$ with prototype of Borexino detector*, Phys. Lett. B 525 (2002) 29 .

2. G. Alimonti et al. *Science and technology of Borexino: a real-time detector for low energy solar neutrinos* , Astroparticle Phys. 16 (2002) 205

3. C.Arpesella et al. *Measurements of extremely low radioactivity levels in Borexino.* Astroparticle Phys. 18 (2002) 1

4. H.O.Back et al. *New limits on nucleon decays into invisible channels with the Borexino counting test facility .* submitted for publication to Phys.Lett.B

5. H.O.Back et al. *Study of the neutrino electromagnetic properties with prototype of Borexino detector.* submitted for publication to Phys.Lett.B.

References

[1] G. Alimonti et *al. Science and technology of Borexino: a real-time detector for low energy solar neutrinos.*, Astroparticle Phys. 16 (2002) 205

[2] G. Alimonti et *al. A Large Scale Low Background Liquid Scintillation Detector: the Counting Test Facility at Gran Sasso.*, Nucl. Instrum. Meth, A406 (1998) 411.

[3] G. Alimonti et *al. Ultralow background measurements in a large volume underground detector.*, Astroparticle Phys., 8 (1998)141.

[4] G. Alimonti et *al. Measurements of the* ^{14}C *abundance in a low-background liquid scintillator.*, Phys. Lett. B, 422 (1998) 349.

[5] G. Alimonti et *al. Light propagation in a large volume liquid scintillator.*, Nucl. Instrum. Meth A 440 (2000) 360.

CRESST. Dark Matter Search

W. Seidel [a] (speaker), G. Angloher [a], C. Bucci [d], N. Bazin [c], S. Cooper [c], C. Cozzini [a], J. Doncev [a], F.v.Feilitzsch [b], T. Frank [a], D. Hauff [a], S. Henry [c], T. Jagemann [b], J. Jochum [b], R. Keeling [c], H. Kraus [c], F. Petricca [a], F. Pröbst [a], Y. Ramachers [c], M. Stark [b], L. Stodolsky [a], H. Wulandari [b]

[a] Max-Planck-Institut für Physik, Föhringer Ring 6, D-80805 Munich, Germany
[b] Technische Universität München, Physik Department, D-85747 Munich, Germany
[c] University of Oxford, Physics Department, Oxford OX1 3RH, UK
[d] Laboratori Nazionali del Gran Sasso, I-67010 Assergi, Italy

Abstract

We are preparing the CRESST (**C**ryogenic **R**are **E**vent **S**earch with **S**uperconducting **T**hermometers) experiment to search for dark matter WIMPs using cryogenic detectors. In the second stage we plan to use cryogenic detectors with strong background rejection due to the simultaneous detection of scintillation light and phonons. Progress of the development of a 300 g prototype module is described.

1 Introduction

The CRESST experiment located at the 'Laboratori Nazionali del Gran Sasso' (LNGS), Italy, was designed to search for particle Dark Matter and to contribute to the elucidation of its properties. CRESST uses low background cryogenic calorimetric detectors with superconducting phase transition thermometers for the direct detection of WIMP-nucleus scattering events.

The search for Dark Matter and the understanding of its nature is of central interest for particle physics, astronomy and cosmology. In astonomy, there is strong observational evidence for its existence on all scales. In addition, the history of the universe is difficult to reconstruct without Dark Matter, be it Big Bang Nucleosynthesis or structure formation.

Particle physics provides a well motivated candidate with the lightest SUSY-particle, the "neutralino". Generically, such particles are called WIMPs (Weakly Interacting Massive Particles). WIMPs are expected to interact with ordinary matter by elastic scattering on nuclei. All direct detection schemes have focused on this possibility.

Conventional methods for direct detection rely on the ionization or scintillation caused by the recoiling nucleus. This leads to certain limitations connected with the relatively

high energy required to produce an ionization and with the sharply decreasing efficiency of ionization by slow nuclei. The cryogenic detectors developed for CRESST use much lower energy excitations – phonons. Obviously, since the dominant physical effect of a WIMP nuclear recoil is the generation of phonons rather than ionization, cryogenic calorimeters are ideally suited for WIMP detection.

2 Detection Principle

The low temperature calorimetric detectors employed in CRESST consist of a target crystal, the so-called absorber, an extremely sensitive superconducting phase transition thermometer, capable of measuring temperature rises in the μK range, and a weak thermal coupling to a heat bath to allow relaxation of the system after an interaction. The thermometer is made of a tungsten film evaporated onto the absorber crystal. Its temperature is stabilized at $\approx 15\,\mathrm{mK}$, in the transition region from the superconducting to the normal conducting state. In this region a small temperature rise (typically some μK), e.g. from a WIMP nucleus scattering event, leads to an increase of resistivity, which can be measured with a SQUID based readout circuit.

This detection principle provides an excellent energy resolution, a low energy threshold, and, particularly important for the investigation of WIMP nucleus scattering, a high detection efficiency for interactions exhibiting a low ionization yield. The combination of these characteristics makes it an ideal tool for WIMP searches.

3 Overview on the CRESST Dark Matter Experiment

The CRESST Dark Matter experiment has been approved for installation in the Gran Sasso Underground Laboratory (LNGS) in 1993 and has been set up in hall B of the laboratory from 1995 to 1998. The central part of the setup is a ^{3}He/^{4}He-dilution refrigerator, capable of sustaining the detector operation temperature of $\approx 10 - 15\,\mathrm{mK}$. In order to fulfill the stringent low-background requirements, the detectors are housed inside a cold box, which was fabricated from low background OFHC-copper. Special care has been taken to minimize the exposure of all construction materials to cosmic rays, in order to avoid activation. The low temperature is transferred from the dilution refrigerator to the cold box through a cold finger, protected by thermal radiation shields, all fabricated of low background copper. Two internal shields consisting of low level lead are attached to the mixing chamber and liquid N_2-shield, respectively, in order to block any line-of-sight from the detectors to non-radiopure parts of the dilution refrigerator. An extensive passive shielding of low background copper and lead surrounds the cold box and serves to shield radioactivity from the outside, particularly the surrounding rock. Fig. 1 shows a sketch of the low background cryostat facility.

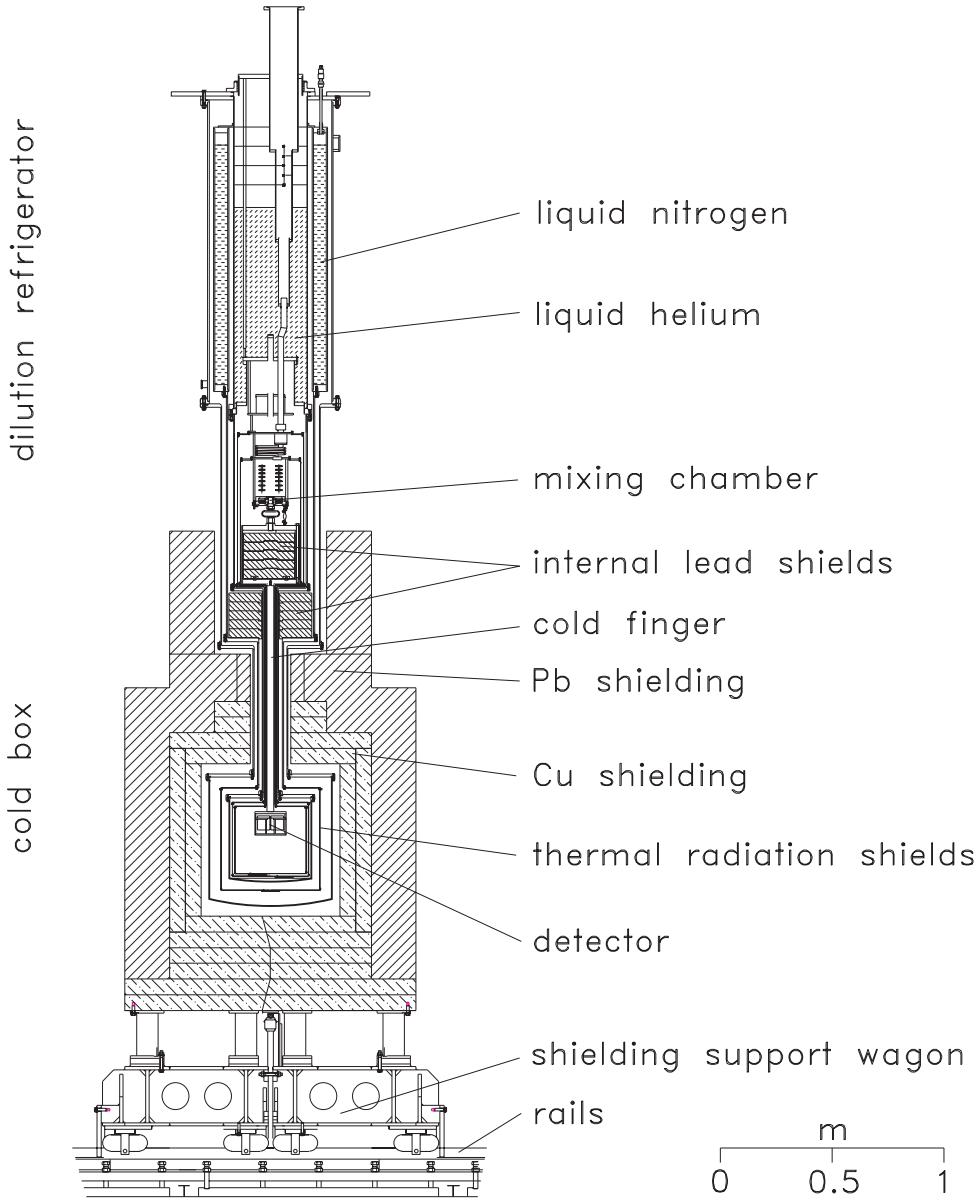

Figure 1: Sketch of the CRESST cryostat with the attached cold box housing the detectors and the passive copper and lead shielding.

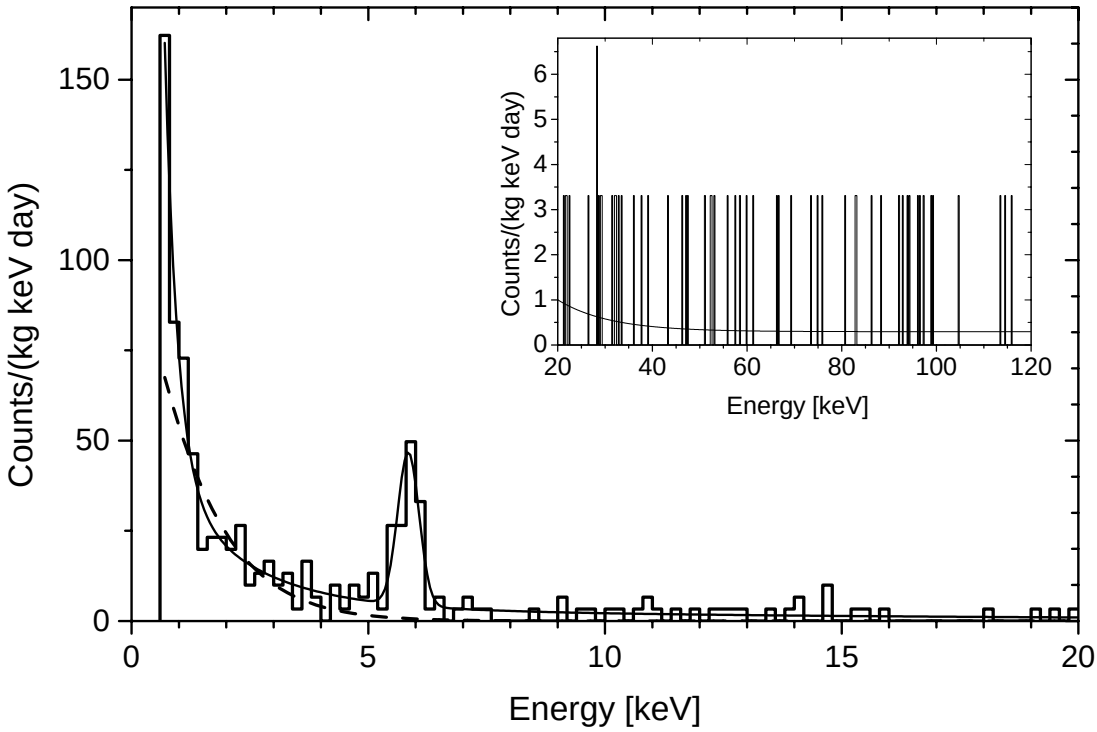

Figure 2: Energy spectrum obtained in the 1.51 kg·d dark matter run. The solid curve is an empirical fit to the measured spectrum. For illustration, the dashed line depicts the recoil spectrum from a 5 GeV WIMP, which is excluded at 90% cl. The prominent line at 5.89 keV is due to a low activity contamination from a previously used ^{55}Fe source and was used for calibration.

4 Results from the Data Taking Phase CRESST-I

To search for WIMP nucleus scattering, CRESST was taking data with up to four sapphire calorimeters during the years 2000 and 2001 (data taking period CRESST-I). This measurement campaign yielded new, restrictive limits for spin-dependent interactions of light-mass WIMPs. The data used to set dark matter limits results from a total run time of 138.8 h of which 0.6 h are dead time following triggers. This dark matter run was preceeded by a 10 h calibration run with an external ^{57}Co source and followed by a second calibration run. The individual detectors varied in their response with detector #8 (numbered by order of fabrication) having the lowest threshold and thus giving the best dark matter limits. The trigger efficiency of this detector was measured to be 100% down to an energy of 580 eV throughout the dark matter run.

To avoid reliance on the detailed behaviour of the trigger efficiency at low-energies a software threshold of 600 eV was used. There were 446 events from the software threshold to 120 keV. Events in coincidence in two or more detectors cannot be due to WIMP interactions and so can be discarded. After a pulse shape cut to remove fake events caused by vibrations or electronic noise the spectrum shown in fig. 2 is obtained. It translates into a background as low as (0.73 ± 0.22) counts/kg/day/keV for the energy range from 15 keV to 25 keV. The background drops to about 0.3 /kg/day/keV at 100 keV. Fig. 3

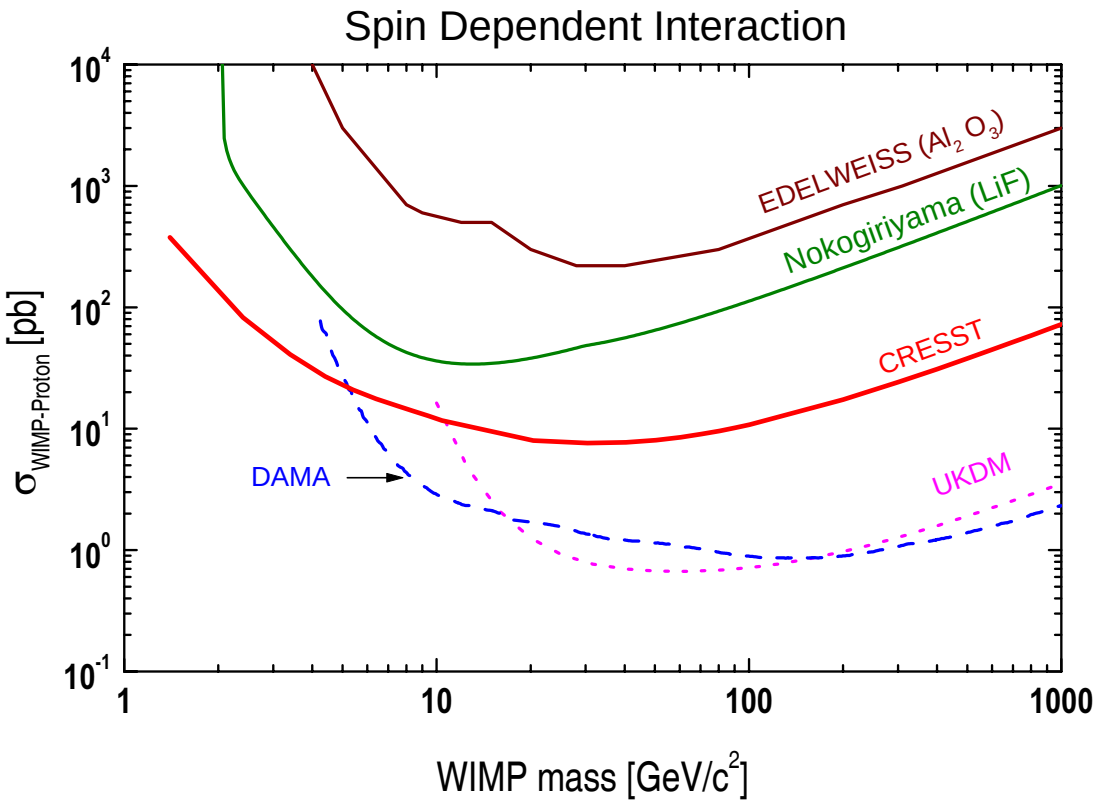

Figure 3: Equivalent WIMP-proton cross section limits (90% cl) for spin-dependent interaction as a function of WIMP mass from 1.51 kg·d exposure of a 262 g sapphire detector. For comparison we show limits from the EDELWEISS dark matter search with cryogenic sapphire detectors, from DAMA with NaI detectors using pulse-shape discrimination, and from the UK dark matter search with NaI detectors.

shows the obtained WIMP limits for spin-dependent interaction.

5 The Upgrade Phase CRESST-II

Detection Principle

For CRESST-I the detector consisted of up to four sapphire crystals of mass 262 g each. At the operation temperature of $\approx$ 15 mK the tiny temperature increase caused by a WIMP or background interaction (order of μK per keV energy deposit) can be measured with superconducting phase transition thermometers. These thermometers consist of a thin metallic tungsten film evaporated onto the sapphire absorber crystal. Stabilised right in the transition region from the superconducting to the normal conducting state, a small temperature increase leads to a substantial change in resistivity which can be detected utilizing a SQUID-based readout circuit.

For CRESST-II, an improved detection principle will be applied. It has been developed at the institute and relies on the coincident detection of phonons and scintillation light created in the absorber crystal after an interaction. Instead of sapphire a scin-

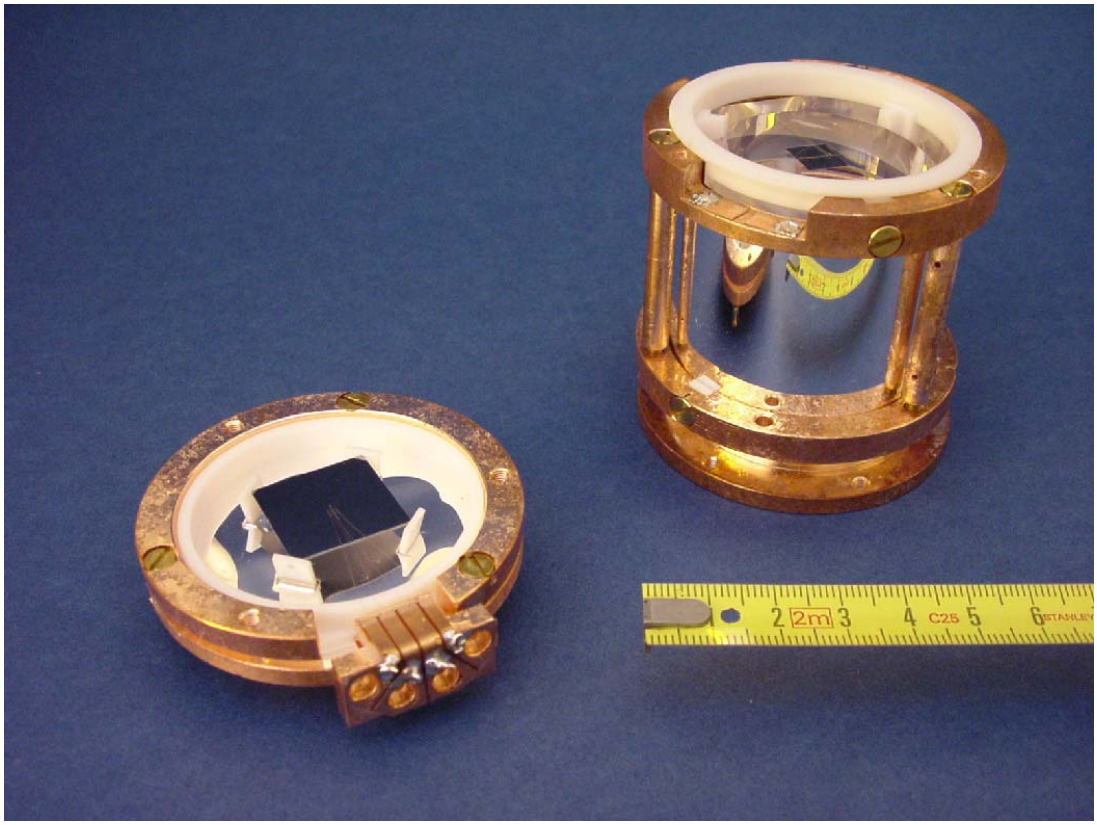

Figure 4: Photograph of a CRESST-II $CaWO_3$-detector for the coincident measurement of phonons and scintillation light. The small crystal in the left holder is the light detector, which is later on mounted facing the top of the large cylindrical detector on the right.

tillating crystal, $CaWO_4$, will be used as absorber. It is equipped with an evaporated superconducting tungsten phase transition thermometer for the detection of the phonons. In addition, the scintillation light will be recorded in coincidence with a dedicated second cryogenic detector, consisting of a sapphire absorber with silicon coating for better light absorption. Fig. 4 shows a photograph of the actual design of the detector and its holder.

The coincident detection of phonons and scintillation light offers a substantial background suppression. For a given energy deposit the ratio of the energy in the phonon channel and the energy in the light channel depends on the type of interaction. Nuclear recoils, such as WIMP or neutron scattering events, emit substantially less scintillation light than ionizing interactions, e.g. gamma or beta absorptions. Therefore, as most of the backgroud consists of ionizing interactions, the simultaneous detection of the phonons and the scintillation light provides an efficient method for background suppression. Fig. 5 illustrates the potential of the novel detection method.

It has been verified, that the suppression for ionizing background with this concept is as high as 99.7 % in the energy region between 15 and 25 keV, and 99.9 % at energies exceeding 25 keV. Following this proof-of-principle, detector fabrication for CRESST-II has been started.

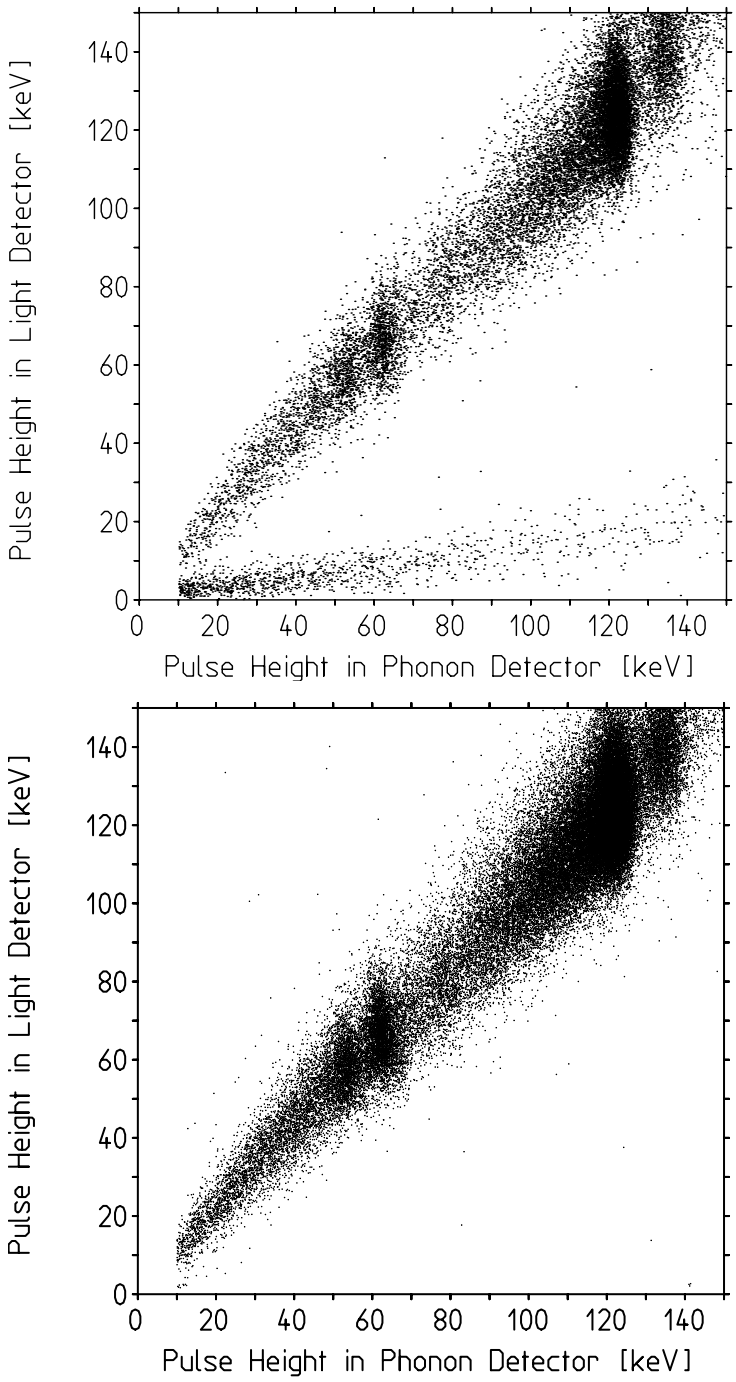

Figure 5: Coincident detection of phonons and scintillation light with a $CaWO_4$ detector. Upper fig.: The lower band consists of nuclear recoils, caused by a neutron calibration source. WIMPs do have the same interaction characteristics. The upper band of events is due to ionizing interactions from electrons and gamma rays. By removing the neutron source (lower fig.), it has been verified that there is no leakage of ionizing events into the nuclear recoil region.

CRESST-II Detector Development

During 2002 several measurements of 300 g $CaWO_4$ prototype modules were performed. Several improvements were made on the phonon detector as well as on the light detector.

CaWO4 phonon detector improvements

The evaporation of a pure tungsten thermometer directly on a $CaWO_4$ crystal leads to high phase transition temperatures of about 40-50 mK and correspondingly low sensitivity performance. Nevertheless, an initial measurement utilizing this technology achieved a threshold of 10 keV for a 300 g $CaWO_4$ crystal. Meanwhile, a new method to produce CRESST tungsten thermometers on a $CaWO_4$ crystal has been developed. A SiO_2 interdiffusion barrier below the tungsten film effectively reduces phase transition temperatures to the desired range of about 10 mK, hence improving sensitivity and giving a better match to the operating temperature of the corresponding light detector. Another important issue for the $CaWO_4$ detectors is their radiopurity, i.e. the amount of radioactive impurities internally present in the crystals from different suppliers. So far, $CaWO_4$ crystals from two suppliers have been prepared for low-level measurements at Gran Sasso. Crystals from a

Hungarian company turned out to show a low-energy alpha-radiation contamination, probably from a Samarium isotope. In addition, a low but non-negligible contamination from one of the natural decay chains is visible. Fig. 6 shows the alpha contaminations found in two different crystals from the Hungarian supplier. Due to the simultaneous detection of scintillation light and phonons alpha contaminations can be clearly separated from beta and gamma background. These spectra were obtained by applying an new pulse shape analysis, which enables us to obtain energy spectra from pulses exceeding the dynamic range of the phase transition thermometer. The energy spectrum in the low energy range of the electron recoil band is shown in fig. 7.

Light Detector Improvements

Initial designs for the light detector thermometer followed the standard CRESST design (see fig. 8, left panel). The detector consisted of a cryogenic calorimeter made from sapphire (10x20x0.5 mm3) that was coated on one 10x20 mm2 surface with silicon to improve the light absorption. The opposite side had the thermometer deposited. The latest design, however, consists of a newly restructured tungsten thermometer on a silicon substrate(30x30x0.5 mm3) . The significantly changed thermometer design is visible in fig. 8 on the right panel.

The design uses aluminum-phonon collectors combined with a reduced tungsten film area and hence reduced heat capacity. Such a thermometer yields larger signals from a light detection. In addition, the new thermal coupling with a thin gold film instead of a mere gold wire contact enlarges integration times. This results then in a better match to the long (millisecond) light emission times of the $CaWO_4$ scintillator.The effect for the signal sensitivity can be most clearly seen in fig. 9 .

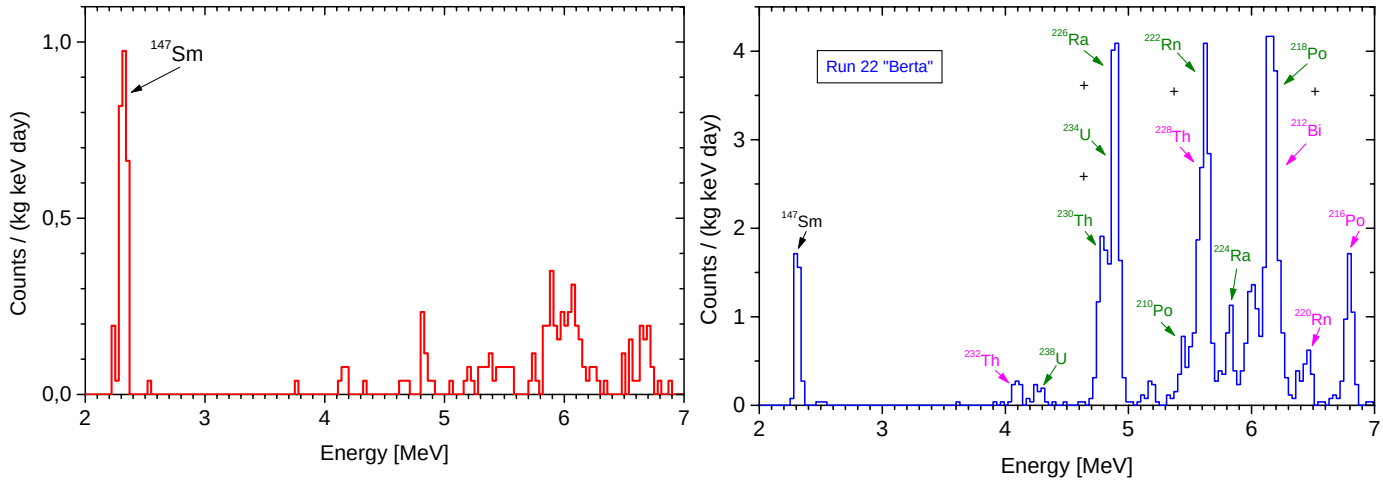

Figure 6: Alpha contaminations found in two different crystals from an Hungarian supplier. The contamiantion is caused by 266Ra and its natural decay chain as well as by 146Sm. The crystal with the higher contamination has a contamination of 5 mBq of 266 Ra

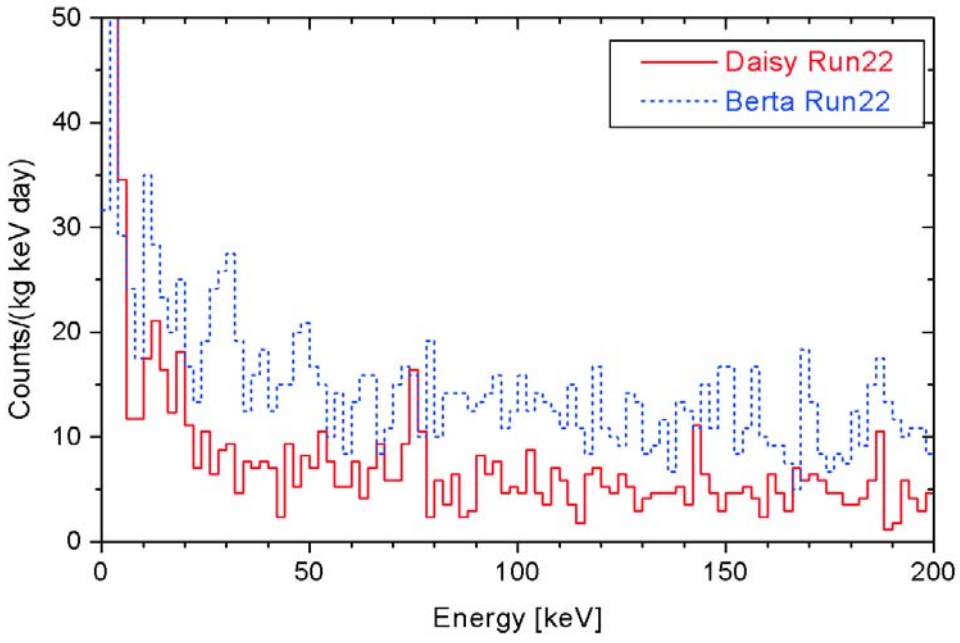

Figure 7: Low Energy spectra of the crystals of fig. 6.

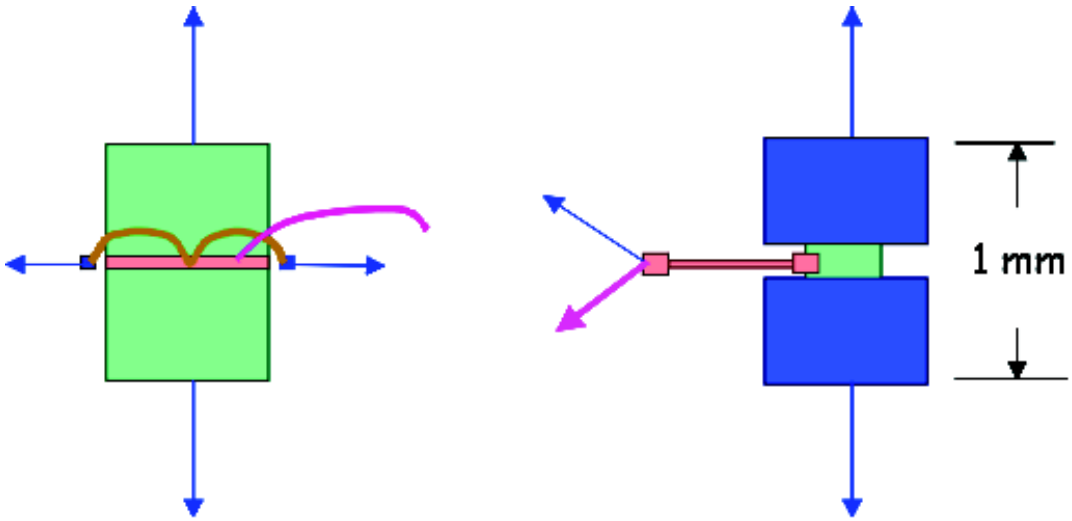

Figure 8: The left picture shows the old thermometer design with a large tungsten thermometer and a thermal coupling and heater realized by gold bonding wires. The new thermometer design in the right picture has only a small tungsten thermometer and large aluminum phonon collectors. The thermal coupling and heater are realized by an evaporated gold structure.

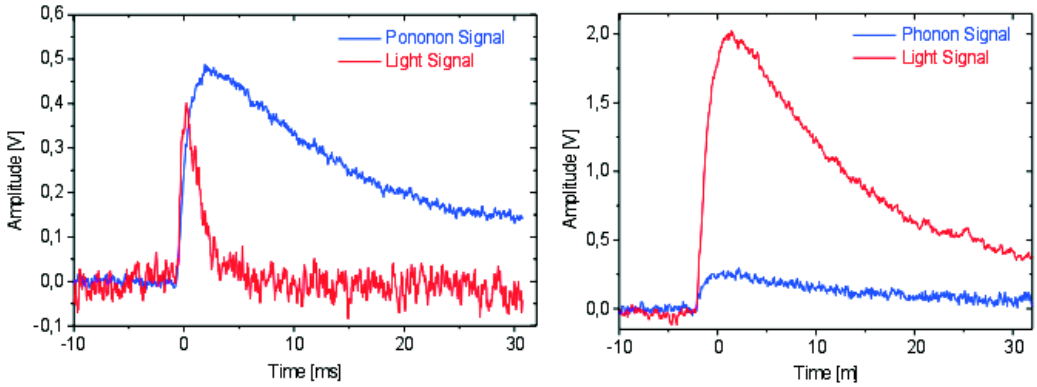

Figure 9: The left picture shows simultaneous light and phonon pulses obtained with an $CaWO_4$ crystal with tungsten thermometer and a light detector of the old design. The right picturse shows pulses of the same $CaWO_4$ crystal and the new light detector. The improvement in the light detection can be clearly seen.

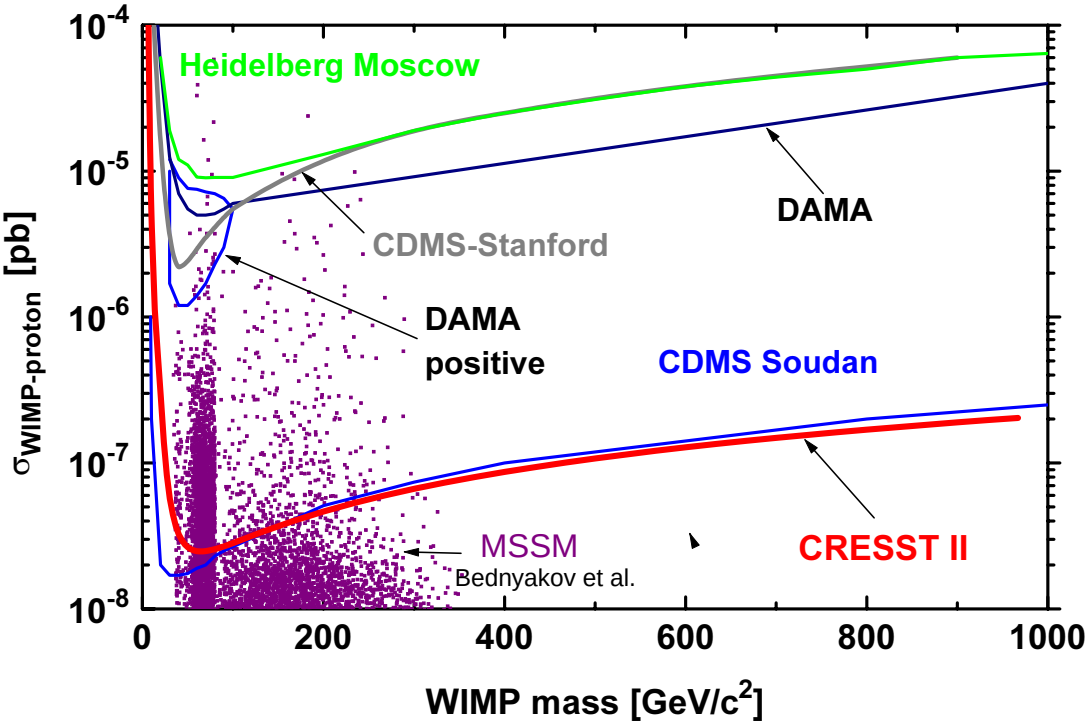

Figure 10: Expected sensitivity of CRESST-II for a 30 kg yr observation time, together with the limits from other experiments. The area labelled 'DAMA positive' is the region in the parameter space suggested by the DAMA evidence for a seasonal variation of the interaction rate.

For equal energy deposition in the scintillator (60 keV here) the pulses from the phonon channel as well as the light detector are shown comparing the old and new design. An improvement by a factor of five for the light detection is visible.

Plans and Perspectives for CRESST-II

It is planed to finalize and freeze the detector design early 2003 so tha a series production can be started.

CRESST-II will be characterized by

- a $CaWO_4$ cryogenic detector capable of performing the coincident detection of phonons and scintillation light,
- a total detector mass of 10 kg, realized as a segmented installation of 33 $CaWO_4$ crystals of mass 300 g each and the corresponding 33 calorimetric light detectors, and
- an extensive radiation shielding, improved with respect to the CRESST-I setup by an additional muon veto and a neutron shielding.

In total, for CRESST-II the accumulation of a 30 kg $\cdot$ yr data sample is planned with a four years' running time. Assuming a background rate of 1/(kg $\cdot$ keV $\cdot$ d) and a rejection of

ionizing background of 99.7 % (both already demonstrated to be achievable), CRESST-II will be in the position not only to probe the positive evidence of WIMP dark matter claimed by the DAMA experiment, but also to cover a significant part of the MSSM parameter space. Fig. 10 illustrates this potential.

DAMA. Dark Matter Search

DAMA collaboration:
P. Belli[a], R. Bernabei[a,@], A. Bussolotti[a,*], F. Cappella[a,b],
R. Cerulli[a], P. Delfini[a,*], F. Montecchia[a,c], F. Nozzoli[a],
A. Incicchitti[d], A. Mattei[d,*], D. Prosperi[d], V.I. Tretyak[d,+],
C.J. Dai[e], Z. P. Ye[e], H.H. Kuang[e], J.M. Ma[e]

in neutron measurements: M.Angelone[f], P.Batistoni[f], M.Pillon[f]

[a]Dip. di Fisica, Università di Roma "Tor Vergata" and INFN-Roma2, 00133 Roma, Italy;
[b]Laboratorio Nazionale del Gran Sasso, INFN, 67010 Assergi (Aq), Italy;
[c] Facoltà di Ingegneria, Università "Campus Bio-Medico" di Roma, 00155 Roma, Italy;
[d]Dip. di Fisica, Università di Roma "La Sapienza" and INFN-Roma, 00185 Roma, Italy;
[e]IHEP, Chinese Academy, P.O. Box 918/3, Beijing 100039, China;
[f]ENEA - C. R. Frascati, P.O. Box 65, I-00044 Frascati, Italy.

@ Spokesman of the DAMA collaboration
* technical staff
+ permanent address: Institute for Nuclear Research, 252650 Kiev, Ukraine

Abstract

DAMA is investigating various rare processes by developing and using several kinds of radiopure scintillators. The main experimental set-ups are: i) the $\simeq$ 100 kg NaI(Tl) set-up, which has completed its data taking in July 2002; ii) the new $\simeq$ 250 kg NaI(Tl) LIBRA (Large sodium Iodide Bulk for RAre processes) set-up, whose installation is started at fall 2002; iii) the $\simeq$ 6.5 kg ($\simeq$ 2 l volume) liquid Xenon (LXe) pure scintillator; iv) the R&D installation for tests and small scale experiments. Moreover, in the framework of devoted R&D for higher radiopure detectors and PMTs, sample measurements are regularly carried out by means of the low background Ge detector of the DAMA experiment and in some cases at Ispra.

1 Introduction

DAMA is devoted to the investigation of rare processes by developing and using low radioactivity scintillators. Its main aim is the investigation of relic particles (WIMPs: Weakly Interacting Massive Particles) embedded in the galactic halo. Thus, our solar

system, which is moving with respect to the galactic system, is continuously hit by a WIMP "wind". The quantitative study of this "wind" allows both to obtain information on the Universe evolution and to investigate Physics beyond the Standard Model.
The WIMPs investigation is mainly carried out by studying the WIMPs' elastic scatterings on the target nuclei, which constitute a scintillation detector. For this purpose, radiopure NaI(Tl), liquid Xenon and CaF_2(Eu) detectors are developed and used (main recent references are given in [1, 2, 3, 4, 5, 6, 7, 8, 9, 10, 11, 12, 13, 14, 15, 16, 17, 18, 19] and in the 2002 publication list quoted in the following). In particular, the $\simeq$ 100 kg NaI(Tl) set-up has been realized to investigate the so-called WIMP "annual modulation signature". In fact, this experiment can effectively exploit such a signature because of its well known technology, of its high intrinsic radiopurity, of its mass and of its suitable control of the operational parameters. The relevance of performing experiments with a proper unambiguous model independent signature is evident.

An R&D activity to develop higher radiopure detectors is continuously carried out toward the creation of ultimate radiopure detectors and studies on their possible new applications (see ref. [20] and publication list in 2002) are also carried out. As a result of one of these R&D efforts, at present a new NaI(Tl) set-up (LIBRA) with exposed target-detector mass enlarged up to $\simeq$ 250 kg has been realized and installed.

Finally, profiting of the radiopurity achieved in the whole set-ups, several searches for other rare processes are also performed, such as: i) $\beta\beta$ decay processes; ii) charge-non-conserving (CNC) processes; iii) Pauli exclusion principle (PEP) violating processes; iv) nucleon instability; v) solar axions; vi) exotics; etc. Also in these cases competitive results have been obtained so far (main recent references are given in [21] and in the 2002 publication list quoted in the following).

The DAMA activities during 2002 are summarised in the following.

2 The $\simeq$ 100 kg highly radiopure NaI(Tl) set-up

The main goal of the $\simeq$ 100 kg NaI(Tl) set-up is the search for WIMPs by the annual modulation signature (see [6, 7, 8, 10, 11, 12, 13, 17] and publication list in 2002); in addition, as mentioned above, it allows also to investigate other rare processes (see ref. [21] and publication list in 2002).
This set-up and its performances have been described in details in ref. [7]; since then some upgradings have been carried out. In particular, in summer 2000 the electronic chain and data acquisition system have been completely upgraded, while during August 2001 the new HV power supply system and the new preamplifiers prepared for the foregoing LIBRA set-up have been installed.
This set-up has completed its data taking in July 2002.
Various kind of data analyses are continuing; some of them have been published during 2002.

2.1 On the WIMP annual modulation signature

The $\simeq$ 100 kg NaI(Tl) set-up has been realized to investigate the so-called WIMP "annual modulation signature". In fact, since the Earth rotates around the Sun, which is moving with respect to the galactic system, it would be crossed by a larger WIMP flux in June (when its rotational velocity is summed to the one of the solar system with respect to the Galaxy) and by a smaller one in December (when the two velocities are subtracted). The fractional difference between the maximum and the minimum of the rate is expected to be $\lesssim 7\%$. The annual modulation signature is very distinctive; in fact, a WIMP-induced seasonal effect must simultaneously satisfy many requirements: the rate must contain a component modulated according to a cosine function (1) with one year period (2) and a phase that peaks around $\simeq 2^{nd}$ June (3); this modulation must be found in a well-defined low energy range, where WIMP induced recoils can be present (4); it must apply to those events in which just one detector of many actually "fires", since the WIMP multi-scattering probability is negligible (5); the modulation amplitude in the region of maximal sensitivity must be $\lesssim$7% (6). Thus, only systematic effects also able to simultaneously satisfy these 6 requirements could mimic this signature; no one able to do it has been found or suggested by anyone so far; this can be easily understood considering the relevant number of peculiarities which have to be simultaneously satisfied.

In particular, we remind that the data collected in four annual cycles, DAMA/NaI-1 to DAMA/NaI-4 (total statistics 57986 kg·day) have been released up to now (see ref. [6, 7, 8, 10, 11, 12, 13, 17] and publication list in 2002). They show evidence at $\simeq 4\ \sigma$ C.L. for the presence of a modulation with the distinctive features expected for a WIMP induced effect. A devoted investigation has not offered any possible known systematics or side process able to mimic a WIMP induced seasonal effect and, thus, to account for the observed effect [12]. In conclusion, the model independent approach, together with the absence of possible systematics or side processes able to mimic such a signature, suggests the presence of a WIMP contribution to the measured rate independently on the nature and coupling with ordinary matter of the involved WIMP particle.

To investigate the nature and coupling with ordinary matter of the possible WIMP candidate, energy and time correlation analyses in some of the possible model frameworks[1] have been performed. In particular, we have published cumulative results for the data of the four annual cycles in some of the possible model frameworks for purely spin independent (SI) coupled WIMPs, for purely spin dependent (SD) coupled WIMPs, for WIMPs with both SI and SD coupling and for WIMP with preferred inelastic scattering, considering WIMP mass above 30 GeV [2] and the constraint arising from the measured upper limit on recoils of ref. [5] (see e.g. [11, 13, 17] and publication in 2002). During 2002 the analysis

[1] We further remind that a model framework is identified not only by general astrophysical, nuclear and particle physics assumptions, but also by the specific set of values used for all the experimental and theoretical parameters needed in the model itself and in related quantities (for example WIMP local velocity, v_0, form factors expressions and parameters, etc.), which are also indeed affected by significant uncertainties. Obviously, varying the parameters values within their allowed intervals as well as varying any of the astrophysical, particle and nuclear physics assumptions, the allowed region (the same is for excluded limits) and the related best fit values will consequently vary.

[2] This bound being inspired by the lower bound on the supersymmetric candidate, as derived from the LEP data in the usually adopted supersymmetric schemes based on GUT unification assumptions.

for the case of purely SI coupled WIMPs has been extended by considering a large class of different halo models (see later).

Finally, the analysis of the data collected in the 5^{th}, 6^{th} and 7^{th} (after completion) annual cycles has been pursued; the cumulative result from DAMA/NaI is planned to be released in 2003.

2.1.1 Effect of the galactic halo modelling on the DAMA/NaI annual modulation result: an extended analysis of the data for WIMPs with a purely SI coupling

This work has been performed in collaboration with N. Fornengo and S. Scopel, Torino University and INFN-To (see publication list in 2002).

The analysis of the data collected during four annual cycles for the case of WIMPs with purely SI coupling has been extended by discussing in details the implications on the results of the uncertainties on the dark matter galactic velocity. Possible departures from the isothermal sphere model, which is the parameterisation usually adopted to describe the halo, have been investigated in a systematic way. Modifications arising from various matter density profiles, effects due to anisotropies of the velocity dispersion tensor and rotation of the galactic halo have been specifically investigated. In particular, halo models with potential and matter density having a spherical symmetry have been investigated as well as halo models with spherical symmetry but anisotropic WIMP velocity distribution and halo models with axial symmetry. Moreover, in these latter cases possible co-rotation or counter-rotation of the dark halo has also been considered. Some phenomenological restrictions have been applied on the considered halo models to account for the experimental observations on: *i)* the allowed values for the local rotational velocity; *ii)* the degree of flatness in the rotational curve; *iii)* the maximal values of the non-dark matter components in the Galaxy.

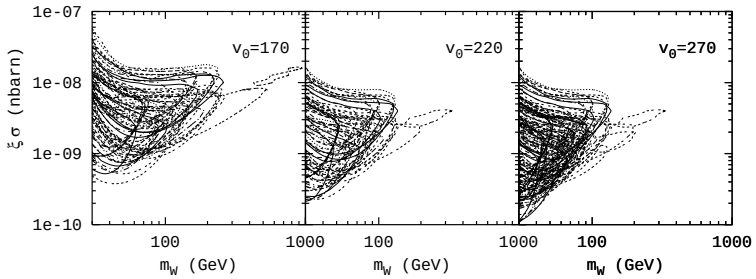

Figure 1: Superposition of the regions allowed at 3σ C.L. in the given model framework for the velocity distribution of each one of the considered halo models (see the publication for details). Three of the possible values of v_0 are considered. Obviously a specific set of best fit values for m_W and $\xi\sigma$ corresponds to each region. Inclusion of other existing uncertainties will further enlarge the regions.

As a result, limit values of the halo density for the considered halo models have also been obtained. The global results of this analysis is shown in Fig. 1, where the allowed regions obtained for the various considered models are superimposed for three of the possible values of the local velocity, v_0. The cumulative result, which gives a direct

impact of the effect induced on the region allowed in the considered scenario only by the halo model uncertainty, is shown in Fig. 2. The obtained region is compared there with

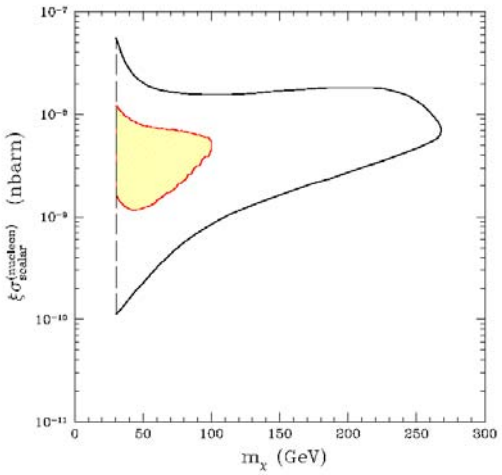

Figure 2: Region allowed at 3σ C.L. obtained considering all the allowed regions obtained in a given model framework considering several possible non-rotating halo models. Note that in these calculation only the uncertainties on the halo model have been considered; the inclusion of the other existing uncertainties would further enlarge the allowed region. It is evident that this cumulative region, as those given e.g. in ref.[11], accounts for a large set of best fit values for WIMP mass and cross section. The shaded region, which corresponds – in the considered scenario – to the particular case of the approximate and non-consistent isothermal sphere halo model when assuming also $v_0 = 220$ km/s e $\rho_0 = 0.3$ GeV/cm^3, is shown only to point out the effect. The increasing of the bound from accelerators with respect to the bound considered here will select further the possible model framework and in particular the halo models.

the one obtained when considering the approximate and non-consistent isothermal sphere model assuming also $v_0 = 220$ km/s e $\rho_0 = 0.3$ GeV/cm^3 in the given scenario. As one can see, the 3σ C.L. allowed region is extended up to $m_W \simeq 270$ GeV with cross section on nucleon in the range $10^{-10}\text{nbarn} \leq \xi\sigma_{SI} \leq 6 \cdot 10^{-8}\text{nbarn}$. Maximal co-rotating and counter-rotating models can extend the allowed region up to $m_W \simeq 500 - 900$ GeV (see Fig. 1). We further stress that in this analysis no other uncertainty than the halo model[3] has been considered; the proper inclusion of the other existing uncertainties will further extend the allowed region.

2.2 A preliminary search for Q-balls by delayed coincidences in NaI(Tl)

Theories with low-energy supersymmetry predict the existence of stable non-topological solitons, named Q-balls, with mass greater than about 10^8 GeV. The Q-balls may be

[3]Although the large number of halo models considered in this analysis, further halo models are still available and not yet considered here.

non-topological solitons stabilised by global charge conservation and may be considered in supersymmetric theories as coherent states of squarks, sleptons and Higgs fields; the condition for stable Q-balls is satisfied when the energy scale, M_S, of the SUSY breaking is low (from 100 GeV and 100 TeV [22]).

A preliminary search for Q-balls has been carried out by re-analysing delayed "downward" and "upward" coincidence patterns among two planes (center-to-center distance: 23.2 cm) of the $\simeq$ 100 kg NaI(Tl) set-up. These data have been collected during 350.05 days (total exposure: 1.1 $\cdot 10^6$ cm^2 sr day) and have been previously considered for other purposes in ref. [23].

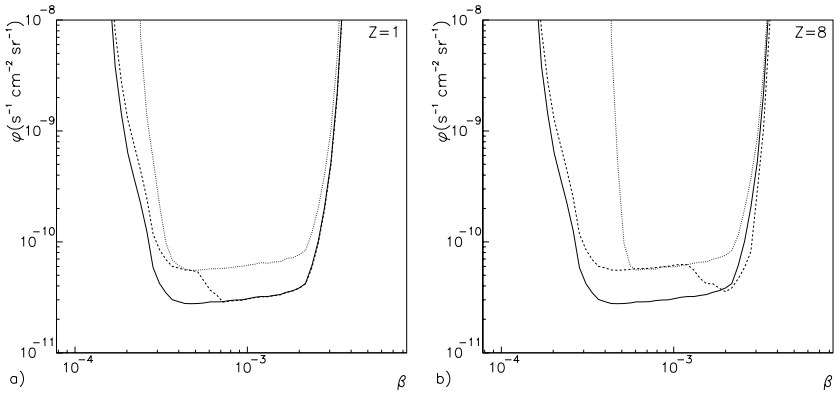

Figure 3: Exclusion plots at 90% C.L. in the plane (ϕ,β) for charged Q-balls with Z=1 (a) and Z=8 (b); the dotted curves correspond to Q-balls with $M_Q = 10^{13}$ GeV, the dashed ones to Q-balls with $M_Q = 10^{16}$ GeV and the solid contour is the geometrical limit. This corresponds to the case when all the Q-balls have sufficient energy to reach the detectors giving rise to a candidate event (in this case $M_Q = 10^{20}$ GeV). Intermediate contours in the (ϕ,β) plane with respect to the case (a) and (b) will correspond to Q-balls having intermediate Z values.

Both the detection efficiency of the experimental set-up and the effect of the matter crossed by the Q-balls have been properly estimated. No Q-balls candidates have been observed, thus 90% C.L. exclusion limits on Q-ball flux, ϕ, as a function of β for charged Q-balls having Z=1 (a) and Z=8 (b) have been calculated and are reported for some M_Q values in Fig. 3, where the solid contours represent the "geometrical limit". Fig. 3 clearly shows the dependence of the limit contour on M_Q. In particular, charged Q-balls with $M_Q \lesssim 10^{16}$ GeV would be absorbed by the Earth (depending also on β and Z values), thus only downward delayed coincidences would be observed in this case. Moreover, it can be noted that for $M_Q = 10^{13}$ GeV Q-balls with $\beta < 5 \cdot 10^{-4}$ are absorbed by the mountain too. Finally, for charged Q-balls with $M_Q \simeq 10^{16}$ GeV and velocity before crossing the mountain or the Earth equal to $\beta \simeq (2-4) \cdot 10^{-3}$, the limit contour is slightly more stringent than the geometrical one, since for a similar M_Q value the Q-ball has a velocity on the set-up in the underground laboratory lower than that it has before crossing the mountain or the Earth. Therefore, its efficiency for producing in the set-up the signal searched for is larger than the one of a Q-ball with $M_Q \simeq 10^{20}$ GeV, which impinges the detector with a higher β.

Fig. 4 shows the 90% C.L. exclusion plots in the plane (ϕ,β) for neutral Q-balls with

the given M_Q and M_S values; the solid contour is again the "geometrical limit". It can be noted that, for a given M_Q, larger M_S values imply smaller cross section (see above). This gives rise to larger mean free path in the detector and, therefore, the detection efficiency sharply drops down. Thus, the limit on ϕ is poorer, as it can be seen in Fig. 4.

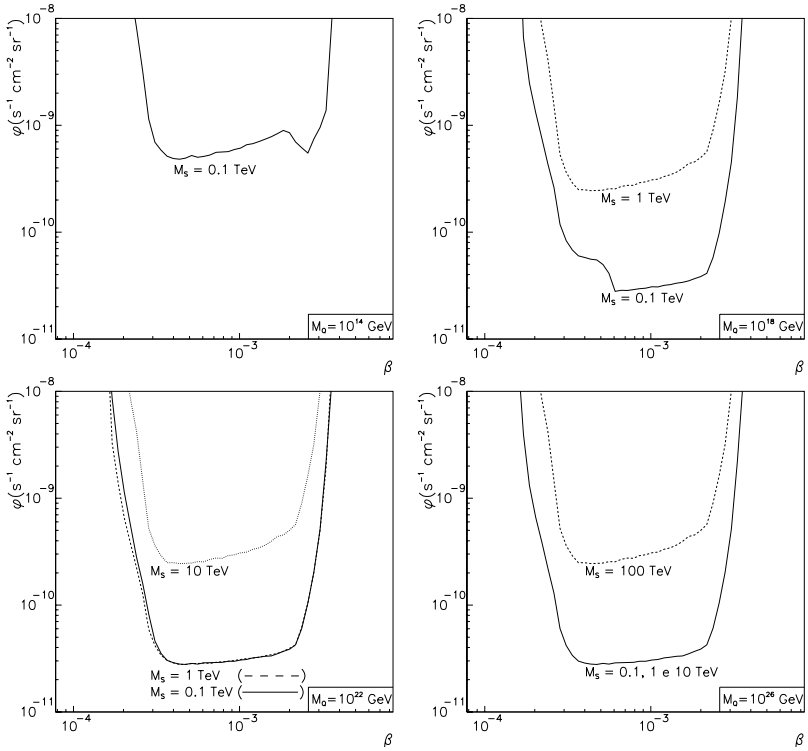

Figure 4: Exclusion plots at 90% C.L. in the plane (ϕ,β) for neutral Q-balls with $M_Q = 10^{14}$ GeV, 10^{18} GeV, 10^{22} GeV and 10^{26} GeV. The solid contour is the "geometrical limit" (see text).

In conclusion, no Q-ball candidate has been found. In particular, the 90% C.L. "geometrical limit" for the flux of charged Q-balls e.g. when Z=1 and $M_Q = 10^{20}$ GeV is: $\phi < 2.8 \cdot 10^{-11}$ s^{-1}cm^{-2}sr^{-1} ($\beta \simeq 10^{-3}$). The same value also holds for the "geometrical limit" of the neutral Q-balls flux when $M_Q = 10^{26}$ GeV and $0.1 < M_S < 10$ TeV. These limits are the first ones obtained by using crystal scintillators and can be significantly improved in future by using LIBRA and a different approach.

3 The new LIBRA set-up

After the completion of the data taking of the $\simeq$ 100 kg NaI(Tl) set-up, we have started the procedures needed to install the new LIBRA set-up.

In particular, the $\simeq$ 100 kg NaI(Tl) set-up has been fully dismounted and improvements have been realized in the experimental site (see e.g. Fig. 5), in the Cu box, in the shield and in the available detectors.

The LIBRA set-up is made of 25 NaI(Tl) detectors, 9.70 kg each one. The new detectors have been realized thanks to a second generation R&D with Crismatec company, by exploiting in particular new radiopurification techniques of the NaI and TlI selected

Figure 5: At work to improve the experimental site (walls, floor, etc.). On the bottom: the passive shield opened.

powders. In the framework of this R&D new materials have been selected, prototypes have been built and a devoted protocol has been fixed.

The full dismounting of the $\simeq$ 100 kg NaI(Tl) set-up, the improvements mentioned above and the installation of all the detectors including the new PMTs' shield has been completed at end 2002.

Figure 6: The dismounting of the detectors of the $\simeq$ 100 kg set-up and the installation of the LIBRA detectors and PMTs' shield have been performed in HP Nitrogen atmosphere by using special masks connected to air bottles to avoid that the inner part of the Cu box, the detectors and the new PMTs' shield would be in contact with the environmental air, that is to reduce at most possible surfaces' contamination by environmental Radon.

The dismounting of the detectors of the $\simeq$ 100 kg set-up and the installation of the LIBRA detectors and of the new PMTs' shield have been performed in HP Nitrogen atmo-

sphere by using special masks connected to air bottles to avoid that the inner part of the Cu box, the detectors, the new PMTs' shield, etc. would be in contact with the environmental air, that is to reduce at most possible surfaces' contamination by environmental Radon (see Fig. 6). In particular since in the $\simeq$ 100 kg set-up we had evidence that contaminations external to the NaI(Tl) crystals themselves were dominant, we prepared and installed the new PMTs' shield. This evidence was obtained by comparing the energy spectrum measured for a single detector with a complete shield of the PMTs, cables and feedthroughs, with respect to the one measured in the running conditions where this full shielding was not possible and the effect of PMTs, cables and feedthroughs of the all installed detectors was present.

Figure 7: Left top picture: some detectors during installation; in the central and right upper detectors the new shaped Cu shield surrounding the light guides and the PMTs has not yet been applied, while it has in the other detectors nearby. Right top picture: in the 3 upper detectors the shaped Cu shield has been applied but the HV dividers are still visible. Left bottom picture: during the detectors installation. Right bottom picture:view at end of the detectors installation. All the used materials have been deeply selected for radiopurity (see for example the cables with teflon envelop).

In Fig. 7 some pictures during the installation of the LIBRA detectors are shown. Before this installation, all the Cu parts have been chemically etched following a devoted protocol and maintained in HP Nitrogen atmosphere until the installation (see Fig. 8).

In Fig. 9 the two sides of a LIBRA low background HV divider (realized in such a way to optimise also the signal/noise) are shown; they are similar to those used in the $\simeq$ 100 kg NaI(Tl) set-up.

Figure 8: Chemical etching of Cu parts in clean room; on the right the sealing procedure in HP Nitrogen atmosphere of the etched materials is shown.

Figure 9: View of the two sides of a LIBRA low background HV divider.

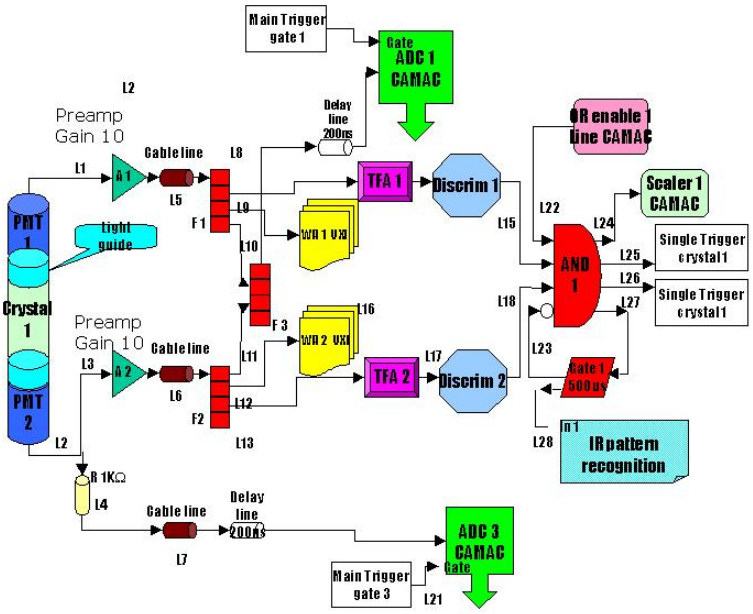

Figure 10: Schema of the electronic chain referred to a single detector and its trigger.

In Fig. 10 the schema of the electronic chain referred to a single detector and its trigger is shown, while in Fig. 11 the schema of the main trigger of the acquisition system and of the trigger of the Waveform Analysers is shown. We mention that to improve the performances of the system some devoted electronic parts have been specially developed.

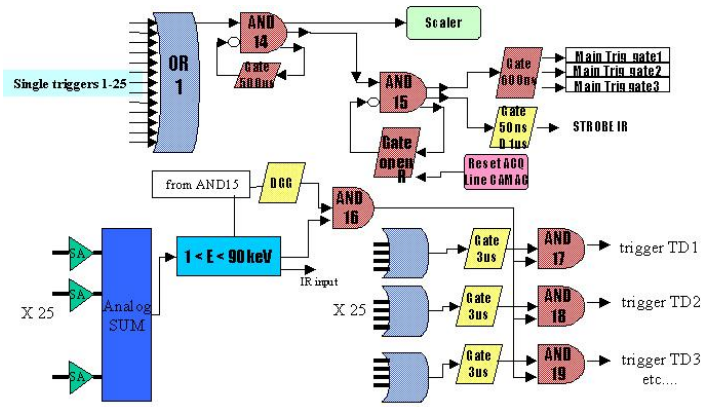

Figure 11: Schema of the main trigger of the acquisition system and of the trigger of the Waveform Analysers.

As regards the data acquisition system, it is briefly summarised in Fig. 12. It is made of a Workstation by Compaq with a Linux SuSe operative system, which is interfaced with the hardware system via MXI-2 and GPIB bus. The GPIB bus allows to communicate with the CAMAC crate housing the ADCs, the scalers and the I/O Registers, while the MXI-2 bus allows to communicate with the VXI mainframes, where the Waveform Analysers are installed.

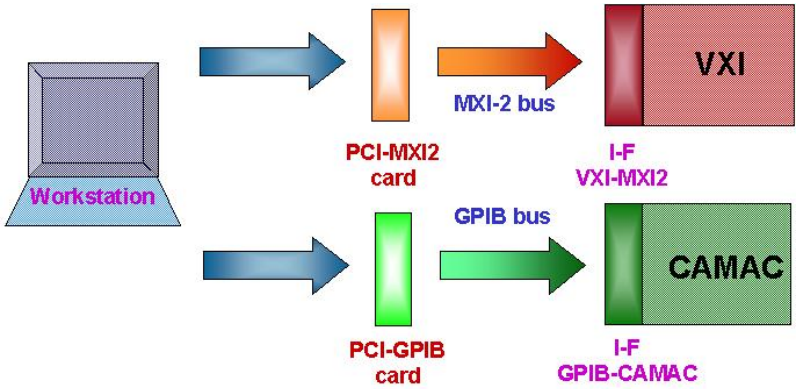

Figure 12: Schema of the LIBRA acquisition system.

The new LIBRA set-up, having an exposed mass of $\simeq$ 250 kg and an higher overall radiopurity will allow us to increase the experimental sensitivity. In particular, the higher statistics which will be collected each single annual cycle will allow to reach very high confidence level for the model independent effect in shorter time and to better identify the nature of the WIMP candidate.

Finally, only to offer a comparison with existing projects, which generally assume in their estimates absence of signal, we note that under the same arbitrary assumption this

set-up (which is already under test) would explore in few years - considering as an example purely SI coupled WIMPs - $\xi\sigma_p \lesssim 10^{-8}$ pb; this further shows the intrinsic competitiveness of LIBRA.

4 The LXe set-up

The low background $\simeq 6.5$ kg liquid Xenon (LXe) DAMA set-up has been largely upgraded two times: in fall 1995 and in summer 2000; moreover, various improvements and/or substitutions have been carried out with time. A recent description of the set-up and its performances is available in NIMA482(2002)728.

During 2002, some data analyses have been completed and further data taking has been continued in large part of the year. The data taking will continue in incoming years.

In particular, during 2002, new investigations on $\beta\beta$ decay processes in ^{136}Xe and in ^{134}Xe have been performed by exploiting the active source technique.

4.1 Preliminary search for neutrinoless $\beta\beta$ decay in ^{134}Xe

Preliminary results have been obtained by investigating the neutrinoless $\beta\beta$ decay in ^{134}Xe considering data collected during 6843.8 hours with the detector filled by by Kr-free Xenon containing 17.1% of ^{134}Xe (and 68.8% of ^{136}Xe), giving a useful statistics for this isotope of 0.87 kg $\times$ y.

The response functions of the detector for the $\beta^-\beta^-0\nu(0^+ \rightarrow 0^+)$ and for the $\beta^-\beta^-0\nu(0^+ \rightarrow 2^+)$ decay modes of ^{134}Xe have been simulated by using EGS4 [24] and an event generator code [25]; they are shown in Fig. 13.

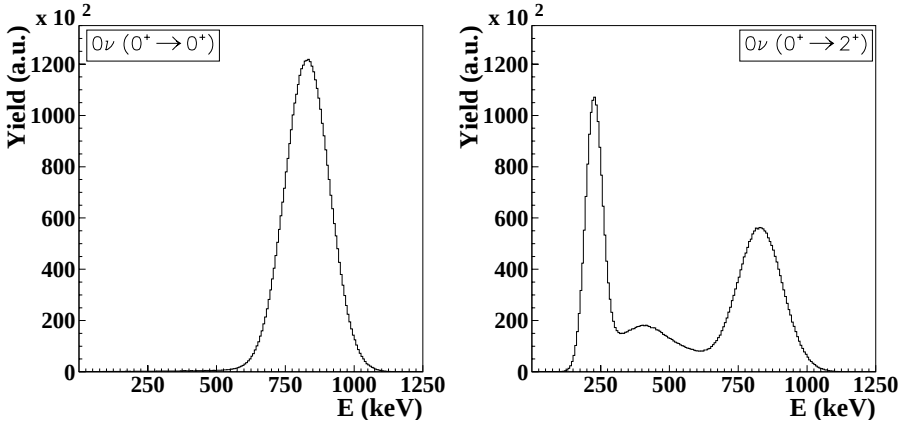

Figure 13: Expected energy distributions for the $\beta^-\beta^-0\nu(0^+ \rightarrow 0^+)$ and the $\beta^-\beta^-0\nu(0^+ \rightarrow 2^+)$ decay modes in ^{134}Xe. In the latter case the first peak corresponds to events where the de-excitation γ escapes, while the higher energy peak corresponds to the case when it is fully contained in the detector.

Fig. 14 shows the experimental energy distribution, where there is no evidence for the peaks arising from the processes searched for. Thus, the half life, $T_{1/2}$, has been estimated according to the standard formula: $T_{1/2} = \frac{N \cdot T}{N_d} ln2$, where N is the number of atoms of ^{134}Xe, T is the running time and N_d is the number of signal events which can be

ascribed to the process searched for on the basis of the experimental data. To estimate

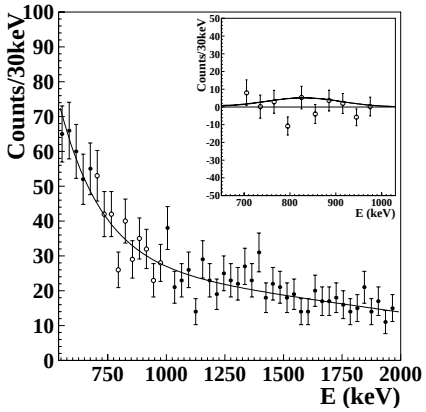

Figure 14: Experimental data (filled and open circles) with superimposed (continuous line) the behaviour of the background. In the inset the residuals of the open circle data are shown; the dashed and dotted curves (there practically indistinguishable) are the expected distributions for the $\beta^-\beta^-0\nu(0^+ \rightarrow 0^+)$ and for the $\beta^-\beta^-0\nu(0^+ \rightarrow 2^+)$ decay modes, respectively, calculated for $T_{1/2}$ equal to the corresponding 90% C.L. limits.

N_d, we have considered various approaches; one of them is depicted in Fig. 14. The more cautious limits on the $\beta^-\beta^-0\nu(0^+ \rightarrow 0^+)$ and on the $\beta^-\beta^-0\nu(0^+ \rightarrow 2^+)$ decay modes in ^{134}Xe resulted to be: $T_{1/2} > 5.8 \cdot 10^{22}$ y (90% C.L.) and $T_{1/2} > 2.6 \cdot 10^{22}$ y (90% C.L.), respectively. The first one improves the previously available best limit of about three orders of magnitude, while the second has been set for the first time.

4.2 Investigation of $\beta\beta$ decay modes in ^{134}Xe and ^{136}Xe

As mentioned above the gas, we use, is enriched in ^{136}Xe at 68.8% and contains also 17.1% of ^{134}Xe. Thus, after the preliminary results of ref. [16] and those given above, a larger statistics has been considered to perform, in particular, a joint analysis of the $0\nu\beta\beta$ decay mode in ^{134}Xe and in ^{136}Xe as suggested in ref. [26]. In principle, this kind of analysis could improve the information obtained when separately studying the two isotopes.

Thus, the data collected over 8823.54 hours (statistics of 1.1 kg $\times$ y for the ^{134}Xe and of 4.5 kg $\times$ y for the ^{136}Xe) have been analysed to investigate further the ^{134}Xe and ^{136}Xe $\beta\beta$ decay modes. The response functions of the detector have been calculated for the considered $\beta\beta$ decay processes by using the EGS4 code and an event generator code [16].

The data collected in the (0.55 – 3.55) MeV energy region are shown in Fig. 15. In particular, in this energy region the $0\nu\beta\beta(0^+ \rightarrow 0^+)$ signals in ^{134}Xe and ^{136}Xe (which show quasi-gaussian energy distributions around 0.83 MeV and 2.47 MeV, respectively) are fully contained. No evidence for these peaks is found. Fig. 15 shows the background estimate (continuous line) superimposed on the experimental data; the obtained residuals as a function of the energy are shown in the inset.

The residuals have been fitted by a linear combination of the expected $0\nu\beta\beta(0^+ \rightarrow 0^+)$ signals in ^{134}Xe and in ^{136}Xe with the half-lives of the two isotopes as free parameters. The results are depicted in Fig. 16a, where the area in the plane $(T^{136}_{1/2})^{-1}$ *versus* $(T^{134}_{1/2})^{-1}$

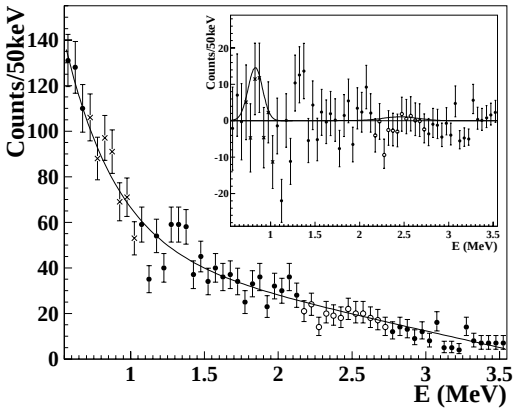

Figure 15: Experimental data (crosses, filled and open circles) with superimposed the background contribution (continuous line). In the inset: the residuals as a function of the energy; the gaussian peaks represent the expected signals for the $0\nu\beta\beta(0^+ \to 0^+)$ decay mode in ^{134}Xe and in ^{136}Xe when $T_{1/2} = 5.8 \cdot 10^{22}$ y and $T_{1/2} = 1.2 \cdot 10^{24}$ y, respectively (they correspond to the 90% C.L. limit values in case of pure ^{134}Xe $0\nu\beta\beta(0^+ \to 0^+)$ decay mode and in case of pure ^{136}Xe $0\nu\beta\beta(0^+ \to 0^+)$ decay mode, respectively.

outside the continuous (dashed) contour is excluded at 68% (90%) C.L. In the particular case of the pure ^{134}Xe $0\nu\beta\beta(0^+ \to 0^+)$ decay mode the limit: $T^{134}_{1/2} = 7.8(5.8) \cdot 10^{22}$ y at 68(90)% C.L. is obtained, while in the particular case of the pure ^{136}Xe $0\nu\beta\beta(0^+ \to 0^+)$ decay mode the limit is: $T^{136}_{1/2} = 4.9(1.2) \cdot 10^{24}$ y at 68(90)% C.L.

According to the model of ref. [26] the half-life of the $0\nu\beta\beta(0^+ \to 0^+)$ decay modes in ^{134}Xe and in ^{136}Xe can be written as a function of the *effective light Majorana neutrino mass*, $< m_\nu >$, and of the *effective inverse heavy Majorana mass*, η_N, (see ref. [26] for detail). In particular, in the plane of Fig. 16a the straight line $\frac{(T^{136}_{1/2})^{-1}}{(T^{134}_{1/2})^{-1}} = 9.66$ would represent the case $< m_\nu > = 0$, while the straight line $\frac{(T^{136}_{1/2})^{-1}}{(T^{134}_{1/2})^{-1}} = 4.02$ would represent the case $\eta_N = 0$. Furthermore, still considering the theoretical model of ref. [26], it is also possible by means of the obtained limits to calculate the exclusion plot in the plane $< m_\nu >$ *versus* η_N. The positive sector of this plane is shown in Fig. 16b, where the values outside the continuous (dashed) contour are excluded at 68(90)% C.L.; for example, we obtain $\eta_N < 2.7 \cdot 10^{-7}$ (90% C.L.) if $\langle m_\nu \rangle = 0$ eV and $\langle m_\nu \rangle < 2.9$ eV (90% C.L.) if $\eta_N = 0$. This limit value on $\langle m_\nu \rangle$ is comparable with those obtained – depending on the adopted model [26, 27, 28, 29, 30] – from the result on the $0\nu\beta\beta(0^+ \to 0^+)$ decay mode in ^{136}Xe alone (from 1.1 eV to 2.9 eV at 90% C.L.), while lower limit values can be derived from the $0\nu\beta\beta(0^+ \to 0^+)$ decay mode in ^{134}Xe alone (between 27 eV for the model of ref. [26] and 17 eV for the model of ref. [30]).

Furthermore, the data shown in Fig. 15 have also been analysed in terms of neutrinoless double beta decay with Majoron (M) obtaining for the half life of this process: $T_{1/2} > 5.0 \cdot 10^{23}$ y (90% C.L.); consequently, upper limit values on the effective Majoron-neutrino coupling constant ranging from $2.0 \cdot 10^{-5}$ to $3.0 \cdot 10^{-5}$ (90% C.L.) have been derived, depending on the considered theoretical model [27, 28, 29, 30].

Finally, by using a very cautious approach, the $2\nu\beta\beta(0^+ \to 0^+)$ and the $2\nu\beta\beta(0^+ \to 2^+)$ decay modes in ^{134}Xe have been investigated, obtaining the following conservative 90%

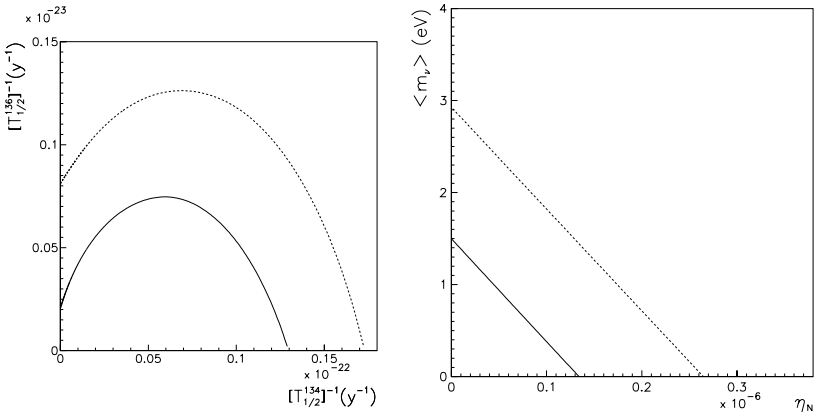

Figure 16: On the left (a): results of the simultaneous analysis of the $0\nu\beta\beta(0^+ \rightarrow 0^+)$ decay mode in ^{134}Xe and in ^{136}Xe. The area outside the continuous (dashed) contour is excluded at 68% (90%) C.L.. On the right (b): Exclusion plot in the positive sector of the plane $< m_\nu >$ *versus* η_N obtained from the results on the $0\nu\beta\beta(0^+ \rightarrow 0^+)$ decay mode in the ^{134}Xe and ^{136}Xe when considering the theoretical model of [26]. The values outside the continuous (dashed) contour are excluded at 68% (90%) C.L.

C.L. limits: $1.0 \cdot 10^{22}$ y and $9.4 \cdot 10^{21}$ y for the $2\nu\beta\beta(0^+ \rightarrow 0^+)$ and the $2\nu\beta\beta(0^+ \rightarrow 2^+)$ decay modes in ^{136}Xe, respectively. It is worth to note that the experimental limit on the $2\nu\beta\beta(0^+ \rightarrow 0^+)$ decay mode is in the range of the theoretical estimate by [31] ($2.11 \cdot 10^{22}$ y) and about a factor 5 higher than that of ref. [32] [4].

5 Measurements in the R&D installation

The set-up named "R&D" is used for prototype tests and small scale experiments. During year 2002 the analysis of the data collected with CeF_3 has been carried out and preliminary data have been collected by using a BaF_2 scintillator.

Moreover, new results have been obtained and published on the investigation of the ordinary highly forbidden β decay, of the $\beta\beta0\nu(0^+ \rightarrow 2^+)$ decay and of the $\beta\beta2\nu(0^+ \rightarrow 2^+)$ in ^{48}Ca by means of the $\beta-\gamma$ coincidence technique using CaF_2(Eu) and NaI(Tl) detectors. Fig. 17 shows that this technique can be effectively employed to study ^{48}Ca decays. In fact, for example, after a ^{48}Ca β decay, γ of 131 keV is expected by the excited nuclear level of ^{48}Sc and, subsequently, γ's of 984, 1037 and 1312 keV are emitted when the daughter ^{48}Sc decays to excited nuclear levels of ^{48}Ti.

Data have been collected deep underground with a 1.11 kg CaF_2(Eu) detector partially surrounded by low background NaI(Tl) detectors The used experimental set-up (see Fig. 18) has been installed inside the low radioactive Cu box of the R&D set-up, which is maintained in high purity Nitrogen atmosphere in slightly overpressure with respect to external environment. The surrounding passive shield was made by 10 cm of low radioactive Cu, 15 cm of low radioactive Pb, Cadmium foils and about 10 cm of polyethylene/paraffin. The shield is enclosed in a plexiglas box also maintained in HP

[4] On the other hand, similar theoretical estimates suffer of the large uncertainties typically associated to the calculations of the nuclear matrix elements.

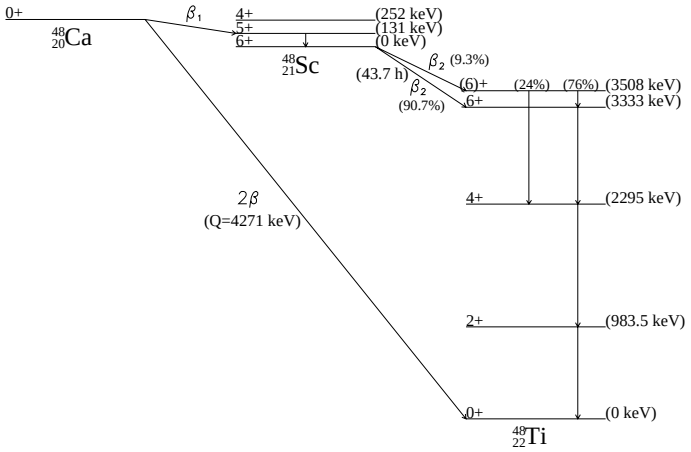

Figure 17: Single and double β decay of ^{48}Ca.

Nitrogen atmosphere. Three CaF_2(Eu) scintillators (3" diameter by 1" length each one)

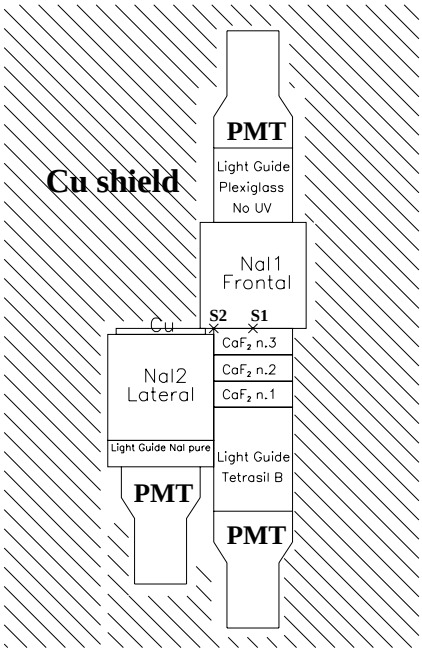

Figure 18: Schema of the detectors' assembling inside the inner Cu box.

have been glued all together by selected optical grease in order to form a single detector, named $3C$. The latter is coupled to a low background EMI9265-B53/FL PMT through a 3" diameter 10 cm long Tetrasil-B light guide. Both the $3C$ detector and the light guide have been wrapped in teflon tape ($\simeq$ 0.5 mm). The considered assembling allows to reduce the number of used PMTs (and related background contribution) and to use two $\simeq$ 4 kg NaI(Tl) as coincidence detectors. The light absorption in the $3C$ detector remains at an acceptable level as verified by devoted calibrations (see the paper for discussion).

5.1 The search for ^{48}Ca single β decay

An ordinary β decay of $^{48}\mathrm{Ca}(0^+) \rightarrow {}^{48}\mathrm{Sc}(6^+,5^+,4^+)$ is possible. The calculated half-life of the most probable transition $^{48}\mathrm{Ca}(0^+) \rightarrow {}^{48}\mathrm{Sc}(5^+)$ ($Q = 281$ keV [33]) is $T_{1/2} = 7.6\times10^{20}$ y [34] and $1.1^{+0.8}_{-0.6}\times10^{21}$ y [35], while the best available experimental limit is $T_{1/2}(^{48}\mathrm{Ca},\beta) > 6.0\times10^{18}$ y (95% C.L.) [36].

Here such a process has been investigated by searching in the experimental data for the β decay of the daughter nuclei $^{48}\mathrm{Sc} \rightarrow {}^{48}\mathrm{Ti}$ with $T_{1/2} = 43.7$ h. With large probability (90.7%) the decay goes to the excited 6^+ level of ^{48}Ti with excitation energy 3333 keV. In this case the emitted electron has energy up to 657 keV, and three γ quanta are emitted as well with energies 1037, 1312 and 984 keV [33]. In the remaining 9.3% of the cases the daughter nucleus ^{48}Sc decays to ^{48}Ti level with energy 3508 keV (electron energy up to 482 keV); the subsequent emitted γ's are depicted in Fig. 17. Thus, the coincidence technique can be used to determine the half life of the β decay of ^{48}Ca since the ^{48}Ca – ^{48}Sc chain is in equilibrium.

The energy distributions expected for the considered processes have been calculated by MonteCarlo method using the EGS4 code [24] and accounting for the physical parameters of the experimental set-up. In this way the related efficiencies in the considered energy windows can be determined. The coincidence data collected during 3235.72 h have been

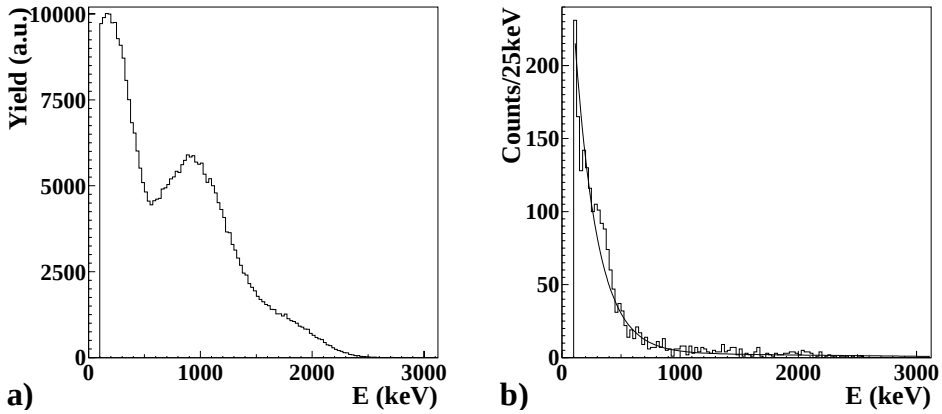

Figure 19: a) Behaviour of the energy distribution expected for the signal in the 3C detector due to single β decay of ^{48}Ca in the case: one γ in NaI-1 in the (945 – 1078) keV energy window and a signal with energy greater than 100 keV in $3C$. Here the energy deposited is the sum of the β energy and of the energy released by either 0 or 1 or 2 de-excitation γ's. b) Experimental energy distribution measured by the $3C$ detector in the same case (superimposed the fit; see the paper).

analysed by investigating all the possible coincidence triggers. The more stringent results have been obtained for the detection channels which require a signal with energy greater than 100 keV in $3C$ and, respectively: a) one γ in NaI-1 in the (945 – 1078) keV energy window; b) one γ in NaI-1 in the (1263 – 1361) keV energy window; c) one γ in NaI-2 in the (937 – 1087) keV energy window; d) one γ in NaI-2 in the (1251 – 1373) keV energy window. As an example, for the trigger condition a), the expected behaviour of the signal energy distribution in the $3C$ detector is shown in Fig. 19 together with the

energy distribution measured by $3C$ deep underground. In Fig. 19a) the energy deposited in the 3C detector is the sum of the β energy and of the energy released by either 0 or 1 or 2 de-excitation γ's.

Following a widely used procedure, the behaviour of the background in the experimental energy distribution has been fitted in the considered energy interval for each case of interest by an empirical formula (see paper for details). The results obtained for the four considered coincidence channels have been given and the cumulative result, obtained by considering the weighted mean of the N_d of each considered coincidence channel, gives $T_{1/2} > 2.4 \times 10^{18}$ y at 90% C.L. for the highly forbidden β decay of ^{48}Ca. This limit is roughly of the same order of magnitude than the best available limit, supporting that competitive results can be achieved by covering the whole solid angle with coincidence detector(s), by achieving a larger exposure and by obtaining further reduction of the U/Th residual contaminations.

5.2 Investigation of $\beta\beta$ decays in ^{48}Ca

The $\beta\beta0\nu(0^+ \rightarrow 2^+)$ decay process has been searched for by investigating $\beta - \gamma$ coincidences (E_γ = 984 keV). The various possibilities for coincidences in the used set-up have been exploited. The more stringent result for this $\beta\beta0\nu(0^+ \rightarrow 2^+)$ decay has been obtained by considering the double coincidence channel given by the photon in the NaI-1 detector (considering an energy window $\pm2\sigma$ around the 984 keV full energy peak) and the two β's with total energy above 2600 keV (efficiency equal to 0.031) in the 3C detector. The behaviour of the energy distribution in the considered energy window expected in the $3C$ detector for the $\beta\beta0\nu(0^+ \rightarrow 2^+)$ signal giving these $\beta-\gamma$ coincidences has been calculated by the MonteCarlo method using the EGS4 code [24] and accounting for the physical parameters of the experimental set-up; it is shown in Fig. 20.

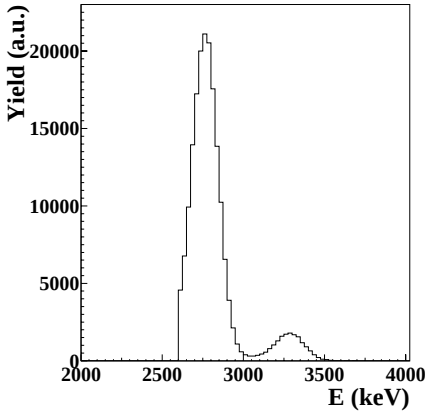

Figure 20: Behaviour of the energy distribution expected in the $3C$ detector for the $\beta\beta0\nu(0^+ \rightarrow 2^+)$ signal considering the $\beta-\gamma$ double coincidence given by the de-excitation photon in the NaI-1 detector (energy window $\pm2\sigma$ around the 984 keV full energy peak) and the two β's with total energy above 2600 keV in the 3C detector. The two peaks are due to the different response of the three CaF_2(Eu) detectors (see the paper for details); in particular, the highest energy one is due to decay processes occurred in the first CaF_2(Eu) detector and is depressed with the respect to the other one because of the geometry.

Zero events have been found satisfying the requirements. This gives an upper limit on the number of events, which could be ascribed to the process equal to 2.3 events at 90% C.L. [37] and, consequently, the limit (90% C.L.) $T_{1/2} > 5.5 \times 10^{19}$ y. We note that this limit is lower than the one quoted in ref. [38].

As regards the $\beta\beta2\nu$ (0^+ - 2^+), it has been investigated by searching for β-γ coincidences (E_γ=984 keV). Two cases have been considered in the analysis requiring a signal with energy greater than 100 keV in $3C$ and : a) the γ in NaI-1 within the energy window: (945–1023) keV (1 σ); b) the γ in NaI-2 within the energy window: (937–1031) keV (1 σ). In particular, Fig. 21 shows the expected behaviour of the signal energy distribution in the $3C$ detector for the case a) and the experimental energy spectrum under the same a) requirements. In both cases the same procedure described in the previous section has

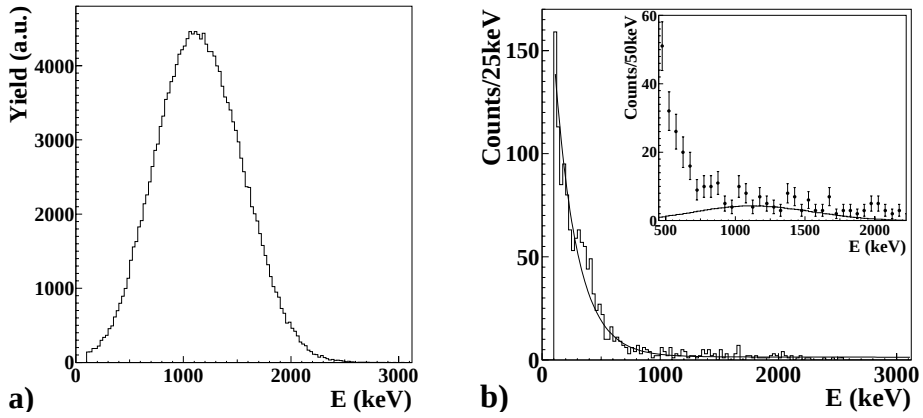

Figure 21: a) Behaviour of the energy distribution expected in the $3C$ detector for the $\beta\beta2\nu(0^+ \rightarrow 2^+)$ signal in the case: one γ in NaI-1 in the (945 – 1023) keV energy window and a signal with energy greater than 100 keV in $3C$; b) experimental energy distribution measured by the $3C$ detector for the same case (superimposed the fit). In the inset the experimental data points are compared with the expectation for the considered decay process when $T_{1/2}$ would be equal to the found 90% C.L. limit (see text).

been followed. The cumulative result, obtained by considering the weighted mean of the N_d of each considered coincidence channel, gives $T_{1/2} > 1.2 \times 10^{18}$ y at 90% C.L. for the $\beta\beta2\nu$ (0^+ - 2^+) decay of ^{48}Ca. This is the first experimental limit for this process.

For the sake of completeness, we note that the background events in the (900 – 1700) keV energy region (where most of the signal is expected) of Fig. 21b) can be mainly ascribed to double coincidences from the standard contaminant ^{208}Tl (e.g. – in the $\simeq$ 44% of the cases – 583 keV and 2614 keV γ's); this is credited by the whole coincidence bidimensional spectrum. Other contributions can arise from the tails of coincidences induced e.g. by ^{214}Bi (mainly 609 – 1120 keV γ's) and ^{40}K (through Compton scatterings).

The considerations, given at end of the previous subsection, hold also for the investigation of these $\beta\beta$ decay modes.

6 The low background DAMA Ge

Various R&D developments to improve low background set-ups and scintillators as well as new developments for higher radiopure PMTs are carried out. The related measurements on samples are regularly performed by means of the DAMA low background Ge detector[5], which is operative deep underground in the low background facility of the Gran Sasso Laboratory since many years.

7 Conclusions

The $\simeq$ 100 kg NaI(Tl) set-up has concluded its data taking in July 2002. Then, the installation of the new LIBRA set-up is started and almost completed in the same year. The effect of consistent halo models in the results already released on the annual modulation signature for WIMPs has been investigated and a preliminary search for Q-balls has been carried out. Furthermore, the analysis of the data of the 5^{th}, 6^{th} and 7^{th} annual cycles has been carried out and results will be released in 2003.

The LXe set-up has runned for part of the year 2002 filled with Xenon enriched in ^{136}Xe; then, works to introduce a new water refrigeration system for the compressor have been started. New results on $\beta\beta$ decay modes in ^{134}Xe and ^{136}Xe have been obtained.

As regards the R&D set-up, the data collected with 1.1 kg of CaF_2(Eu) have been published. Moreover, work has been done on the data collected with CeF_3 detector (as it will be described in the annual report 2003) and preliminary data have been taken with a BaF_2 scintillator.

The idea of using anisotropic scintillators, originally suggested by P. Belli et al. in ref. [39] has also been revisited (see publication list in 2002).

The low background Ge detector is continuing the measurements on samples' materials.

Further data analyses to investigate various rare processes are in progress.

8 List of Publications during 2002

1. R. Bernabei, P. Belli, A. Bussolotti, F. Cappella, R. Cerulli, C.J. Dai, A. Incicchitti, A. Mattei, F. Montecchia, D. Prosperi, The liquid Xenon set-up of the DAMA experiment, Nucl. Instr. & Meth. A482 (2002), 728.

2. R. Bernabei, M. Amato, P. Belli, F. Cappella, R. Cerulli, C.J. Dai, H.H. He, G. Ignesti, A. Incicchitti, H.H. Kuang, J.M. Ma, F. Montecchia, F. Nozzoli, D. Prosperi, Results with the DAMA/NaI(Tl) experiment at LNGS, Nucl. Phys. B(Proc. Supp.) 110 (2002), 61.

3. R. Bernabei, P. Belli, F. Cappella, R. Cerulli, C.J. Dai, A. Incicchitti, F. Montecchia, D. Prosperi, Results with the DAMA/LXe experiment at LNGS, Nucl. Phys. B(Proc. Supp.) 110 (2002), 88.

[5]This detector was specially realized with a low Z window.

4. R. Bernabei, M. Amato, P. Belli, F. Cappella, R. Cerulli, C.J. Dai, H.H. He, G. Ignesti, A. Incicchitti, H.H. Kuang, J.M. Ma, F. Montecchia, F. Nozzoli, D. Prosperi, Results with the DAMA experiment at LNGS , Nucl. Phys. B(Proc. Supp.) 1098 (2002), 329.

5. R. Bernabei, P. Belli, R. Cerulli, F. Montecchia, M. Amato, A. Incicchitti, D. Prosperi, C.J. Dai, H.L. He, H.H. Kuang, J.M. Ma, Investigating the DAMA annual modulation data in the framework of inelastic Dark Matter, Eur. Phys. J. C23 (2002), 61.

6. R. Bernabei, Dark Matter search, Prog. Part. Nucl. Phys. 48 (2002), 263.

7. R. Bernabei, P. Belli, F. Cappella, R. Cerulli, F. Montecchia, A. Incicchitti, D. Prosperi, C.J. Dai, Search for neutrinoless $\beta\beta$ decay in ^{134}Xe at Gran Sasso, Phys. Lett. B527 (2002), 182.

8. R. Bernabei, P. Belli, F. Cappella, R. Cerulli, F. Montecchia, F. Nozzoli, A. Incicchitti, D. Prosperi, C.J. Dai, V. I. Tretyak, Yu. G. Zdesenko, O.A. Ponkratenko, Search for β and $\beta\beta$ decays in ^{48}Ca, Nucl. Phys. A705 (2002), 29

9. R. Bernabei, M. Amato, P. Belli, F. Cappella, R. Cerulli, C.J. Dai, H.L. He, G. Ignesti, A. Incicchitti, H. H. Kuang, J. M. Ma, F. Montecchia, F. Nozzoli, D. Prosperi, WIMP search by DAMA at Gran Sasso, astro-ph/0205047 to appear in the Proc. of "Dark2002" Cape Town, South Africa, Feb. 2002.

10. R. Bernabei, M. Amato, P. Belli, F. Cappella, R. Cerulli, C.J. Dai, H.L. He, G. Ignesti, A. Incicchitti, H. H. Kuang, J. M. Ma, F. Montecchia, F. Nozzoli, D. Prosperi, DAMA status report and perspectives for the new LIBRA set-up, to appear on the Proceed. of Vulcano2002, Vulcano, Italy.

11. F. Cappella, R. Cerulli, A. Incicchitti, A preliminary search for Q-balls by delayed coincidences in NaI(Tl), Eur. Phys. J.-direct C14 (2002), 1.

12. P. Belli, R. Cerulli, N. Fornengo, S. Scopel, Effect of the galactic halo modeling on the DAMA/NaI annual modulation result: an extended analysis of the data for WIMPs with a purely spin-independent coupling, Phys. Rev. D66 (2002), 043503.

13. R. Bernabei, M.Amato, P. Belli, F. Cappella, R. Cerulli, C.J. Dai, G. Ignesti, A. Incicchitti, H. H. Kuang, J. M. Ma, F. Montecchia, F. Nozzoli, Z.P. Ye, D. Prosperi, Searching for the Dark Universe by the DAMA experiment, ROM2F/2002/26 to appear on the Proceed. of the Conf. "Beyond the Desert 02", Oulu, Finland.

14. R. Bernabei, M. Amato, P. Belli, F. Cappella, R. Cerulli, C.J. Dai, H.L. He, G. Ignesti, A. Incicchitti, H. H. Kuang, J. M. Ma, F. Montecchia, F. Nozzoli, D. Prosperi, DAMA results and status report, to appear on the Proceed. of IDM2002, York, UK.

15. R. Bernabei, M. Amato, P. Belli, F. Cappella, R. Cerulli, C.J. Dai, G. Ignesti, A. Incicchitti, H. H. Kuang, J. M. Ma, F. Montecchia, F. Nozzoli, Z.P. Ye, D. Prosperi, Searching for the Dark Universe by the DAMA experiment, to appear on the Proceed. of NPDC-17, Debrecen, Hungary.

16. R. Bernabei, P. Belli, F. Cappella, R. Cerulli, F. Montecchia, A. Incicchitti, D. Prosperi, C.J. Dai, Investigation of $\beta\beta$ decay modes in ^{134}Xe and ^{136}Xe, Phys. Lett. B546 (2002), 23.

17. R. Bernabei, P. Belli, F. Nozzoli, A. Incicchitti, Anisotropic scintillators for WIMP direct detection: revisited, ROM2F/2002/34, submitted for publication.

References

[1] P. Belli et al., Il N. Cim. C19 (1996), 537.

[2] R. Bernabei et al., Phys. Lett. B387 (1996), 222; Phys. Lett. B389 (1996), 783.

[3] R. Bernabei et al., Phys. Lett. B436 (1998), 379.

[4] R. Bernabei et al., New J. of Phys. 2 (2000), 15.1.

[5] R. Bernabei et al., Phys. Lett. B389, (1996), 757.

[6] R. Bernabei et al., Phys. Lett. B424, (1998), 195.

[7] R.Bernabei et al., Il N. Cim. A112 (1999), 545.

[8] R. Bernabei et al., Phys. Lett. B450 (1999), 448.

[9] R. Bernabei et al., Il N. Cim. A112 (1999), 1541.

[10] P. Belli et al., Phys. Rev. D61 (2000), 023512.

[11] R. Bernabei et al., Phys. Lett. B480 (2000), 23.

[12] R. Bernabei et al., Eur. Phys. J. C18 (2000), 283.

[13] R. Bernabei et al., Phys. Lett. B509 (2001), 197.

[14] R. Bernabei et al., Phys. Lett. B515 (2001), 6.

[15] R. Bernabei et al., Eur. Phys. J.-direct **C11** (2001), 1.

[16] R. Bernabei et al.,INFN/AE-01/19 to appear in the volume XENON-01.

[17] R. Bernabei et al., Eur. Phys. J. C23 (2002) 61.

[18] R. Bernabei et al., Astrop. Phys. 7 (1997), 73.

[19] P. Belli et al., Nucl. Phys. B563 (1999), 97.

[20] R. Bernabei et al., Astrop. Phys. 4 (1995), 45; R. Bernabei,"Competitiveness of a very low radioactive ton scintillator for particle Dark Matter search", in the volume *The identification of Dark Matter*, World Sc. pub. (1997), 574; I. R. Barabanov et al., Astrop. Phys. 8 (1997), 67; I. R. Barabanov et al., Nucl. Phys. B546 (1999), 19. I. R. Barabanov et al., New Journal of Physics **3** (2001), 5.1.

[21] P. Belli et al., Astrop. Phys. 5 (1996), 217; R. Bernabei et al., Il N. Cim. A110 (1997), 189; R. Bernabei et al., Phys. Lett. B408 (1997), 439; R. Bernabei et al., Il N. Cim. A111, 347 (1998) & Il N. Cim. A, oct. 1998; P. Belli et al., Astrop. Phys. 10 (1999), 115; P. Belli et al., Phys. Rev. C60 (1999), 065501; P. Belli et al., Phys. Lett. B460 (1999), 236; P. Belli et al., Phys. Lett. B465 (1999), 315; R. Bernabei et al., Phys. Rev. Lett. 83 (1999), 4918; P. Belli et al., Phys. Rev. D61 (2000), 117301; R. Bernabei et al., Phys. Lett. B493 (2000), 12.

[22] A. Kusenko et al., Phys. Rev. Lett. 80 (1998) 3185; S. Coleman, Nucl. Phys. B262 (1985) 263; A. Kusenko, Phys. Lett. B404 (1997) 285; A. Kusenko, Phys. Lett. B405 (1997) 108; A. Kusenko, Phys. Lett. B406 (1997) 26; G. Dvali et al., Phys. Lett. B417 (1998) 99; A. Kusenko et al., Phys. Lett. B418 (1998) 46.

[23] R. Bernabei et al., Phys. Rev. Lett. 83 (1999) 4918.

[24] W. R. Nelson et al., SLAC-265, UC-32 (E/I/A).

[25] F. Cappella, Thesis, Univ. Roma "Tor Vergata" A.A. 2000/2001.

[26] F. Simkovic, P. Domin, A. Faessler, hep-ph/0204278.

[27] J. Suhonen et al., Nucl. Phys. A535 (1991) 91.

[28] J. Engel et al., Phys. Rev. C37 (1988) 731.

[29] T. Tomoda, Rep. Prog. Phys. 54 (1991) 53.

[30] K. Muto, E. Bender and H. V. Klapdor, Z. Phys. A334 (1989b) 187.

[31] A. Staudt, K. Muto and H. V. Klapdor, Europhys. Lett. 13 (1990) 31.

[32] E. Caurier et al., Nucl. Phys. A654 (1999) 973.

[33] Table of Isotopes, ed. by C.M. Lederer and V.S. Shirley, VII ed. , John Wiley, NY, 1978.

[34] E. K. Warburton, Phys. Rev. C 31 (1985) 1896.

[35] M. Aunola et al., Europhys. Lett. 46 (1999) 577.

[36] D. E. Alburger and J. B. Cumming, Phys. Rev. C 32 (1985) 1358.

[37] K. Hikasa et al., *Particle Data Group*, Phys. Rev. D 45 (1992).

[38] R. K. Bardin et al., Nucl. Phys. A 158 (1970) 337; A. S. Barabash, Phys. Lett. B 216 (1989) 257.

[39] P. Belli et al., Nuovo Cim. C15 (1992) 475.

GENIUS-TF. Test Facility for the GENIUS Project

H.V. Klapdor-Kleingrothaus*[a], T. Kihm[a], A. Dietz[a], C. Dörr[a], I.V. Krivosheina[a,b], D. Mazza[a], H. Strecker[a], C. Tomei[a,c], V. Bednyakov[d], V. Bobrakov[d]

[a] Max-Planck Institut für Kernphysik, Heidelberg, Germany
[b] Institute of Radiophysical Research, Nishnij Novgorod, Russia
[c] University of L'Aquila, Italy
[d] JINR, Dubna, Russia
* Spokesman of the Collaboration; E-mail: klapdor@gustav.mpi-hd.mpg, Home-page: http://www.mpi-hd.mpg.de.non_acc/

1 Introduction

GENIUS-TF is a test-facility for the GENIUS project [1, 2], which has been proposed aiming at a dramatic increase of the sensitivity in the field of dark matter and double beta decay search.

GENIUS suggests to operate conventional High-Purity Germanium (HPGe) detectors directly in liquid nitrogen. This has the advantage that the background can be lowered by three or four orders of magnitude with respect to the same detectors operated in the usual way (e.g. the HEIDELBERG-MOSCOW experiment), essentially by removing most of the material in the vicinity of the detectors.

The GENIUS experiment would have the potential to look for Dark Matter, covering the major part of the MSSM parameter space predicted for neutralinos as cold dark matter candidates (also by looking for the annual modulation effect).

The sensitivity of GENIUS for searching the neutrinoless double-beta decay of ^{76}Ge would reach the level of 0.01 eV mass range. Moreover, by using 100 kg of enriched ^{76}Ge GENIUS would allow to confirm the present indication for neutrinoless double beta decay (see [3]) with a confidence level of 7 sigma after 3 years of measurement.

It was suggested by the Scientific Committee of LNGS to build up a smaller test facility (GENIUS-TF) before realizing the final large setup. This would allow to test important prerequisites for the realization of the GENIUS experiment, such as:

1. long term stability of the detectors in liquid nitrogen,

2. stability of the low energy spectrum to mechanical vibrations (microphonic noise),

3. implementation of the detector holder system

4. data acquisition system.

The GENIUS Test Facility which is described, also with its physics potential, in [4] is under construction since summer of 2001 between hall A and B at LNGS. The final version foreseen for the test facility consists of 40 kg of natural Ge detectors in a box of liquid nitrogen.

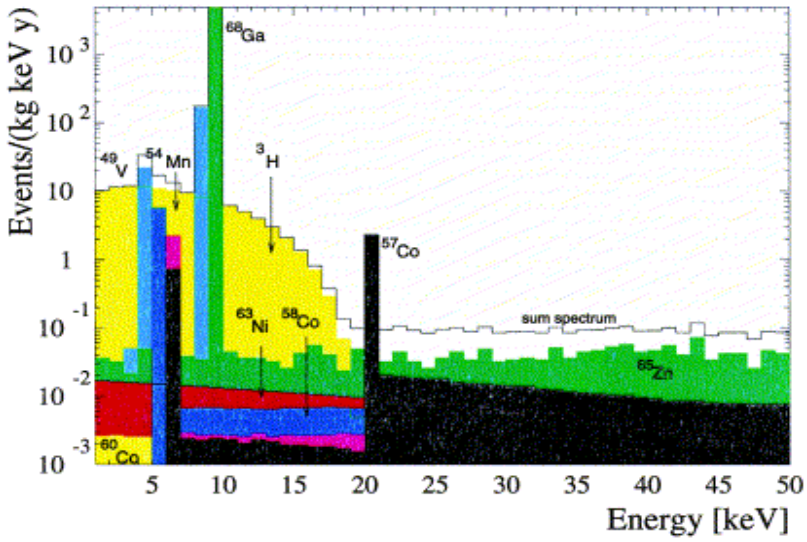

Figure 1: Background originating from cosmic activation of the Ge-crystals at sea level with 10 days exposure and 1 y deactivation below ground. Below 11 keV the X-rays from the decays of the various isotopes and the decay of ^3H will be dominating the overall sum spectrum of the experiment (from [4]).

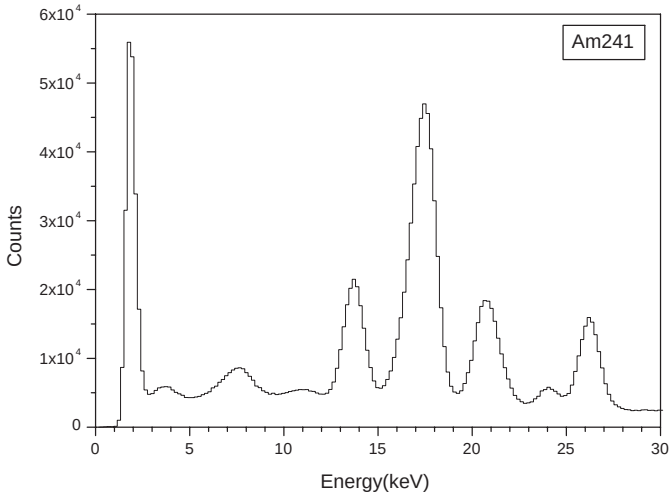

Figure 2: Low-energy part of the spectrum measured with an ^{241}Am source.

During 2001 and 2002 6 detectors of 2.5 kg each and with an extremely low energy threshold of ∼500 eV have been produced. Four of them have been brought to Gran Sasso meanwhile.

Fig. 1. shows the result of the simulation of the expected background from cosmic activation of the Ge crystals. For ^3H an upper limit is given.

The setup will start operation in early 2003 with 4 detectors (about 10 kg of Ge) and a new digital data acquisition system which has been developed during 2002 [5] especially for GENIUS-TF and GENIUS. The new system allows to perform digitally all essential data processing functions, including precise energy measurements over a range of a few keV to 3 MeV, rise time analysis, ballistic deficit correction and pulse shape analysis.

Fig. 2 shows a spectrum measured with an ^{241}Am source and demonstrates the low threshold reached with a test Ge detector, and the very good energy resolution.

With 40 kg of natural Ge and a background of 2-4 events/(kg yr keV) in the energy region below 50 keV, GENIUS-TF can cover the evidence region in the MSSM parameter space for neutralinos as dark matter candidates singled out by the DAMA experiment [6]. It would deliver an independent test by using a different technology and raw data without background subtraction.

2 Acknowledgment

The authors acknowledge the support by the BOREXINO group and by G. Heusser with the liquid nitrogen purification system for GENIUS-TF.

3 List of Proceedings (2002)

1. H.V. Klapdor-Kleingrothaus and R. Viollier (eds.), Dark Matter in Astro- and Particle Physics., Proc. of DARK2002, Cape Town, South Africa, February 4 - 9, 2002, Heidelberg, Germany: Springer (2002) 663 pp.

2. H.V. Klapdor-Kleingrothaus (ed.) Physics Beyond the Standard Model: Beyond the Desert 02, Proc. of Intern. Conf. BEYOND'02, Oulu, Finland, 2-7 Jun 2002, IOP, Bristol, 2003 (in preparation).

4 List of Publications (2002)

1. H.V. Klapdor-Kleingrothaus, Nucl. Instrum. Meth. A 481 (2002) 149-159.

2. H.V. Klapdor-Kleingrothaus, Int. J. Mod. Phys. A 17 (2002) 3421-3431.

3. H.V. Klapdor-Kleingrothaus, Nucl. Phys. Proc. Suppl. 110 (2002) 58-60, and e-Print Archive: hep-ph/0206250.

4. V.A. Bednyakov, H.V. Klapdor-Kleingrothaus, V. Gronewold, Phys. Rev. D 66 (2002) 115005, and e-Print Archive: hep-ph/0208178.

5. H.V. Klapdor-Kleingrothaus et al. Astropart. Phys. 17 (2002) 383-391.

6. V.A. Bednyakov, H.V. Klapdor-Kleingrothaus, E. Zaiti, Phys. Rev. D 66 (2002) 015010, and e-Print Archive: hep-ph/0203108.

7. H. V. Klapdor-Kleingrothaus et al., Astroparticle Physics, Volume 18, Issue 5, February 2003, Pages 525-530.

5 List of Conference (2002)

1. H.V. Klapdor-Kleingrothaus and I. Krivosheina, in Proc. of DARK2002, Cape Town, South Africa, February 4 - 9, 2002, Springer, Heidelberg (2002), 473-484.

2. V.A. Bednyakov, H.V. Klapdor-Kleingrothaus, E. Zaiti, Deutsche Physikalische Gesellschaft e. V. (DPG), 18. - 22. März 2002, Leipzig, GERMANY.

3. C. Tomei, H.V. Klapdor-Kleingrothaus, A. Dietz, Ch. Dörr, I. Krivosheina, D. Mazza and H. Strecker, Deutsche Physikalische Gesellschaft e. V. (DPG), 18. - 22. März 2002, Leipzig, GERMANY.

4. H.V. Klapdor-Kleingrothaus and I. Krivosheina, Zacatecas Forum in Physics 2002, 11-13 MAY, 2002 Zacatecas, Mexico.

5. V.A. Bednyakov and H.V. Klapdor-Kleingrothaus, in Proc. of Intern. Conf. on Physics Beyond the Standard Model: Beyond the Desert 02, BEYOND'02, Oulu, Finland, 2-7 Jun 2002, IOP, Bristol, 2003, ed. H.V. Klapdor-Kleingrothaus.

6. H.V. Klapdor-Kleingrothaus and I. Krivosheina, in Proc. of Intern. Conf. on Physics Beyond the Standard Model: Beyond the Desert 02, BEYOND'02, Oulu, Finland, 2-7 Jun 2002, IOP, Bristol, 2003, ed. H.V. Klapdor-Kleingrothaus.

7. H.V. Klapdor-Kleingrothaus and C. Tomei, in IIIrd International Workshop on Low Energy Solar Neutrinos, LowNu 2002, 22-24 May, 2002, Heidelberg, Germany.

8. H.V. Klapdor-Kleingrothaus and C. Tomei, in Proc. of IDM2002, York, England, 22-24 Sep. 2002, World Scientific (2003).

9. H.V. Klapdor-Kleingrothaus and I. Krivosheina, in Proc. of IDM2002, York, England, 22-24 Sep. 2002, World Scientific (2003).

10. I. Krivosheina, International School on CP Violation, Baryogenesis and Neutrinos, Prerow, Germany, September 15 - 21, 2002.

11. I. Krivosheina, Meeting of Russian Academy of Science, Nuclear Physics Section, Moscow, ITEP, 3-5 December, 2002.

References

[1] H.V. Klapdor-Kleingrothaus, J. Hellmig and M. Hirsch, *J. Phys.* **G 24**, 483-516 (1998).

[2] H.V. Klapdor-Kleingrothaus, *Int. J. Mod. Phys.* **A 13** (1998) 3953 .

[3] H.V. Klapdor-Kleingrothaus, A. Dietz and I.V. Krivosheina, *Foundations of Physics* **31**, 1181-1223 (2002).

[4] H.V. Klapdor-Kleingrothaus et al., Nucl. Instrum. Meth. A 481 (2002) 149-159.

[5] T. Kihm, H.V. Klapdor-Kleingrothaus, V. Bobrakov, to be publ. (2003).

[6] R. Bernabei et al., Phys. Lett. B 424 (1998) 195; B 450 (1999) 448; B 480 (2000) 23.

GNO. Gallium Neutrino Observatory

M. Altmann[a], M. Balata[b], P. Belli[c], E. Bellotti[d], R. Bernabei[c], E. Burkert[e], C. Cattadori[d], G. Cerichelli[f], R. Cerulli[c], M. Chiarini[e], M. Cribier[g], S. d'Angelo[c], G. Del Re[f], K. Ebert[h], F. von Feilitzsch[a], N. Ferrari[b], W. Hampel[e], E. Henrich[h], G. Heusser[e], F.Kaether[e], J. Kiko[e], T. Kirsten[e], D. Motta[d,e], T. Lachenmaier[a], J. Lanfranchi[a], M. Laubenstein[b], L. Pandola[b], S. Nisi[b], H. Richter[e], M. Weneser[a], L. Zanotti[d]

[a] Physik Department E15, Technische Universität München (TUM), James-Franck Straße, D-85748 Garching b. München, Germany

[b] INFN, Laboratori Nazionali del Gran Sasso (LNGS), S.S. 17/bis Km 18+910, I-67010 L'Aquila - Italy

[c] Dip. di Fisica, Università di Roma "Tor Vergata" and INFN, Sez. Roma II, Via della Ricerca Scientifica, I-00133 Roma - Italy

[d] Dip. di Fisica, Università di Milano "Bicocca", and INFN Sez. Milano, Via Emanueli, I-20126 Milano - Italy

[e] Max-Plank-Institut für Kernphysik (MPIK), P.O.B. 103980, D-69029 Heidelberg - Germany

[f] Dip. di Ingegneria Chimica e Materiali, Università dell'Aquila, Località Monteluco di Roio, L'Aquila - Italy

[g] DAPNIA/Service de Physique de Particules, CE Saclay, F-91191 Gif-sur-Yvette Cedex - France

[h] Institut für Technische Chemie, Forschungszentrum Karlsruhe (FZK), Postfach 3640, D-76021 Karlsruhe, Germany

Abstract

GNO (Gallium Neutrino Observatory) is monitoring the low energy solar neutrino flux with a 30 tons gallium detector at LNGS. During the year 2002, 12 solar runs and 1 blank run have been successfully done; in total 54 solar runs (corresponding to $\approx$ 1578 days of live time) have been accumulated since spring 1998 when GNO started the data taking. The result of the first 43 solar runs is: 65.2 $\pm$ 6.4 (stat.) $\pm$ 3.0 (sys.) SNU. The combined result from both GNO and GALLEX together (108 solar runs) is 70.8$\pm$4.5(stat.)$\pm$3.8(syst.) SNU. The data taking and the various activities performed during 2002 and the R&D in progress are also discussed in this report.

1 Introduction

GNO (Gallium Neutrino Observatory) is the experiment successor of GALLEX; it is devoted to the measurement of the interaction rate of solar neutrinos on gallium with a low energy threshold (233 keV), well below the maximum energy of the so called pp neutrinos.
The aims of GNO can be summarized as follow:

- to refine the measurement of the mean (i.e. mediated over the entire period of data taking) solar neutrino interaction rate on gallium, reducing the systematic and statistical errors to a level of 5% or less;
- to provide a monitor of the low energy neutrinos over a long period (one solar cycle);
- to investigate possible (unexpected) short and long term time variations of the signal.

The efforts of GNO are addressed to collect continously data on the interaction rate and to improve many details of the experimental procedure, in order to lower the systematic errors as much as possible.

In this section we briefly recall the experimental aspects of the GNO detector, and we give an up to date overview of the solar neutrino physics, concentrating in particular on the scientific motivation of the GNO experiment. In section 2 we describe the GNO solar neutrino observations performed in 2002 and the results obtained from data analysis up to December 2001. In section 3 we discuss the experimental activities (besides data taking) performed in 2002. In section 4 we describe the plan of future activities.

1.1 The GNO detector

The gallium solar neutrino experiment at Laboratori Nazionali del Gran Sasso detects solar neutrinos via the reaction $^{71}Ga\,(\nu_e, e\,)^{71}Ge$, which has a threshold of 233 keV. The detector is sensitive mainly to pp-neutrinos (53% of the interaction rate according to the standard solar model [1]), with smaller contributions to the signal from ^{7}Be ν (27%), ^{8}B ν (12%), and CNO ν (8%).

The target consists of 101 tons of a $GaCl_3$ solution in water and HCl, containing 30.3 tons of natural gallium; this amount corresponds to $\sim 10^{29}$ ^{71}Ga nuclei.

The ^{71}Ge atoms produced by solar neutrinos (at a rate of about 0.7 per day, one half of the amount predicted by solar models) are extracted from the gallium tank every 4 weeks [2] and introduced in low-background gas proportional counters [3] as germane gas (GeH_4). The decay of ^{71}Ge (e.c., τ=16.5 days) produces a signal in the counters consisting of a point-like ionization at 10.4 keV, or 1.1 keV. The signal is recorded by fast digitizers to allow background reduction by pulse shape analysis. The solar neutrino interaction rate on ^{71}Ga is deduced from the number of ^{71}Ge atoms observed. For a complete description of the experimental procedure see [4].

The gallium detector was operated between 1991 and 1997 by the GALLEX collaboration: 65 'solar runs' were performed. The solar neutrino capture rate on ^{71}Ga was measured with a global uncertainty of 10 % as: 77.5 $\pm$6.2(stat.)$^{+4.3}_{-4.7}$(syst.) SNU [1] (1σ) [4]. This result has important physical implications both for astrophysics and for particle physics (for discussion see for example [5]).

After maintenance of the chemical plants and renovation of the DAQ and electronics, a new series of measurements was started in April 1998, within the GNO (Gallium Neutrino Observatory) project [6]. The experiment is presently running with 30 tons of gallium.

1.2 The role of GNO in the solar neutrino research

After the pioneering studies of R. Davis with the Homestake chlorine detector, Gallex had a very important role in the so-called *solar neutrino problem*, i.e. the deficit of electron solar neutrinos with respect to the predictions of the Standard Solar Model.

The experimental determination of the solar neutrino energy spectrum is very important both for astrophysics and for particle physics. We have now very precise measurements of the ^{8}B ν flux and its energy spectrum. Data recorded by the water Cerenkov experiment SuperKamiokande [17], based on the neutrino electron scattering, shows that the ^{8}B ν energy spectrum above $\approx$ 6 MeV is what we expect from the beta decay of ^{8}B; also the time dependence of the signal is what is expected from the annual variation of the Earth-Sun distance. However the flux is strongly suppressed (about 1/2) with respect to the Standard Solar Model prediction. The recent results of SNO [18], the heavy water detector able to discriminate the neutral current and the charged current ν interactions on deuterons, demonstrate that the deficit observed by SuperKamiokande is due to a conversion of the electron neutrinos produced in the Sun into neutrinos with a different active flavour. SNO measured the flavour components of the ^{8}B ν flux as [18]:

$\Phi_e(^8B) = (1.8 \pm 0.1) \cdot 10^6$ cm^{-2} s^{-1} (^{8}B ν with electronic flavour);
$\phi_{\mu,\tau}(^8B) = (3.4 \pm 0.6) \cdot 10^6$ cm^{-2} s^{-1} (^{8}B ν with active flavours other than electronic).

The sum agrees very well with the predictions of the Standard Solar Model within the theoretical uncertainties [1].
^{8}B ν are only a very small fraction of the solar neutrino flux; the bulk of solar neutrinos concentrates in the sub-MeV energy region, with the most important contributions from

[1] 1 SNU (Solar Neutrino Unit) = 10^{-36} captures per second and per absorber nucleus

the pp ν and the ^{7}Be ν. Recent results from the long baseline reactor experiment KamLand [19] definitely confirm the oscillation scenario and restrict the allowed parameter region for the oscillations to the LMA region $\sin^2(2\theta) > 0.4$ and $\Delta m^2 > 10^{-5}$ eV^2. Next generation high statistic, real-time experiments able to lower the threshold to cover the pp energy region are still in a R&D phase and are not expected to start observations at least in the next 5 years (for a review see for example [20]).

Gallium experiments are the presently "available instrument" to measure well below 1 MeV. Therefore it is of crucial importance to push their sensitivity to the best: an increased sensitivity on the measured gallium rate combined with a direct precise measurement of the ν capture cross section on Ga, will allow in the next years, once the measurement of the ^{7}Be flux by Borexino will be available, to extract the pp ν flux with an accuracy of the order of 10-15% or better.

2 Solar neutrino observations.

GNO started solar neutrino observations in May 1998: the list of the main parameters of the solar runs performed in 2002 is reported in Table 1. Data for runs performed before 2002 can be found in the LNGS Annual Reports of past years [7, 8, 9, 10] 12 solar runs and 2 blank runs were successfully performed in the year 2002.

At the beginning of January 2003, counting is completed for 50 solar runs; other 4 solar runs and 1 blank are counting (January 2003). Data from the first 43 GNO solar runs (extractions performed from May 1998 until December 2001) have been evaluated and results have been presented at the Neutrino 2002 conference [11]. A total of 198 decaying ^{71}Ge atoms were identified from the 1236 days of exposure in solar runs SR1-SR41. The corresponding ν interaction rate is **65.2±6.4±3.0 SNU** [11]. The combined result for GALLEX and GNO (65+43=108 solar runs, corresponding to 1594+1236=2830 days of live time) is **70.8±4.5(stat.)±3.8(syst) SNU** [11]. Results from the single GNO solar runs are reported in Table 2 and displayed in Figures 1 and 3. It is important to remark that during year 2002 we adopted, after a long validation phase, a new data analysis technique for the pulse shape discrimination. We changed the pulse shape discrimination criteria (already adopted in GALLEX) based on a simple two parameters cut (energy-risetime) and adopted a more sophisticated selection, based on pulse fit followed by a neural network discrimination stage. The whole GNO data set is now analyzed using the new technique, which gives a result fully compatilble with the old method, but with improved signal/background. More details on this new analysis are given in section 3.4.

The measured interaction rate (see table 2) is lower than the rate expected from pp neutrinos only, which, for a large class of solar models, is independent from the details of the models themselves. Therefore, as discussed in section 1, the gallium results strongly support by themselves that the solution of the solar neutrino problem must be found in the ν physics domain.

In figure 2 we show the energy spectrum of all the counts observed in the GNO solar runs SR1-SR43.

In figure 3 we show the distributions of single run results of Gallex and GNO (histograms) superimposed with the expected distributions (dots) coming from a constant ν interaction

Table 1: Summary of GNO runs performed between January 2002 and December 2002. For each extraction the following data are reported: extraction label; DAQ lable (SR=Solar Run, BL=BLank); extraction date, referred to the end of the extraction; exposure time in days; counter type and number used for ^{71}Ge counting (Fe=Iron cathode, Si=Silicon cathode, FC=Iron shaped cathode, SC=Silicon shaped cathode); counting time (status at 20-Jan-2003); chemical yield (tank to counter), measured by non-radioactive Ge carrier.

Extraction label	Type	Date	Exposure (days)	Counter	Counting time (days) (20-Jan-2003)	Chemical yield (%)
EX57	SR43	08-jan-02	26	SC-156	172.5	96.2
EX58	SR44	06-feb-02	28	Fc-126	174.7	98.7
EX59	SR45	06-mar-02	28	SC-151	172.5	96.1
EX60	BL9	07-mar-02	1	FC-174	140.9	93.7
EX61	SR46	10-apr-02	34	SC-136	183.0	94.8
EX62	SR47	08-may-02	28	Si-106	165.6	97.3
EX63	SR48	05-jun-02	28	Fe-112	166.7	95.1
EX64	-	06-jun-02	1	Si-119	165.7	95.0
EX65	SR49	03-jul-02	27	FC-093	166.6	93.8
EX66	SR50	31-jul-02	28	FC-174	167.9	97.8
EX67	SR51	28-aug-02	28	FC-102	145(*)	93.6
EX68	SR52	23-oct-02(+)	56	SC-136	89(*)	97.3
EX69	SR53	20-nov-02	28	Si-106	61(*)	96.4
EX70	BL10	21-nov-02	1	Fe-112	60(*)	96.4
EX71	SR54	18-dec-02	27	SC-150	33(*)	98.3

(*) counters still counting (at 20-jan-2003) (+) the extraction foreseen for september 2002 was cancelled because of infrastructural troubles

Table 2: Measured solar neutrino capture rate (SNU) in the GNO solar runs SR1-SR43. For comparison we give also the results with the Rise time selection previously used. The new absolute efficiencies for counters Si138, Si108, Si139 and Si150 have not been yet taken into account.

Extraction lable	DAQ lable	SNU (NN sel)	SNU (RT sel)
EX003	SR01		$\mathbf{75^{+45}_{-36}}$
EX004	SR02		$\mathbf{51^{+45}_{-34}}$
EX005	SR03(*)		$\mathbf{93^{+62}_{-50}}$
EX006	SR04		$\mathbf{67^{+50}_{-39}}$
EX007	SR05(*)		$\mathbf{0^{+40}_{-34}}$
EX008	SR06		$\mathbf{36^{+49}_{-37}}$
EX009	SR07	$\mathbf{124^{+56}_{-47}}$	115^{+55}_{-46}
EX010	SR08	$\mathbf{0^{+35}_{-28}}$	0^{+46}_{-37}
EX011	SR09	$\mathbf{89^{+50}_{-41}}$	93^{+52}_{-42}
EX013	SR10	$\mathbf{137^{+56}_{-46}}$	129^{+53}_{-43}
EX014	SR11	$\mathbf{75^{+47}_{-35}}$	56^{+41}_{-30}
EX015	SR12	$\mathbf{35^{+67}_{-50}}$	19^{+66}_{-50}
EX016	SR13	$\mathbf{112^{+54}_{-45}}$	91^{+51}_{-41}
EX017	SR14	$\mathbf{121^{+70}_{-56}}$	118^{+70}_{-56}
EX018	SR15	$\mathbf{45^{+38}_{-28}}$	53^{+40}_{-29}
EX019	SR16	$\mathbf{53^{+43}_{-33}}$	47^{+46}_{-36}
EX020	SR17	$\mathbf{38^{+32}_{-24}}$	36^{+32}_{-23}
EX021	SR18	$\mathbf{55^{+45}_{-35}}$	53^{+45}_{-34}
EX022	SR19	$\mathbf{71^{+48}_{-37}}$	69^{+51}_{-39}
GNO-I Combined		$\mathbf{64.5^{+10.1}_{-9.5}}$	$63.7^{+10.1}_{-9.4}$
EX024	SR20	$\mathbf{55^{+43}_{-32}}$	75^{+51}_{-39}
EX025	SR21	$\mathbf{50^{+57}_{-42}}$	28^{+52}_{-33}
EX026	SR22	$\mathbf{0^{+34}_{-23}}$	3^{+36}_{-24}
EX028	SR23	$\mathbf{122^{+52}_{-42}}$	140^{+57}_{-47}
EX029	SR24	$\mathbf{75^{+48}_{-37}}$	84^{+51}_{-39}
EX032	SR25	$\mathbf{61^{+55}_{-43}}$	74^{+58}_{-46}
EX033	SR26	$\mathbf{97^{+48}_{-38}}$	91^{+48}_{-38}
EX034	SR27	$\mathbf{33^{+48}_{-34}}$	47^{+52}_{-40}
EX036	SR28	$\mathbf{62^{+40}_{-29}}$	58^{+41}_{-29}
EX037	SR29	$\mathbf{2^{+45}_{-32}}$	0^{+36}_{-24}
EX038	SR30	$\mathbf{113^{+52}_{-43}}$	112^{+54}_{-44}
EX040	SR31	$\mathbf{115^{+62}_{-50}}$	99^{+60}_{-49}
EX041	SR32	$\mathbf{69^{+40}_{-30}}$	85^{+44}_{-34}
EX042	SR33	$\mathbf{28^{+37}_{-26}}$	50^{+47}_{-36}
EX044	SR34	$\mathbf{160^{+58}_{-51}}$	117^{+63}_{-52}
EX045	SR35	$\mathbf{63^{+39}_{-29}}$	45^{+36}_{-25}
EX046	SR36	$\mathbf{21^{+44}_{-26}}$	57^{+58}_{-41}
EX048	SR37	$\mathbf{83^{+56}_{-43}}$	63^{+57}_{-42}
EX049	SR38	$\mathbf{49^{+49}_{-38}}$	59^{+49}_{-38}
EX050	SR39	$\mathbf{71^{+51}_{-42}}$	46^{+51}_{-41}
EX051	SR40	$\mathbf{9^{+39}_{-28}}$	1^{+31}_{-31}
EX053	SR41	$\mathbf{92^{+47}_{-38}}$	108^{+49}_{-40}
EX054	SR42	$\mathbf{31^{+33}_{-21}}$	27^{+31}_{-20}
EX057	SR43	$\mathbf{111^{+54}_{-43}}$	85^{+52}_{-42}
GNO-II Combined		$\mathbf{65.9^{+8.8}_{-8.3}}$	$65.5^{+8.8}_{-8.4}$
GNO Combined		$\mathbf{65.3^{+6.6}_{-6.3}}$	$64.7^{+6.6}_{-6.3}$

(*) No RT cuts applied

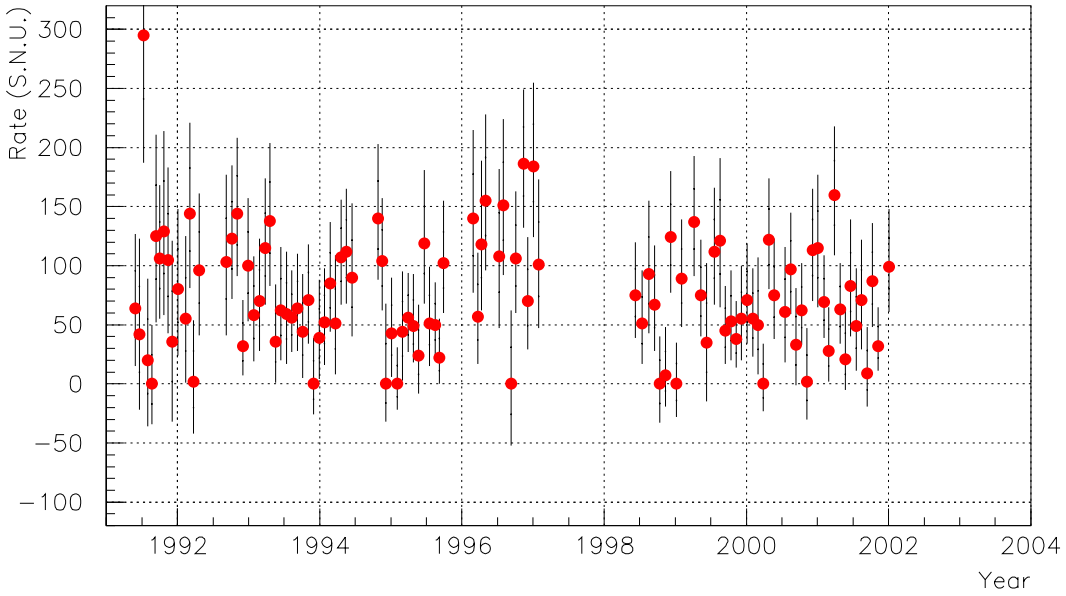

Figure 1: Measured solar neutrino capture rate (atoms/day) in the single 65 GALLEX solar runs, and in GNO solar runs SR1-SR43. A signal of 100 SNU corresponds to a production rate of 0.90 ^{71}Ge atoms per day inside the 30 tons gallium tank.

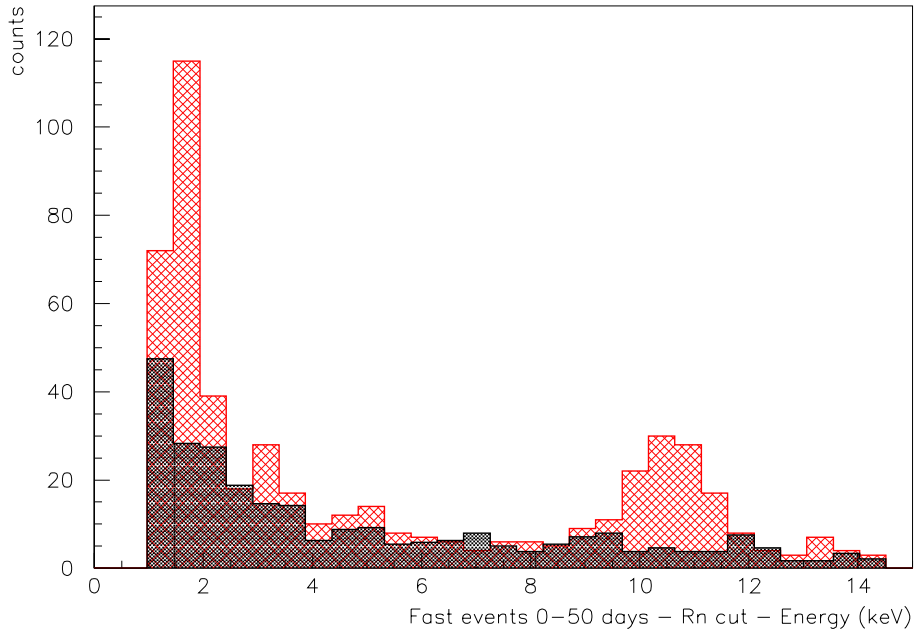

Figure 2: Energy spectrum of "fast" events (i.e. ^{71}Ge candidates). The red hystogram represents all fast counts detected in SR1-SR43 during the the first 2 ^{71}Ge half lives; the black hystogram plots all fast counts detected in the remaining of the counting time (i.e. after 2 ^{71}Ge half lives).

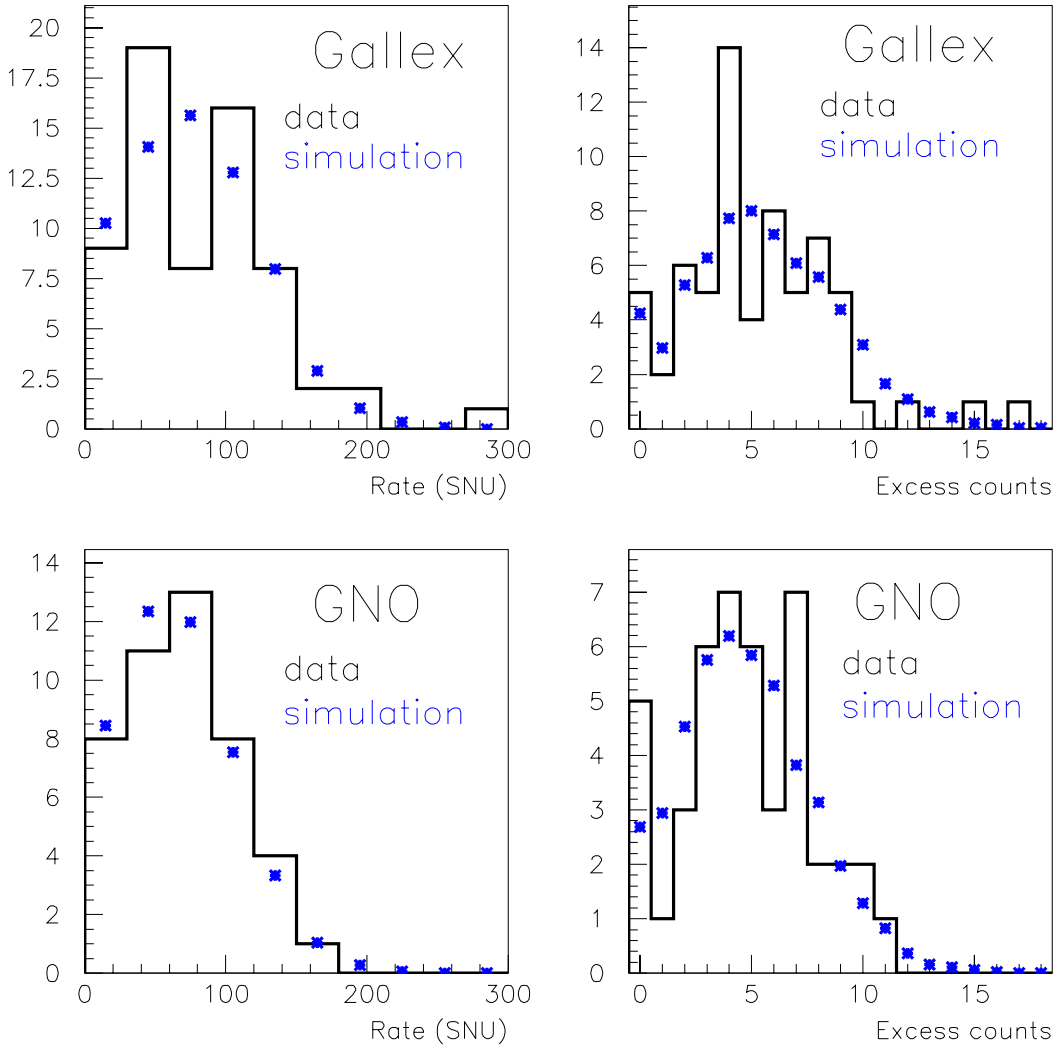

Figure 3: Comparison of the distribution of single run results of GALLEX and GNO (histograms) with the expectations from a constant ν interaction rate (dots). The single run results are expressed both in SNUs (left) and in excess counts (right).

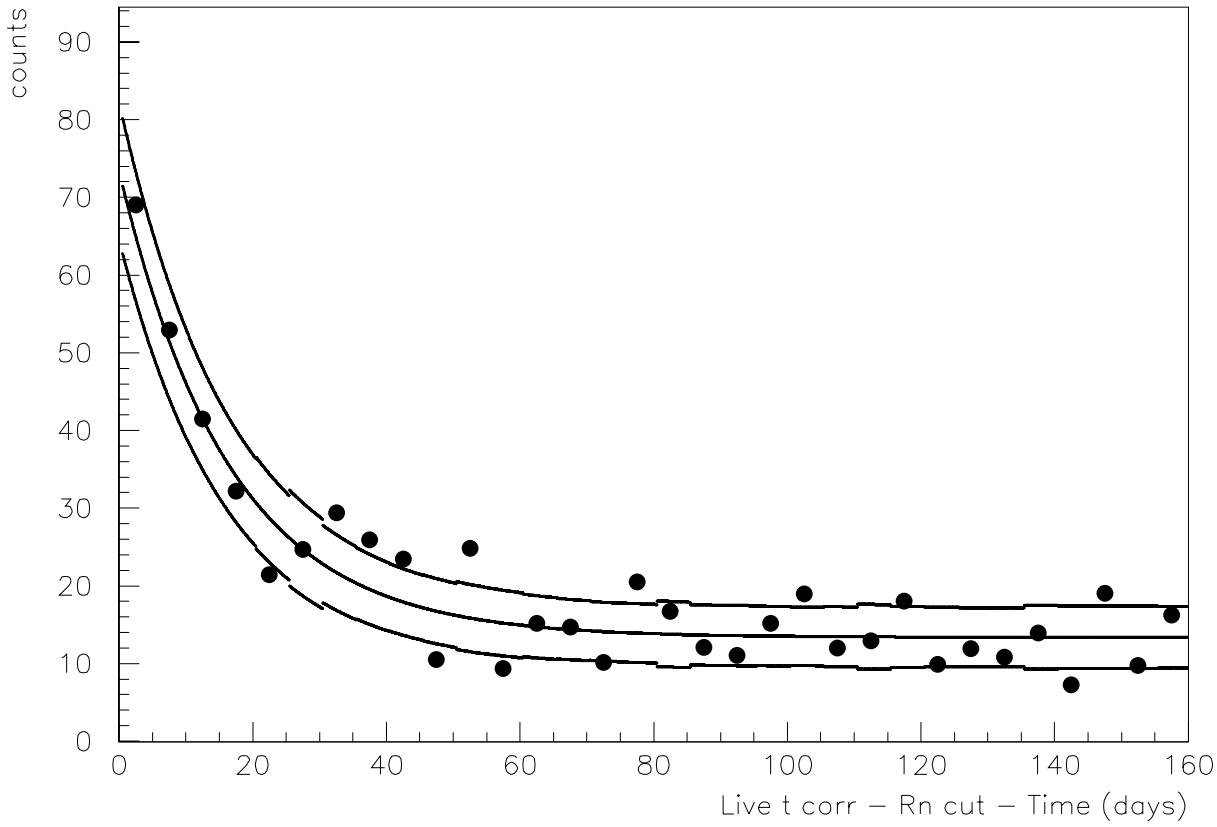

Figure 4: Distribution of candidate ^{71}Ge counts vs. counting time.

rate. These were obtained with a simulation taking into account the exposure times and the selection efficiencies of the actual runs. In the figure 3 the single run results are expressed both in SNUs (left) and in excess counts (right).
Figure 4 shows the time distribution of the candidate ^{71}Ge events obtained from solar runs SR1-SR43. This has been superimposed with the curve obtained from the maximum likelihood fit (assuming a time dependence $f(t) = ae^{-t/\tau} + b$, with τ = life time of ^{71}Ge) and the corresponding $\pm\sigma$ error band.
In Table **??** the envisaged components of the systematic errors both for GALLEX and GNO are summarized and compared. The overall systematic error decreased from 4.5 to 2.7 SNU due to the actions described in sect. 3.

3 Experimental activity during 2002

3.1 Extraction system and synthesis line

During 2002 the following activities were performed at the extraction and synthesis plants:

- preparation and carrying out of 14 extractions, see table 1;
- maintenance of the building safety equipment: building ventilation system, tank leak sensor, HCl leak detector;
- maintenance of gallium tank, absorber plant, auxiliary plants;
- maintenance of the main building, containing the gallium tank: care of the structure, of the electrical plant, water distribution piping, etc.;
- 46 kg of highly pure HCl were added to the 53 m^3 of the gallium solution (about 3 kg of HCl are removed during each run for extracting the ^{71}Ge);
- atomic absorption analysis has been carried out for each run to control the extraction yield;
- in collaboration with the L'Aquila University Chem. Eng. department several tests were performed, to further study the behaviour of the Ge during absorption in the columns and during the acidification.

3.2 Electronics and DAQ

Electronics and DAQ didn't change since the beginning of the experiments. A synthetic bottom-up description of the system follows

- 16 independent line are equipped; one counter is connected to one line. The analog signal from the preamp is splitted and amplified of two different factors and digitized at 0.2 nsec/point during 400 nsec by two independent channels of a 8 bit, 1 GHz transient digitizer (TDF) to have sensitivity both in the 10 keV and in the 1 keV regions (see 6). A reduced bandwidth (20 MHz) output of the fast amplifier is splitted in two and digitized by two slower (400 nsec/point during 800 μs, and 4 nsec/point during 8 μs) to look with proper sensitivity for Bismuth-Polonium events and any events preceeding/following each pulse.
- step like pulses are sent to preamps once each 90 minutes to check for proper functionality, stability and response function of the electronics (see **??**)
- Analog and Digital electronics is placed in a Faraday Cage to avoid background pulses from electromagnetic interferences.
- DAQ is performed by an alpha-server placed outside the Faraday Cage interconnected to the digital (VXI standard) electronics via an Optical GPIB bus. DAQ is always alived and monitored by automatic and manual procedures: the live time over almost 5 years is ca. 97%.

TDF & TDS LOGIC

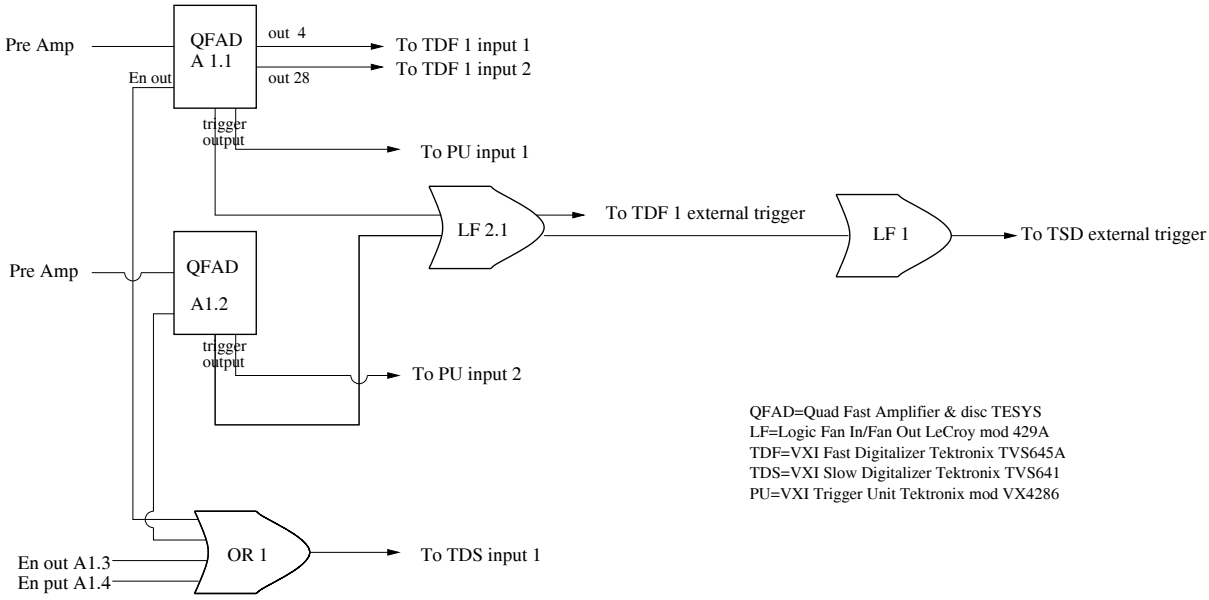

Figure 5: Schematic of the single line electronic chain in GNO.

TEST PULSE LOGIC

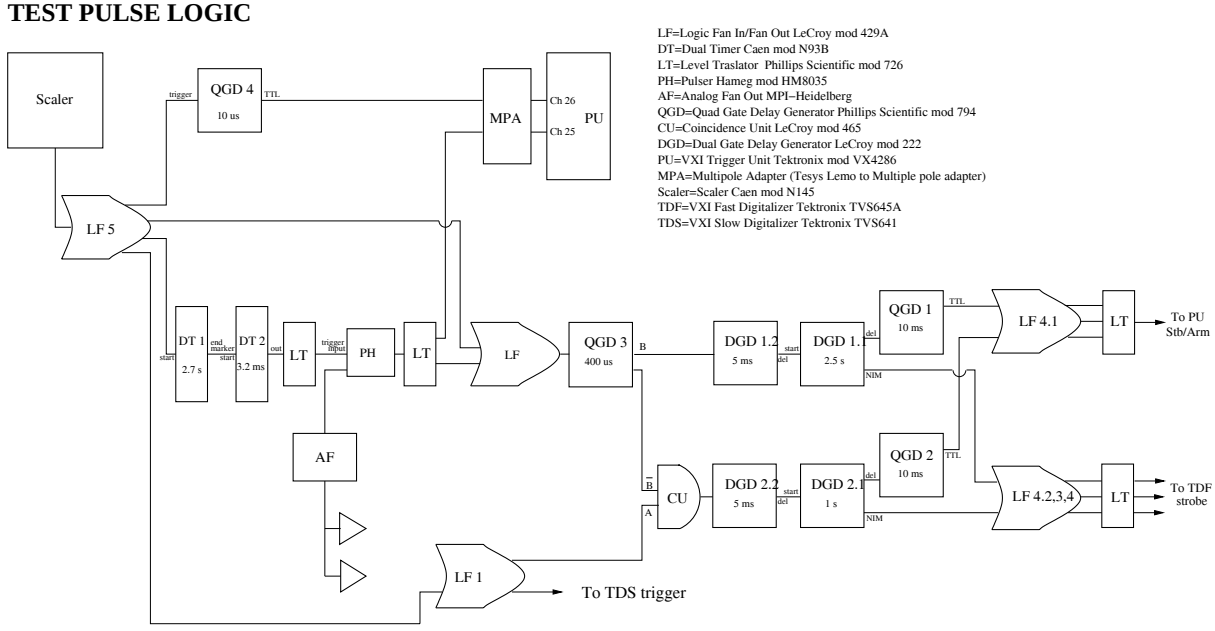

Figure 6: Schematic of the Test Pulses distribution system.

Table 3: Counting efficiencies for absolutely calibrated counters.

Counter	Counting efficiency (%)			GNO		GALLEX		
	new calib.	old calib.	diff.	Solar	Blank	Solar	Blank	Source
Fe43*		76.7±2.1		1	0	4	0	0
FC93	79.9±0.7	80.0±4.0	-0.1	5	1	1	0	1
Fe39$^+$	74.6±1.0	76.4±2.1	-1.8	4	2	5	1	3
FC102	78.9±0.9	81.4±4.0	-2.5	4	1	0	0	1
Si106	74.8±1.0	77.1±4.0	-2.3	5	0	3	3	2
FC174	78.8±0.6	81.7±4.0	-2.9	3	1	0	0	1
Si119*		77.2±2.1		0	1	4	3	3
SC136	80.9±0.7	82.3±4.0	-1.4	6	0	2	2	1
Si138$^+$	79.2±1.0	81.4±4.0	-2.2	4	1	2	3	0
Si108$^+$	75.2±1.0	77.9±4.0	-2.7	4	1	5	3	1
Si139$^+$	80.5±1.0	81.3±2.1	-0.8	5	0	2	2	0
Si150$^+$	78.7±1.0			2	0	0	0	0
SC151$^+$	-	-	-	2	0	0	0	0
FC126$^+$	-	-	-	3	1	0	0	0
Fe103				0	0	3	3	4
Total				46	9	31	22	17

$^+$ Counters calibrated in 2002 with ^{69}Ge; * Counters calibrated in former time with ^{71}Ge.

3.3 ^{71}Ge calibrations

One of the most important goals for GNO is to substantially reduce the systematic error that affected the final GALLEX result. For that reason in 2001 we started to work for the determination of the counting efficiency of individual counters at 1% level. In fact, the major component ($\approx 4\%$) of the systematic error comes from the actual knowledge of this parameter (see table **??**). In former time (GALLEX) the counting efficiency was determined for a few counters filled with a calibrated ^{71}Ge activity and extrapolating to other counters of the same type using individual total volume and longitudinal moltiplication curves. For the absolute calibration we fill the counter with ^{69}Ge activity. Details on the calibration procedure are given in the 2001 Annual report [10]. Table 3 lists the counting efficiency for all the calibrated counters, and gives the total number of solar runs and blanks for which the counters were employed; in 2002 we calibrated 6 counters.

3.4 Implementation of a new pulse shape analysis

During 2001 a more sophisticated pulse-shape (PS) analysis based on fitting the whole pulse rather than the rise time (RT) only was developed. In 2002 the work of refinement and validation of the method was completed. Also the component of the induced systematic error (see Tab. **??**) was fully evaluated, so that data analysis is presently carried on with the this new method.
The main features of the PS analysis can be found in [10]. The pulses are first selected

Table 4: Selection and background rejection efficiencies for RT and NN analysis methods.

Window	Selection eff. [%]		Background rejection eff. [%]	
	L window	K window	L window	K window
NN analysis	96.4	95.2	79.5	78.8
RT analysis	96.4	96.4	65.7	73.5

according to their amplitudes: the subsequent PS analysis is applied only to those pulses that pass the energy selection. The procedure is then logically divided into two different steps: a) fit of the pulse; b) events selection through neural network (NN). The pulses are fitted with a semi-empirical function (fig. 7d) obtained by the numerical convolution of the ideal pulse produced by a cylindrical proportional counter (fig. 7a) with the experimental response function of the electronic chain (fig. 7b) and a gaussian charge distribution function (fig. 7c), to modelize a not point-like energy deposition.

The information obtained by the fit about the shape of the pulses are fed to a feed-forward 3-levels NN, in order to distinguish between genuine ^{71}Ge decays and background events originated by β/γ environmental radioactivity.

The training stage of the network is very important as it heavily affects the results when an unknown sample is analyzed. In order to perform a reliable analysis, a library of known reference pulses was collected for the training process: ^{71}Ge reference pulses come from actual calibrations of the counters with ^{71}Ge activity (see sect 3.3); background reference pulses are obtained from calibrations with a ^{137}Cs γ source, which is assumed to simulate environmental radioactivity. Once the training stage is completed, the network is switched on the execution mode and it is used analyze the data.

As L and K e-captures originate two distinct classes of events, two NNs are used: this also allows to take into account the possibility of observing double-ionization pulses after K-capture ^{71}Ge decays. Since the pulse shapes are *a priori* dependent on the particular proportional counter and on its filling/working conditions (i.e. pressure, gas composition, high voltage), we got reference ^{71}Ge pulses from 10 different counters. However, since the composition of the counting gas and the reduced field E/P for the actual runs vary in a very narrow range, all these ^{71}Ge reference sets proved to give equivalent trainings: the final results of the analysis are then insensitive to the particular counter and setting which was used for the collection of the reference pulses.

Table 4 shows the selection and background rejection efficiencies, both for L and K amplitude windows, which are estimated from the present data. Selection efficiencies of the NN analysis are of the same order than those for RT analysis, whereas background rejection efficiencies are clearly higher, expecially in the L energy window.

When the first 43 GNO solar runs are analyzed with the maximum likelihood algorithm after the NN event selection, the solar neutrino interaction rate is $65.3^{+6.6}_{-6.3}$(stat)$\pm$2.9(syst) SNU (see also Tab. 5 for separate L and K analysis).

The reduction of the flat background level is 7% compared to RT selection: this means that more background events are recognized and rejected by the NN selection, i.e. the NN provides a "cleaner" sample of candidate events than RT selection for the subsequent

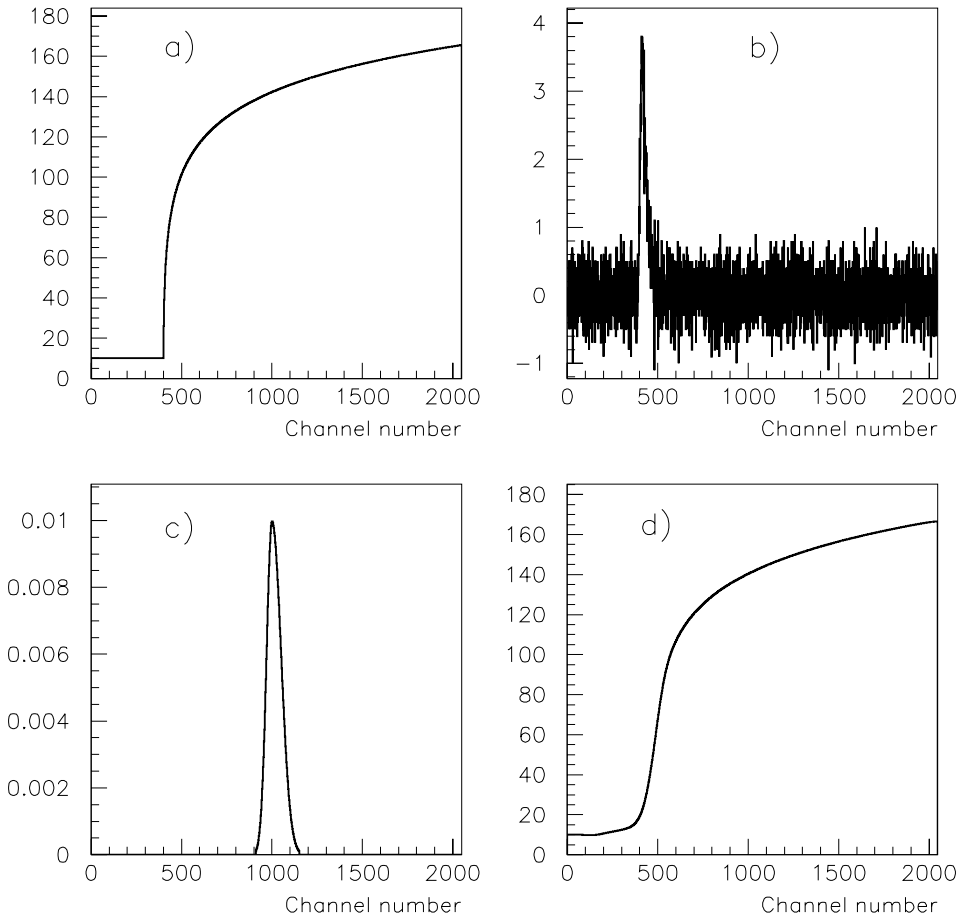

Figure 7: Model used for pulse fitting. a) Ideal pulse produced by a cylindrical proportional counter. b) Experimental response function of the actual electronic chain. c) Gaussian charge distribution function. d) Final convoluted pulse.

Table 5: For each selection method are shown: the solar neutrino interaction rate (all corrections included), the number of events that are attribuited to ^{71}Ge decay from the maximum likelihood analysis and the number of those attributed to the flat background. The quoted errors are only statistical. The analysis is applied to the first 43 solar runs.

		rate (SNU)	^{71}Ge counts	bck counts
NN	L+K	$65.3^{+6.6}_{-6.3}$	199.2	401.8
	L only	$70.1^{+10.6}_{-10.1}$	101.8	245.2
	K only	$62.1^{+8.4}_{-7.9}$	99.2	154.8
RT	L+K	$64.7^{+6.6}_{-6.3}$	200.5	430.5
	L only	$69.2^{+10.7}_{-10.2}$	101.0	267.0
	K only	$61.9^{+8.3}_{-7.9}$	101.2	161.8

statistical analysis. Some tests of the NN method robustness are the following:

- the results obtained from the separate analysis of L and K events are well compatible, as shown in Tab. 5. The difference of the SNU values is of the same order of RT analysis and is well within the statistical errors;
- the ratio of double-ionization to total K events is found to be 16.7% in the ^{71}Ge calibrations and 15.5%($\pm$2%) in the solar runs (after the neural selection). The expected theoretical value is 20.9%[2];
- when the life time τ of ^{71}Ge is a free parameter in the maximum likelihood analysis, the resulting value is (16.6$\pm$2.3) days, consistent with the "true" known life time $\tau = (16.49 \pm 0.04)$ days.

All the NN results are consistent, within the statistical uncertanties, with those from RT analysis.
The component of the systematic error connected to the neural analysis has been evaluated to be 1.3%; in the RT analysis, the contribution to the systematics coming from the PS cuts is 1.5%. The systematic error connected with the new analysis comes from the choice of the training examples and from the fact that the network is trained on ^{71}Ge pulses collected only in given counters and in particular working conditions. A simulation was performed in order to fully evaluate the NN-induced systematics: the network is trained with randomly extracted sets of examples and is then used to select the events from all the presently available solar runs. These candidate events are analyzed with the usual maximum likelihood algorithm, in order to evaluate the solar neutrino rate. This procedure is repeated 1000 times (starting with different training sets) and the distribution of rates is reconstructed: the width of the distribution is an estimate of the effective NN-induced systematic error. Such distribution is well fitted with a gaussian curve: the

[2]This value should be regarded as an upper limit, as the two components cannot be resolved if they are too close in time.

Table 6: Characteristics of the Cr isotopes

isotope	^{50}Cr	^{52}Cr	^{53}Cr	^{54}Cr
natural abundance (%)	4.35	83.8	9.5	2.35
sample abundance (%)	38.6	60.7	0.7	<0.3
neutron cross section (barn)	15.9	0.76	18.2	0.36

mean rate is 65.67 SNU with rms 0.84 SNU (=1.3%), which is much lower than the statistical error (about 6 SNU).

4 Plans for the future and R&D in progress

4.1 Solar neutrino observations

We plan to go on with 4-week exposure solar runs over the next years. The only planned interruptions are foreseen for the ν calibration (see sect. 4.4) and for 1-day exposure blanks every three months.

4.2 Counters

We will complete the absolute determination of counting efficiency of all available proportional counters.
longitudinal moltiplication curves z-scan of the counters! Da scrivere!

4.3 The Chromium source

In order to test the entire procedure of the experiment, GALLEX was exposed twice to a strong artificial source of neutrinos emitted in E.C. of ^{51}Cr [13],[14]. ^{51}Cr transforms, via E.C., in ^{51}V with a mean life of 39.97 days; it emits two doublets of monochromatic neutrino lines at 426 (9%), 431 (1%), 746 (81%) and 751 (9%) keV respectively. These lines are very close in energy to the ^{7}Be lines at 386 (10%) and 863 (90%) keV. In 10% of the cases, the final state is an excited level of ^{51}V; the 320 keV γ ray can be used to determine the source strength with excellent accuracy. An enriched ^{50}Cr sample (36 kg) was irradiated two times at the Siloe reactor in Grenoble. The isotopic composition of the sample is reported in table 6; as it can be seen, the sample is not only enriched in the interesting isotope (^{50}Cr), but also depleted in the high neutron capture cross section ^{53}Cr.

The strenght of the two sources are reported in the table 7. The ratio between the measured values and the expected one of the interaction rate is also reported in the table 7; combining both experiments, we obtain $R = 0.93 \pm 0.08$. After the pubblication of this result, the efficiency of some of the counters used in the second exposure was directly measured and their values resulted slightly higher than previously computed; the final

Table 7: GALLEX sources

Source I	$63.4\ ^{+1.1}_{-1.6}$ PBq	$R = 1.01^{+0.12}_{-0.11}$
Source II	$69.1\ ^{+3.3}_{-2.1}$ PBq	$R = 0.84^{+0.12}_{-0.11}$

value (unpublished) is $R = 0.89 \pm 0.07$. Also SAGE performed a similar measurement leading to a value $R = 0.95$ [15].

Two factors enter in the determination of R: the efficiency, in a wide sense, of the detector (extraction, synthesis, counting...) and the neutrino-gallium cross sections. Assuming that the value of the efficency is provided by the "ancillary" tests on the relevant quantities (first of all the arsenic test, which guarantees that the extraction efficiency is well known and close to 100%), R gives an estimate of the neutrino cross section. At the ^{51}Cr lines, the cross section can be written as [16]:

$$\sigma = \sigma_{g.s.}\Big[1 + \alpha\frac{BGT(175)}{BGT(g.s.)} + \beta\frac{BGT(500)}{BGT(g.s.)}\Big] \tag{1}$$

where α and β are "kinematical factors". Their values are 0.67 and 0.22 respectively [16]. The BGT's can be deduced from the E.C. rate for the ground state-ground state transition and from the (p,n) measurements for the excited states. These data provide only an upper limit (0.056) for the transition BGT(175)/BGT(g.s.) to the first (175 keV) excited state. In the cross section computation, a value of 0.028 is assumed. The central value of R implies instead a zero contribution from this state.

4.4 The proposed source

We plan to make a third exposure of the GNO solution to a ^{51}Cr source. The two above mentioned sources used in GALLEX have been prepared at Siloe (Grenoble). This was a very effective solution from the technical point of view and very practical for many reasons (transportation, customs, uniformity of legal rules for radioactive source handling and so on). However, the Siloe reactor is no more in operation and, moreover, no other suitable reactors are available in Western Europe. Therefore, after some investigations, we decided to contact the Research Institute of Atomic Reactors (RIAR) in Dimitrovgrad. As a matter of fact, one of us (T. Kirsten) was responsible for the INTAS project n.96-0145 [12] aimed to the determination of the optimum conditions for the production of very intense ^{51}Cr sources.

The irradiation could be carried at a SM reactor, which is designed for the production of radioactive isotopes with high specific activity. The neutron flux ranges from 1 to $1.2{\cdot}10^{14}$ n/cm$^2\cdot$ s, depending on the specific irradiation channel. Thank to the above mentioned and other preliminary studies and after direct contact, RIAR has provided a specific technical and economical offer.
In conclusion, the relevant points are:

- the irradiation of about 12 kg, subdivided in three sources of 3600 g of enriched Cr for 50 days will produce an activity of about 300 Ci/g, i.e more than 3 MCi in total;

- with this activity, and assuming a mean cross section on gallium of $58.1 \cdot 10^{-46}$ cm^2, the production of about 300 ^{71}Ge atoms is expected, corresponding to a statistical error on R of 6% and a total error of about 8%;
- the source can be provided in one year from the time of the signature of the contract;
- the overall cost for a source of at least 2.5 MCi (preliminary studies, irradiation, shipping container and transportation to an italian airport) is 1.5 million dollars.

5 Conclusions

The gallium detector at LNGS is monitoring low energy solar neutrinos since May 1991 with 30 tons of natural gallium. From the 65 GALLEX solar runs plus the 43 GNO solar runs, the solar neutrino interaction rate on gallium has been measured with an overall accuracy of $\sim 8.3\%$. Data taking is going on regularely with four-week-exposure runs, with the aim to reach an accuracy of the order of 5%, and to study possible unexpected time dependences of the signal at the level of 10-15 % . During year 2002 we continued the experimental activity on the absolute counter calibrations, necessary for the reduction of the systematics. A new pulse shape analysis (pulse fit+neural network) has been developed and applied to the whole GNO data set: the results are fully compatible with the old method but with improved signal to noise ratio.

6 Acknowledgemnts

7 List of Publications (2002)

1. GNO collaboration, "GNO progress report for 2001", LNGS annual Report 2001, 79-94, GNO report n.18
2. T. Kirsten, "Progress in GNO", to be published in Nuclear Physics B (Proceedings supplement)
3. N. Ferrari and L. Pandola, "Gallium Neutrino Observatory: data analysis and systematic error reduction", to be published in Nuclear Physics B (Proceedings supplement)
4. J.C. Lanfranchi, "Development of highly efficient cryogenic detectors for GNO", to be published in Nuclear Physics B (Proceedings supplement)
5. N. Ferrari, "Detection of Sub MeV solar neutrinos", to be published in the Vulcano Workshop 2002 Proceedings

8 List of Conference Presentations (2002)

1. T. Kirsten, "Progress in GNO", XXth International Conference on Neutrino Physics and Astrophysics (Neutrino 2002), May 2002, Munich

2. L. Pandola, "Neural network analysis for GNO events: methods and results", IIIrd International Workshop on Low Energy Solar Neutrinos (LowNu 2002), May 2002, Heidelberg

3. T. Lachenmaier, "Low temperature detectors: an alternative counting technique for GNO", IIIrd International Workshop on Low Energy Solar Neutrinos (LowNu 2002), May 2002, Heidelberg

4. N. Ferrari, "Detection of sub MeV solar neutrinos", Vulcano Workshop 2002, Vulcano, May 2002

5. P. Belli,"L'esperimento GNO ai Laboratori Nazionali del Gran Sasso", Meeting of the Italian Physics Society (SIF), Alghero, October 2002

6. T. Lachenmaier, "Measuring solar neutrinos with the Gallium Neutrino Observatory", Spring meeting of the German Physics Society (DPG), 2002, Leipzig

7. J.C. Lanfranchi, "Highly efficient and low-level cryogenic detectors for GNO", Spring meeting of the German Physics Society (DPG), 2002, Leipzig

8. T. Lachenmaier, "Low temperature detectors for GNO", Meeting of the EU TMR Network on "Cryogenic detectors", 2002, Paris

References

[1] J.N. Bahcall, Phys. Rept. 333 (2000) 47-62; S. Turck-Chiéze et al, Nucl. Phys. (Proc. Suppl.) 87 (2000) 162-171; V. Castellani et al., Nucl. Phys. (Proc. Suppl.) 70 (1999) 301-314.

[2] E.Henrich, K.H.Ebert, Angew. Chemie Int. Ed. (Engl.) 31 (1992) 1283; E.Henrich et al., 'GALLEX, a challange for chemistry', Proc. IV Int'l. Solar Neutrino Conf., ed. W.Hampel, MPI Kernph., Heidelberg (1997) 151-162.

[3] R. Wink et al. Nucl. Inst. and Meth. A329 (1993) 541.

[4] GALLEX collaboration, Phys.Lett. B285 (1992) 376; Phys.Lett. B314 (1993) 445; Phys.Lett. B327 (1994) 377; Phys.Lett. B342 (1995) 440; Phys.Lett. B357 (1995) 237; Phys.Lett. B388 (1996) 384, Phys.Lett. B447 (1999) 127.

[5] T.Kirsten, Rev.Mod.Phys., 71 (1999) 1213-1232.

[6] E.Bellotti et al., GNO collaboration, LNGS report INFN/AE-96-27.

[7] GNO collaboration, LNGS annual report 1998, pag. 55-69.

[8] GNO collaboration, LNGS annual report 1999, pag. 57-68.

[9] GNO collaboration, LNGS annual report 2000, pag. 57-68.

[10] GNO collaboration, LNGS annual report 2001, pag. 79-94.

[11] T.Kirsten, "Progress in GNO", Talk at XXth International Conference on Neutrino Physics and Astrophysics, Munich (2002), to appear in the proceeding.

[12] INTAS 06-0145 Feasibility of re-activation of the GALLEX Cr source at Russian reactors for the use in the BOREXINO and GNO Solar neutrino experiments at Gran Sasso - Final Report - Proj. coordinator T. Kirsten.

[13] W.Hampel et al., GALLEX coll., Phys. Lett. B420 (1998) 114.

[14] M. Cribier et al., Nucl. Instr. and Meth. A378 (1996) 233.

[15] SAGE collaboration, Phys. Rev. C59 (1999) 2246-2263

[16] J.N.Bahcall, Phys.Rev.C56 (1997) 3391.

[17] SuperKamiokande Collaboration, Phys.Rev.Lett. 86 (2001) 4651.

[18] SNO collaboration, Phys.Rev.Lett. 87 (2001) 071301; Phys.Rev.Lett. 89 (2002) 011302

[19] KamLAND Collaboration, K.Eguchi et al., submitted to PRL (2002)

[20] S.Schoenert, "Future solar and reactor experiments", TAUP2001, LNGS, September 2001.

HDMS. Dark Matter Search

H.V. Klapdor-Kleingrothaus*[a], A. Dietz[a], C. Dörr[a],
I.V. Krivosheina[a,b], D. Mazza[a], H. Strecker[a], C. Tomei[a,c]

[a] Max-Planck Institut für Kernphysik, Heidelberg, Germany
[b] Institute of Radiophysical Research, Nishnij Novgorod, Russia
[c] University of L'Aquila, Italy
* Spokesman of the Collaboration
E-mail: klapdor@gustav.mpi-hd.mpg,
Home-page: http://www.mpi-hd.mpg.de.non_acc/

1 Introduction

There is strong observational and theoretical evidence that dark, nonbaryonic matter accounts for about a quarter of the critical density of the Universe. Many candidates have been proposed and some of them (cosmions, heavy Dirac neutrinos) have already been rejected. Slow thermal relics born in an early phase of the Universe, stable or very long lived, are excellent candidates for nonbaryonic dark matter. These weakly interacting, massive (1 GeV - 1 TeV) particles (WIMPs) arise independently from cosmological considerations in supersymmetric models as neutralinos - the lightest supersymmetric particles. Direct detection of neutralinos can occur in very low background experiments, where the elastic neutralino scattering off target nuclei is exploited

HDMS is a new Germanium experiment aiming to test the hypothesis that the dark halo of our Galaxy is made of WIMPs.

HDMS operates two ionization HPGe detectors in a unique configuration. A small, p-type Ge crystal is surrounded by a well-type Ge crystal, both being mounted into a common cryostat system. To shield leakage currents on the surfaces, a 1 mm thin insulator made from vespel is placed between them. Two effects are expected to reduce the background of the inner,

1. The anticoincidence between the two detectors acts as an effective suppression for multiple scattered photons,

2. The detection crystal is surrounded by Ge, which is one of the radio-purest known materials.

From previous measurements (the HEIDELBERG-MOSCOW experiment) we know that the main radioactive background of Ge detectors comes from materials situated in the immediate vicinity of the crystals, i.e. from the copper parts of the cryostats.

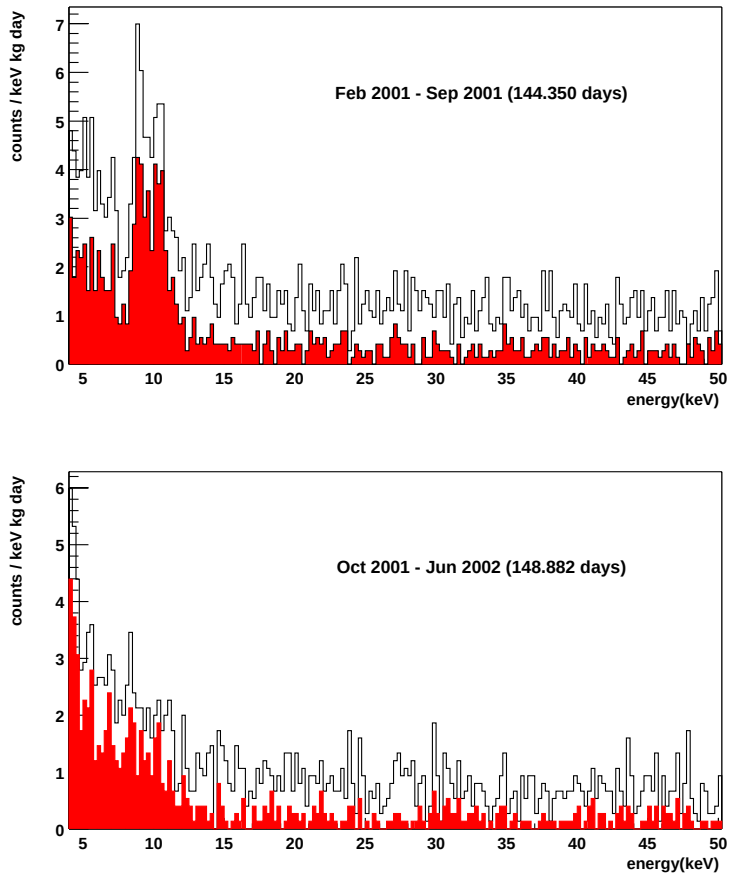

Figure 1: Low-energy spectrum of the inner, enriched Ge detector before and after (open and solid histograms, respectively) the anti-coincidence is applied with the outer Ge detector. The internal, low-energy X-rays are not removed by the anti-coincidence.

HDMS has the goal to achieve an absolute background counting rate of 0.07 events per kg, day and keV in the region between 2 keV and 30 keV, and thus to test the evidence region singled out by the DAMA experiment in the MSSM parameter space [1]. It would be an independent test by using only raw data and a completely different detection technique.

The HDMS experiment started in 1998 with a prototype phase: the HDMS-prototype (for which both inner and outer detectors were made of natural Ge) took successfuly data over a period of about 15 month in the Gran Sasso Underground Laboratory. The full scale experiment was installed at LNGS in August 2000: the main difference was the use of enriched of ^{73}Ge which means at the same time a de-enrichment in the isotope ^{68}Ge, whose X-rays are a known source of background in the low energy region. The reduction of the background due to the anticoincidence between the two detectors can be seen in the figure 1. Also seen is the clear reduction in the course of the measurementof the gamma-peaks around 10 keV (X-rays from ^{68}Ge etc.) which originate from the decay of isotopes produced by spallation via cosmic rays during the time of production and transport of

the detectors (compare Figs. 1a and 1b).

References

[1] H. V. Klapdor-Kleingrothaus et al., Astroparticle Physics, Volume 18, Issue 5, February 2003, Pages 525-530.

2 List of Proceedings (2002)

1. H.V. Klapdor-Kleingrothaus and R. Viollier (eds.), Dark Matter in Astro- and Particle Physics., Proc. of DARK2002, Cape Town, South Africa, February 4 - 9, 2002, Heidelberg, Germany: Springer (2002) 663 pp.

2. H.V. Klapdor-Kleingrothaus (ed.) Physics Beyond the Standard Model: Beyond the Desert 02, Proc. of Intern. Conf. BEYOND'02, Oulu, Finland, 2-7 Jun 2002, IOP, Bristol, 2003 (in preparation).

3 List of Publications (2002)

1. H.V. Klapdor-Kleingrothaus, Int. J. Mod. Phys. A 17 (2002) 3421-3431.

2. H.V. Klapdor-Kleingrothaus, Nucl. Phys. Proc. Suppl. 110 (2002) 58-60 e-Print Archive: hep-ph/0206250.

3. V.A. Bednyakov, H.V. Klapdor-Kleingrothaus, V. Gronewold, Phys. Rev. D 66 (2002) 115005 and e-Print Archive: hep-ph/0208178

4. V.A. Bednyakov, H.V. Klapdor-Kleingrothaus, E. Zaiti, Phys. Rev. D 66 (2002) 015010 and e-Print Archive: hep-ph/0203108.

5. H. V. Klapdor-Kleingrothaus et al., Astroparticle Physics, Volume 18, Issue 5, February 2003, Pages 525-530.

4 List of Conferences (2002)

1. H.V. Klapdor-Kleingrothaus and I. Krivosheina, in Proc. of DARK2002, Cape Town, South Africa, February 4 - 9, 2002, Springer, Heidelberg (2002), 473-484.

2. V.A. Bednyakov, H.V. Klapdor-Kleingrothaus, E. Zaiti, Deutsche Physikalische Gesellschaft e. V. (DPG), 18. - 22. März 2002, Leipzig, GERMANY.

3. C. Tomei, H.V. Klapdor-Kleingrothaus, A. Dietz, Ch. Dörr, I. Krivosheina, D. Mazza and H. Strecker, Deutsche Physikalische Gesellschaft e. V. (DPG), 18. - 22. März 2002, Leipzig, GERMANY.

4. H.V. Klapdor-Kleingrothaus and I. Krivosheina, Zacatecas Forum in Physics 2002, 11-13 MAY, 2002 Zacatecas, Mexico.

5. V.A. Bednyakov and H.V. Klapdor-Kleingrothaus, in Proc. of Intern. Conf. on Physics Beyond the Standard Model: Beyond the Desert 02, BEYOND'02, Oulu, Finland, 2-7 Jun 2002, IOP, Bristol, 2003, ed. H.V. Klapdor-Kleingrothaus.

6. H.V. Klapdor-Kleingrothaus and I. Krivosheina, in Proc. of Intern. Conf. on Physics Beyond the Standard Model: Beyond the Desert 02, BEYOND'02, Oulu, Finland, 2-7 Jun 2002, IOP, Bristol, 2003, ed. H.V. Klapdor-Kleingrothaus.

7. H.V. Klapdor-Kleingrothaus and I. Krivosheina, in Proc. of IDM2002, York, England, 22-24 Sep. 2002, World Scientific (2003).

8. I. Krivosheina, International School on CP Violation, Baryogenesis and Neutrinos, Prerow, Germany, September 15 - 21, 2002.

9. I. Krivosheina, Meeting of Russian Academy of Science, Nuclear Physics Section, Moscow, ITEP, 3-5 December, 2002.

HEIDELBERG-MOSCOW Experiment on Neutrinoless Double Beta Decay

H.V. Klapdor-Kleingrothaus*, A. Dietz, I.V. Krivosheina
Max-Planck-Institut für Kernphysik,
P.O. Box 10 39 80, D-69029 Heidelberg, Germany

Abstract

The HEIDELBERG-MOSCOW experiment in GRAN SASSO, which is the most sensitive experiment worldwide since nine years, has been regularly continued in 2002. Since its starting in 1990, it has collected until end of 2002 about 75 kg y of data. The statistics collected for the $2\nu\beta\beta$ spectrum amounts to $\sim$ 147 000 events.

The experiment has found the first indication for the neutrinoless decay mode [1, 2, 4]. This is the first evidence for lepton number violation and proves the neutrino to be a Majorana particle. It excludes several of the neutrino mass scenarios allowed from present neutrino oscillation experiments - only degenerate scenarios and those with inverse mass hierarchy survive. This result allows neutrinos to still play an important role as dark matter in the Universe. To improve the accuracy of the present result, considerably enlarged experiments are required, such as GENIUS. A GENIUS Test Facility has been funded and will come into operation by early 2003.

1 Introduction

Double beta decay is the most sensitive probe to test lepton number conservation. Further it seems to be the only way to decide about the Dirac or Majorana nature of the neutrino. Observation of $0\nu\beta\beta$ decay would prove that the neutrino is a Majorana particle and would be another clear sign of beyond standard model physics. Recently atmospheric and solar neutrino oscillation experiments have shown that neutrinos are massive. This was the first indication of beyond standard model physics. The absolute neutrino mass scale, however, cannot be determined from oscillation experiments alone. Double beta decay is indispensable also to solve this problem.

The observable of double beta decay is the effective neutrino mass

$$\langle m \rangle = |\sum U_{ei}^2 m_i| = |m_{ee}^{(1)}| + e^{i\phi_2}|m_{ee}^{(2)}| + e^{i\phi_3}|m_{ee}^{(3)}|,$$

*Spokesman of HEIDELBERG-MOSCOW and GENIUS Collaborations,
E-mail: klapdor@gustav.mpi-hd.mpg, Home-page: http://www.mpi-hd.mpg.de.non_acc/

with U_{ei} denoting elements of the neutrino mixing matrix, m_i neutrino mass eigenstates, and ϕ_i relative Majorana CP phases. It can be written in terms of oscillation parameters (see [7]).

The effective mass $\langle m \rangle$ is related with the half-life for $0\nu\beta\beta$ decay via $\left(T^{0\nu}_{1/2}\right)^{-1} \sim \langle m_\nu \rangle^2$, and for the limit on $T^{0\nu}_{1/2}$ deducible in an experiment we have

$$T^{0\nu}_{1/2} \sim \epsilon \times a \sqrt{\frac{Mt}{\Delta E B}}, \tag{1}$$

Here a is the isotopical abundance of the $\beta\beta$ emitter; M is the active detector mass; t is the measuring time; ΔE is the energy resolution; B is the background count rate and ϵ is the efficiency for detecting a $\beta\beta$ signal. Determination of the effective mass fixes the absolute scale of the neutrino mass spectrum. [7, 8].

Although in the HEIDELBERG-MOSCOW experiment we also have the highest statistics ($\sim$ 147 000 events) for $2\nu\beta\beta$ decay (see [5] and [6]) we shall concentrate in this report on the neutrinoless decay mode. We shall, in section 2, discuss the status of evidence for the neutrinoless decay mode, from the first 55 kg y of measurement of the HEIDELBERG-MOSCOW experiment and the consequences for the neutrino mass scenarios which could be realized in nature. In section 3 we shall discuss briefly possible future experiments, which could improve the present accuracy.

2 Evidence for the Neutrinoless Decay Mode

The status of present double beta experiments is shown in Fig. 1 and is extensively discussed in [9]. The HEIDELBERG-MOSCOW experiment using the largest source strength of 11 kg of enriched ^{76}Ge (enrichment 86%) in form of five HP Ge-detectors is running since August 1990 in the Gran-Sasso underground laboratory [9, 4, 5, 1, 31, 27], and is since nine years now the most sensitive double beta experiment worldwide.

2.1 *Data from the HEIDELBERG-MOSCOW Experiment*

The data taken in the period August 1990 - May 2000 (54.9813 kg y, or 723.44 mol-years) are shown in Fig. 2 in the section around the $Q_{\beta\beta}$ value of 2039.006 keV [15, 16]. Fig. 2 is identical with Fig. 1 in [1], except that we show here the original energy binning of the data of 0.36 keV. These data have been analysed [1, 2, 4] with various statistical methods, with the Maximum Likelihood Method and also with the Bayesian method. This method is particularly suited for low counting rates. Details and the results of the analysis are given in [1, 2, 4]. The data taken since May 2000 are at present under analysis.

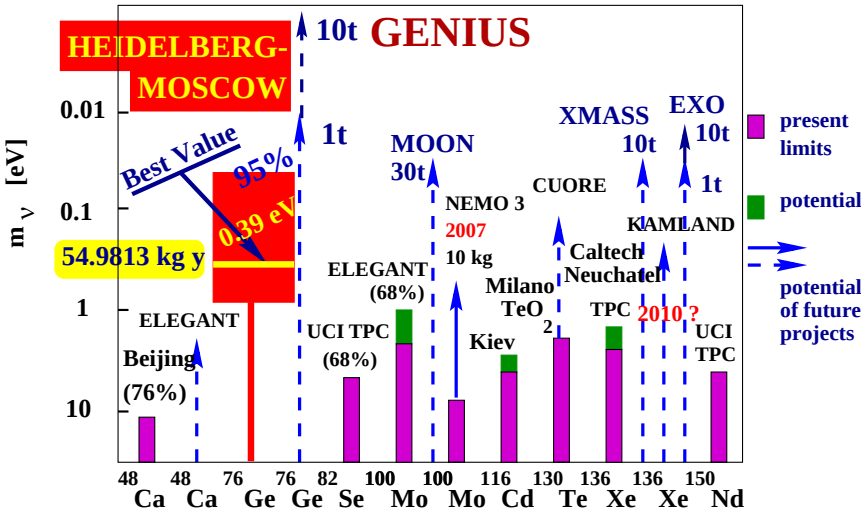

Figure 1: Present sensitivity, and expectation for the future, of the most promising $\beta\beta$ experiments. Given are limits for $\langle m \rangle$, except for the HEIDELBERG-MOSCOW experiment where the recently observed *value* is given (95% c.l. range and best value). Framed parts of the bars: present status; not framed parts: future expectation for running experiments; solid and dashed lines: experiments under construction or proposed, respectively. For references see [9, 2, 4, 34, 38].

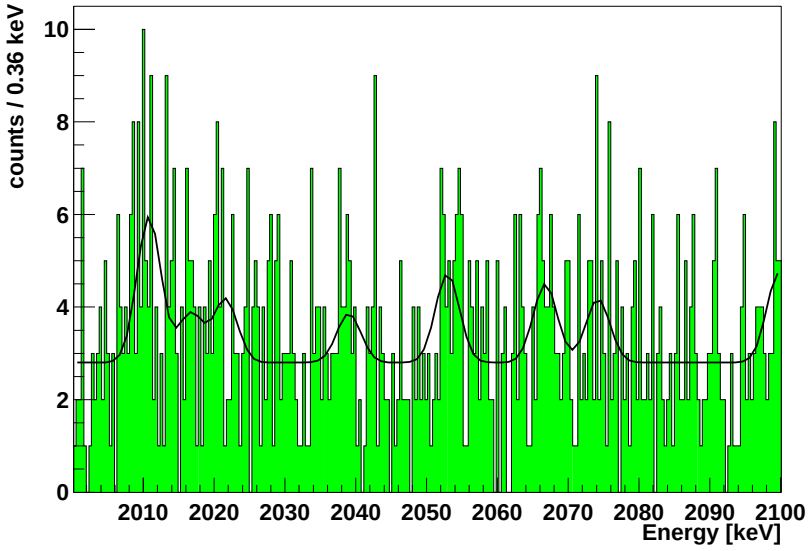

Figure 2: The spectrum taken with the ^{76}Ge detectors Nr. 1,2,3,4,5 over the period August 1990 - May 2000 (54.9813 kg y) in the original 0.36 keV binning, in the energy range 2000 - 2100 keV. Simultaneous fit of the ^{214}Bi lines and the two high-energy lines yield a probability for a line at 2039.0 keV of 91%.

Details and the results of the analysis are given in [1, 2, 4]. The data taken since May 2000 are at present under analysis.

Our peak search procedure (for details see [2, 4]) reproduces (see [1, 2, 4]) γ-lines at the positions of known weak lines from the decay of ^{214}Bi at 2010.7, 2016.7, 2021.8 and 2052.9 keV [14]. In addition, a line centered at 2039 keV shows up (see Fig. 3). This is compatible with the Q-value [15, 16] of the double beta decay process. The Bayesian analysis yields, when analysing a $\pm 5\sigma$ range around $Q_{\beta\beta}$ (which is the usual procedure when searching for resonances in high-energy physics) a confidence level (i.e. the probability K) for a line to exist at 2039.0 keV of 96.5 % c.l. (2.1 σ) (see Fig. 3). We repeated the analysis for the same data, but except detector 4, which had no muon shield and a slightly worse energy resolution (46.502 kg y). The probability we find for a line at 2039.0 keV in this case is 97.4% (2.2 σ) [1, 2, 4].

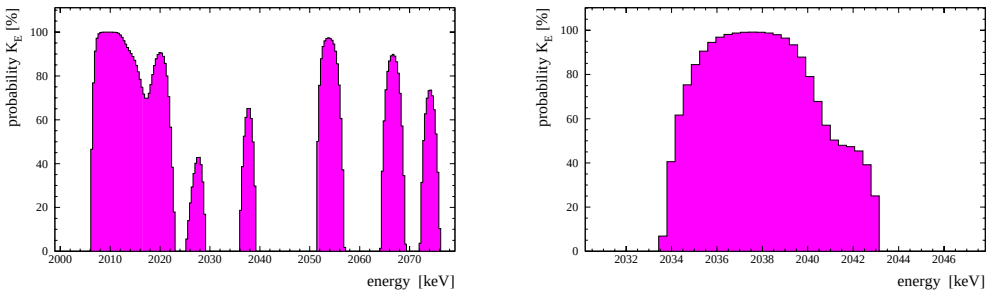

Figure 3: Left: Probability K that a line exists at a given energy in the range of 2000-2080 keV derived via Bayesian inference from the spectrum shown in Fig. 2. Right: Result of a Bayesian scan for lines as in the left part of this figure, but in an energy range of $\pm 5\sigma$ around $Q_{\beta\beta}$.

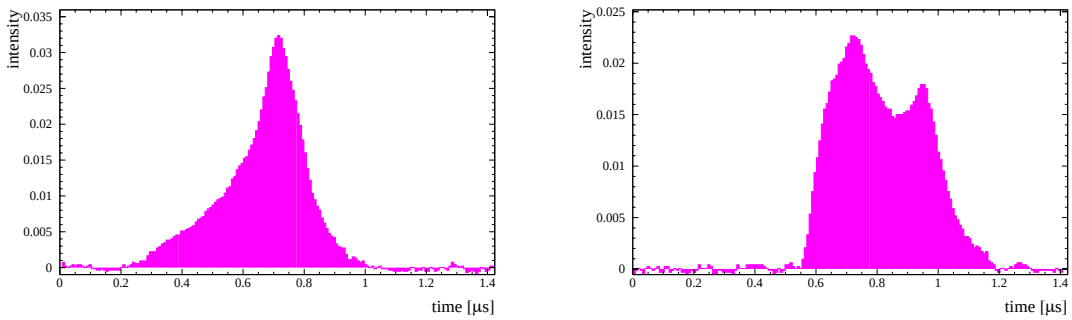

Figure 4: Left: Shape of one candidate for $0\nu\beta\beta$ decay classified as SSE by all three methods of pulse shape discrimination. Right: Shape of one candidate classified as MSE by all three methods.

Fitting a wide range of the spectrum yields a line at 2039 keV at 91% c.l. (see Fig.2).

We also applied the Feldman-Cousins method. This method (which does not use the information that the line is Gaussian) finds a line at 2039 keV on a confidence level of 3.1 σ (99.8% c.l.). In addition to the line at 2039 keV we find candidates for lines at energies

beyond 2060 keV and around 2030 keV, which at present cannot be attributed. This is a task of nuclear spectroscopy.

Important further information can be obtained from the *time structures* of the individual events. Double beta events should behave as single site events (see Fig. 4 left), i.e. clearly different from a multiple scattered γ-event (see Fig. 4 right). It is possible to differentiate between these different types of events by pulse shape analysis. We have developped three methods of pulse shape analysis [10, 11, 12] during the last seven years, one of which has been patented and therefore only published recently.

Installation of Pulse Shape Analysis (PSA) has been performed in 1995 for the four large detectors. Detector Nr.5 runs since February 1995, detectors 2,3,4 since November 1995 with PSA. The measuring time with PSA from November 1995 until May 2000 is 36.532 kg years, for detectors 2,3,5 it is 28.053 kg y.

In the SSE spectrum obtained under the restriction that the signal simultaneously fulfills the criteria of *all three* methods for a single site event, we find again indication of a line at 2039.0 keV (see Figs. 5, 6). We have used a ^{228}Th source to test our PSA method again in 2002 and found that it works properly [6].

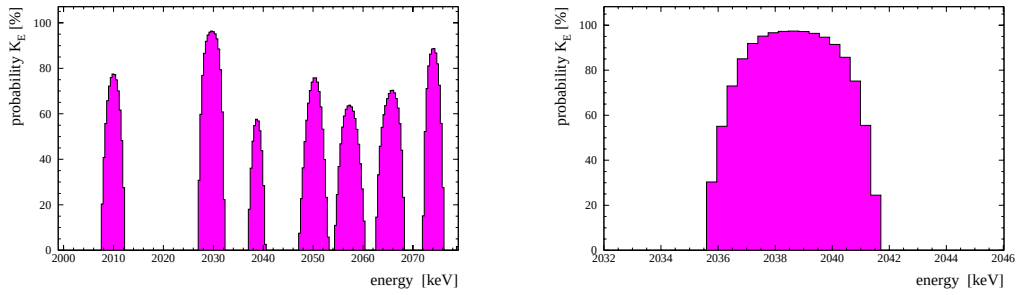

Figure 5: Scan for lines in the single site event spectrum taken from 1995-2000 with detectors Nr. 2,3,5, (Fig. 6), with the Bayesian method. Left: Energy range 2000 - 2080 keV. Right: Energy range of analysis $\pm 4.4\sigma$ around $Q_{\beta\beta}$.

A very careful simulation of the different components of radioactive background, has been performed [6, 17] by a new Monte Carlo program basing on GEANT4 in 2002. This simulation uses a new event generator for simulation of radioactive decays basing on ENSDF-data and describes the decay of arbitrary radioactive isotopes including α, β and γ emission as well as conversion electrons and X ray emission. Also included in the simulation is the influence of neutrons in the energy range from thermal to high energies up to 100 MeV on the measured spectrum. Elastic and inelastic reactions, and capture have been considered, and the corresponding production of radioactive isotopes in the materials of the setup. The neutron fluxes and energy distributions were taken from published measurements performed by other group in the Gran Sasso. Also simulated was the influence of the cosmic muon flux measured in the Gran Sasso, on the measured spectrum.

The simulation gives no indication that the signal at 2039 keV could come from a known background line. In particular, the simulation shows, that e.g. decays of ^{77}Ge,

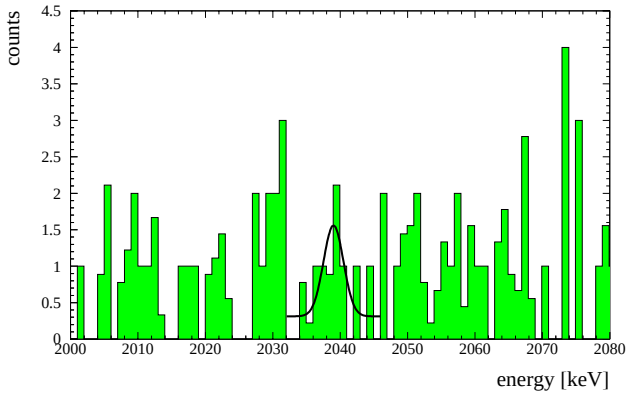

Figure 6: Sum spectrum of single site events, measured with the detectors Nr. 2,3,5 operated with pulse shape analysis in the period November 1995 to May 2000 (28.053 kg y), summed to 1 keV bins. Only events identified as single site events (SSE) by all three pulse shape analysis methods [10, 11, 12] have been accepted. The curve results from Bayesian analysis. When corrected for the efficiency of SSE identification (see text), this leads to a half-life of $T^{0\nu}_{1/2}$=(0.88 - 22.38)$\times$ 10^{25} y (90% c.l.).

^{76}Ga or ^{228}Ac, should not lead to signals visible in our measured spectra near the signal at $Q^{\beta\beta}$. For details we refer to [6].

2.2 Comparison with Earlier Results

We applied the same methods of peak search as used the analysis of our data to the spectrum, measured in the Ge experiment by Caldwell et al. [18] more than a decade ago. These authors had the most sensitive experiment using *natural* Ge detectors (7.8% abundance of ^{76}Ge). With their background being a factor of 9 higher than in the present experiment, and their measuring time of 22.6 kg y, they have a statistics for the background larger by a factor of almost 4 in their experiment. This allows helpful conclusions about the nature of the background.

The peak scanning finds (see [4] and Fig. 7) indications for peaks essentially at the same energies as in Fig. 3. This shows that these peaks are not fluctuations. In particular it sees the 2010.78, 2016.7, 2021.6 and 2052.94 keV ^{214}Bi lines. It finds, however, *no line at* $Q_{\beta\beta}$. This is consistent with the expectation from the rate found from the HEIDELBERG-MOSCOW experiment. About 16 observed events in the latter correspond to 0.6 *expected* events in the Caldwell experiment, because of the use of non-enriched material and the shorter measuring time.

The first experiment using enriched (but not high-purity) ^{76}Ge detectors performed by Kirpichnikov and coworkers [19] because of their low statistics of 2.95 kg y would expect 0.9 counts. Their result is consistent with this expectation. Another Ge experiment (IGEX) using 8.8 kg of enriched ^{76}Ge, but collecting since beginning of the experiment in the early nineties till shutdown in end of 1999 only 8.8 kg y of statistics, could expect, according to our result, about 2.6 events. The result of that measurement is consistent

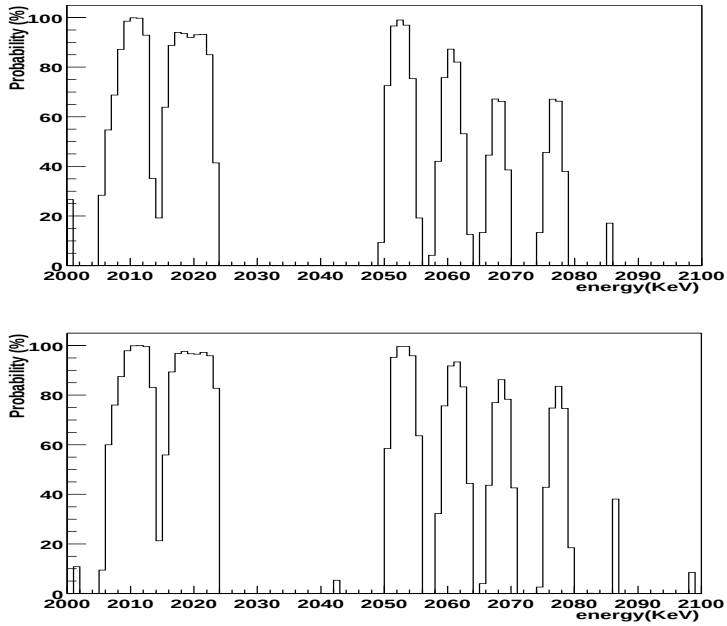

Figure 7: Peak scanning of the spectrum measured by Caldwell et al. [18], with the Maximum Likelihood method (upper part), and with the Bayesian method (lower part) (as in Figs. 3,6) (see [4]).

with this expectation.

The result described in section 2.1 has been questioned in some papers (Aalseth et al, hep-ex/0202018; Feruglio et al., Nucl. Phys. B 637(2002)345; Zdesenko et al., Phys. Lett. B 546(2002) 206, and Kirpichnikov, talk at Meeting of Physical Section of Russian Academy of Sciences, Moscow, December 2, 2002, and priv. communication, Dec. 3, 2002.) These claims against our results are incorrect in various ways. The answers are given in detail in [2, 4] and in [3].

2.3 *Half-Life and Effective Neutrino Mass*

Translating the observed number of events into half-lifes, we obtain [1, 2, 4] $T^{0\nu}_{1/2} = (0.8 - 18.3) \times 10^{25}$ y (95% c.l.) with a best value of 1.5×10^{25}y.

The result obtained is consistent with all other double beta experiments - which still reach less sensitivity. The most sensitive experiments following the HEIDELBERG-MOSCOW experiment are the geochemical ^{128}Te experiment with $T^{0\nu}_{1/2} > 2(7.7) \times 10^{24}$ y (68% c.l.), [20] the ^{136}Xe experiment by the DAMA group with $T^{0\nu}_{1/2} > 1.2 \times 10^{24}$ y (90% c.l.)[21], a second ^{76}Ge experiment with $T^{0\nu}_{1/2} > 1.2 \times 10^{24}$ y [19] and a ^{nat}Ge experiment with $T^{0\nu}_{1/2} > 1 \times 10^{24}$ y [18, 19]. Other experiments are already about a factor of 100 less sensitive concerning the $0\nu\beta\beta$ half-life: the Gotthard TPC experiment with ^{136}Xe yields [22] $T^{0\nu}_{1/2} > 4.4 \times 10^{23}$ y (90% c.l.) and the Milano Mibeta cryodetector experiment $T^{0\nu}_{1/2} > 1.44 \times 10^{23}$ y (90% c.l.). Another experiment with enriched ^{76}Ge, which has

stopped operation in 1999 after reaching a significance of 8.8 kg y, yields (if one believes their method of 'visual inspection' in their data analysis), in a conservative analysis, a limit of about $T^{0\nu}_{1/2} > 5 \times 10^{24}$ y (90% c.l.).

As a consequence of our result, lepton number is not conserved. Further the neutrino is a Majorana particle. If the $0\nu\beta\beta$ amplitude is dominated by exchange of a massive neutrino the effective mass $\langle m \rangle$ is deduced to be $\langle m \rangle = (0.11 - 0.56)$ eV (95% c.l.), with best value of 0.39 eV. Allowing conservatively for an uncertainty of the nuclear matrix elements of $\pm$ 50% (for detailed discussions of the status of nuclear matrix elements we refer to [9, 4] and references therein) this range may widen to $\langle m \rangle = (0.05 - 0.84)$ eV (95% c.l.).

Assuming other mechanisms to dominate the $0\nu\beta\beta$ decay amplitude, the result allows to set stringent limits on parameters of SUSY models, leptoquarks, compositeness, masses of heavy neutrinos, the right-handed W boson and possible violation of Lorentz invariance and equivalence principle in the neutrino sector. For a discussion and for references we refer to [9, 23, 26, 33, 38].

With the limit deduced for the effective neutrino mass, the HEIDELBERG-MOSCOW experiment excludes several of the neutrino mass scenarios allowed from present neutrino oscillation experiments (see Fig. 8) - allowing only for degenerate and inverse hierarchy mass scenarios [8].

Assuming the degenerate scenarios to be realized in nature we fix - according to the formulae derived in [7] - the common mass eigenvalue of the degenerate neutrinos to m = (0.05 - 3.4) eV. Part of the upper range is already excluded by tritium experiments, which give a limit of m $<$ 2.2-2.8 eV (95% c.l.) [29]. The full range can only partly (down to $\sim$ 0.5 eV) be checked by future tritium decay experiments, but could be checked by some future $\beta\beta$ experiments (see, e.g., next section). The deduced best value for the mass is consistent with expectations from experimental $\mu \rightarrow e\gamma$ branching limits in models assuming the generating mechanism for the neutrino mass to be also responsible for the recent indication for as anomalous magnetic moment of the muon [42]. It lies in a range of interest also for Z-burst models recently discussed as explanation for super-high energy cosmic ray events beyond the GKZ-cutoff [41, 44]. A recent model with underlying A_4 symmetry for the neutrino mixing matrix also leads to degenerate neutrino masses consistent with the present result from $0\nu\beta\beta$ decay [43]. The range of $\langle m \rangle$ fixed in this work is, already now, in the range to be explored by the satellite experiments MAP and PLANCK [7].

The neutrino mass deduced leads to $0.002 \geq \Omega_\nu h^2 \leq 0.1$ and thus may allow neutrinos to still play an important role as hot dark matter in the Universe [32].

3 The Future

With the HEIDELBERG-MOSCOW experiment, the era of the small smart experiments is over. New approaches and considerably enlarged experiments (as discussed, e.g. in [9, 26, 39, 25, 28]) will be required in future to fix the neutrino mass with higher accuracy.

Since it was realized in the HEIDELBERG-MOSCOW experiment, that the remaining small background is coming from the material close to the detector (holder, copper cap,

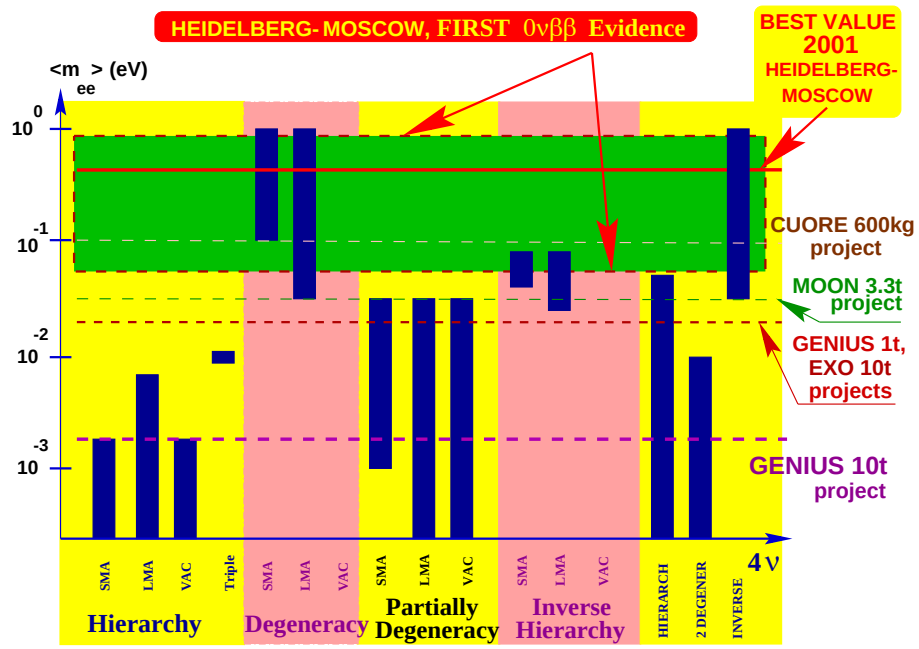

Figure 8: The impact of the evidence obtained for neutrinoless double beta decay in this paper (best value of the effective neutrino mass $\langle m \rangle = 0.39\,\mathrm{eV}$, 95% confidence range (0.05 - 0.84) eV - allowing already for an uncertainty of the nuclear matrix element of a factor of $\pm$ 50%) on possible neutrino mass schemes. The bars denote allowed ranges of $\langle m \rangle$ in different neutrino mass scenarios, still allowed by neutrino oscillation experiments (see [8]). Hierarchical models are excluded by the new $0\nu\beta\beta$ decay result. Also shown are the expected sensitivities for the future potential double beta experiments CUORE, MOON, EXO and the 1 ton and 10 ton project of GENIUS [9, 33, 39, 25].

...), elimination of *any* material close to the detector will be decisive. Experiments which do not take this into account, like, e.g. CUORE, and MAJORANA, will allow at best only rather limited steps in sensitivity. Furthermore there is the problem in cryodetectors that they cannot differentiate between a β and a γ signal, as this is possible in Ge experiments.

Another crucial point is - see eq. (4) - the energy resolution, which can be optimized *only* in experiments using Germanium detectors or bolometers. It will be difficult to probe evidence for this rare decay mode in experiments, which have to work - as result of their limited resolution - with energy windows around $Q_{\beta\beta}$ of several hundreds of keV, such as NEMO III, EXO, CAMEO.

Another important point is (see eq. 4), the efficiency of a detector for detection of a $\beta\beta$ signal. For example, with 14% efficiency a potential future 100 kg ^{82}Se NEMO experiment would be, because of its low efficiency, equivalent only to a 10 kg experiment (not talking about the energy resolution).

In the first proposal for a third generation double beta experiment, the GENIUS proposal [23, 24, 26, 39, 25], the idea is to use 'naked' Germanium detectors in a huge tank of liquid nitrogen. It seems to be at present the *only* proposal, which can fulfill *both* requirements mentioned above - to increase the detector mass and simultaneously reduce

the background drastically. GENIUS would - with only 100 kg of enriched ^{76}Ge - increase the confidence level of the present pulse shape discriminated $0\nu\beta\beta$ signal to 4σ within one year, and to 7σ within three years of measurement (a confirmation on a 4σ level by the MAJORANA project would at least need $\sim$230 years, the CUORE project would need (ignoring for the moment the problem of identification of the signal as a $\beta\beta$ signal) 3700 years). With ten tons of enriched ^{76}Ge GENIUS should be capable to investigate also whether the neutrino mass mechanism or another mechanism (see, e.g. [9]) is dominating the $0\nu\beta\beta$ decay amplitude. A GENIUS Test Facility is at present under construction in the GRAN SASSO Underground Laboratory [36, 35].

4 Conclusion

The observed indication for a non-vanishing Majorana neutrino mass by the HEIDELBERG-MOSCOW experiment opens a new era in space-time structure [40]. It has been shown [40] that the Majorana nature of the neutrino tells us that spacetime does realize a construct that is central to construction of supersymmetric theories.

From future projects to improve the present accuracy of the effective neutrino, the most sensitive and perhaps at the same time most realistic one, is the GENIUS project. GENIUS is the only of the new projects which simultaneously has a huge potential for cold dark matter search, and for real-time detection of low-energy neutrinos (see [23, 28, 30, 33, 37, 34, 38]).

5 Acknowledgement

The authors are indebted to their colleaques D. Mazza, C. Tomei, C. Dörr, G. Heusser and H. Strecker for their continuous help in running the HEIDELBERG-MOSCOW experiment, and C. Tomei, C. Dörr for the help in the analysis of the Bi lines. They are further grateful to their colleagues U. Sarkar, E. Ma, V. Bednyakov, S. Stoica for the efficient collaboration on the side of theory.

6 List of Proceedings During 2002

1. H.V. Klapdor-Kleingrothaus and R. Viollier (eds.), Dark Matter in Astro- and Particle Physics., Proc. of DARK2002, Cape Town, South Africa, February 4-9, 2002, Heidelberg, Germany: Springer (2002) 663 pp.

2. H.V. Klapdor-Kleingrothaus (ed.) Physics Beyond the Standard Model: Beyond the Desert 02, Proc. of Intern. Conf. BEYOND'02, Oulu, Finland, 2-7 Jun 2002, IOP, Bristol, 2003 (in preparation).

7 List of Publications During 2002

1. G. Bhattacharyya, H.V. Klapdor-Kleingrothaus, H. Päs and A. Pilaftsis, hep-ph/0212169, *"Neutrinoless Double Beta Decay from Singlet Neutrinos in Extra Dimensions."*

2. H.V. Klapdor-Kleingrothaus and U. Sarkar, hep-ph/0211274, Accept. for Publ. in Phys. Lett. B (2002) B, *"Neutrinoless double beta decay with scalar bilinears."*

3. H.V. Klapdor-Kleingrothaus, L. Baudis, A. Dietz, G. Heusser, I. Krivosheina, B. Majorovits and H. Strecker, Nucl. Instrum. Meth. A 481 (2002) 149-159, *"GENIUS-TF: a test facility for the GENIUS project."*

4. H.V. Klapdor-Kleingrothaus, Int. J. Mod. Phys. A 17 (2002) 3421-3431, *"Dark Matter Search"*.

5. H.V. Klapdor-Kleingrothaus, A. Dietz, I.V. Krivosheina, Part. Nucl. Lett. 110 (2002) 57-79, *"First Evidence for Neutrinoless Double Beta Decay."*

6. H.V. Klapdor-Kleingrothaus, A. Dietz, I.V. Krivosheina, Foundations of Phys. 32 (2002) 1181-1223, *"Neutrinoless Double Beta Decay: Status of Evidence."*

7. H.V. Klapdor-Kleingrothaus, E. Ma and U. Sarkar, Mod. Phys. Lett. A 17 (2002) 2221, e-Print Archive: hep-ph/0210156, *"Baryon and Lepton Number Violation with Scalar Bilinears."*

8. H.V. Klapdor-Kleingrothaus, *"Is the Neutrino a Majorana Particle?", Phys. in unserer Zeit 33 (2002) 155."*

9. I.V. Krivosheina, Prog. Part. Nucl. Phys. 48 (2002) 283-286, and e-Print Archive: hep-ph/0206149, *"Search for Cold Dark Matter and Solar Neutrinos with GENIUS and GENIUS-TF."*

10. H.V. Klapdor-Kleingrothaus, *"Reply to a Comment of Article "Evidence for Neutrinoless Double Beta Decay", hep-ph/0205228. "*

11. H.V. Klapdor-Kleingrothaus and U. Sarkar, Phys. Lett. B 532 (2002) 71-76, and e-Print Archive: hep-ph/0202006 *"Neutrino mixing schemes and neutrinoless double beta decay."*

12. H.V. Klapdor-Kleingrothaus and U. Sarkar, Phys. Lett. B 541 (2002) 332-337, e-Print Archive: hep-ph/0201226, *"Majorana neutrinos with split fermions in extra dimensions."*

13. H.V. Klapdor-Kleingrothaus, Nucl. Phys. Proc. Suppl. 110 (2002) 58-60, e-Print Archive: hep-ph/0206250, *"Search for Dark Matter by GENIUS-TF and GENIUS."*

14. H.V. Klapdor-Kleingrothaus, Nucl. Phys. Proc. Suppl. 110 (2002) 364-368, e-Print Archive: hep-ph/0206249, *"GENIUS - A New Underground Observatory for Non-Accelerator Particle Physics."*

15. V.A. Bednyakov, H.V. Klapdor-Kleingrothaus, V. Gronewold, Phys. Rev. D 66 (2002) 115005 and e-Print Archive: hep-ph/0208178, *"Squark-, Slepton- and Neutralino-Chargino coannihilation effects in the low-energy effective MSSM. "*

16. V.A. Bednyakov, H.V. Klapdor-Kleingrothaus, E. Zaiti, Phys. Rev. D 66 (2002) 015010, and e-Print Archive: hep-ph/0203108, *"Slepton and Neutralino/Chargino Coannihilations in MSSM."*

17. H. V. Klapdor-Kleingrothaus, A. Dietz, G. Heusser, I.V. Krivosheina, D. Mazza, H. Strecker, C. Tomei, Astroparticle Physics, Volume 18, Issue 5 (2003) pp.525-530, and e-Print Archive: hep-ph/0206151, *"First Results from the HDMS experiment in the Final Setup"*.

18. H.V. Klapdor-Kleingrothaus, Yad. Fiz. 65 (2002) 2135-2146 *"Neutrinoless Double-Beta Decay - Status of evidence and Future."*

19. I.V. Krivosheina, Yad. Fiz. 65 (2002) 2228-2233, *"Search for Cold Dark Matter and Solar Neutrinos with GENIUS and GENIUS-TF."*

20. H.V. Klapdor-Kleingrothaus, L. Baudis, A. Dietz, G. Heusser, B. Majorovits, H. Strecker, Astropart. Phys. 17 (2002) 383-391, *"Direct dark matter detection and neutrinoless double beta decay with an array of 40 kg of 'naked' natural Ge and 11 kg of enriched ^{76}Ge detectors in liquid nitrogen."*

8 List of Presentations at Conferences During 2002

1. I. Krivosheina, Meeting of Russian Academy of Science, Nuclear Physics Section, Moscow, ITEP, 3-5 December, 2002, *"GENIUS and GENIUS-TF - Future Detectors for Double Beta, Dark Matter and Solar Neutrino Search"*.

2. H.V. Klapdor-Kleingrothaus, Gran Sasso, Italy, 11 November 2002, DBD meeting, *"GENIUS - a Supersensitive Germanium Detector System for Rare Events"*.

3. H.V. Klapdor-Kleingrothaus, Intern. Conf. "Neutrinos and Implications for Physics Beyond the Standard Model", Stony Brook, USA, Oct. 11-13, 2002, *"Heidelberg-Moscow Experiment and First Evidence for Neutrinoless Double Beta Decay"*.

4. H.V. Klapdor-Kleingrothaus, International School on CP Violation, Baryogenesis and Neutrinos, Prerow, Germany, September 15 - 21, 2002, *"Heidelberg-Moscow Experiment and First Evidence for Neutrinoless Double Beta Decay"*.

5. I. Krivosheina, International School on CP Violation, Baryogenesis and Neutrinos, Prerow, Germany, September 15 - 21, 2002, *"GENIUS-TF and GENIUS: Future Detectors for Dark Matter and Solar Neutrinos"*.

6. H.V. Klapdor-Kleingrothaus, 4th International Workshop on the Identification of Dark Matter (IDM02), St. William's College, York Minster, York, England, 22-24 Sep. 2002, *"First Evidence for Neutrinoless Double Beta Decay"*.

7. H.V. Klapdor-Kleingrothaus and *I. Krivosheina, 4th International Workshop on the Identification of Dark Matter (IDM02), St. William's College, York Minster, York, England, 22-24 Sep. 2002, *"GENIUS-TF and GENIUS: Future Detectors for Dark Matter and Solar Neutrinos"*.

8. H.V. Klapdor-Kleingrothaus and *C. Tomei, 4th International Workshop on the Identification of Dark Matter (IDM02), St. William's College, York Minster, York, England, 22-24 Sep. 2002, *"Annual Modulation of Dark Matter Signal with GENIUS-TF"*.

9. H.V. Klapdor-Kleingrothaus, "Third International Conference on Physics Beyond the Standard Model "Accelerator, Non-Accelerator and Space Approaches", (BEYOND THE DESERT 02) Oulu, Finland, 2-7 Jun 2002, *"Majorana Neutrino Mass and Future Double Beta Experiments"*.

10. H.V. Klapdor-Kleingrothaus and *A. Dietz, "Third International Conference on Physics Beyond the Standard Model "Accelerator, Non-Accelerator and Space Approaches", (BEYOND THE DESERT 02) Oulu, Finland, 2-7 Jun 2002, *"Statistics of Rare Events"*.

11. H.V. Klapdor-Kleingrothaus and *I. Krivosheina, "Third International Conference on Physics Beyond the Standard Model "Accelerator, Non-Accelerator and Space Approaches", (BEYOND THE DESERT 02) Oulu, Finland, 2-7 Jun 2002, *"Dark Matter Search by GENIUS-TF and GENIUS"*.

12. *V.A. Bednyakov and H.V. Klapdor-Kleingrothaus, "Third International Conference on Physics Beyond the Standard Model "Accelerator, Non-Accelerator and Space Approaches", (BEYOND THE DESERT 02) Oulu, Finland, 2-7 Jun 2002, *"Slepton and Neutralino/Chargino Coannihilations in MSSM"*.

13. H.V. Klapdor-Kleingrothaus, Zacatecas Forum in Physics 2002, 11-13 May, 2002 Zacatecas, Mexico, *"Status of Double Beta Decay Research"*.

14. H.V. Klapdor-Kleingrothaus and *I. Krivosheina, Zacatecas Forum in Physics 2002, 11-13 MAY, 2002 Zacatecas, Mexico, *"GENIUS and GENIUS-TF: Future of dark matter and solar neutrino experiments"* .

15. H.V. Klapdor-Kleingrothaus and *C. Tomei, in IIIrd International Workshop on Low Energy Solar Neutrinos, LowNu 2002, 22-24 May, 2002, Heidelberg, Germany, *"GENIUS, a real-time detector for solar pp-neutrinos"*.

16. *A. Dietz, H.L. Harney, I.V. Krivosheina und H.V. Klapdor-Kleingrothaus, Deutsche Physikalische Gesellschaft e. V. (DPG), 18. - 22. März 2002, Leipzig, GERMANY, *"Statistische Methode für die Analyse von seltenen Zerfällen"*.

17. V.A. Bednyakov, H.V. Klapdor-Kleingrothaus, *E. Zaiti, Deutsche Physikalische Gesellschaft e. V. (DPG), 18. - 22. März 2002, Leipzig, GERMANY, *"Co-Annihilationen im MSSM"*.

18. *C. Dörr, V. Bobrakov, T. Kihm und H. V. Klapdor-Kleingrothaus, Deutsche Physikalische Gesellschaft e. V. (DPG), 18. - 22. März 2002, Leipzig, GERMANY, *"Neues Datenaufnahmesystem für GENIUS-TF."*

19. *A. Dietz, I. Krivosheina, D. Mazza, H. Strecker, C. Tomei, H.V. Klapdor-Kleingrothaus Deutsche Physikalische Gesellschaft e. V. (DPG), 18.-22. März 2002, Leipzig, GERMANY, *"Das Heidelberg Dark Matter Search Experiment (HDMS)"*.

20. *C. Tomei, H.V. Klapdor-Kleingrothaus, A. Dietz, Ch. Dörr, I. Krivosheina, D. Mazza and H. Strecker, Deutsche Physikalische Gesellschaft e. V. (DPG), 18. - 22. März 2002, Leipzig, GERMANY, *"Potential of GENIUS-TF in searching for the annual modulation of a Dark Matter signal.*

21. *H.V. Klapdor-Kleingrothaus, A. Dietz, I.V. Krivosheina, 5th Intern. UCLA Symposium on "Sources and Detection of Dark Matter and Dark Energy in the Universe" (dm2002), February 20-22, 2002, Marina del Rey, CA, USA, *"Evidence for Neutrinoless Double Beta Decay and Search for Dark Matter with GENIUS and GENIUS TF"* .

22. *H.V. Klapdor-Kleingrothaus, A. Dietz, I.V. Krivosheina, Fourth International Heidelberg Conference on "DARK MATTER IN ASTRO AND PARTICLE PHYSICS " (DARK 2002). Cape Town, South Africa, February 4-9, 2002, *"Evidence for Neutrinoless Double Beta Decay and Hot Dark Matter"* .

23. H.V. Klapdor-Kleingrothaus and *I. Krivosheina, Fourth International Heidelberg Conference on "DARK MATTER IN ASTRO AND PARTICLE PHYSICS " (DARK 2002). Cape Town, South Africa, February 4-9, 2002, *"Dark Matter Search by GENIUS-TF and GENIUS"*.

24. H.V. Klapdor-Kleingrothaus, Double Beta Experiments in EUROPE, ApPEC, January 21 - 22, 2002, Paris, France, *"Double Beta Decay and its Potential for Neutrino Mass and Other Beyond Standard Model Physics"*.

9 List of Conference Contributions Published in 2002

1. A. Dietz, H.L. Harney, I.V. Krivosheina and H.V. Klapdor-Kleingrothaus, Deutsche Physikalische Gesellschaft e. V. (DPG), 18. - 22. März 2002, Leipzig, GERMANY, *"Statistische Methode für die Analyse von seltenen Zerfällen"*, T 405.1, p.109.

2. V.A. Bednyakov, H.V. Klapdor-Kleingrothaus, E. Zaiti, Deutsche Physikalische Gesellschaft e. V. (DPG), 18. - 22. März 2002, Leipzig, GERMANY, *"Co-Annihilationen im MSSM"*, T. 204.7, p.92.

3. C. Dörr, V. Bobrakov, T. Kihm und H. V. Klapdor-Kleingrothaus, Deutsche Physikalische Gesellschaft e. V. (DPG), 18. - 22. März 2002, Leipzig, GERMANY, *"Neues Datenaufnahmesystem für GENIUS-TF"*, T. 209.4, p.96.

4. *A. Dietz, I. Krivosheina, D. Mazza, H. Strecker, C. Tomei, H.V. Klapdor-Kleingrothaus Deutsche Physikalische Gesellschaft e. V. (DPG), 18. - 22. März 2002, Leipzig, GERMANY, *"Das Heidelberg Dark Matter Search Experiment (HDMS)"*, T. 501.2, p. 114.

5. C. Tomei, H.V. Klapdor-Kleingrothaus, A. Dietz, Ch. Dörr, I. Krivosheina, D. Mazza and H. Strecker, Deutsche Physikalische Gesellschaft e. V. (DPG), 18. - 22. März 2002, Leipzig, GERMANY, *"Potential of GENIUS-TF in searching for the annual modulation of a Dark Matter signal*, T. 501.3, p.114.

6. H.V. Klapdor-Kleingrothaus, A. Dietz, I.V. Krivosheina, in Proc. of 5th Intern. UCLA Symposium on "Sources and Detection of Dark Matter and Dark Energy in the Universe" (dm2002), February 20-22, 2002, Marina del Rey, CA, USA, *"Evidence for Neutrinoless Double Beta Decay and Search for Dark Matter with GENIUS and GENIUS TF"* .

7. H.V. Klapdor-Kleingrothaus, A. Dietz, I.V. Krivosheina, in Proc. of DARK2002, Cape Town, South Africa, February 4-9, 2002, eds. H.V. Klapdor-Kleingrothaus and R. Viollier, Springer, Heidelberg (2002), 367-403, *"Evidence for Neutrinoless Double Beta Decay and Hot Dark Matter"* .

8. H.V. Klapdor-Kleingrothaus, A. Dietz, I.V. Krivosheina, in Proc. of DARK2002, Cape Town, South Africa, February 4-9, 2002, eds. H.V. Klapdor-Kleingrothaus and R. Viollier, Springer, Heidelberg (2002), 404-411, *"Evidence for Neutrinoless Double Beta Decay and Revisited - Reply to a Comment"*.

9. H.V. Klapdor-Kleingrothaus and I. Krivosheina, in Proc. of DARK2002, Cape Town, South Africa, February 4 - 9, 2002, eds. H.V. Klapdor-Kleingrothaus and R. Viollier, Springer, Heidelberg (2002), 473-484, *"Dark Matter Search by GENIUS-TF and GENIUS"*.

10. I.V. Krivosheina, in Proc. of Intern. Conf. on Flavor Physics (ICFP2001), May 31-June 6, 2001, Zhang-Jia-Jie City, Hunan, China, World Scientific (2002) 387-406, *"Latest Results from the HEIDELBERG-MOSCOW Experiment for Neutrino Mass and Cold Dark Matter"*.

11. H.V. Klapdor-Kleingrothaus, in Proc. of ICFP2001, May 31-June 6, 2001, Zhang-Jia-Jie City, Hunan, China, World scientific (2002) 93-110, *"Complementary information to the Neutrino Mass Matrix from Double Beta Decay"*.

12. H.V. Klapdor-Kleingrothaus, in Proc. of ICTP 6th School on Nonaccelerator Astroparticle Physics, Trieste, Italy, 9-20 Jul 2001, "Trieste 2001, Non-accelerator astroparticle physics" World Scientific, Singapure (2002) 148-174, and e-Print Archive: hep-ph/0211033. *"Searches for Dark Matter and for Neutrino Masses with Underground Detectors"*.

10 List of Colloquia and Seminars Made During 2002

1. H.V. Klapdor-Kleingrothaus, Double Beta Experiments in Europe, ApPEC, Paris, France, 21-22.01.2002, *"Double Beta Decay and its Potential for Neutrino Mass and Other Beyond Standard Model Physics"*.

2. H.V. Klapdor-Kleingrothaus, CERN Particle Physics Seminar, April 16, 2002, CERN, Main Auditorium at CERN, Switzerland, *"Status of Double Beta Decay Search"*.

3. H.V. Klapdor-Kleingrothaus, Kaffeepalaver im Bothelabor, April 25, 2002, Max-Planck-Institut für Kernphysik, Heidelberg, Germany, *"Status of Double Beta Decay Search"*.

4. H.V. Klapdor-Kleingrothaus, DESY-Seminar, 7.05.2002, DESY, Main Auditorium at DESY, Hamburg, Germany, *"Status of Double Beta Decay Search"*.

5. H.V. Klapdor-Kleingrothaus, Seminar I. Physikalisches Institut, July 2, 2002, Aachen, Germany, *"Status of Double Beta Decay Search"*.

6. H.V. Klapdor-Kleingrothaus, Seminar in Institut für Kernphysik, Forschungszentrum Karlsruhe, Germany, 9.07.2002, *"Status of Double Beta Decay Search"*.

7. H.V. Klapdor-Kleingrothaus, Seminar PPD - Rutherford Appleton Lab., 9 September, 2002, England, *"First Evidence for Neutrinoless Double Beta Decay - and Future of the Field"*.

8. H.V. Klapdor-Kleingrothaus, Department of Particle Physics, ELEMENTARY PARTICLE PHYSICS SEMINARS, Oxford, England, 10 September, 2002, *"First Evidence for Neutrinoless Double Beta Decay - and Physics Beyond the Standard Model"*.

9. H.V. Klapdor-Kleingrothaus, The P/T Colloquium, Los Alamos, Theoretical Division, Los Alamos Nat. Lab., USA, 3 October 2002 *"Status of Evidence for Neutrinoless Double Beta Decay Search - and the Future"*.

10. H.V. Klapdor-Kleingrothaus, Dept. of Chemistry, University of Missouri, Rolla, USA, 7 October, 2002, *"First Evidence for Neutrinoless Double Beta Decay - and Implications"*.

11. H.V. Klapdor-Kleingrothaus, Brookhaven National Laboratory, Physics Dept., Upton, USA, 15 October, USA, *"First Evidence for Neutrinoless Double Beta Decay - and Implications"*.

12. H.V. Klapdor-Kleingrothaus, Physics Department Colloquium, Princeton University, Jadwin Hall A10, USA, 16 October, 2002, *"First Evidence for Neutrinoless Double Beta Decay - and Implications"*.

13. H.V. Klapdor-Kleingrothaus, Northeastern University, 216 DANA Physics Building, Boston, USA, 17.10.2002, *"First Evidence for Neutrinoless Double Beta Decay - and Implications"*.

14. H.V. Klapdor-Kleingrothaus, Dept of Physics, University of Maryland, College Park, USA, 22 October, 2002, *"First Evidence for Neutrinoless Double Beta Decay - and Implications"*.

15. H.V. Klapdor-Kleingrothaus, Texas A&M University Physics Department, College Station, Texas, 24.10.2002, *"First Evidence for Neutrinoless Double Beta Decay - and Implications"*.

16. H.V. Klapdor-Kleingrothaus, GRAN SASSO National Laboratory, "B. Pontecorvo" Room, Assergi, Italy, 7.11.2002 *"First Evidence for Neutrinoless Double Beta Decay - and Future of the Field"*.

17. H.V. Klapdor-Kleingrothaus, NIKHEF, Amsterdam, Netherlands, 22 November, 2002 *"First Evidence for Neutrinoless Double Beta Decay - and Future of the Field"*.

18. Physics Department of Moscow State University, Moscow, Russia, 3.12.2002 *"First Evidence for Neutrinoless Double Beta Decay - and Future of the Field"*.

19. Laboratory of Nuclear Problems, Joint Institute for Nuclear Research, Dubna, Russia, 4 December, 2002 *"First Evidence for Neutrinoless Double Beta Decay - and Future of the Field"*.

References

[1] H.V. Klapdor-Kleingrothaus et al. hep-ph/0201231 and *Mod. Phys. Lett.* **A 16** (2001) 2409-2420.

[2] H.V. Klapdor-Kleingrothaus, A. Dietz and I.V. Krivosheina, *Part. and Nucl.* **110** (2002) 57-79.

[3] H.V. Klapdor-Kleingrothaus, hep-ph/0205228, and in Proc. of DARK2002, Cape Town, South Africa, February 4-9, 2002, Springer, Heidelberg (2002), 404 - 411.

[4] H.V. Klapdor-Kleingrothaus, A. Dietz and I.V. Krivosheina, *Foundations of Physics* **31** (2002) 1181-1223, and Corrigenda, 2003, and home-page: http://www.mpi-hd.mpg.de/non_acc/main_results.html.

[5] H.V. Klapdor-Kleingrothaus et al., (HEIDELBERG-MOSCOW Collaboration), Eur. Phys. J. **A 12** (2001) 147 and hep-ph/0103062, and in Proc. of DARK2000, H.V. Klapdor-Kleingrothaus (Editor), Springer-Verlag Heidelberg, (2001) 520-533 and *http* : *//www.mpi* − *hd.mpg.de/non_acc/*.

[6] H.V. Klapdor-Kleingrothaus et al., to be publ. in 2003.

[7] H.V. Klapdor-Kleingrothaus, H. Päs and A.Yu. Smirnov, *Phys. Rev.* **D 63** (2001) 073005 and *hep-ph/***0003219**; in Proc. of DARK'2000, Heidelberg, 10-15 July, 2000, Germany, ed. H.V. Klapdor-Kleingrothaus, *Springer, Heidelberg* (2001) 420-434.

[8] H.V. Klapdor-Kleingrothaus and U. Sarkar, *Mod. Phys. Lett.* **A 16** (2001) 2409.

[9] H.V. Klapdor-Kleingrothaus, "60 Years of Double Beta Decay - From Nuclear Physics to Beyond the Standard Model", *World Scientific, Singapore* (2001) 1281 p.

[10] J. Hellmig and H.V. Klapdor-Kleingrothaus, *Nucl. Instrum. Meth.* **A455** (2000) 638.

[11] J. Hellmig, F. Petry and H.V. Klapdor-Kleingrothaus, *Patent* **DE19721323A**.

[12] B. Majorovits and H.V. Klapdor-Kleingrothaus. *Eur. Phys. J.* **A 6** (1999) 463.

[13] A. Staudt, K. Muto and H.V. Klapdor-Kleingrothaus, *Eur. Lett.* **13** (1990) 31.

[14] R.B. Firestone and V.S. Shirley, Table of Isotopes, 8-th Edition, *John Wiley and Sons*, Incorp., N.Y. (1998).

[15] G. Douysset et al., *Phys. Rev. Lett.* **86** (2001) 4259 - 4262.

[16] J.G. Hykawy et al., *Phys. Rev. Lett.* **67** (1991) 1708.

[17] Ch. Dörr, Diplomarbeit (2002), Univ. of Heidelberg, unpublished.

[18] D. Caldwell, *J. Phys. G* **17**, S137-S144 (1991).

[19] A.A. Vasenko, I.V. Kirpichnikov et al., *Mod. Phys. Lett.***A 5** (1990) 1299-1306.

[20] O. Manuel et al., in Proc. Intern. Conf. Nuclear Beta Decays and the Neutrino, eds. T. Kotani et al., World Scientific (1986) 71, *J. Phys. G: Nucl. Part. Phys.* **17** (1991) S221-S229; T. Bernatovicz et al. *Phys. Rev. Lett.* (1992) 2341.

[21] R. Bernabei et al., *Phys. Lett.* (2002) 23-28.

[22] R. Lüscher et al., *Phys. Lett.* (1998) 407.

[23] H.V. Klapdor-Kleingrothaus in Proc. of BEYOND'97, Castle Ringberg, Germany, 8-14 June 1997, edited by H.V. Klapdor-Kleingrothaus and H. Päs, *IOP Bristol* (1998) 485 - 531 and in *Int. J. Mod. Phys.* **A 13** (1998) 3953.

[24] H.V. Klapdor-Kleingrothaus, J. Hellmig and M. Hirsch, *J. Phys.* **G 24** (1998) 483.

[25] H.V. Klapdor-Kleingrothaus et al. **MPI-Report MPI-H-V26-1999** and Proc. of BEYOND'99, Castle Ringberg, Germany, 6-12 June 1999, eds. by H.V. Klapdor-Kleingrothaus and I.V. Krivosheina, *IOP Bristol* (2000) 915 - 1014.

[26] H.V. Klapdor-Kleingrothaus, in Proc. of 18th Int. Conf. on NEUTRINO 98, Takayama, Japan, 4-9 Jun 1998, (eds) Y. Suzuki et al. *Nucl. Phys. Proc. Suppl.* **77** (1999) 357 - 368.

[27] HEIDELBERG-MOSCOW Coll. (M. Günther et al.), Phys. Rev. **D55** (1997) 54.

[28] H.V. Klapdor-Kleingrothaus, in Proc. of Int. Conference NOW2000 - "Origins of Neutrino Oscillations", ed. G. Fogli, *Nucl. Phys.* **B 100** (2001) 309 - 313.

[29] J. Bonn et al., in Proc. of NEUTRINO2000, (2000), ed. J. Law et al. *Nucl. Phys.* **B 91** (2001) 273 - 279.

[30] V.A. Bednyakov and H.V. Klapdor-Kleingrothaus, *hep-ph/***0011233** and *Phys. Rev.* **D 63** (2001) 095005.

[31] H.V. Klapdor-Kleingrothaus, in Proc. of the Int. Sympos. on Advances in Nuclear Physics, eds.: D. Poenaru and S. Stoica, *World Scientific, Singapore* (2000) 123-129.

[32] H.V. Klapdor-Kleingrothaus, *Int. J. Mod. Phys.* **A17** (2002) 3421-3431, in Proc. of Intern Conf. LP01, Rome, Italy, July 2001.

[33] H.V. Klapdor-Kleingrothaus, *Springer Tracts in Modern Physics*, **163** (2000) 69-104, *Springer-Verlag, Heidelberg, Germany* (2000).

[34] H.V. Klapdor-Kleingrothaus, in Proc. Int. Workshop on Low Energy Solar Neutrinos, LowNu2, Dec. 4-5. ed: Y. Suzuki et al. *World Scientific, Singapore* (2001) 116-132.

[35] H.V. Klapdor-Kleingrothaus, Internal Report **MPI-H-V32-2000**.

[36] H.V. Klapdor-Kleingrothaus et al., *hep-ph/*0103082, *Nucl.Instr.Meth.* **A481** (2002) 149-159.

[37] H.V. Klapdor-Kleingrothaus and I.V. Krivosheina, in Proc. of "Forum of Physics", Zacatecas, Mexico, 11-13 May, 2002, eds. D.V. Ahluwalia et al.

[38] H.V. Klapdor-Kleingrothaus, in Proc. of NANPino-2000, Dubna, July 19-22, 2000, *Particles and Nuclei, Letters* iss. 1/2 (2001) and *hep-ph/* **0102319**.

[39] H.V. Klapdor-Kleingrothaus, hep-ph/0103074 and in Proc. of NOON 2000, Tokyo, Japan, 6-18 Dec. 2000, ed: Y. Suzuki et al., *World Scientific* (2001).

[40] D.V. Ahluwalia in Proc. of Beyond the Desert 2002, BEYOND02, Oulu, Finland, June 2002, IOP 2003, ed. H.V. Klapdor-Kleingrothaus: D.V. Ahluwalia and M. Kirchbach *Phys. Lett.* **B 529** (2002) 124.

[41] D. Fargion et al., in Proc. of DARK2000, Heidelberg, Germany, July 10-15, 2000, Ed. H.V. Klapdor-Kleingrothaus, *Springer, Heidelberg*, (2001) 455-468, and in Proc. of BEYOND02, Oulu, Finland, June 2002, IOP 2003, ed. H.V. Klapdor-Kleingrothaus.

[42] E. Ma and M. Raidal, *Phys. Rev. Lett.* **87** (2001) 011802; Erratum-ibid. **87** (2001) 159901.

[43] K.S. Babu, E. Ma and J.W.F. Valle, hep-ph/0206292.

[44] Z. Fodor et al., *JHEP* (2002) 0206:046, or hep-ph/0203198, and Z. Fodor, in Proc. of BEYOND'02, Oulu, Finland, 2-7 Juny 2002, IOP, Bristol, 2003, ed. H.V. Klapdor-Kleingrothaus and hep-ph/0210123.

ICARUS. Imaging Cosmic and Rare Underground Signals

S. Amoruso[a], P. Aprili[b], F. Arneodo[b], B. Babussinov[c], B. Badełek[d], A. Badertscher[e], M. Baldo Ceolin [c], G. Battistoni [f], B. Bekman[g], P. Benetti [h], M. Bischofberger[e], A. Borio di Tigliole[h], R. Brunetti[h], R. Bruzzese[a], A. Bueno[i], E. Calligarich[h], F. Carbonara[a], D. Cavalli[f], F. Cavanna[j], P. Cennini[k], S. Centro[c], A. Cesana[l], C. Chen[m], Y. Chen[m], D. Cline[n], A.G. Cocco[a], P. Crivelli[e], A. Dąbrowska[o], Z. Dai[e], C. De Vecchi[h], R. Dolfini[h], A. Ereditato[a], M. Felcini[e], A. Ferrari[k], F. Ferri[j], G. Fiorillo[a], S. Galli[j], Y. Ge[e], D. Gibin [c], A. Gigli Berzolari[h], I. Gil-Botella[e], K. Graczyk[p], L. Grandi[h], A. Guglielmi [c], K. He[m], J. Holeczek[g], X. Huang[m], C. Juszczak[p], D. Kiełczewska[d], J. Kisiel[g], L. Knecht[e], T. Kozłowski[q], H. Kuna-Ciskał[r], M. Laffranchi[e], J. Łagoda [d], Z. Li[m], B. Lisowski[n], F. Lu[m], J. Ma[m], N. Makrouchina[n], G. Mangano[a], G. Mannocchi[t], M. Markiewicz[s], A. Martinez de la Ossa[i], M. Maślak[r], C. Matthey[n], F. Mauri[h], G. Meng [c], M. Messina[e], C. Montanari[h], S. Muraro[f], G. Natterer[e], S. Navas-Concha[i], M. Nicoletto [c], S. Otwinowski[n], O. Palamara[b], D. Pascoli[c], L. Periale[t], G. Piano Mortari[j], A. Piazzoli[h], P. Picchi[t], F. Pietropaolo[c], W. Półchłopek [s], T. Rancati[f], A. Rappoldi[h], G.L. Raselli[h], J. Rico[e], E. Rondio[q], M. Rossella[h], A. Rubbia[e], **C. Rubbia**[h,*] P. Sala[e], D. Scannicchio[h], E. Segreto[j], Y. Seo[n], F. Sergiampietri[u], J. Sobczyk [p], N. Spinelli[a], J. Stepaniak[q], M. Szarska[o], M. Szeptycka[q], M. Terrani[l], L. Velotta[a], S. Ventura[c], C. Vignoli[h], H. Wang[n], X. Wang[a], M. Wójcik [v], G. Xu[m], X. Yang[n], A. Zalewska[o], J. Zalipska [q], C. Zhang[m], Q. Zhang[m], S. Zhen[m], W. Zipper [g]

[*] **Spokesman of the ICARUS Collaboration**

[a] Dip. Di Scienze Fisiche UniversitFederico II and INFN Sezione di Napoli, Italy
[b] Lab. Naz. del Gran Sasso, INFN, Assergi (AQ), Italy
[c] Dip. di Fisica and INFN, Università di Padova, Italy
[d] Institute of Experimental Physics, Warsaw University, Warszawa, Poland
[e] Institute for Particle Physics, ETH Hönggerberg, Zürich, Switzerland
[f] Dip. di Fisica and INFN, Università di Milano, Italy
[g] Institute of Physics, University of Silesia, Katowice, Poland
[h] Dip. di Fisica and INFN, Università di Pavia, Italy
[i] Dep. de Fsica Terica y del Cosmos and Centro Andaluz de Fsica de Partculas Elementales, Universidad de Granada, Spain
[j] Dip. di Fisica and INFN, Università dell'Aquila, Italy
[k] CERN, CH 1211 Geneva 23, Switzerland
[l] Politecnico di Milano and INFN, Milano, Italy
[m] IHEP – Academia Sinica, 19 Yuqnan Road, Beijing, People's Republic of China
[n] Department of Physics UCLA, Los Angeles, CA, USA
[o] H.Niewodniczański Institute of Nuclear Physics, Kraków, Poland
[p] Institute of Theoretical Physics, Wrocław University, Wrocław, Poland
[q] A.Sołtan Institute for Nuclear Studies, Warszawa, Poland
[r] Cracow University of Technology, Kraków, Poland
[s] University of Mining and Metallurgy, Kraków, Poland
[t] ICGF del CNR, Torino, Italy
[u] INFN Pisa, San Piero a Grado,Italy
[v] Institute of Physics, Jagellonian University, Kraków, Poland

Abstract

The major achievements of the 2002 activity of the ICARUS Collaboration have been the completion of the assembly of the inner detector of the second T600 half-module and the analysis of the events collected during the 2001 surface run in Pavia, aimed at the development of algorithms for the geometrical and kinematical reconstruction of future underground events. In addition, the ICARUS Collaboration undertook the developmentof the "Final Project" of the LNGS site installation needed in particular to produce the "Risk Analysis" document of the ICARUS underground plant.

1 Introduction

Since the original proposal [1] an extensive R&D program lasting more than 12 years has demonstrated the feasibility of the liquid Argon (LAr) technology for the realization of large mass TPC detectors for astroparticle experiments. During this time several devices with fiducial volume up to 2000 l have been realized and successfully operated.

In 1997 the ICARUS T600 [2] detector was approved and the realization of a two semi-modules detector with total mass of about 600 ton started. This program was completed in August 2001 with an 100-days cosmic-ray run of the first 300 ton semimodule. No

major problems were experienced during the data taking. All the detector functionalities have been extensively tested and more than 20,000 cosmic rays events have been recorded. The run was performed at surface in the Pavia Laboratory with a cosmic event rate about one million times higher then in the underground hall at LNGS. Events were efficiently taken and reconstructed in 3D with a readout granularity of a few millimeters all over the large inner volume. Calorimetric information from ionizating particles were also exploited obtaining the excellent resolution of $\Delta E/E \approx 4\%$.

The tested detector is to be considered as the basic module to build-up a larger total fiducial mass (3000 ton) required to exploit the CNGS neutrino beam for oscillation searches. After the major achievement of the first T600 half-module commissioning the ICARUS Collaboration started to work on other demanding subjects:

- The analysis of the collected cosmic-ray events with the main aim of developing algorithms for the geometrical and kinematical reconstruction of the events taken in the underground operation.
- The development of the site installation project to provide information to the Risk Analysis of the ICARUS underground plant and to prepare the following tenders for the plant implementation. The tenders will concern the "Executive Project" together with the realization of the ICARUS site in the underground Laboratory. The project activity started rigth after the LNGS management assigned to ICARUS the LNGS Hall B.
- The design of the next 1200 ton detector (ICARUS T1200) [3].

All above activities have been basically completed. We are only missing the final agreement of LNGS on safety matters required to start-up the tendering procedure for the T600 installation (planned for 2003).

2 The ICARUS T600 Detector

The ICARUS T600 detector has been extensively described in several papers; among these we refer in particular to the LNGS Annual Report of 2000 and 2001 [4]. ICARUS T600 is a large cryostat split in two identical, adjacent half-modules ($3.6 \times 3.9 \times 19.3 m^3$) each one housing an inner detector composed by two Time Projection Chambers (TPC), the field shaping system, monitors and probes, and by a system for the LAr scintillation light detection. The inner detector is externally surrounded by a set of thermal insulation layers. Outside the detector is placed the read-out electronics (on the top side) and the cryogenic plant composed of a liquid Nitrogen cooling circuit needed to maintain uniform the LAr temperature, and of a system of LAr purifiers to keep the LAr purity at the required level.

3 The assembly of the second 300 ton half-module inner detector

The second half-module of the ICARUS T600 detector was delivered to the assembly hall in Pavia in August 2000. The mounting of the inner detector was delayed until completion of the tests of the first half-module (beginning of 2002). As for the first half-module, the assembly of the secon half-module was performed in a 100,000 class clean room and made use of a suitable mechanical platform (assembly island) to ease the mounting procedures.

The wire chambers' sustaining structure was mounted outside the cryostat, on the assembly island, and then moved inside the cryostat by means of rails. The alignment of the components of the whole structure has been carefully measured, using optical theodolite devices. A precision of the order of 0.3 mm, namely the device precision limit, was obtained, in accordance with the figure for the first half-module. This result is important because the accuracy in the event reconstruction, that depends on the distance between adjacent wires pairs and on the parallelism of the three wire planes, entirely relies on the mechanical quality of the sustaining structure. Furthermore, the quality of the mechanics assures that during the cooling phase and at the cryogenic temperature (87 K), no stress is induced on the wires and all components remain in the required precision range.

In June 2002 the nearly 30,000 wires in the three wire planes of the second half-module started to be positioned onto the sustaining frame. The wiring of the corresponding 832 modules (32 wires each) had been done months earlier, by using a semi-automatic wiring table. The positioning operation resulted to be very fast (of the order of 12 modules per hour).

The scintillation light detection system and the slow control devices were anchored to the sustaining structure as well. The use of a set of 54 PMTs in a suitable geometrical arrangement allows event-by-event the detection of the light produced in the detector drift volume. The PMTs (9354FLA Electron Tubes Ltd.) were characterised in laboratory for what concerns their functioning at low temperature. The sand-blasted window of each PMT was coated with a wavelengh shifter (tetra-phenil-butatiene). A voltage divider designed to work at low temperature was welded directly on the PMT output leads. The PMT dimensions were compatible with the T600 mechanical constraints which imposed their mounting in the 300 mm space left behind the wire planes by means of a dedicated sustaining structure. The sustaining system allowed the PMT positioning behind the collection planes 5 mm far from the wires (Fig. 1). The PMT bases were electrically connected via 8 m long RG316 cables to dedicated H.V. feed-through flanged on the detector signal chimneys.

4 Analysis of events taken 10m^3 prototype and with the 300 ton half-module

A detailed analysis of the performance of the ICARUS LAr TPC operating at LNGS in a $10m^3$ cryostat was carried out and the results published (publication n. 1). The main

Figure 1: The 27 photomultipliers of one wall used for the detection of the scintillation ligth.

issues were: optimization of the signal extraction procedures, measurement of the electron drift velocity and of the electron life-time in Lar, calorimetric reconstruction of the events.

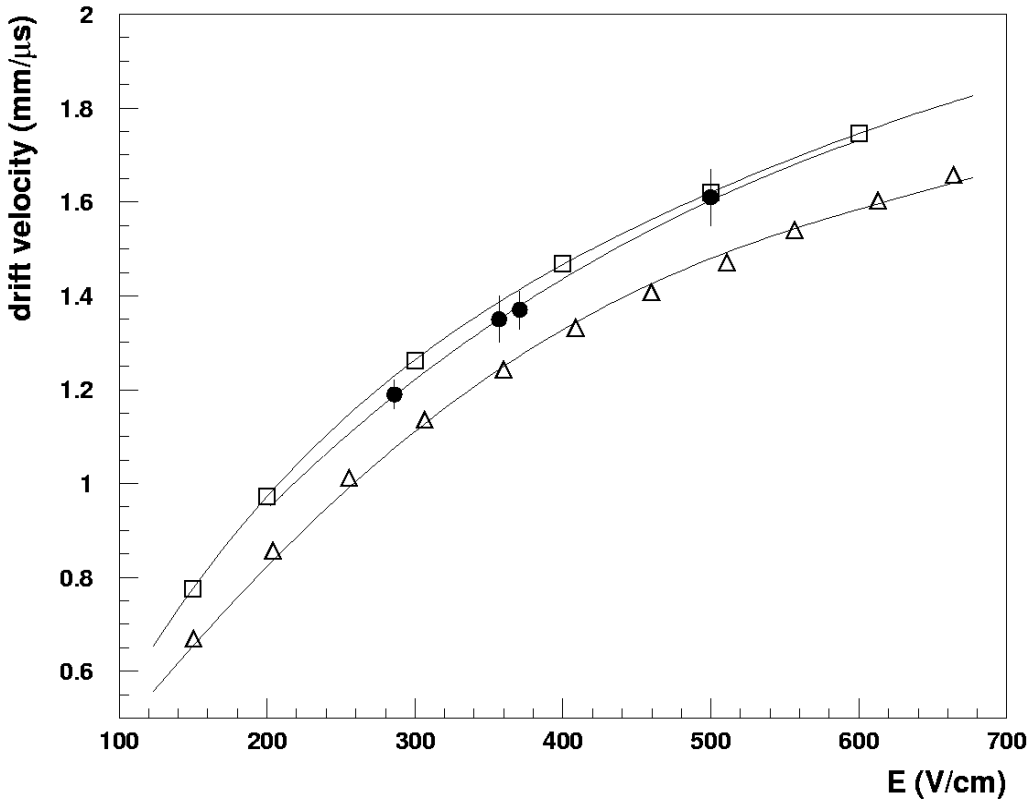

Figure 2: Mean values of the drift velocity for different electric fields. Data of "3 t prototype" are open squares at 87K and open triangles at 92K, data of 10 m^3 are full dots at 88K.

The mean value and relative error of the drift velocity from the track samples at different electric fields are reported in Fig. 2. On the same plot, for comparison, the measurements done with the ICARUS "3 t prototype" in the same range of electric fields are also shown. The values corresponding to the "3 t prototype" (open squares) are close to the measurements with the $10m^3$ (full dots). Estimates of the drift electron life-time are obtained directly from the attenuation of the signal amplitude observed at increasing drift distance from the wire chamber. In order to evaluate the evolution of the electron life-time during the test, groups of consecutive runs taken in periods of 24 h each have been analysed separately. In Fig. 3 life-time measurements for six consecutive periods are reported. These results are in good agreement with the values obtained independently using the Lar purity monitors.

We then analized data taken with the 300 ton half-module to prove the observation of long ionizing tracks with lengths up to 20 meters. As mentioned above, the data were

collected during a 100 days exposure of the detector to cosmic rays at see level (in Pavia, Italy May-July 2001). The primary goal of the test was to check the detector performance, before it is transported to the Gran Sasso underground Laboratory, and demonstrate that a complete scaling-up from small sized prototypes has been achieved. Pictures of typical events showing the excellent imaging capabilities and granularity are given in Fig. 4 where the horizontal axis is the wire coordinate and the vertical one is the drift-time coordinate.

The analysis of δ rays produced along the muon track collected with the T300 detector provides a direct check of the "scaling up" by comparison with similar analyses performed with smaller size prototypes. A total of 328 δ ray events were selected and their energy was individually measured with over a total length of 68 m of muon tracks. The measured δ rays energy spectrum is shown in Fig. 5. The continuous line represents the best fit by the Mott formula. The results show consistency between predictions and data. Accounting for the different cut-off criteria and geometrical efficiency of the detector the results also agree with those obtained with a 50-litres prototype.

The LAr purity is potentially a critical item to obtain the best achievable performance of the detector. The proper modeling of the observed purity curve is important because in principle it allows to extrapolate the purity behaviour after long period of time (asymptotic trend) or to a detector with longer (3 meter) drift length, as foreseen for the T1200 detector. The imput data come from on-line measurements with purity monitors immersed in the LAr volume and from the off-line analysis based on the fit of long tracks to a Landau distribution to find the most probable energy loss as a function of the drift length. The two analyses yield compatible results. In Fig. 6 the drift electron life-time is shown versus the run elapsed time. The maximum obtained life-time is 1.7 ms, providing good expectations for the final multi kton detector. Data are consistent with a purity recirculation efficiency of 100%. The regions with decreasing trend correspond to LAr and GAr recirculation off.

We also used stopping muon tracks in the 300 ton half-module to verify the expected multiple scattering behavior and to check the consistency with Monte Carlo predictions. The method used to determine the muon momentum from the multiple scattering experienced by its track is based on the measurement of the truncated RMS (in order to get rid of the Moliere tail) of the scattering angles projected onto the plane containing the drift coordinate. The FLUKA Monte Carlo prediction of the RMS as a function of the muon momentum is given in Fig. 7 and is compared with data. The energy range is limited to 1 GeV because this is the upper limit for a muon stopping in the chamber. In Fig. 8 the behaviour of the measured resolution (%) is shown against the muon energy extrapolated to 5 GeV. It is worth nothing that in this energy range the resolution is comparable with what obtained with dedicated muon spectrometers.

We also exploited the signals produced by very 'large' events to measure the electron drift velocity in the 300 ton half-module. For a given high voltage and for each analyzed event, the signal from all wires is projected on the drift time coordinate. The signal window is defined as shown in Fig. 9. The number of time samples gives the drift velocity: The result of the measurements performed as a function of the high voltages is shown in Fig. 10. The agreement with previous measurements is evident (continuous line).

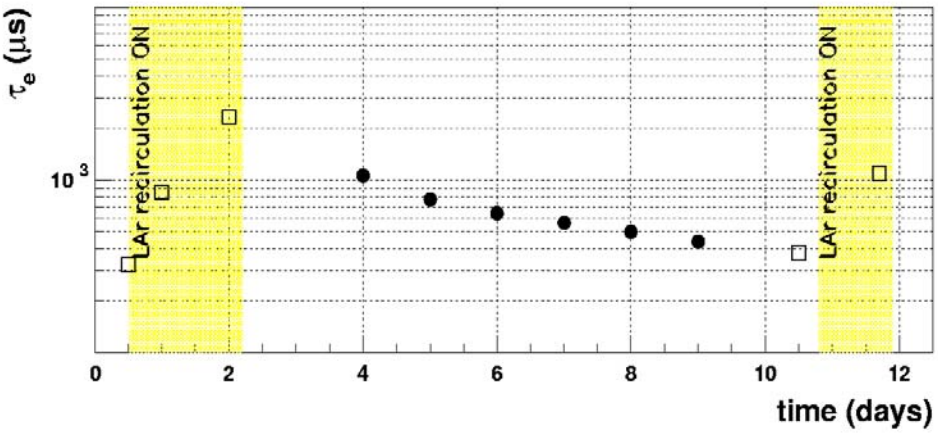

Figure 3: Measurements of the electron life-time in a 12 days long period during the test run. Data from the analysis of the selected crossing muon sample (full dots) and values from the LAr purity monitors (open squares). During this period the LAr purification unit was on in the shaded intervals and the GAr purification system was off.

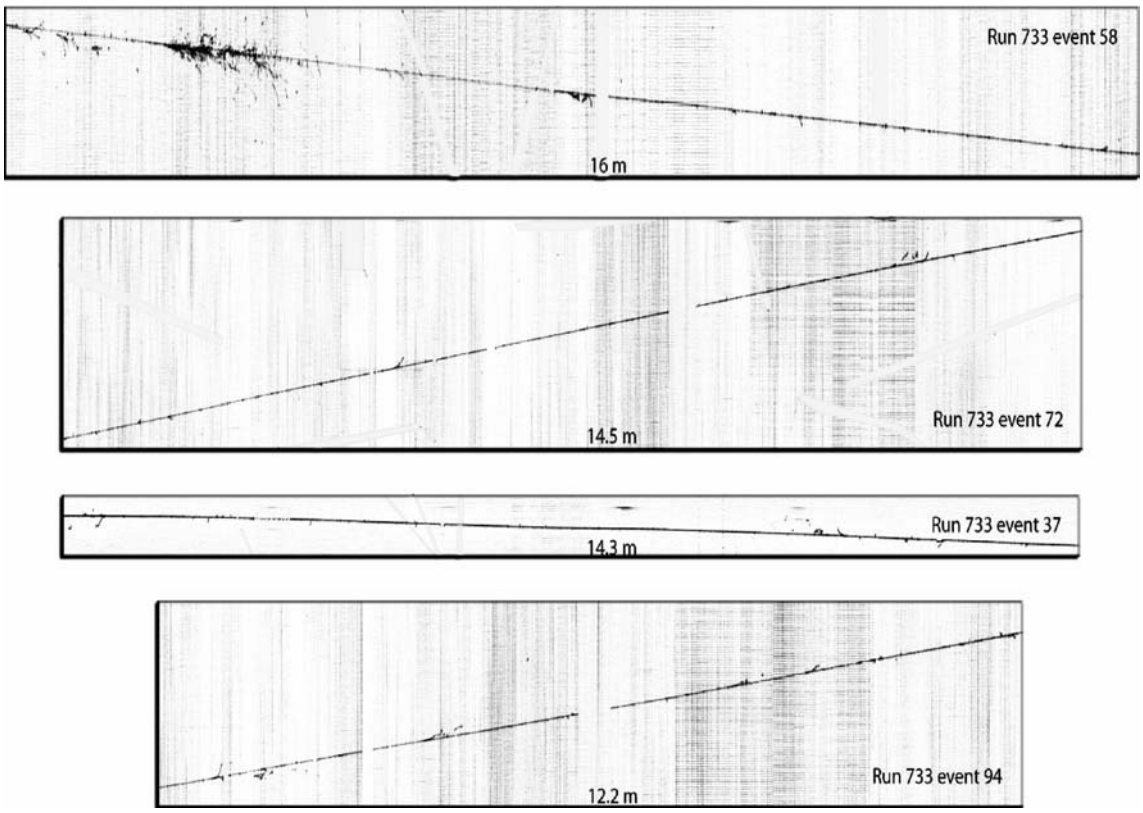

Figure 4: Four typical long muon-tracks crossing the ICARUS 300 ton half-module.

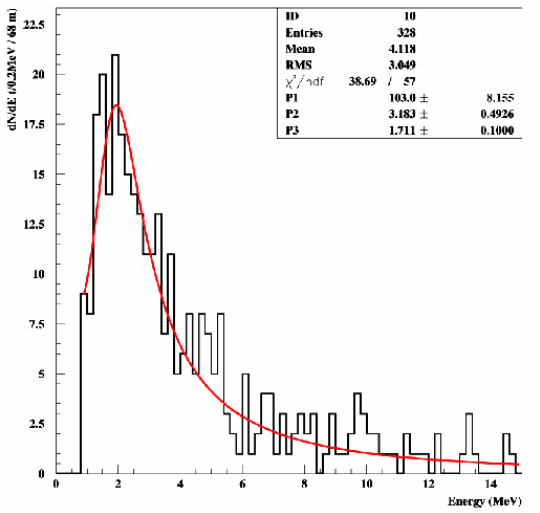

Figure 5: Number of δ-rays / MeV / 68 m tracks. The continuous line represents the fit with a Mott cross-section. The parameters are P_1 normalization factor, P_2 the slope and P_3 the flex point (MeV) in the sigmoid function.

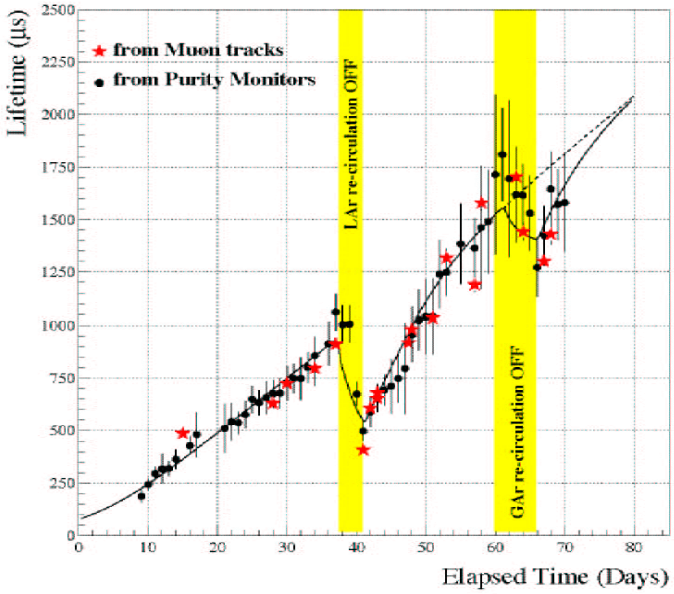

Figure 6: Drift electron life-time versus run time. Purity monitors data are the full dots, whereas stars are the data obtained with crossing muons. The continuous line represents the result of a matematical model.

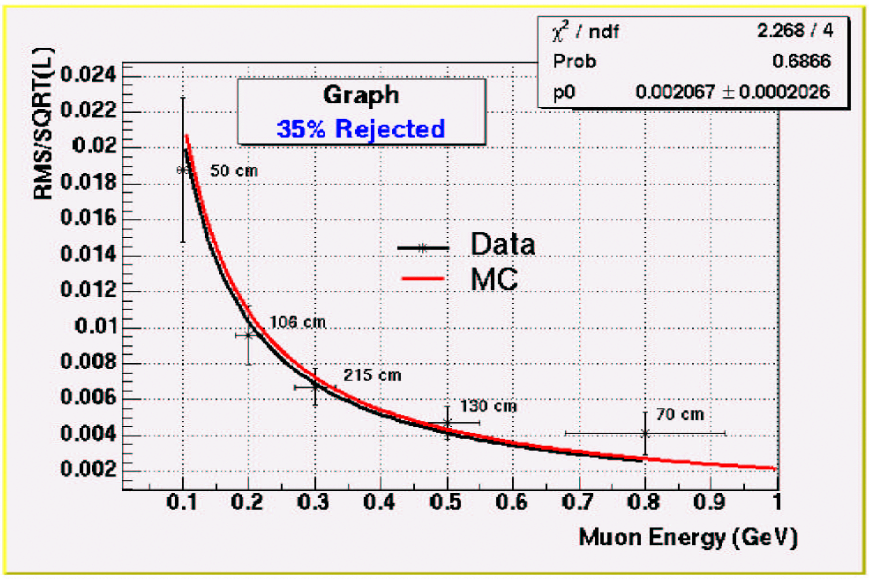

Figure 7: Muon multiple scattering: normalized and truncated RMS as a function of the muon momentum. Data are compared with the predictions of the FLUKA Monte Carlo (continuous line).

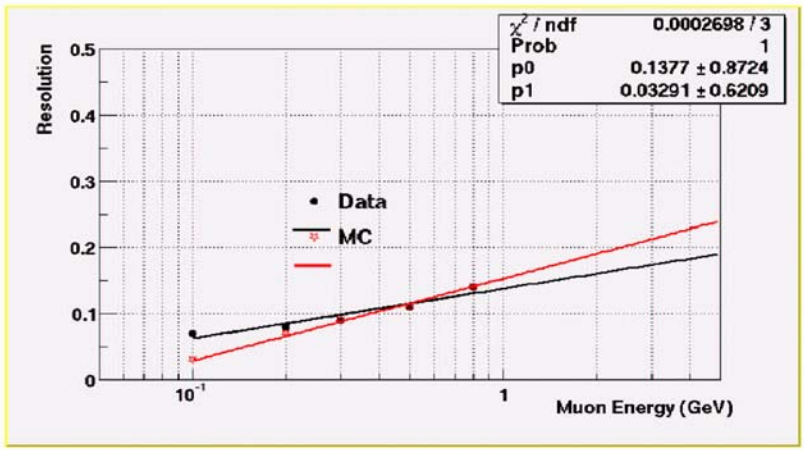

Figure 8: Resolution in percent versus muon energy. Extrapolation is presented up to 5 GeV energy.

$$v_{drift} = Length(cathode - wire)/(N_{bins} \times 0.4ms)$$

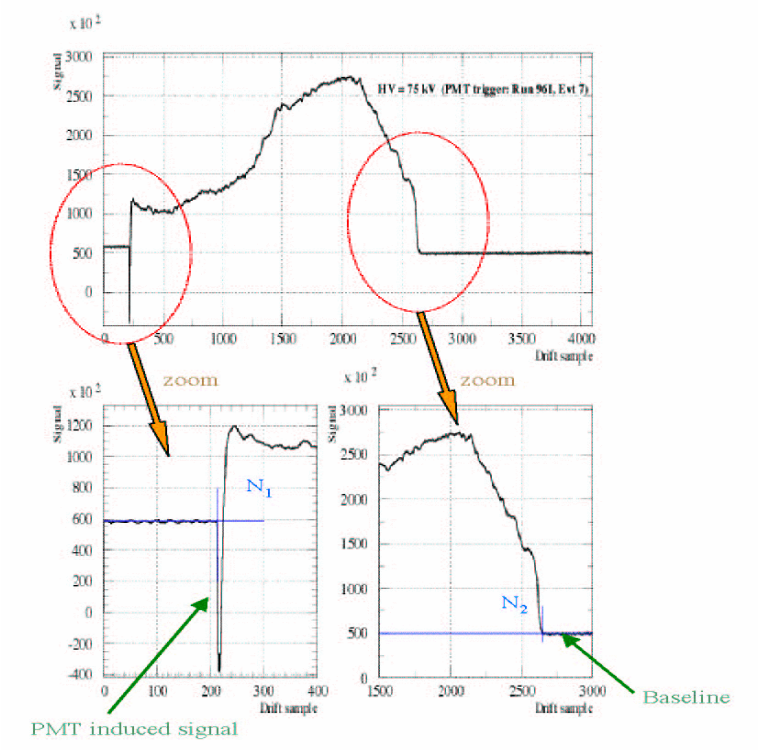

Figure 9: Signal versus drift time sample.

A very detailed analysis was then performed on Michel electrons produced by stopping muons. The electron energy is measured with two different methods: the range-energy correlation and the stopping power reconstruction. The resulting energy spectrum is shown in Fig. 11, where the data are compared with simulations and with a Michel formula fit. The result of the fit for the first Michel parameter is $\rho = 0.77 \pm 0.22 \pm 0.10$.

5 Some of the other activities carried out by the Collaboration.

An upgrade of the solar neutrino analysis was performed by introducing a new variable, the total visible energy associated with the absorption neutrino-nucleus events, i.e. the sum of the Compton electron energies. In Fig. 12 the results from simulations of the neutron capture in 40Ar and 36Ar and for neutrino absorption (pure Fermi and Gamow-Teller events) are shown. Rates are normalized to 1 year T600 detector run. In order to reduce the neutron capture background the correlation between the leading electron energy and the visible energy (photon total energy) can be exploited, as shown in Fig. 13. A cut-off in this plane allows to get a neutron background-free solar neutrino sample reducing at an acceptable level the number of events to be analysed. In particular, we

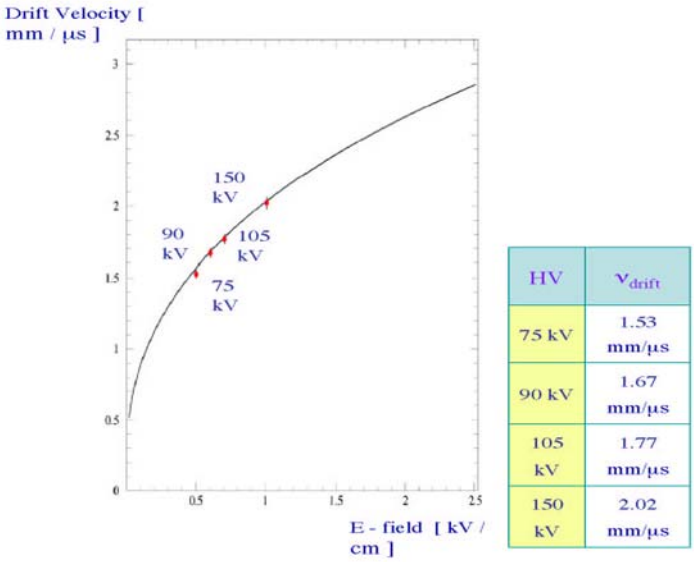

HV	v_{drift}
75 kV	1.53 mm/μs
90 kV	1.67 mm/μs
105 kV	1.77 mm/μs
150 kV	2.02 mm/μs

Figure 10: Measured drift velocity for four different high voltage values.

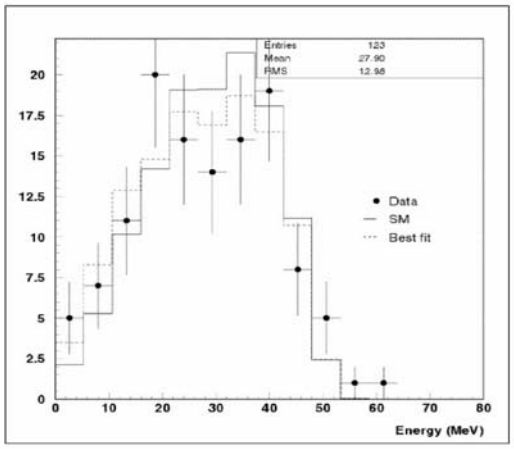

Figure 11: Michel electron energy spectrum . Reconstructed data are full dots, Montecarlo events are the histogram and the dotted histogram is the best fit result with the Michel formula.

expect with a 8.8 MeV cut in the visible energy to obtain 38, 165 or 295 events/year with the T600 detector for elastic scattering, pure Fermi and Gamow-Teller interactions, respectively.

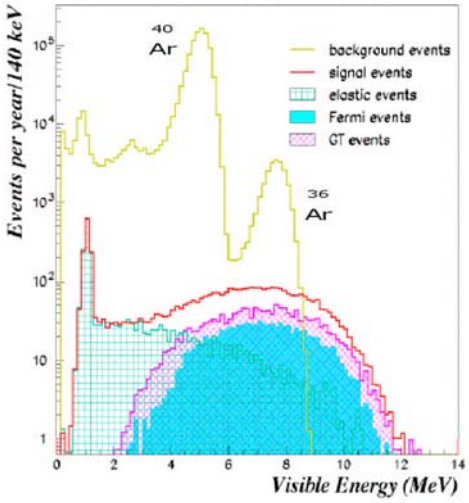

Figure 12: Visible energy for solar neutrino events and for neutron background.

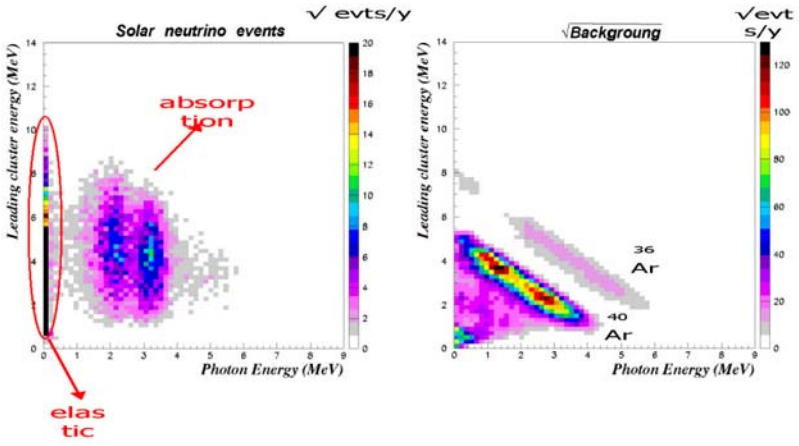

Figure 13: Correlation between the leading electron energy and the total photon energy.

During the year 2002, a substantial fraction of the ICARUS *R&D* activity was devoted to a series of items that could help improving the performance of the LAr-TPC. Based on the experience gained with the Pavia T600 test-run analysis which took place during 2001, we concentrated on:

- Absolute energy calibration of the T600 detector by means of test-pulses and through-going crossing muons (the 50 liter chamber on a muon beam at CERN was also used

for cross-calibration)[5]. Three calibration capacitances are foreseen along the read-out electronic chain; the first is placed on the *analogue board* before the front-end pre-amplifier; the second is positioned on the *decoupling board*; the third (built with the printed circuit board technique) is mounted on the far end of the read-out wire, immersed in Liquid Argon. During the technical run in Pavia only the first two test capacitance have been exploited.

- Optimization of the front-end preamplifiers (especially those for the middle induction plane)[6].

- Optimization of the on-line data-reduction, by means of both the DAEDALUS chip and some data compression scheme (lossy or lossless) implementable in pipe-line with the data stream[7]. The size of a full event from the T600 semi-module is about 200 Mbytes. The DAEDALUS chip is foreseen to perform zero skipping and hit-finding on-line; however it requires a careful optimization of its parameters to reach finding efficiencies close to 100% while minimizing the false detections. This activity is underway using the T600 data as test ground.

  A new proposal of data compression with denoising is based on the Fully Integer Interpolating Wavelet Transform (IWT). The study is based on the possibility of exploiting important aspects of the IWT, namely good computational efficiency, very good decorrelation and fast post-processing for compression and denoising. (The lifting scheme is an efficient implementation of filtering operations when computing a discrete wavelet transform). The compression factors achieved on the data from the T600 Pavia test runs are very satisfactory;

These activities took place both in Padova and CERN.

Other studies started concerning another possible method for the detector calibration. The principle of UV laser calibration is the possibility of producing ionisation electrons and hence tracks along the light beam inside the volume of liquid Argon. These tracks are analogous to those generated by ionising particles, but for which the ionisation yield, the position and the timing are a priori known. Laser induced tracks are obviously not affected by multiple coulomb scattering and by Landau fluctuations. UV laser beams can be used to measure the detector drift velocity and possibly distortions in the drifting of the electrons induced by errors in the applied electric field We are presently evaluating the possibility of using UV laser beams to monitor the liquid Argon purity. The goal is to design and construct a laser purity monitoring system for the first T1200 module, after an R&D study conducted on prototype detectors at CERN and in Naples.

We finally briefly mention some studies of the global ICARUS trigger system. In a possible scheme each detector signal, e.g. PMs, wires, veto detectors, CNGS beam timing signals, could be separately treated in different trigger control units which collect data and send trigger proposals to the trigger box. The system should be segmented in order to cope with the specific requirements imposed by bursts of low energy localized events, i.e. from supernovae. The intrinsic trigger granularity is given by the single readout crate, which corresponds to 1/8 of a chamber, 1350 samples (80 cm in drift). A signal from a single crate could be useful to form a local trigger for low energy events. The total number of arguments is (24 left + 24 right) times 4 chambers = 192 sum signals to which N from

PMs and external signals should be added. The 48 arguments from a chamber should feed a programmable logic unit where the trigger is formed within a time less than 5The logic unit can be realized by means of FPGA devices and can be interfaced to the full detector general trigger system.

6 Conclusions

The main activities of the ICARUS Collaboration in 2002 concerned:

- the completion of the assembly of the inner detector of the second 300 ton half module after the test run conducted in 2001 on the first half;
- the analysis of the events collected in the 2001 test run aimed at the development of algorithms to be used for the geometrical and kinematical recontruction of events taken in the operation of ICARUS in the underground Hall;
- the development of the final project of the ICARUS underground plant;
- the design of the further T1200 detector.

In the next future the Collaboration is focusing on two main streams:

- the installation and commissioning of the first T600 module to the LNGS, after the formal approval of the underground plant project by the Laboratory management;
- the design, construction and assembly of "clones" of the T600 module in order to reach the sensitive mass required for the ICARUS physics program.

7 List of Publications

1. "Performance of the 10^3 ICARUS liquid Argon Prototype" - Nucl. Instr. and Meth. A498 (2002) 292-311.
2. "Status of ICARUS" - Proceedings of the XXXVI Rencontre de Moriond, Les Arcs, March 2002.
3. "The atmospheric and solar neutrino experiment with the ICARUS T600 detector" - Nucl. Phys. (Proc. Sup.) B110 (2002), 329-332.
4. "Cloning of the T600 modules to reach the design sensitive mass" - CERN SPSC 2002-027.

References

[1] C.Rubbia, "The Liquid Argon Time Projection Chamber: a new concept for Neutrino Detector", CERN-EP/77-08. (1977) .

[2] ICARUS Collaboration, "A first 600 ton ICARUS detector installed at the Gran Sasso Laboratory", Addendum to Proposal LNGS - 95/10. (1995).

[3] ICARUS Collaboration, "A second generation Proton Decay Experiment and Neutrino Observatory at the Gran Sassd Laboratory",.LNGS - EXP 13/89 add. 2/01. (2001).

[4] ICARUS Collaboration, "The ICARUS T600 Experiment", LNGS Annual Report 2000, 89. (2001)

ICARUS Collaboration, "The ICARUS T600 Experiment", LNGS Annual Report 2001, 113. (2002)

[5] S. Navas-Concha et al., A measurement of the electron lifetime and the electron recombination factor with the T600 data, ICARUS-TM/2002-04, 2002.

[6] S. Amerio et al., Considerations on the ICARUS read-out and on data compression, ICARUS-TM/2002-05, 2002

[7] W. Polchlopek et al., Wavelet Transform Compression and Denoising in Real-Time System (Proposal for the ICARUS DAQ System), ICARUS-TM/2002-12, 2002.

LUNA. Laboratory for Underground Nuclear Astrophysics

M.L.Aliotta[1], D.Bemmerer[2], R.Bonetti[3], C.Broggini[4*], F.Confortola[5], P.Corvisiero[5], H.Costantini[5], J.Cruz[6], A.D'Onofrio[7], A.Formicola[8], Z.Fülöp[9], G.Gervino[10], L.Gialanella[11], A.Guglielmetti[3], C.Gustavino[12], G.Gyürky[9], G.Imbriani[11], A.P.Jesus[6], M.Junker[12], A.Lemut[5], R.Menegazzo[4], A.Ordine[11], P.Prati[5], V.Roca[11], D.Rogalla[8], C.Rolfs[8], M.Romano[11], C.Rossi Alvarez[4], F.Schümann[8], O.Straniero[13], F.Strieder[8], E.Somorjai[9], F.Terrasi[7], H.P.Trautvetter[8], S.Zavatarelli[5]

[1] Department of Physics and Astronomy, University of Edinburgh, Great Britain
[2] Technical University of Berlin, Germany
[3] Università di Milano, Dipartimento Di Fisica and INFN, Milano, Italy
[4] INFN, Padova, Italy
[5] Università di Genova, Dipartimento di Fisica and INFN, Genova, Italy
[6] Centro de Fisica Nuclear, Universidade de Lisboa, Portugal
[7] Dipartimento di Scienze Ambientali, Seconda Univerità di Napoli, Caserta, Italy
[8] Institut für Experimentalphysik III, Ruhr-Univerität Bochum, Germany
[9] ATOMKI, Debrecen, Hungary
[10] Politecnico di Torino, Dipartimento di Fisica and INFN, Torino, Italy
[11] Università di Napoli, Dipartimento di Fisica and INFN, Napoli, Italy
[12] Laboratori Nazionali del Gran Sasso, Assergi, Italy
[13] Osservatorio Astronomico di Collurania, Teramo, Italy

Abstract

LUNA is measuring fusion cross sections down to the energy of the nucleosynthesis inside stars. We show the preliminary results obtained last year on the study of $^{14}N(p,\gamma)^{15}O$, the slowest reaction of the CNO cycle, the key one to know the CNO solar neutrino flux, as well as to determine the age of the oldest components of the Milky Way. We then describe the set-up we constructed to measure $^{14}N(p,\gamma)^{15}O$ to the lowest energies with a windowless gas target and a 4π BGO detector. Finally, we tell the unexpected results we obtained on the electron screening measurement in $d(d,p)t$ for deuterated metals.

*Spokesperson

Introduction

Nuclear reactions that generate energy and synthesize elements take place inside the stars in a relatively narrow energy window: the Gamow peak. In this region, which is in most cases below 100 keV, far below the Coulomb energy, the reaction cross-section σ(E) drops almost exponentially with decreasing energy E:

$$\sigma(E) = \frac{S(E)}{E}\, exp(-2\,\pi\,\eta), \tag{1}$$

where $S(E)$ is the astrophysical factor and η is the Sommerfeld parameter, given by $2\,\pi\,\eta = 31.29\,Z_1\,Z_2(\mu/E)^{1/2}$. Z_1 and Z_2 are the nuclear charges of the interacting particles in the entrance channel, μ is the reduced mass (in units of amu), and E is the center of mass energy (in units of keV).

The extremely low value of the cross-section, from pico to femto-barn and even below, has always prevented its measurement in a laboratory at the Earth's surface, where the signal to background ratio would be too small because of cosmic ray interactions. Instead, the observed energy dependence of the cross-section at high energies is extrapolated to the low energy region, leading to substantial uncertainties. In particular, there might be a change of the reaction mechanism or of the centrifugal barrier, or there might be the contribution of narrow or sub-threshold resonances, not accounted for by the extrapolation, but which could completely dominate the reaction rate at the Gamow peak.

In addition, another effect can be studied at low energies: the electron screening. The electron cloud surrounding the interacting nuclei acts as a screening potential, thus reducing the height of the Coulomb barrier and leading to a higher cross-section. The screening effect has to be measured and taken into account in order to derive the bare nuclei cross-section, which is the input data to the models of stellar nucleosynthesis.

In order to explore this new domain of nuclear astrophysics we have installed two electrostatic accelerators underground in LNGS: a 50 kV accelerator and a 400 kV one. The qualifying features of both the accelerators are a very small beam energy spread and a very high beam current even at low energy.

Outstanding results obtained up to now are the only existing cross-section measurements within the Gamow peak of the sun: $^3He(^3He, 2p)^4He$ [1] and $d(p,\gamma)^3He$ [2]. The former plays a big role in the proton-proton chain, largely affecting the calculated solar neutrino luminosity, whereas the latter is the reaction that rules the proto-star life during the pre-main sequence phase.

With these measurements LUNA has shown that, by going underground and by using the typical techniques of low background physics, it is possible to measure nuclear cross sections down to the energy of the nucleosynthesis inside stars.

In the following we report on the activity during the year 2002. First, we show the results obtained on the cross section measurement of $^{14}N(p,\gamma)^{15}O$ with solid targets and germanium detectors and we describe the set-up prepared to study the same reaction down to the lowest energies with a gas target and a 4π BGO detector. Then, we give the status of the 400 kV accelerator, with the design of a second beam line. Finally, we show the unexpected results we obtained at the Bochum 100 kV accelerator on the electron screening in $d(d,p)t$ for deuterated metals.

1 The $^{14}N(p,\gamma)^{15}O$ reaction

$^{14}N(p,\gamma)^{15}O$ is the slowest reaction of the CNO cycle, the key one to know the CNO solar neutrino flux, as well as to determine the age of the globular clusters, the oldest components of the Milky Way. As a matter of fact, the CNO solar neutrino flux depends almost linearly on this cross section [3][4]. The position of the Turn Off point in the HR diagram of a globular cluster is also determined by the value of the $^{14}N(p,\gamma)^{15}O$ cross section and it gives the age of the cluster [5].

The energy region studied so far in nuclear physics laboratories is well above the region of interest for the CNO burning in astrophysical conditions (20-80 keV). At solar energies the cross section of $^{14}N(p,\gamma)^{15}O$ is dominated by a sub-threshold resonance at -504 keV, whereas at energies higher than 100 keV it is dominated by the 278 keV resonance, with transitions to the ground-state of ^{15}O or to the excited states at energies of 5.18 MeV, 6.18 MeV and 6.79 MeV. According to Schröder et al. [6], who measured down to 0.2 MeV, the main contribution to the total S-factor at zero energy, S(0),comes from the transitions to the ground state of ^{15}O and to its excited state at E_x = 6.79 MeV. In particular, they give S(0) = 3.20 ± 0.54 $keV \cdot b$. On the other hand, Angulo et al. [7] re-analyzed Schröder's experimental data using a R-matrix model and they obtained S(0) = 1.77 ± 0.20 $keV \cdot b$, which is a factor 1.7 lower than the values used in the recent compilations. The difference mainly comes from the different contribution of the direct capture to the ^{15}O ground state: Angulo et al. have a value lower by a factor 19 than the one of Schröder et al.. We underline that at the lowest energies Schröder et al. give only upper limits to the cross section, due to the presence of a strong cosmic ray background in the spectrum.

In summary, new measurements of the $^{14}N(p,\gamma)^{15}O$ cross section at energies E $\leq$ 200 keV are strongly demanded. In particular it is necessary to well measure the contribution of the direct capture to the ground state of ^{15}O. The peculiarities of the 400 kV LUNA facility [5] are particularly well suited for this study, where γ-rays with energy up to $\simeq$ 7.5 MeV have to be detected at very low count-rate. As a matter of fact, in such a measurement the cosmic ray background has to be strongly suppressed and ultra-low background detectors have to be employed. In addition, high beam intensities and detectors with excellent energy resolution have to be coupled to targets of high stability and purity, in order to minimize the beam-induced background.

Due to the strong energy dependence of the cross section, we carefully determined the uncertainties of our accelerator: $\pm$300 eV on the absolute energy from E_p = 130 to 400 keV, proton energy spread of better than 100 eV and long term energy stability of 5 eV per hour [5].

The data discussed in this report have been obtained with the beam passing through a Ta collimator and focused to a spot of about 1.5 cm diameter. A liquid nitrogen cooled Cu tube has been placed between the collimator and the target in order to avoid carbon deposition on the target itself. A negative voltage (-300 V) was applied to this tube in order to minimize the secondary electron emission from the target, used as a Faraday cup to measure the beam current. A 126% HpGe detected the γ rays from the reaction: it was placed at 55^o from the beam direction at about 1.5 cm distance from the target. Both the detector and the target chamber were surrounded by a 5 cm thick lead shielding.

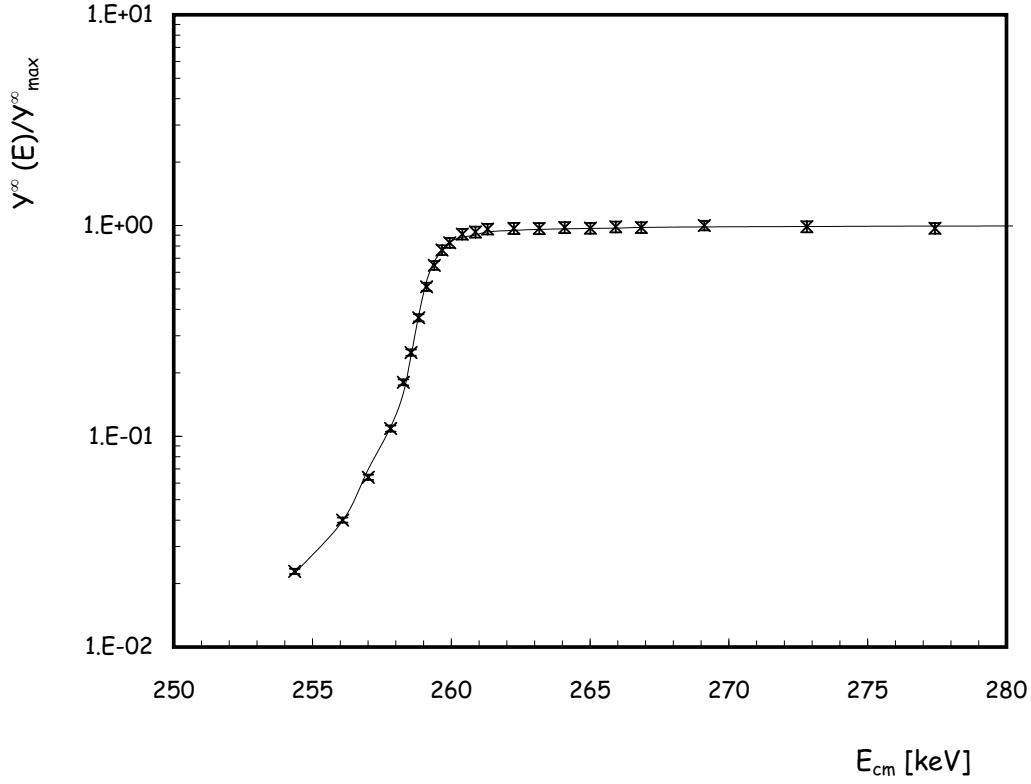

Figure 1: Excitation function of primary γ-rays from the ^{14}N(p, γ)^{15}O.

1.1 The resonance at $E_p = 278\ keV$

The excitation function of the ^{14}N(p, γ) reaction ($Q = 7.297\ MeV$) to four final states in ^{15}O was measured in the region of the 1.2 keV broad resonance at $E_p = 278\ keV$. The beam energy is given by the accelerator calibration curve [5], whereas the measured yield is fitted by a function which is the sum of a non resonant cross section and of a Breit-Wigner, numerically integrated:

$$f(E) = \int \sigma(E)dE = \int \left(\frac{S \exp[-2\pi\eta]}{E} + \frac{\lambda^2 \omega}{4\pi} \frac{\Gamma_\gamma \Gamma_p(E)}{(E - E_R)^2 + [(\Gamma_\gamma + \Gamma_p(E))/2]^2} \right) dE \quad (2)$$

where S is the value of the astrophysical S-factor, assumed constant in the small energy range. The result of this fit is shown in figure 1 and the preliminary values obtained for the resonance parameters are: $E^R_{cm} = 259.1 \pm 0.3\ keV$ and $\Gamma_p = 1.07 \pm 0.05 keV$.

By analyzing a resonance spectrum it is possible to determine the energies of the ^{15}O excited states and the Q-value of the ^{14}N + p reaction. From the constrained fit to the observed γ-ray positions in the spectrum, using as free parameters the ^{15}O energy levels and the Q-value, we obtained the following preliminary results: $E1 = 5180.3 \pm 0.3\ keV$; $E2 = 6172.0 \pm 0.3\ keV$; $E3 = 6791.6 \pm 0.3\ keV$ and $Q = 7297.2 \pm 0.3\ keV$.

In order to have a new determination of the resonance strength and of the branching ratios to the different final states, we had first to measure the γ-ray detection efficiency: with ^{137}Cs and ^{60}Co calibrated sources placed at the target position in the low energy region and from the γ-ray cascade structure of the resonant state at high energies. The preliminary results we finally obtained on the resonance strength and on the branching ratios are the following: $\omega\gamma = 13.5 \pm 0.5\, meV$, $b_0 = 1.6 \pm 0.1$ %, $b_1 = 16.8 \pm 0.2$ %, $b_2 = 58.2 \pm 0.3$ % and $b_3 = 23.4 \pm 0.3$ %. Such values were then used to get the absolute normalization of the cross section outside the resonance.

1.2 Preliminary results on $^{14}N(p,\gamma)^{15}O$

The yield of the ^{14}N(p,γ)^{15}O reaction has been measured down to the proton energy $E_p = 147\ keV$ by using sputtered targets of TiN on Ta backing, with thickness larger than 60 keV. In order to extract the absolute cross section from the observed γ-ray spectra, we studied in detail the expected line shape. This shape is determined by the cross section behavior $\sigma(E_p)$ in the proton energy interval spanned by the incident beam during the slowing-down process in the target (once the transformation from the energy E_p at which the reaction takes place to the corresponding γ-ray energy $E_\gamma = E_p^{cm} + Q$ is made).

The number of counts per unit charge, N_i, observed in the channel i, which corresponds to the energy bin from E_{γ_i} to $E_{\gamma_i} + \delta E_\gamma$, is given by the expression:

$$N_i = \frac{\sigma(E_{p_i})\delta E_\gamma \varepsilon(E_{\gamma_i}) b_j W_j(\theta)}{\frac{dE}{dx}(E_{p_i})} \tag{3}$$

for $E_{p_i} \leq E_p$ (E_{p_i} is the proton energy corresponding to channel i), where $\sigma(E_{p_i})$ is the ^{14}N(p,γ)^{15}O cross section, $\varepsilon(E_{\gamma_i})$ is the γ-ray detection efficiency, b_j is the branching of the j-decay, $W_j(\theta)$ is the angular distribution and dE/dx(E_p) is the proton stopping power in TiN. The conversion from E_{γ_i} to E_{p_i} must of course take into account the averaged Doppler and recoil effects. Finally, the result is folded with the detector resolution to obtain the experimental line shape.

Since N_i depends on the stechiometry of the target, in order to extract the absolute value of the cross section $\sigma(E_{pi})$ it is necessary to normalize N_i to the corresponding infinite resonance yield measured with the same target [8]:

$$Y^\infty = \frac{\lambda^2}{2}\frac{\omega\gamma b_j \varepsilon(E_\gamma^R)}{\frac{dE}{dx}(E^R)} \tag{4}$$

To fit the ratio N_i/Y^∞ we write the cross section $\sigma(E_{p_i})$ as a sum of a non resonant component and a resonant one, given by the Breit-Wigner formula. In this way one obtains the following expression:

$$\sigma(E_{p_i}) = \frac{S_{NR}(\overline{E}_p^{cm})\exp[-2\pi\eta]}{E_{p_i}^{cm}} + \frac{\lambda^2\omega}{4\pi}\frac{\Gamma_\gamma\Gamma_p(E_{p_i}^{cm})}{(E_{p_i}^{cm} - E_R)^2 + [(\Gamma_\gamma + \Gamma_p(E_{p_i}^{cm}))/2]^2} \tag{5}$$

where $S_{NR}(E)$ is the non resonant astrophysical factor, ω is the statistical factor and

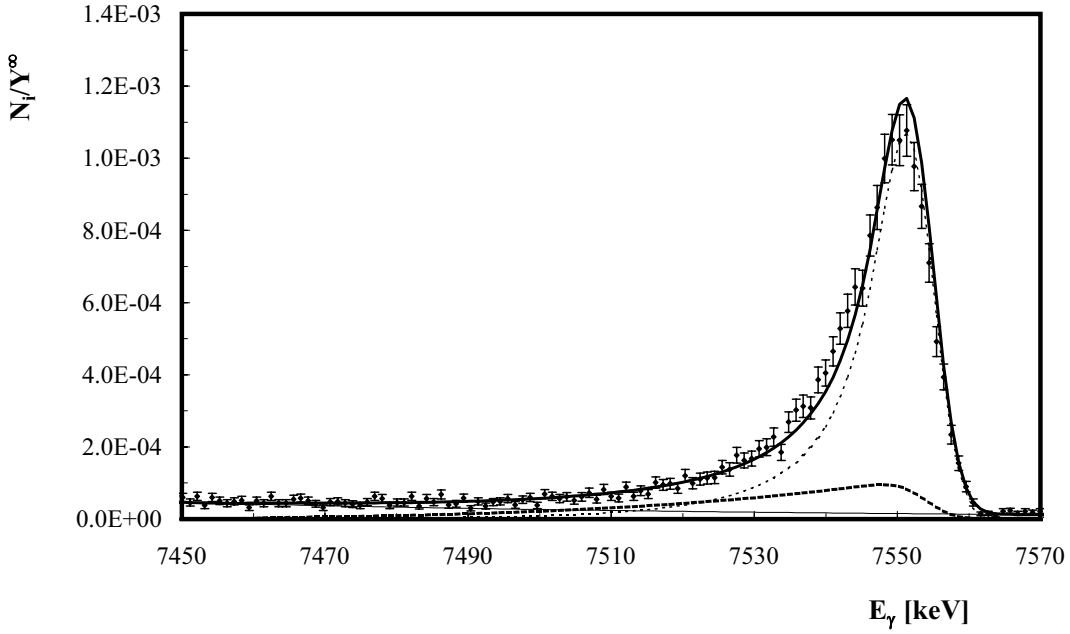

Figure 2: The γ-spectrum for the ground-state transition at $E_{cm} = 270\ keV$.

Γ are the resonance widths. An example of the fit is given in figure 2, where the γ-spectrum for the ground-state transition at $E_{cm} = 270\ keV$ is plotted: the thin solid line is the background, the bold and the thin dotted lines represent the non resonant and the resonant part of the cross section, respectively. The bold solid line is the sum of all the previous functions and it gives the fit to the data. It is worth observing that we obtain such a fit by using as free parameters only the non resonant astrophysical factor $S_{NR}(E)$ and the background parameters.

If we reduce the target thickness then the fit improves since the $S_{NR}(E)$ function actually varies with energy. Unfortunately it is very difficult to produce stable thin targets. A way to simulate a thin target is to differentiate channel by channel two spectra acquired at different energies, after normalization to the charge. The resulting spectrum will be equivalent to one acquired at the higher energy and with a target thickness equal to the difference in incident energy. An example of this procedure is shown in figure 3.

Finally, figure 4 shows our preliminary results on the ground-state transition S-factor (filled symbol), obtained using the differential method, together with the results of [6].

At the end of the year we also studied the γ ray angular distribution of the $^{14}N(p,\gamma)^{15}O$ reaction with 3 HpGe detectors placed at about 7 cm from the target and at angles of 0^o, 90^o and 125^o. Angular distributions were measured for primary and secondary transitions at the proton energies of 220 and 388 keV, whereas spectra taken at the 278 keV resonance (where all the γ transitions are isotropic) were used to get the relative efficiency between the different detectors. The spectra at 388 keV were taken for comparison to Schroeder's angular distribution data at 500 keV. The analysis of this data is in progress.

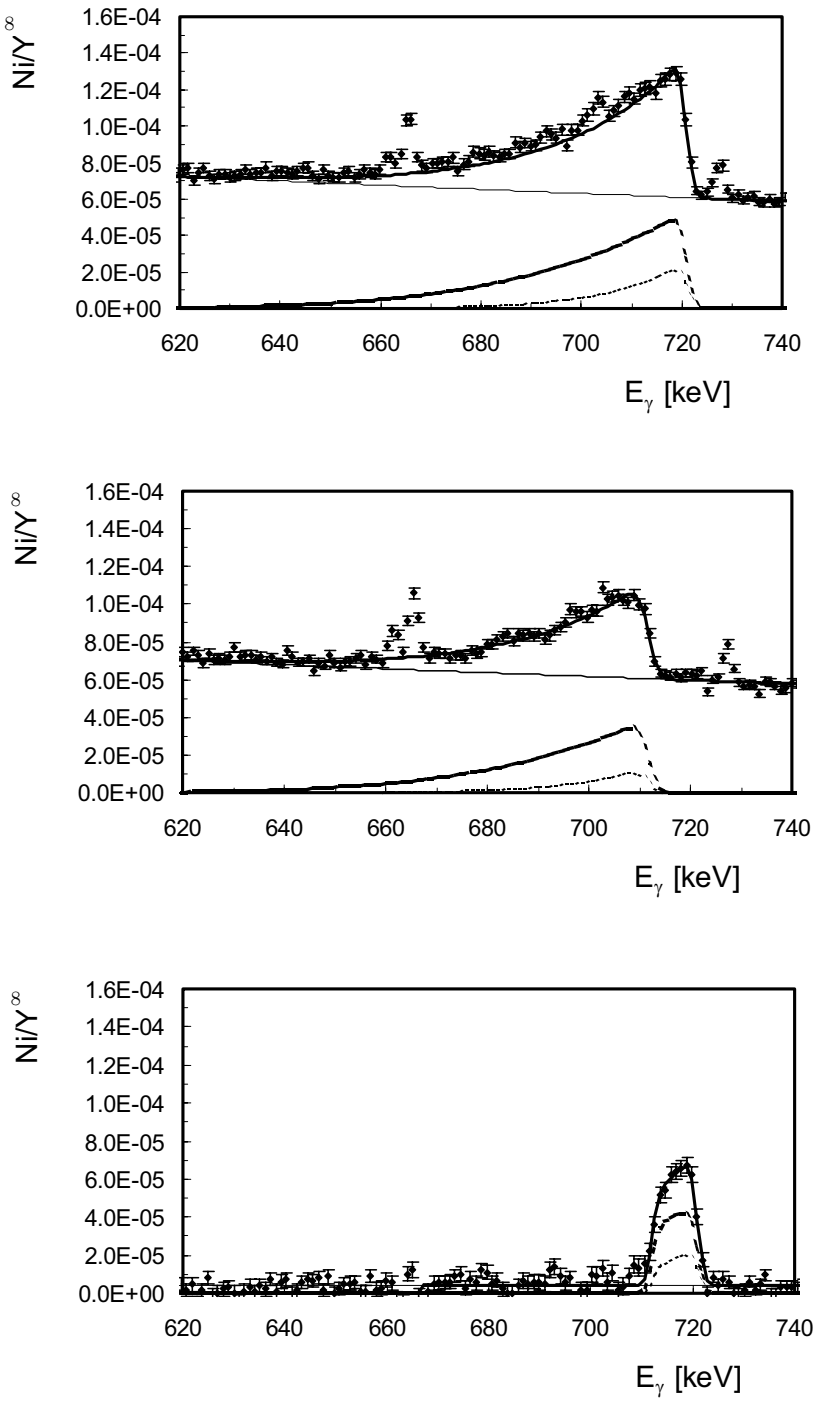

Figure 3: The upper panel shows the γ line shape corresponding to the transition at 6.79 MeV with a beam energy of $E_p^{cm} = 230\ keV$ and the middle one the same transition but with a beam energy of $E_p^{cm} = 221\ keV$. The lower panel shows the γ-spectrum resulting from the differential procedure, which is equivalent to a spectrum acquired at $E_p^{cm} = 230\ keV$ with a 9 keV thick target.

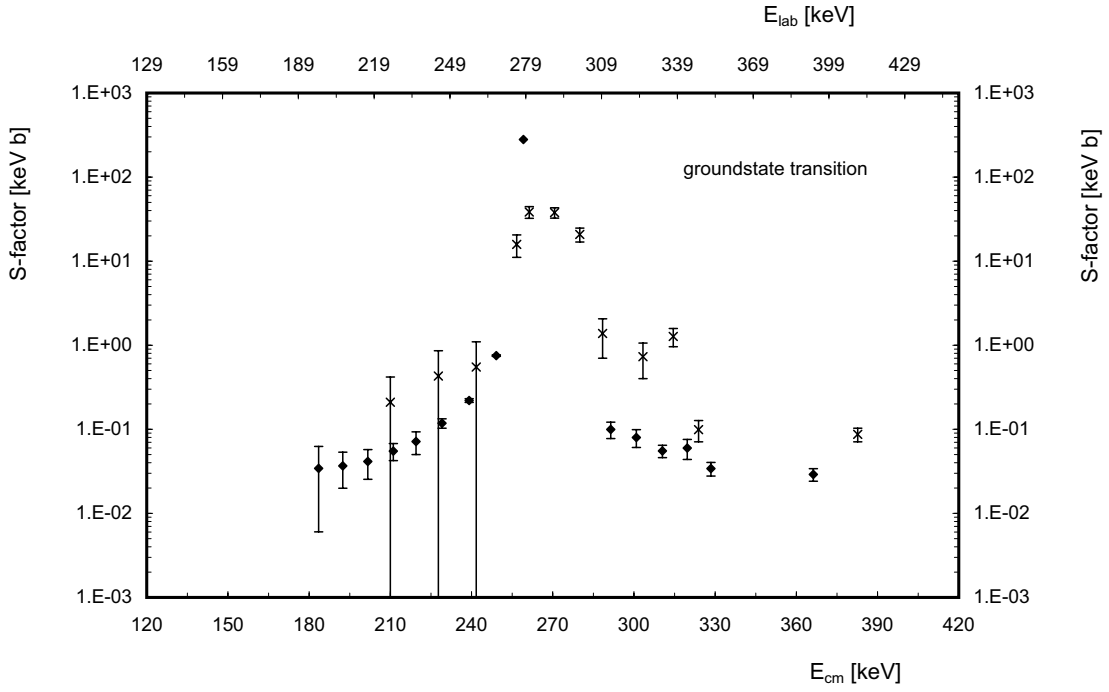

Figure 4: preliminary results for the ground-state transition.

2 The new gas target setup

In order to explore the energy region below 140 keV it is essential to have both a γ ray detector with very high efficiency, to compensate for the rapidly decreasing cross section, and a very thin ^{14}N target, to minimize the straggling on the energy loss. This can be achieved with the same 4π BGO summing detector (about 80% efficiency) [9] used in the measurement of $d(p,\gamma)^3He$ [2] and with a new windowless gas target. A schematic diagram of the gas target is shown in Fig. 5. The ion beam enters the target chamber through three apertures of high pass flow impedance (A_3–A_1, Fig. 5) and it is stopped in a beam calorimeter placed at the downstream part of the chamber. The chamber is designed to fit inside the central hole (diameter $\phi = 6\ cm$) of the BGO crystal detector. The target chamber has one port for gas inlet and one extended port for pressure measurement. A Cu pipe (inner diameter $\phi = 6\ mm$, length $L = 30\ cm$) goes from the target chamber to the pressure manometer outside the BGO crystal. The measurement is carried out with a capacitance gauge (MKS Baratron Type 626A) to an accuracy better than 0.25 %; such a measurement is absolute and independent of the gas used.

Fig. 6 shows the special setup used to check the target chamber pressure homogeneity, the pressure gradient along the beam axis and the pressure gradient along the 30 cm long Cu pipe connecting the chamber to the manometer. The gas, filled into the target chamber from a reservoir, is pumped through the water cooled aperture A_1 ($\phi = 7\ mm$, $L = 40\ mm$) by a windowless gas target system with three pumping stages. The third of

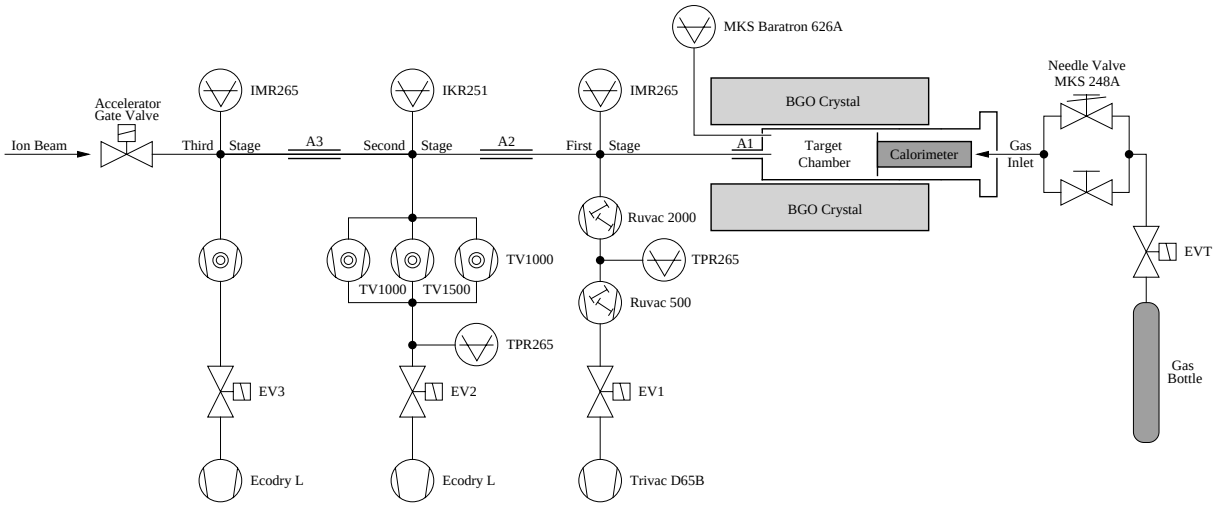

Figure 5: ^{14}N(p,γ)^{15}O windowless gas target schematic diagram.

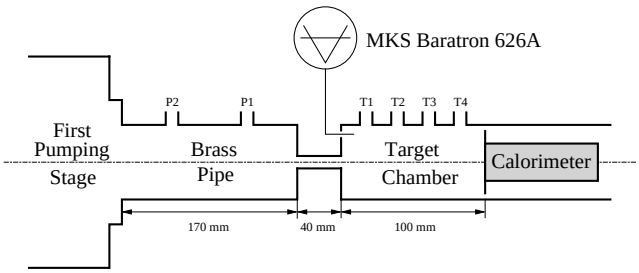

Figure 6: Target set-up dedicated to the pressure profile measurement.

them is connected to the accelerator by a gate valve. The pumping stages are separated by apertures A_2 ($\phi = 20\ mm$, $L = 80\ mm$) and A_3 ($\phi = 25\ mm$, $L = 80\ mm$). When the target is filled with ^{14}N at the pressure of $P_t = 2\ mbar$, the pumping system reduces the pressure to about 10^{-2}, 10^{-5} and $10^{-6}\ mbar$ in the regions between A_1, A_2 and A_3, respectively (such pressures are measured by Penning and Pirani gauges). At the same time the pressure in the target chamber is kept constant by an electronically regulated needle valve (MKS model 248A, controller MKS Type 250).

No deviation > 0.5 % have been observed at four position along the chamber (position T1, T2, T3 and T4) with the target filled with Nytrogen in the pressure range between P_t 0.8 and 15 $mbar$.

The pressure drop between the target chamber and the first pumping stage is critical. As a matter of fact, the ^{14}N(p,γ)^{15}O reactions occurring in this segment of the beam line produceγ-rays which can be detected by the BGO crystal and which cannot be separated from the ones produced inside the target chamber. At a given beam energy this additional γ-ray flux is proportional to the product between the beam current and the gas pressure profile in the first pumping stage. Fig. 7 shows the pressure profile values observed at the two positions P1 and P2. These data are used in the Monte Carlo program. Simulation

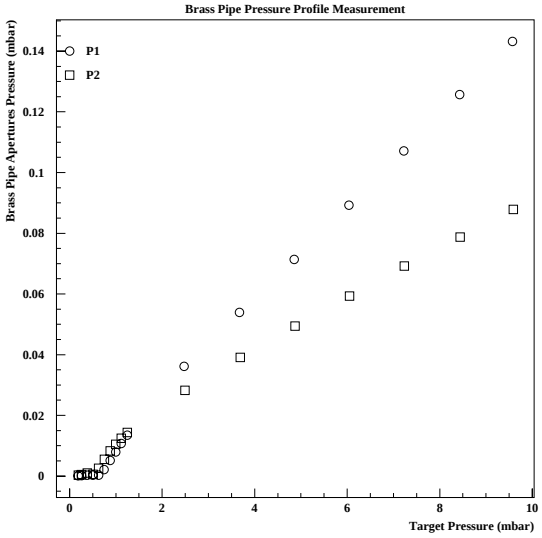

Figure 7: Brass pipe pressure profile measurement results.

gives the following result: the fraction of γ-rays detected by the BGO crystal from the first pumping stage is lower than about 1 % of the total number of detected γ rays.

A LABVIEW application controls the gas target system. The application has been developped as a remote control tool of the gas target and it can automatically check the status of the pumps and of the valves. If there is a system failure the program is able to switch off safely the entire system.

2.1 The beam calorimeter

When the ion beam goes through the gas target, the ion charge state fluctuates, preventing this way a precise current measurement. Instead, the current can be determined by a beam calorimeter with a constant gradient between a hot and a cold side, at temperature T_h and T_c, respectively [8]. When there is no beam, the heating power needed to maintain the T_h temperature, W_{zero}, is provided by the heater (power transistor and/or thermo-resistors) controlled by a feedback circuit. When the ion beam hits the hot side, then it also contributes to the heating and it correspondingly reduces the electric power down to W_{run}. This way, the number of projectiles per second reaching the calorimeter, N_p, is simply given by the difference of the heater powers divided by the kinetic energy, E_{cal}, of the projectile at the hot side of the calorimeter:

$$N_p = \frac{W_{beam}}{E_{cal}} = \frac{(W_{zero} - W_{run})}{E_{cal}} \tag{6}$$

This energy is obtained [10] by subtracting the energy lost in the target gas to the original beam energy.

The hot side of the calorimeter, which works as a beam stop, is a Cu disk ($\phi = 48\ mm$, 41 mm thick), heated up by eight resistors (25 Ω, 50 W each) electrically connected in

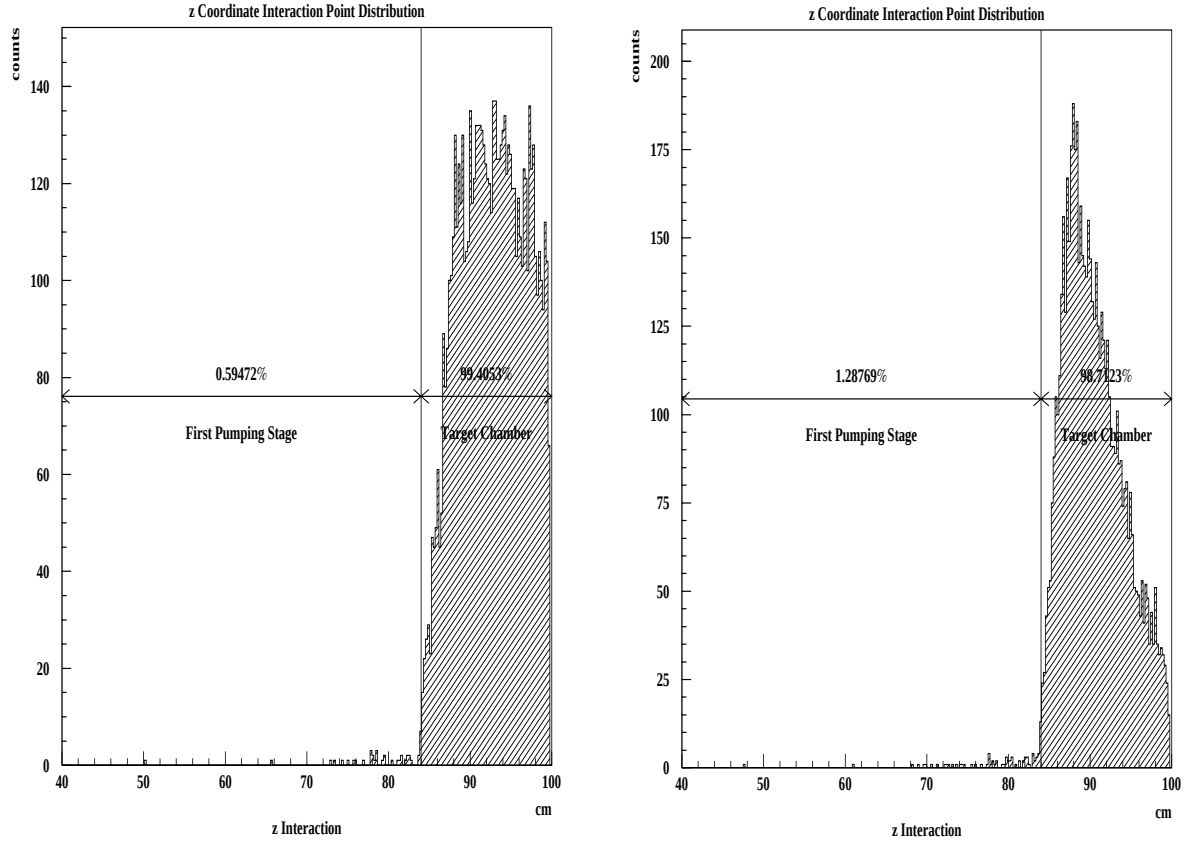

Figure 8: On the left: Simulated z distribution of the interaction point at beam energy = 200 keV and target pressure = 1 $mbar$. On the right: As on the left at beam energy = 70 keV and target pressure = 1 $mbar$.

parallel. The current through the resistors is provided by a standard DC power supply (32 V, 10 A) controlled by a 0–10 V signal to keep the constant temperature $T_h = 60\ ^\circ C$. The diameter of the Cu disk is much larger than the beam diameter ($< 10\ mm$) at the the calorimeter.

The cold side is kept at $T_c = 0\ ^\circ C$ by a cooling circuit connected to a refrigerator (cooling capacity = 500 W, temperature stability = 0.01 $^\circ C$). The temperatures are monitored via PT100 thermoresistors with a precision of 0.01 $^\circ C$: three PT100 on the hot side and one on the cold side of the calorimeter. With this arrangement the maximum beam power is 200 W, whereas the heating power stability is 0.1 W.

The calorimeter has been designed to work also as a Faraday cup. As a matter of fact, the calorimeter and the target chamber are electrically insulated from the upstream part of the gas target by a 10 mm thick Teflon disk with a $\phi = 12\ mm$ central hole; furthermore, an insulating cooling liquid is used in the refrigerator.

During the calibration, the calorimeter and the target chamber are connected together to become a Faraday cup. A metallic ring, at -100 V, is inserted in the Teflon insulator to minimize the effect of secondary electrons. At the pressure of $5 \times 10^{-5} mbar$ in the

target chamber (no fluctuations in beam charge are expected at such a low pressure), both the calorimetric and the Faraday cup measurements give a consistent result within a 1 % systematic uncertainty.

3 The 400 kV accelerator and the second beam line

In 2002 the 400 kV accelerator has delivered proton beams in the energy range between 50 keV and 400 keV for an overall time of 8 months. During these runs stable beams of up to 750 μA have been delivered to the target mounted on the 45^o line, while no beam was available for 2 months due to the maintenance of the accelerator itself. The duration of the maintenance time has been significantly decreased in the course of the year thanks to the gained experience and to the optimization of the procedure. A normal maintenance, which requires the opening of the accelerator tank, takes now about eight hours.

The facility is equipped with all necessary interlocks to allow for the handling of the accelerator by selected members of the collaboration after a short training period.

In the course of the year the complete vacuum system has been modified in order to use only oil free pumps. In particular, the Leybold rotary vane foreline pumps have been exchanged with Alcatel ACP28 pumps and diaphragm pumps, while keeping the previously used turbo pumps. This solution allows for a vacuum of 10^{-7} $mbar$ in the beam line (10^{-5} with source in operation) in a completely oil free setup. Finally, the LUNA II site has been equipped with an alignment system which allows for the correct positioning of the experimental equipments along the beam line.

A set of measurements has also been performed to analyse the beam optics of the accelerator. The obtained data have been used to develop models, based on the codes COSY INFINITY and TRACE3D, which describe the optic properties of the accelerator itself. By using such models, and by taking advantages of the precious help of the INFN-Legnaro accelerator experts, we could design a second beam line.

It starts at the 0^o beam exit port of the 45^o bending magnet we have, it enters a new bending magnet, equal to the first one and at 1.6 m from it, and it runs parallel to the existing line at 1.2 m distance. This line is now under construction. It will give us the possibility of having a beam line dedicated to the windowless gas target set-up, and one dedicated to the solid target measurements. In particular, on the second line we are planning to study the key reactions of the NeNa and MgAl cycles in order to understand the origin and the history of the chemical elements that build up our Universe.

4 Electron screening in $d(d,p)t$ for deuterated metals

For nuclear reactions studied in the laboratory the target nuclei and the projectiles are usually in the form of neutral atoms or molecules and ions, respectively. The electron clouds surrounding the interacting nuclei reduce the height of the Coulomb barrier and lead to a higher cross section, $\sigma_{\rm s}(E)$, than would be the case for bare nuclei, $\sigma_{\rm b}(E)$, with an exponential enhancement factor [8]:

$$f_{\rm lab}(E) = \sigma_{\rm s}(E)/\sigma_{\rm b}(E) \simeq E(E+U_{\rm e})^{-1}\exp(\pi\eta\, U_{\rm e}/E), \qquad (7)$$

where U_e is an electron screening potential energy and η is the Sommerfeld parameter.

Recently, the electron screening effect on the $d(d,p)t$ reaction has been studied in the metals Al, Zr and Ta [11], where deuterated metals were produced via implantation of low-energy deuterons. The resulting $S(E)$ data show an exponential enhancement, however the extracted U_e values are about one order of magnitude larger than the value U_e =25±5 eV found in the corresponding gas target experiment [12]. An anomalous enhancement was reported earlier [13] for deuterated Pd and deuterated Au/Pd/PdO multi-layer, while deuterated Ti and Au exhibited a normal (gaseous) enhancement.

In order to test these surprising results, we started a complete experimental program at the 100 kV accelerator of the Bochum Tandem Laboratory. Briefly, the $d(d,p)t$ cross section has been measured in 29 deuterated metals and 5 deuterated insulators or semiconductors [14][15] by detecting the emitted particles with four Si detectors (active area=600 mm^2, effective thickness=100 μm) installed at an angle of 130^0 around the beam axis.

As compared to measurements performed with a gaseous deuterium target, a large effect has been observed in all the metals (the highest enhancement is in deuterated Rh, with U_e =840± 70 eV). In contrast, a comparatively small effect is found for the insulators and semiconductors. An explanation of this apparently novel feature of the periodic table is missing. The experimental program is still going on in Bochum, in particular the temperature dependence of the enhancement will be studied as well as reactions with different ions.

References

[1] R. Bonetti et al., Phys. Rev. Lett. 82(1999)5205

[2] C. Casella et al., Nucl. Phys. A 706(2002)203

[3] J.N. Bahcall, Neutrino Astrophysics (Cambridge Univ. Press, 1989)

[4] V. Castellani et al., Phy. Rep. 281(1997)309

[5] R. Bonetti *et al.*, Annual Report LNGS 2001

[6] Schroeder et *al*, Nucl. Phys. A 467(1987)240.

[7] C. Angulo and P. Descouvemont, Nucl. Phys. A 690(2001)755.

[8] C. Rolfs and W.S. Rodney, Cauldrons in the cosmos (Univ. of Chicago Press, 1988)

[9] C. Casella et al., Nucl. Instr. Meth. A 489(2002)160

[10] C. Arpesella et al., Nucl. Instr. Meth. A 360(1995)607

[11] K. Czerski et al., Europhys. Lett. 54(2001)449

[12] U. Greife et al., Phys. A 351(1995)107

[13] H. Yuki et al., JETP Lett. 68(1998)823

[14] F. Raiola et al., Eur. Phys. J. A 13(2002)377

[15] F. Raiola et al., Phys. Lett. B 547(2002)193

5 Publications and Conferences

1. C. Casella et al., First measurement of the $d(p,\gamma)^3He$ cross section down to the solar Gamow peak, Nucl. Phys. A 706(2002)203
2. C. Casella et al., A new setup for underground study of capture reactions, Nucl. Instr. Meth. A 489(2002)160
3. F. Raiola et al., Enhanced electron screening in $d(d,p)t$ for deuterated Ta, Eur. Phys. J. A 13(2002)377
4. F. Raiola et al., Electron screening in $d(d,p)t$ for deuterated metals and the periodic table, Phys. Lett. B 547(2002)193
5. H.Costantini, invited talk at the CAARI 2002 Conference, Denton
6. A.Formicola, invited talk at the EPS Conference, Debrecen
7. G. Imbriani, 11th Workshop on Nuclear Astrophysics, Ringberg Castle
8. G. Imbriani, EPS Conference, Debrecen
9. M. Junker, invited talk at Int. School of Phys. E. Fermi, Villa Monastero
10. F.Raiola, EPS Conference, Debrecen
11. C. Rolfs, invited talk at the Neutrino 2002 Conference, Muenchen
12. C. Rolfs, invited talk at the Sevilla Conference, Sevilla
13. C. Rolfs, invited talk at the EPS Conference, Debrecen
14. C. Rolfs, invited talk at the SNIT summer school, Triumf
15. F. Strieder, 33rd Nucl. Phys. Meeting of the Max Planck Institut, Schleching
16. F. Strieder, 7th Int. Symp. on Nuclei in the Cosmos, Fuji-Yoshida
17. F. Strieder, CAARI 2002 Conference, Denton

LVD. Large Volume Detector

LVD COLLABORATION

M.Aglietta[14], E.D.Alyea[7], P.Antonioli[1], G.Badino[14], G.Bari[1], M.Basile[1], V.S.Berezinsky[9], M.Bertaina[14], R.Bertoni[14], G.Bruni[1], G.Cara Romeo[1], C.Castagnoli[14], A.Chiavassa[14], J.A.Chinellato[3], L.Cifarelli[1], F.Cindolo[1], A.Contin[1], V.L.Dadykin[9], L.G.Dos Santos[3], R.I.Enikeev[9], W.Fulgione[14], P.Galeotti[14], M.Garbini[1], P.L.Ghia[14], P.Giusti[1], F.Gomez[14], F.Grianti[4], G.Iacobucci[1], E.Kemp[3], F.F.Khalchukov[9], E.V.Korolkova[9], P.V.Korchaguin[9], V.B.Korchaguin[9], V.A.Kudryavtsev[9], M.Luvisetto[1], A.S.Malguin[9], H.Menghetti[1], N.Mengotti Silva[3], C.Morello[14], R.Nania[1], G.Navarra[14], K.Okei[10], L.Periale[14], A.Pesci[1], P.Picchi[14], I.A.Pless[8], A.Porta[14], A.Romero[14], V.G.Ryasny[9], O.G.Ryazhskaya[9], O.Saavedra[14], K.Saitoh[13], G.Sartorelli[1], M.Selvi[1], N.Taborgna[5], N.Takahashi[12], V.P.Talochkin[9], G.C.Trinchero[14], S.Tsuji[11], A.Turtelli[3], P.Vallania[14], S.Vernetto[14], C.Vigorito[14], L.Votano[4], T.Wada[10], R.Weinstein[6], M.Widgoff[2], V.F.Yakushev[9], G.T.Zatsepin[9], A.Zichichi[1]

[1] *University of Bologna and INFN-Bologna, Italy*
[2] *Brown University, Providence, USA*
[3] *University of Campinas, Campinas, Brazil*
[4] *INFN-LNF, Frascati, Italy*
[5] *INFN-LNGS, Assergi, Italy*
[6] *University of Houston, Houston, USA*
[7] *Indiana University, Bloomington, USA*
[8] *Massachusetts Institute of Technology, Cambridge, USA*
[9] *Institute for Nuclear Research, Russian Academy of Sciences, Moscow, Russia*
[10] *Okayama University, Okayama, Japan*
[11] *Kawasaki Medical School, Kurashiki, Japan*
[12] *Hirosaki University, Hirosaki, Japan*
[13] *Ashikaga Institute of Technology, Ashikaga, Japan*
[14] *CNR-IFSI, Torino; University of Torino and INFN-Torino, Italy*

Abstract

The Large Volume Detector (LVD) in the INFN Gran Sasso National Laboratory, Italy, is a ν observatory mainly designed to study low energy neutrinos from the gravitational collapse of galactic objects.

The experiment has been monitoring the Galaxy since June 1992, under increasing larger configurations: in January 2001 it has reached its final active mass $M = 1$ kt. After ten years of running, LVD still remains one of the largest liquid scintillator apparatus for the detection of stellar collapses and, togheter with SNO and SuperKamiokande it is part of the SNEWS network. Furthermore, the ability of LVD to detect muons will allow the experiment to provide a good monitor for the forthcoming CNGS beam.

1 Introduction

LVD, located in Hall A of the INFN Gran Sasso National Laboratory, is a multipurpose detector consisting of a large volume of liquid scintillator interleaved with limited streamer tubes in a compact geometry. The major purpose of the LVD experiment is the search for neutrinos from Gravitational Stellar Collapses (GSC) in our Galaxy [1].

In spite of the lack of a "standard" model of the gravitational collapse of a massive star, some features of its dynamics and, in particular, of the correlated neutrino emission appear to be well established. At the end of its burning phase a massive star ($M > 8M_{\odot}$) explodes into a supernova (SN), originating a neutron star which cools emitting its binding energy $E_B \sim 3 \cdot 10^{53}$ erg mostly in neutrinos.

The largest part of this energy, almost equipartitioned among neutrino and antineutrino species, is emitted in the cooling phase: $E_{\bar{\nu}_e} \sim E_{\nu_e} \sim E_{\nu_x} \sim E_B/6$ (where ν_x denotes generically $\nu_\mu, \bar{\nu}_\mu, \nu_\tau, \bar{\nu}_\tau$ flavors). The energy spectra are approximatively a Fermi-Dirac distribution, but with different mean temperatures, since ν_e, $\bar{\nu}_e$ and ν_x have different couplings with the stellar matter: $T_{\nu_e} < T_{\bar{\nu}_e} < T_{\nu_x}$. LVD is able to detect $\bar{\nu}_e$ interactions with protons, which give the main signal of supernova neutrinos, with a very good signature. Moreover, it can detect ν_e through the elastic scattering reactions with electrons, and it is also sensitive to neutrinos of all flavors detectable through neutral and charged currents interactions with the carbon nuclei of the scintillator.

The described features of stellar collapses are in fact common to all existing models and lead to rather model independent expectations for supernova neutrinos. Thus, the signal observable in LVD, in different reactions and due to different kinds of neutrinos, besides providing astrophysical informations on the nature of the collapse, is sensitive to intrinsic ν properties, as oscillation of massive neutrinos and can give an important contribution to define some neutrino oscillation properties still missing.

2 The LVD experiment

2.1 The detector

The LVD experiment has been in operation since 1992, under different increasing configurations. During 2001 the final upgrade took place: LVD became fully operational, with

an active scintillator mass $M = 1000$ t. LVD now consists of an array of 840 scintillator counters, 1.5 m^3 each. These are interleaved by streamer tubes, and arranged in a compact and modular geometry. There are two subsets of counters: the external ones (43%), operated at energy threshold $\mathcal{E}_h \simeq 7$ MeV, and inner ones (57%), better shielded from rock radioactivity and operated at $\mathcal{E}_h \simeq 4$ MeV. In order to tag the delayed γ pulse due to n-capture, all counters are equipped with an additional discrimination channel, set at a lower threshold, $\mathcal{E}_l \simeq 1$ MeV.

The top level counters, more exposed to the tunnel walls, and thus characterized by a higher background counting rate and a minor capability to disentangle $\bar{\nu}_e$ interactions, have been shielded by a 2 cm thick iron layer. With respect to the neutron background, the 72 counters which belonged to the Mont Blanc LSD telescope, have been placed as a shield on the top of LVD. In figure 1 you can see a view of the ν telescope.

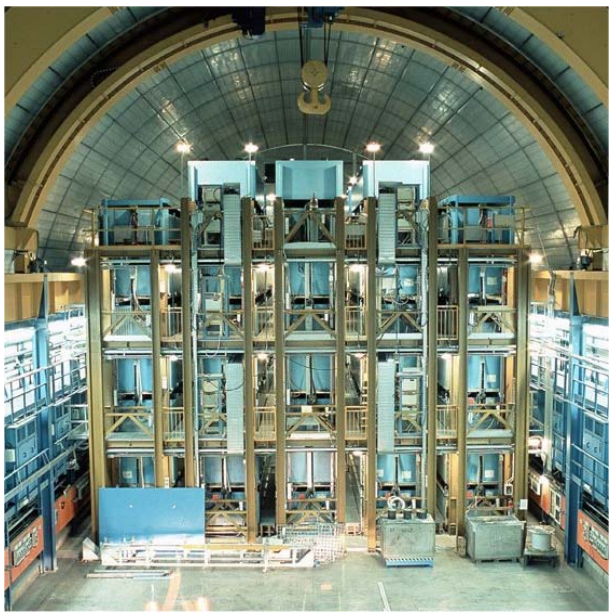

Figure 1: LVD

The tracking system consists of L-shaped detectors, one for each module. Each element contains two staggered layers of 6.3 m long limited streamer tubes. The bidimensional read-out is made by means of 4 cm strips, parallel and perpendicular to the tubes, providing high detection efficiency and an angular resolution better than 4 mrad.

Relevant features of the detector are:

- (i) good event localization and muon tagging;
- (ii) accurate absolute and relative timing: $\Delta t_{abs} = 1\,\mu s$, $\Delta t_{rel} = 12.5\,ns$;

- (*iii*) energy resolution: $\sigma_E/E = 0.07 + 0.23 \cdot (E/\mathrm{MeV})^{-0.5}$;
- (*iv*) very high duty cycle, i.e. 99.7% in the last year;
- (*v*) fast event recognition.

2.2 SN neutrino interactions

The observable neutrino reactions are:

- *(1)* $\bar{\nu}_e p, e^+ n$, observed through a prompt signal from e^+ above threshold $\mathcal{E}_h$ (detectable energy $E_d \simeq E_{\bar{\nu}_e} - 1.8$ MeV $+2m_e c^2$), followed by the signal from the $np, d\gamma$ capture ($E_\gamma = 2.2$ MeV), above $\mathcal{E}_l$ and with a mean delay $\Delta t \simeq 180$ μs.
- *(2)* ν_e ^{12}C,^{12}N e^-, observed through two signals: the prompt one due to the e^- above $\mathcal{E}_h$ (detectable energy $E_d \simeq E_{\nu_e} - 17.8$ MeV) followed by the signal, above $\mathcal{E}_h$, from the β^+ decay of ^{12}N (mean life time $\tau = 15.9$ ms).
- *(3)* $\bar{\nu}_e$ ^{12}C,^{12}B e$^+$, observed through two signals: the prompt one due to the e^+ (detectable energy $E_d \simeq E_{\bar{\nu}_e} - 13.9\,\mathrm{MeV} + 2m_e c^2$) followed by the signal from the β^- decay of ^{12}B (mean life time $\tau = 29.4$ ms). As for reaction *(2)*, the second signal is detected above the threshold $\mathcal{E}_h$.
- *(4)* $\overset{(-)}{\nu}_\ell$ ^{12}C, $\overset{(-)}{\nu}_\ell$ ^{12}C* ($\ell = e, \mu, \tau$), whose signature is the monochromatic photon from carbon de-excitation ($E_\gamma = 15.1$ MeV), above $\mathcal{E}_h$.
- *(5)* $\overset{(-)}{\nu}_\ell$ e^-, $\overset{(-)}{\nu}_\ell$ e^-, which yields a single signal, above $\mathcal{E}_h$, due to the recoil electron.

3 Supernova and ν physics

3.1 Monitoring

LVD has been continuously monitoring the Galaxy since 1992 in the search for neutrino bursts from GSC [1]. Its active mass has been progressively increased from about 330 t in 1992 to the present 1000 t, always guaranteeing a sensitivity to GSC up to distances $d = 20$ kpc from the Earth, even for the lowest ν-sphere temperature.

The telescope duty cycle has been continuously improving since 1992, as it can be seen in Fig.2; in the last years the average duty cycle was $> 99\%$.

The reliability of LVD to detect and recognize ν-bursts with different characteristics, has been tested by inducing clusters of pulses - with different multiplicity and duration - in the LVD counters. The cluster injector, consisting of a generator of light pulses in a certain number of counters, was realized during 2001 and allowed us to evaluate the system efficiency on detecting and disentangling bursts from the background, even with different background conditions.

[1] The results of this search have been periodically updated and published[2, 3, 4, 5, 6]. The latest update, including the 10 years interval between 1992 and 2002, will be presented at the next ICRC Conference, to be held in Tokyo in August 2003.

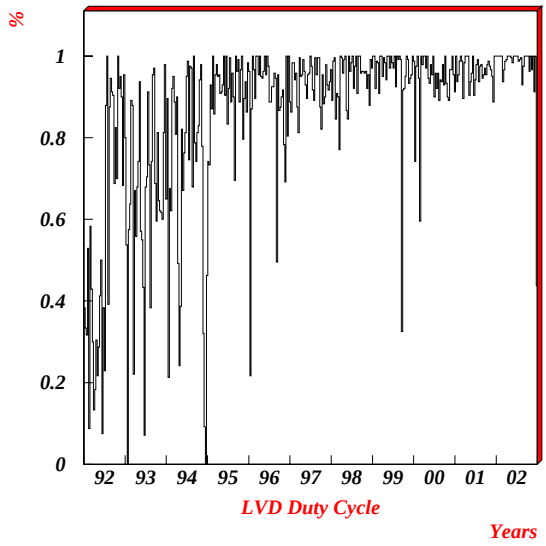

Figure 2: LVD duty cycle.

The observation of a neutrino burst due to the explosion of a galactic supernova can add precious informations about neutrino mass and mixing scenarios, in a complementary way with respect to solar, atmospheric and terrestrial ν experiments. The combination of well separated classes of events, namely those due to charged (reactions *(2)* and *(3)*) and neutral current *(4)* interactions on carbon and those due to inverse β decay *(1)*, can help to distinguish between different scenarios of massive neutrinos and astrophysical parameters.

The signal at LVD from a SN exploding at $D = 10$ kpc for 3-flavor ν oscillation, assuming the LMA-MSW solution for solar ν, and normal or inverted mass hierarchy has been calculated [7] [8]. As shown in figure 3, a large increase with respect to the no-oscillation case is present in the number of inverse β decay $\bar{\nu}_e$ interactions if the temperature T_{ν_x} of the μ and τ flavours is sensibly higher then $T_{\bar{\nu}_e}$. For normal mass hierarchy the number of $\bar{\nu}_e p$ events is practically the same both for adiabatic and non-adiabatic conditions, since, MSW effect takes place in the neutrino sector only. Quite a different picture appears, assuming inverse mass hierarchy: the increment in the number of interactions is the same as in the case of normal hierarchy for non-adiabatic conditions while it is more then double for the adiabatic case.
At the same time, the neutrino flavour mixing results in an increase of the total number of c.c. interactions with ^{12}C (see figure 4), due to both ν_e and $\bar{\nu}_e$. In case of high neutrinosphere temperature, LVD could be sensitive to the adiabaticity of the oscillation process. In addition, as recently discussed [9], the comparison of the results of a *network* of detectors could allow to fully exploit the supernova neutrino signal, thus learning much more on neutrino intrinsic properties.

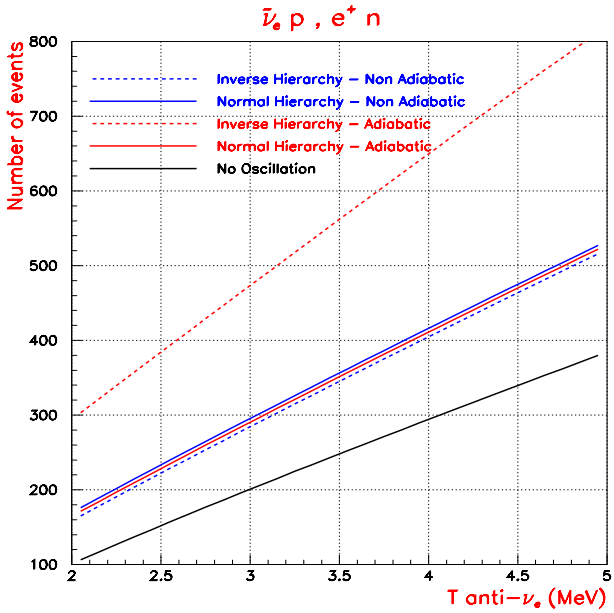

Figure 3: Number of inverse beta decay interactions expected in the LVD detector (1000 t) in case of a supernova exploding at $d = 10$ kpc, with neutrinosphere temperatures $T_{\bar{\nu}_e} = T_{\nu_e}$ and $T_{\nu_x} = 2\ T_{\nu_e}$. Neutrino oscillation parameters used in the calculation are $U^2_{e2} = 0.33$; $U^2_{e3} = 10^{-2}$ in the adiabatic case, $U^2_{e3} = 10^{-6}$ in the non adiabatic case.

4 SNEWS

The SNEWS (SuperNova Early Warning System) is a collaboration among experiments of several major neutrino detectors with sensitivity to supernova neutrinos. The primary goal of SNEWS is to provide the astronomical community with a completely automated alert[10]. At present Super-K, SNO and LVD are charter members of the SNEWS network. Representative of AMANDA, KamLAND, Borexino, and OMNIS are members of the SNEWS Working Group, and will eventually join the active members of the network.

Two coincidence machines are currently on line, at the Kamioka site and at Gran Sasso. Additional machines will be deployed in the future. These machines continuously run coincidence programs, which wait for alarm signals from the experiments and provide an alert if there is a coincidence within a specified time window (10 seconds for normal running).

At present, the SNEWS network is in a test phase, to ensure the continued reliability of operations.

During 2001 Super-K, SNO and LVD performed a "high rate test" of the coincidence software during two months. The purpose was two-fold: first, to check the robustness of the software and work out any remaining bugs, and second, to increase confidence in our understanding of the predicted coincidence rates. The analysis of the data was completed during 2002. The data shows that the test was highly successful. A few minor bugs were found during the first week of the test, but on the whole the software performed extremely well [11]. The High Rate Test shows that although individual experiment rates

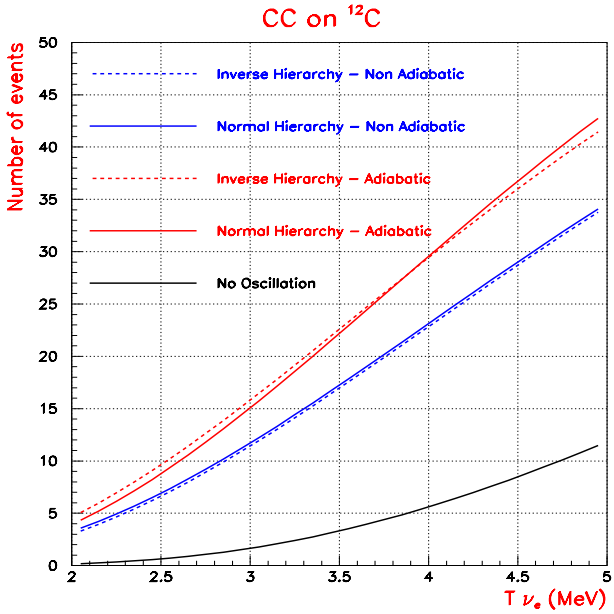

Figure 4: Number of CC interactions on ^{12}C expected in the LVD detector (1000 t) in case of a supernova exploding at $d = 10$ kpc, with neutrinosphere temperatures $T_{\bar{\nu}_e} = T_{\nu_e}$ and $T_{\nu_x} = 2\ T_{\nu_e}$. Neutrino oscillation parameters used in the calculation are $U^2_{e2} = 0.33$; $U^2_{e3} = 10^{-2}$ in the adiabatic case, $U^2_{e3} = 10^{-6}$ in the non adiabatic case.

are slightly non-stationary, they are clearly uncorrelated as it is shown by the results of the Time Shift Method analysis. In the last few years, the existing neutrino telescopes, with the SNEWS network and the gravitational waves (GW) detectors, with the IGEC Collaboration, are studying their signals in correlation among them. It is desirable that in the near future the two communities will correlate their results. With this aim, we began to explore this possibility (as it was done in occasion of SN1987a) studying the possible correlation between the data collected in 2001 by the LVD detector and the two cryogenic GW antennas EXPLORER and NAUTILUS. Data analysis of the combined data is in progress.

5 CNGS beam monitor

The CNGS beam from CERN to the Gran Sasso Laboratory (LNGS) is a wide-band high-energy ν_μ beam ($< E > \sim 23\ GeV$) optimized for τ appearance. It provides $\sim$ 2600 $CC/kt/y$ and $\sim$ 800 $NC/kt/y$ at Gran Sasso [12], that is, assuming 200 days of beam-time per year, a total number of $\sim 17\ (CC + NC)/kt/day$.

In order to provide an adequate monitoring of the beam performance it has been estimated [13] that one should be able to collect an event sample affected by a statistical error of the order of 3% in a few days time.

Even considering an overall mass of the various experiments which will be active in GS at the beam start up as large as 5 kt, the number of CC and NC interaction per

day, internal to the detectors, will be only $\sim$ 80 and therefore more than 14 days will be needed to collect a sample with the statistical significance mentioned above.

The number of events observed per day can be increased considering the muons produced by the ν_μ CC interactions in the upstream rock, emerging into the experimental halls and detected either by a simple wide area dedicated monitor or by the running experiments.

We have investigated the beam monitor capabilities of the LVD detector [1], whose beam orthogonal surface is $13 \times 11\ m^2$, larger than the other foreseen CNGS experiments. A detailed MonteCarlo simulation to estimate both the muon flux inside LVD and the number of detectable CC and NC internal interactions has been developed.

5.1 MonteCarlo simulation description

The interactions, both in the rock and in the LVD detector, of the CNGS beam neutrinos have been simulated using the Lipari generator [14] and the neutrino energy from the reference CNGS beam spectrum [12]. To estimate the number of events we assumed $5.85 \times 10^{-17}\ CC/pot/kt$ and $4.5 \times 10^{19}\ pot/year$ (1 year $\equiv$ 200 days).

The muon energy loss and the angular scatterings in the rock between the production point and the detector are taken into account with MUSIC [16], a three dimensional code for the muon propagation through the rock, that includes ionization, bremsstrahlung, pair production, nuclear interactions and multiple coulomb scattering.

Finally, the detector geometry and the particles' interactions inside the detector have been described with a GEANT simulation of LVD. A typical events of a muon emerging from the rock and entering LVD is shown in figure 5, while a CC neutrino interaction inside the detector is shown in figure 6.

5.2 Results

The number of μ hitting the GEANT reference volume enclosing the LVD apparatus in one "200-days year" is $\sim$ 33600, that is $\sim$ 170 per day. 79% of them go through a sensitive part of the detector (scintillator) and 92% of this latter sample release more than 200 MeV at least in one scintillation counter. Choosing it as the muon selection criteria, the number of detected muons in LVD is 24200 per year, that is $\sim$ 120 per day. Moreover, $\sim$ 30 events per day are expected due to ν_μ CC and NC inside the whole apparatus, for a total number of $\sim$ 150 CNGS events per day. The results are summarized in tables 1 and 2. It is, therefore, possible to get a 3% statistical error in 7 days of running. These results fulfill the requirements made by CNGS beam experts [13]. The main background source is due to cosmic muons. The rate in the whole LVD detector is about 9300 muons/day (about 6.5 per minute), considering the events with at least one scintillation counter fired by the muon. The requirement of at least one counter with an energy loss greater than 200 MeV rejects 20% of them, leaving about 7500 muons per day. Considering the 10^4 reduction factor due to the CNGS beam timing characteristics (10.5 μs of spill length and 50 ms inter-spill gap [18]), the actual number of background μ per day is $\sim$ 1.5, practically negligible. Preliminary results of the analysis have been presented in the poster session of the Neutrino 2002 Conference [19].

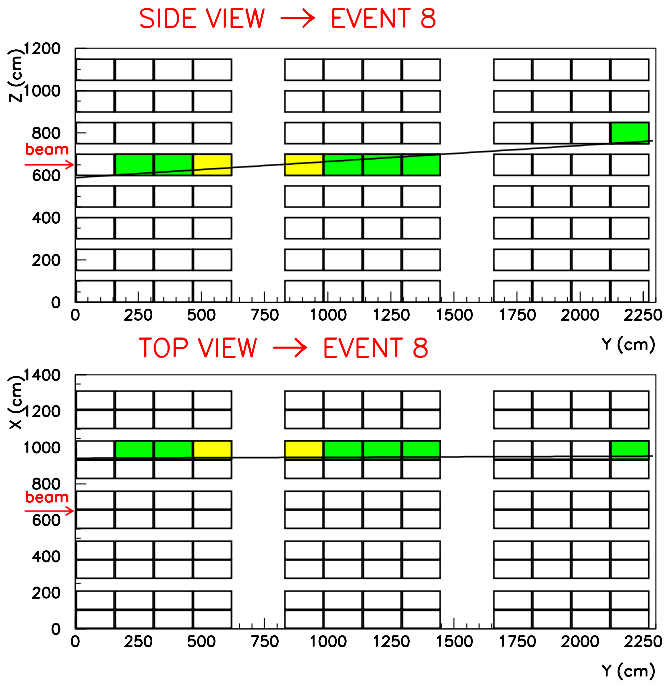

Figure 5: Event display of a *CNGS* μ crossing 8 scintillation counters.

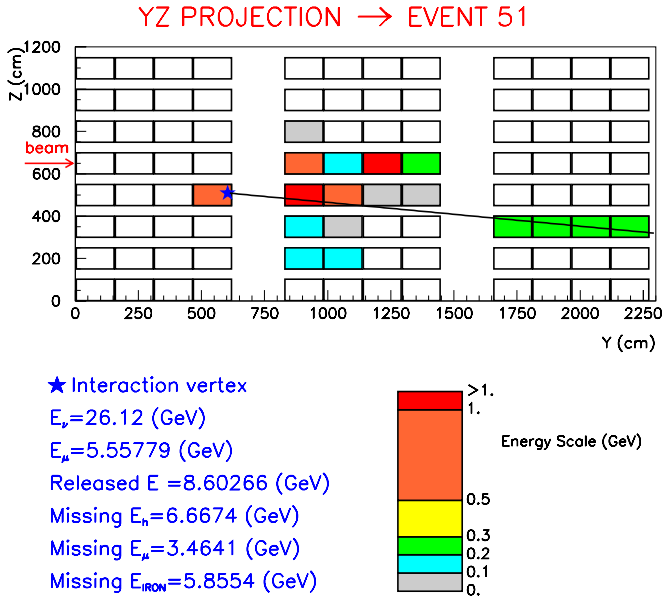

Figure 6: Event display of CNGS ν_μ charged current internal interaction.

Rock cylinder Volume	726493 m^3
Rock cylinder Mass	1969 kt
Nominal CNGS beam intensity	$4.5 \times 10^{19} pot/year$
CC Interaction Probability	5.85×10^{-17} $CC/pot/kt$
ν_μ CC interactions in the rock	5.18×10^6 *per year*
μ survival probability at LNGS	6.8%
Nb. of μ at the LNGS entrance wall	351600 *per year*
Probability to hit LVD "mother volume"	9.6%
Nb. of μ hitting LVD "mother volume"	33600 *per year*
Geometrical efficiency	79%
Nb. of μ hitting LVD sensitive volume	26200 *per year*
Selection cut efficiency	92%
Nb. of detected μ	24200 *per year*

Table 1: Number of *CNGS muons* detected in LVD.

	Volume	**Mass**
Scintillator	1340 m^3	1044 t
Stainless Steel	98.5 m^3	770 t
Total Target		$\sim$ 1810 t
	CC	**NC**
ν_μ interactions in LVD	4770 *per year*	1460 *per year*
efficiency for the selection cut	97%	91%
Nb. of detected events	4630 *per year*	1330 *per year*
Total nb. of detected events	5960 *per year*	

Table 2: Number of internal CC and NC events in LVD.

References

[1] LVD Collaboration, Il Nuovo Cimento **A105** (1992) 1793

[2] LVD Collaboration, 23th ICRC Conf.Proc.,HE 5.1.1,Vol.4,468,1993

[3] LVD Collaboration, 24th ICRC Conf.Proc., HE 5.3.6,Vol.1,1035,1995

[4] LVD Collaboration, 25th ICRC Conf.Proc., HE 4.1.12,1997

[5] LVD Collaboration, 26th ICRC Conf.Proc., HE 4.2.08,Vol.2,223,1999

[6] LVD Collaboration, 27th ICRC Conf.Proc., HE230,1093,2001

[7] LVD Collaboration, Nucl. Phys. B Proc. Sup. 110 (2002) pp 410-413, astro-ph/0112312

[8] A. Zichichi, *The most powerful scintillator supernova neutrino detector*, talk presented at the symposium *LVD: the First Ten Years*, LNGS, 28-29 October, 2002).

[9] C.Lunardini and A.Yu.Smirnov, hep-ph/0106149

[10] http://hep.bu.edu/∼snnet/

[11] SNEWS Subgroup "Proposal for an Automated Supernova Alert for the Astronomical Community"

[12] A.E.Ball et al., CERN-SL-2000-063 EA.

[13] A.E.Ball et al., CERN-SL-2001-016 EA.

[14] P. Lipari et al., Phys. Rev. Lett. **74** (1995), 4384.

[15] M. Gluck, E. Reya and A. Vogt, Z. Phys. **C 67** (1995) 433.

[16] P. Antonioli et al., Astrop. Phys. **7** (1997), 357.

[17] M. Selvi, *Misura del flusso di muoni nell'esperimento LVD, presso i Laboratori Nazionali del Gran Sasso.* - Degree thesis - Bologna University (1996). (see http://www.bo.infn.it/lvd/pubdocs/STESI.PS)

[18] B. Goddard et al., Proc. of EPAC 2000, 2240.

[19] *The CNGS beam monitor with LVD*. Poster presented at the "Neutrino 2002" Conference - Munich, Germany - 25-30 May 2002.

MACRO. Monopole Astrophysics Cosmic Ray Observatory

M. Ambrosio[12], R. Antolini[7], A. Baldini[13], G. C. Barbarino[12], B. C. Barish[4], G. Battistoni[6,b], Y. Becherini[2], R. Bellotti[1], C. Bemporad[13], P. Bernardini[10], H. Bilokon[6], C. Bloise[6], C. Bower[8], M. Brigida[1], S. Bussino[18], F. Cafagna[1], D. Campana[12], M. Carboni[6], R. Caruso[9], S. Cecchini[2,c], F. Cei[13], V. Chiarella[6], T. Chiarusi[2], B. C. Choudhary[4], S. Coutu[11,i], M. Cozzi[2], G. De Cataldo[1], H. Dekhissi[2,17], C. De Marzo[1], I. De Mitri[10], J. Derkaoui[2,17], M. De Vincenzi[18], A. Di Credico[7], C. Favuzzi[1], C. Forti[6], P. Fusco[1], G. Giacomelli[2], G. Giannini[13,d], N. Giglietto[1], M. Giorgini[2], M. Grassi[13], A. Grillo[7], C. Gustavino[7], A. Habig[3,p], K. Hanson[11], R. Heinz[8], E. Iarocci[6,e], E. Katsavounidis[4,q], I. Katsavounidis[4,r], E. Kearns[3], H. Kim[4], A. Kumar[2,t], S. Kyriazopoulou[4], E. Lamanna[14,l], C. Lane[5], D. S. Levin[11], P. Lipari[14], N. P. Longley[4,h], M. J. Longo[11], F. Loparco[1], F. Maaroufi[2,17], G. Mancarella[10], G. Mandrioli[2], S. Manzoor[2,n], A. Margiotta[2], A. Marini[6], D. Martello[10], A. Marzari-Chiesa[16], D. Matteuzzi[2], M. N. Mazziotta[1], D. G. Michael[4], P. Monacelli[9], T. Montaruli[1], M. Monteno[16], S. Mufson[8], J. Musser[8], D. Nicolò[13], R. Nolty[4], C. Orth[3], G. Osteria[12], O. Palamara[7], V. Patera[6,e], L. Patrizii[2], R. Pazzi[13], C. W. Peck[4], L. Perrone[10], S. Petrera[9], V. Popa[2,g], A. Rainò[1], F. Ronga[6], C. Satriano[14,a], E. Scapparone[7], K. Scholberg[3,q], A. Sciubba[6], M. Sioli[2], G. Sirri[2], M. Sitta[16,o], P. Spinelli[1], M. Spinetti[6], M. Spurio[2], R. Steinberg[5], J. L. Stone[3], L. R. Sulak[3], A. Surdo[10], G. Tarlè [11], V. Togo[2], M. Vakili[15,s], C. W. Walter[3,4], R. Webb[15].

[1] Dipartimento di Fisica dell'Università di Bari and INFN, 70126 Bari, Italy
[2] Dipartimento di Fisica dell'Università di Bologna and INFN, 40126 Bologna, Italy
[3] Physics Department, Boston University, Boston, MA 02215, USA
[4] California Institute of Technology, Pasadena, CA 91125, USA
[5] Department of Physics, Drexel University, Philadelphia, PA 19104, USA
[6] Laboratori Nazionali di Frascati dell'INFN, 00044 Frascati (Roma), Italy
[7] Laboratori Nazionali del Gran Sasso dell'INFN, 67010 Assergi (L'Aquila), Italy
[8] Depts. of Physics and of Astronomy, Indiana University, Bloomington, IN 47405, USA
[9] Dipartimento di Fisica dell'Università dell'Aquila and INFN, 67100 L'Aquila, Italy
[10] Dipartimento di Fisica dell'Università di Lecce and INFN, 73100 Lecce, Italy
[11] Department of Physics, University of Michigan, Ann Arbor, MI 48109, USA
[12] Dipartimento di Fisica dell'Università di Napoli and INFN, 80125 Napoli, Italy
[13] Dipartimento di Fisica dell'Università di Pisa and INFN, 56010 Pisa, Italy
[14] Dipartimento di Fisica dell'Università di Roma "La Sapienza" and INFN, 00185 Roma, Italy
[15] Physics Department, Texas A&M University, College Station, TX 77843, USA
[16] Dipartimento di Fisica Sperimentale dell'Università di Torino and INFN, 10125 Torino, Italy
[17] L.P.T.P., Faculty of Sciences, University Mohamed I, B.P. 524 Oujda, Morocco
[18] Dipartimento di Fisica dell'Università di Roma Tre and INFN Sezione Roma Tre, 00146 Roma, Italy
[a] Also Università della Basilicata, 85100 Potenza, Italy
[b] Also INFN Milano, 20133 Milano, Italy
[c] Also Istituto TESRE/CNR, 40129 Bologna, Italy
[d] Also Università di Trieste and INFN, 34100 Trieste, Italy
[e] Also Dipartimento di Energetica, Università di Roma, 00185 Roma, Italy
[f] Also Institute for Nuclear Research, Russian Academy of Science, 117312 Moscow, Russia
[g] Also Institute for Space Sciences, 76900 Bucharest, Romania
[h] Also Macalester College, Dept. of Physics and Astr., St. Paul, MN 55105
[i] Also Department of Physics, Pennsylvania State University, University Park, PA 16801, USA
[l] Also Dipartimento di Fisica dell'Università della Calabria, Rende (Cosenza), Italy
[m] Also Department of Physics, James Madison University, Harrisonburg, VA 22807, USA
[n] Also RPD, PINSTECH, P.O. Nilore, Islamabad, Pakistan
[o] Also Dipartimento di Scienze e Tecnologie Avanzate, Università del Piemonte Orientale, Alessandria, Italy
[p] Also U. Minn. Duluth Physics Dept., Duluth, MN 55812
[q] Also Dept. of Physics, MIT, Cambridge, MA 02139
[r] Also Intervideo Inc., Torrance CA 90505 USA
[s] Also Resonance Photonics, Markham, Ontario, Canada
[t] Also Department of Physics, SLIET,Longowal,India

Abstract

In this 2002 Status Report of the MACRO experiment, we present the final stringent upper limits on GUT magnetic monopoles, nuclearites and lightly ionizing particles, and the shadow of primary cosmic rays by the Moon and the Sun. We also describe the MACRO results on atmospheric neutrino oscillations, high energy muon neutrino astronomy, searches for WIMPs, search for low energy stellar gravitational collapse neutrinos, high energy downgoing muons and primary cosmic ray composition

1 Introduction

MACRO was a large area multipurpose underground detector designed to search for rare events in the cosmic radiation. It was optimized to look for the supermassive magnetic monopoles predicted by Grand Unified Theories (GUT) of the electroweak and strong interactions; it also included the study of atmospheric neutrinos and neutrino oscillations, high energy ($E_\nu \gtrsim 1$ GeV) neutrino astronomy, indirect searches for WIMPs, search for low energy ($E_\nu \gtrsim 7$ MeV) stellar collapse neutrinos, studies of various aspects of the high energy underground muon flux (which is an indirect tool to study the primary cosmic ray composition, origin and interactions), searches for fractionally charged particles and other rare particles that may exist in the cosmic radiation.

The detector was built and equipped with electronics during the years $1988-1995$. It started data taking with part of the apparatus in 1989; it was completed in 1995 and it was running in its final configuration until December 19, 2000. It may be worth pointing out that all the physics and astrophysics items proposed in the 1984 Proposal were covered and good results were obtained on each of them, even beyond the most rosy anticipations.

In the year 2002 nine papers were published on refereed journals [1]-[9]; six more papers are in an advanced state of preparation [10]-[15]. Several results appeared in preliminary form in the 2001 Status Report [16], in 15 paper contributions to 2002 Conferences, Summer Schools and in communications at the meeting of the Società Italiana di Fisica in Alghero 26/9-1/10 [17] - [31].

2 The Detector

The MACRO detector had global dimensions of $76.5 \times 12 \times 9.3\,\mathrm{m}^3$ and provided a total acceptance to an isotropic flux of particles of $\sim 10,000\,\mathrm{m}^2\,\mathrm{sr}$. [1] [32].

The detector was composed of three sub-detectors: liquid scintillation counters, limited streamer tubes and nuclear track detectors. Each one of them could be used in "stand-alone" and in "combined" mode.

3 Atmospheric neutrino oscillations

Upward going muons are identified using the streamer tube system (for tracking) and the scintillator system (for time-of-flight measurement). The number of events measured and expected for the three measured topologies deviate from the MC expectations; the deviations point out to the same $\nu_\mu \to \nu_\tau$ oscillation scenario [16]. This is confirmed by the shape of the zenith distributions and by the L/E_ν distribution [5] [17] [33].

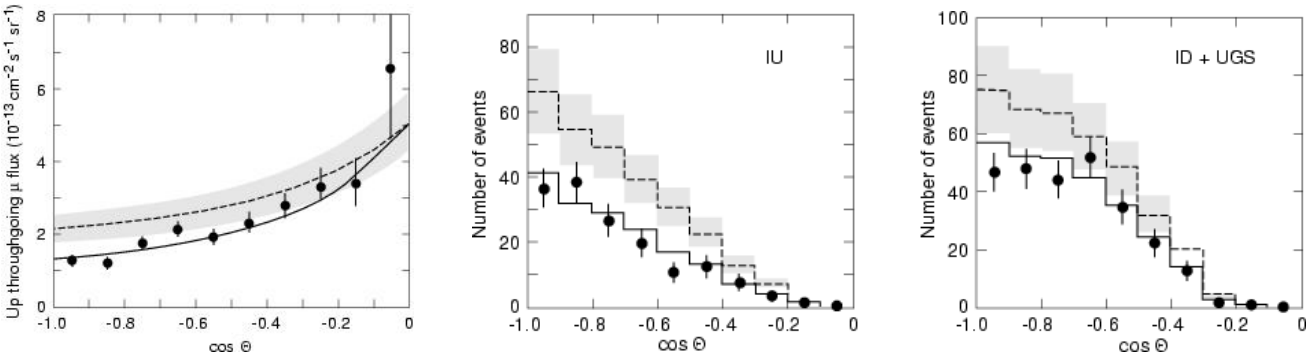

Figure 1: Zenith distributions for the MACRO data (black points) for (a) upthroughgoing, (b) semicontained and (c) up-stopping muons + down semicontained. The dashed lines are the no-oscillation MC predictions (with scale error bands); the solid lines refer to oscillation $\nu_\mu \to \nu_\tau$ with maximum mixing and $\Delta m^2 = 2.5 \cdot 10^{-3}$ eV^2.

Several checks were performed using redundant electronics; also different sources of background were studied in detail [16] [34].

The *upthroughgoing muons* come from ν_μ interactions in the rock below the detector; the ν_μ's have a median energy $\overline{E_\nu} \sim$ 50 GeV. The upthroughgoing muons with $E_\mu > 1$ GeV cross the whole detector. The total data taking livetime was slightly over 6 years (full detector equivalent) [16] [33]. The data deviate in absolute value and in shape from the MC predictions. This was first pointed at TAUP 1993 and in 1995 in [33].

We studied a large number of possible systematic effects that could affect our measurements: no significant systematic problems exist in the detector or in the data analyses. One of the most significant checks was performed using only the scintillator system with the PHRASE Wave Form Digitizers, completely independent of the ERP system in [33].

The measured data have been compared with Monte Carlo simulations. The total systematic uncertainty on the expected muon flux, obtained adding in quadrature the errors from neutrino flux, cross section and muon propagation, is estimated to be 17 %. This uncertainty is mainly a scale error; the error on the shape of the angular distribution is $\sim 5\%$. Fig. 1 shows the zenith angle distribution of the measured flux of upthroughgoing muons. The Monte Carlo expectation for no oscillations is shown as a dashed line with a $\pm 17\%$ band.

For oscillations the best fit parameters are $\Delta m^2 = 2.5 \cdot 10^{-3}$ eV^2 and maximal mixing; the result of the fit is the solid line in Fig. 1.

Fig. 2 shows the allowed regions for the $\nu_\mu \to \nu_\tau$ oscillation parameters in the $sin^2 2\theta - \Delta m^2$ plane. The MACRO 90% c.l. allowed region for $\nu_\mu \to \nu_\tau$ is compared in Fig. 2 with those obtained by the SuperKamiokande (SK) [36] and Soudan 2 experiments [37].

Matter effects due to the difference between the weak interaction effective potential for muon neutrinos with respect to sterile neutrinos would produce a different total number and a different zenith distribution of upthroughgoing muons. We found that $\nu_\mu \to \nu_s$ oscillations are disfavoured at 99% c.l. compared to the $\nu_\mu \to \nu_\tau$ channel [35].

The oscillation probability is a function of the ratio L/E_ν. E_ν was estimated by measuring the muon energy E_μ, which was done using their Multiple Coulomb Scattering (MCS) in the rock absorbers in the lower MACRO. Two methods were used. The second method used the streamer tubes in "drift mode", using the TDC's included in the QTP system, originally designed to search for magnetic monopoles. The space resolution achieved is $\simeq 3$ mm. For each muon,

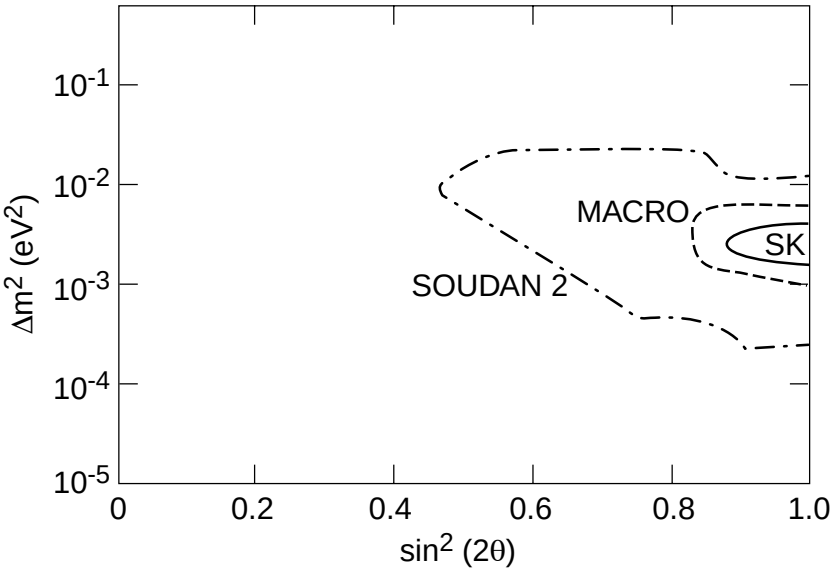

Figure 2: 90% C.L. contour plots of the allowed regions of SK, MACRO and Soudan 2 (the figure is being improved on the basis of recent reanalyses).

seven variables were given in input to a Neural Network (NN) previously trained to estimate the muon energy with MC events of known input energy crossing the detector at different zenith angles. The distribution of the ratio $R = (Data/MC_{noosc})$ obtained by this analysis is plotted in Fig. 3 as a function of $log_{10}(L/E_\nu)$ [5] [11]. Notice that the data extend from $(L/E_\nu) \sim 30$ km/GeV to about 5000 km/GeV. The *Internal Upgoing* (IU) muons ($\sim$ 150 events) come from 4.2 GeV ν_μ's interacting in the lower apparatus. Notice that compared to the no-oscillation prediction there is a reduction of about a factor of two in the flux of these events, without any distortion in the shape of the zenith distribution, Fig. 1b.

The *upstopping muons* (UGS) are due to 3.5 GeV ν_μ's interacting below the detector and yielding upgoing muons stopping in the detector. The *semicontained downgoing muons* (ID) are due to ν_μ-induced downgoing tracks with vertex in the lower MACRO (260 events). The two types of events are identified by means of topological criteria; the lack of time information prevents to distinguish the two sub-samples. The zenith distribution shows a uniform deficit of about 25 % of the measured number of events for the whole angular distribution with respect to no-oscillation prediction, Fig. 1c.

The average value of the double ratio $R = (Data/MC)_{IU}/(Data/MC)_{ID+UGS}$ over the measured zenith angle range is $R \simeq 0.77 \pm 0.07$; the error includes statistical and theoretical uncertainties; $R = 1$ is expected in case of no oscillations.

In [11] we combined our high energy data for the zenith distribution, $A = (N_{vert}/N_{horiz})$, with the neutrino energy measurement, $R = N_{low}/N_{high}$. They are both independent of the neutrino absolute flux; with these two informations the significance of our observation of neutrino oscillations is well above 4 σ. In [14] we combine these two measurements with the absolute flux of the high energy data and the ratio of the two set of low energy data, obtaining a considerable improvement in the significance of our observation of neutrino oscillations, $\gtrsim 6\sigma$ (the predicted flux is being reevaluated on the basis of new experimental data).

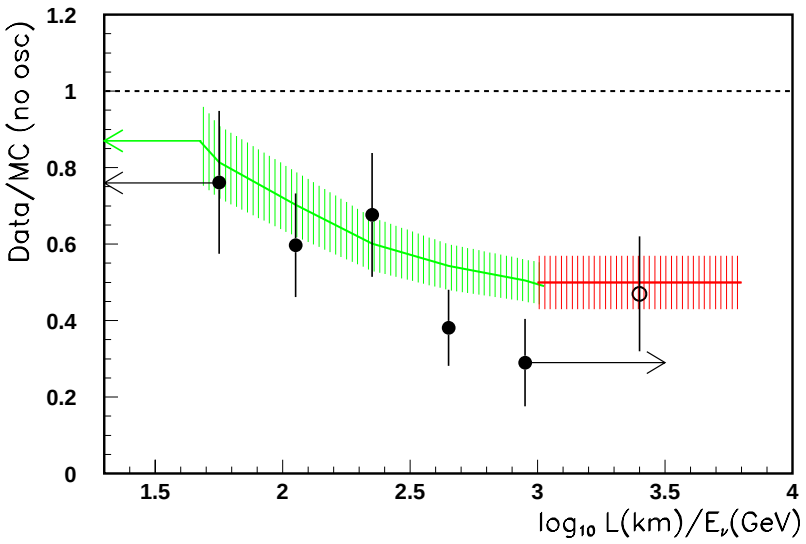

Figure 3: Ratio (Data/MC) as a function of estimated L/E_ν for the upthrougoing muon sample (black circles) and the semicontained up-μ (open circle). For upthroughgoing muons the muon energy was estimated by multiple Coulomb scattering and E_ν by MC methods. The shaded regions represent the uncertainties in the MC predictions assuming $\sin^2 2\theta = 1$ and $\Delta m^2 = 0.0025$ eV^2. The horizontal dashed line at Data/MC=1 is the expectation for no oscillations.

4 Search for Astrophysical Point Sources of High Energy Muon Neutrinos

High energy ν_μ's are expected to come from several galactic and extragalactic sources. Neutrino production requires astrophysical accelerators of charged particles and some kind of astrophysical beam dumps. The excellent angular resolution of our detector allowed a sensitive search for upgoing muons, produced by neutrinos coming from celestial sources, interacting below the detector. An excess of events was searched for around the positions of known sources in 3° (half width) angular bins. We established 90% c.l. upper limits on the muon fluxes from specific celestial sources; the limits lay in the range $10^{-15} - 10^{-14}\,\mathrm{cm}^{-2}\,\mathrm{s}^{-1}$. We have two cases, GX339-4 ($\alpha = 255.71^o$, $\delta = -48.79^o$) and Cir X-1 ($\alpha = 230.17^o$, $\delta = -57.17^o$), with 7 events; we have considered these events as background, therefore the upper flux limits are higher; but the events could also be indication of signals [38].

We searched for time coincidences of our upgoing muons with γ-ray bursts. No statistically significant time correlation was found.

We have also searched for a diffuse astrophysical neutrino flux for which we establish a flux upper limit at the level of $1.5 \cdot 10^{-14}\,\mathrm{cm}^{-2}\,\mathrm{s}^{-1}$ [3].

5 Indirect Searches for WIMPs

Weakly Interacting Massive Particles (WIMPs) could be part of the galactic dark matter; they could be intercepted by celestial bodies, slowed down and trapped in their centers, where WIMPs and anti-WIMPs could annihilate and yield upthroughgoing muons. The annihilations in these celestial bodies would yield neutrinos of GeV or TeV energy, in small angular windows from their centers.

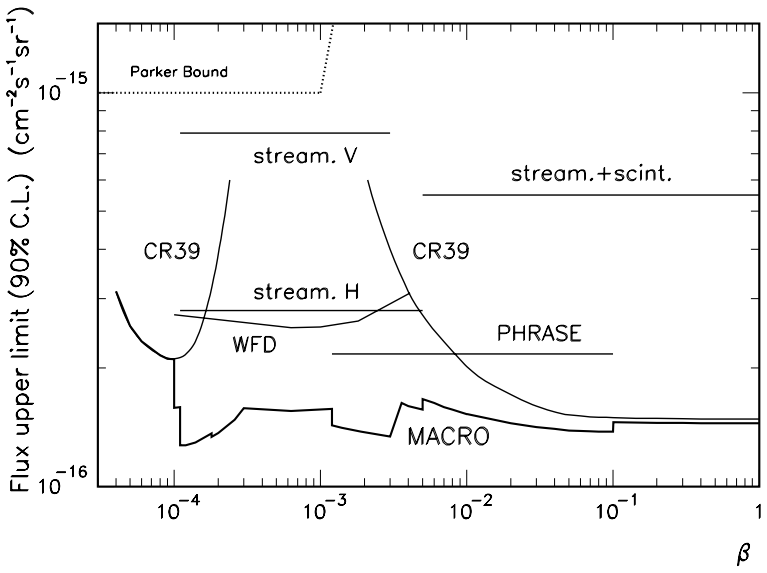

Figure 4: 90% C.L. upper limits vs β for an isotropic flux of MMs obtained from different searches with the 3 subdetectors (both in stand alone and combined ways), and the MACRO global limit.

For the Earth we obtained limits which vary from about 0.8 to 0.5 $10^{-14}\,\mathrm{cm}^{-2}\,\mathrm{s}^{-1}$ [39].

A similar procedure was used to search for muon neutrinos from the Sun: the upper limits are at the level of about $1.5 - 2 \cdot 10^{-14}\,\mathrm{cm}^{-2}\,\mathrm{s}^{-1}$ [39].

6 Magnetic Monopoles and Nuclearites

The search for magnetic monopoles (MM) was one of the main objectives of our experiment. Supermassive monopoles predicted by Grand Unified Theories (GUT) of the electroweak and strong interactions should have masses of the order of $m_M \sim 10^{17}\,\mathrm{GeV}$.

These monopoles could be present in the penetrating cosmic radiation and are expected to have typical galactic velocities, $\sim 10^{-3}c$, if trapped in our Galaxy. MMs trapped in our solar system or in the supercluster of galaxies may travel with typical velocities of the order of $\sim 10^{-4}c$ and $\sim 10^{-2}c$, respectively. Monopoles in the presence of strong magnetic fields may reach higher velocities. Possible intermediate mass monopoles could reach relativistic velocities.

The reference sensitivity level for a significant MM search is the Parker bound, the maximum monopole flux compatible with the survival of the galactic magnetic field. This limit is of the order of $\Phi \lesssim 10^{-15}\,\mathrm{cm}^{-2}\,\mathrm{s}^{-1}\,\mathrm{sr}^{-1}$, but it could be reduced by almost an order of magnitude when considering the survival of a small galactic magnetic field seed [6].

Our experiment was designed to reach a flux sensitivity well below the Parker bound, in the MM velocity range of $4 \times 10^{-5} < \beta < 1$. The three MACRO sub-detectors have sensitivities in wide β-ranges, with overlapping regions; thus they allow multiple signatures of the same rare event candidate. No candidates were found in several years of data taking by any of the three subdetectors. Fig. 4 shows the 90% C.L. flux upper limits for $g = g_D$ MMs (one unit of Dirac magnetic charge) obtained by various subdetectors of MACRO and different analysis methods [6]. The validity of the used search methods was verified in different papers [9] [2] [40]. The MM

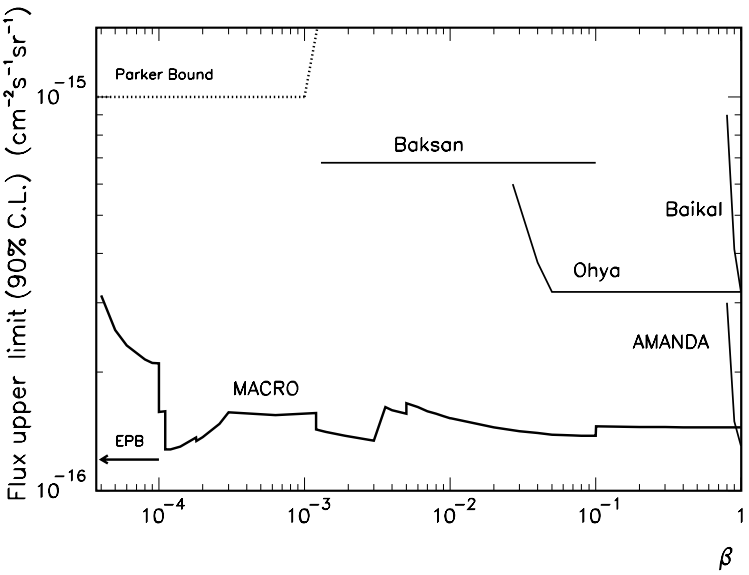

Figure 5: The global MACRO MM upper limit compared with limits from other experiments.

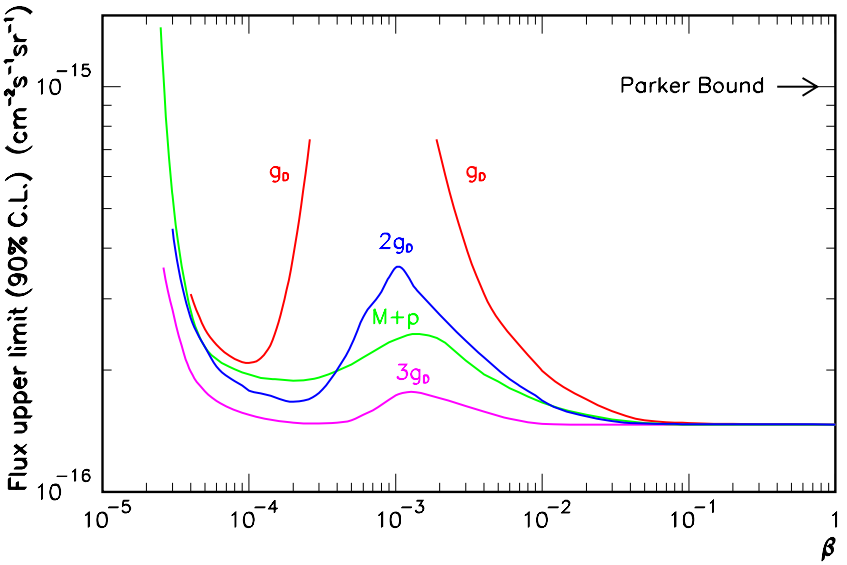

Figure 6: Upper limits (90% C.L.) for an isotropic flux of MMs obtained with the CR39 sub-detector of MACRO, for poles with magnetic charge $g = g_D, 2g_D, 3g_D$ and for M+p composites.

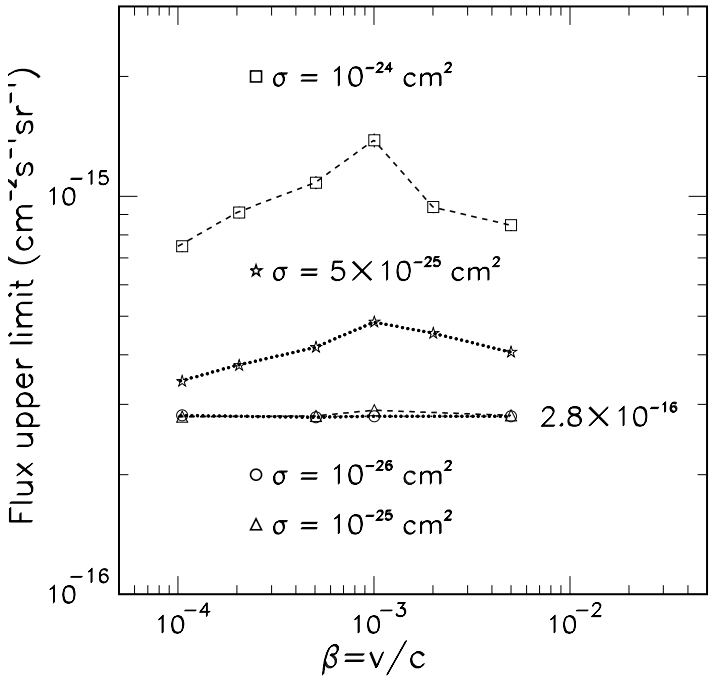

Figure 7: Upper limits for a MM flux as a function of the MM velocity for various catalysis cross sections.

flux limits set by several different analyses using the three subdetectors over different β-range were combined to obtain a global MACRO limit. For each β value, the global time integrated acceptance was computed as the sum of the independent portions of each analysis. Our limit is shown in Fig. 5 versus β together with the limits set by other experiments [41]; other limits are quoted in [17]. Our MM limits are by far the best existing over a very wide range of β , $4 \times 10^{-5} < \beta < 1$.

Fig. 6 shows the flux upper limits obtained with the CR39 nuclear track detector for MMs with different magnetic charges, $g = g_D, 2g_D, 3g_D$ and for M+p composites [40].

The interaction of the GUT monopole core with a nucleon can lead to a reaction in which the nucleon decays (monopole catalysis of nucleon decay), f.e. $M + p \rightarrow M + e^+ + \pi^o$ [7] [42]. The cross section for this process is of the order of the core size, $\sigma \sim 10^{-56}\,\mathrm{cm}^2$, practically negligible. But the catalysis process could proceed via the Rubakov-Callan mechanism with a cross section of the order of the strong interaction cross section. [43]. We developed a dedicated analysis procedure aiming to detect nucleon decays induced by the passage of a GUT MM in our streamer tube system (a fast track from a slow ($\beta \sim 10^{-3}$) MM track). The 90% C.L. flux upper limit established by this search as a function of the MM velocity and of the catalysis cross section is shown in Fig. 7 [7]. The limits are at the level of $\sim 3 \cdot 10^{-16}\, cm^{-2} s^{-1} sr^{-1}$ for $10^{-4} \lesssim \beta \lesssim 5 \cdot 10^{-3}$, and valid for large catalysis cross sections, $5 \cdot 10^2 < \sigma_{cat} < 10^3\, mb$. The flux limit for our standard direct MM search with streamer tubes is valid for $\sigma_{cat} < 100\, mb$.

As a byproduct of our scintillator and nuclear track detector searches, we obtained upper limits for a flux of nuclearites and of Q-balls in the penetrating cosmic radiation.
Nuclearites (Strangelets, Strange Quark Matter) should consist of aggregates of u,d and s quarks in almost equal proportion. They could have been produced shortly after the Big Bang or in

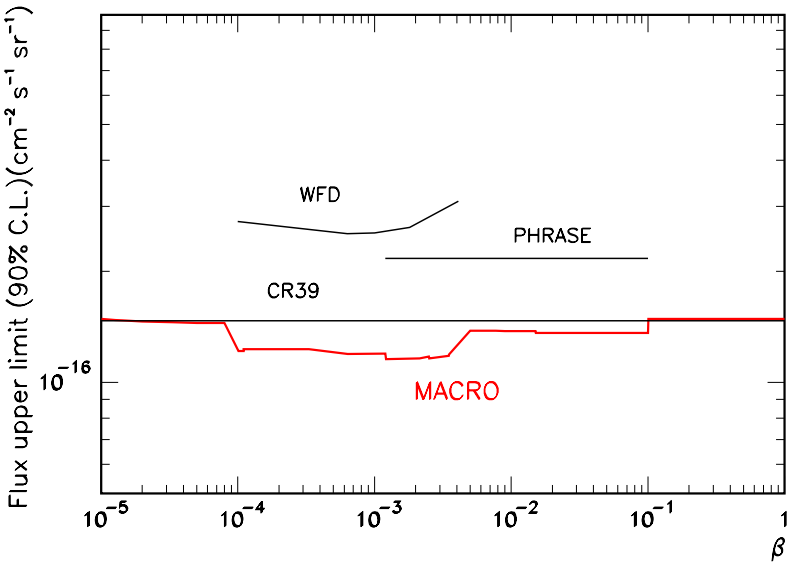

Figure 8: The 90 % C.L. upper limits for an isotropic flux of nuclearites obtained with the liquid scintillators (WFD and PHRASE) and the CR39 subdetectors. The bottom line is the MACRO global limit.

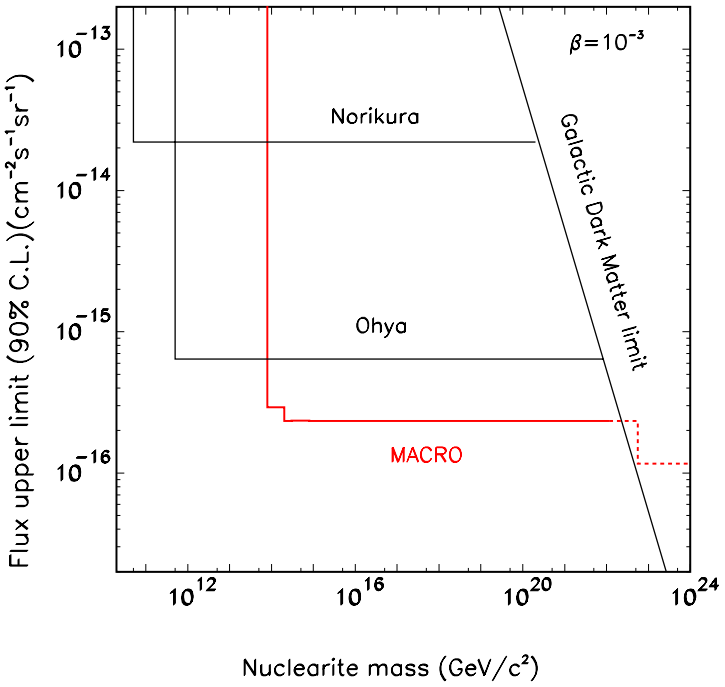

Figure 9: The MACRO flux upper limit for nuclearites with $\beta = 10^{-3}$ at ground level vs nuclearite mass, compared with those obtained by other experiments and with the dark matter bound.

violent astrophysical processes, and may have survived as remnants; they could be part of the present cold dark matter and would have typical galactic velocities, $\beta \sim 10^{-3}$. They should yield a large amount of light in scintillators and large Restricted Energy Losses in the nuclear track detectors. Fig. 8 shows our upper limits for an isotropic flux of nuclearites obtained with the scintillator and the CR39 subdetectors; also the MACRO combined limit is shown [6], [44]. Fig. 9 shows a compilation of limits for a flux of nuclearites compared with the dark matter limit, assuming a velocity at ground level of $\beta \sim 10^{-3}$.

Q-balls should be aggregates of squarks $\widetilde{q}$, sleptons $\widetilde{l}$, and Higgs fields [45] [42]. The scalar condensate inside a Q-ball core should have a global baryon number Q. There could exist neutral and charged Q-balls and they could be possible cold dark matter candidates. Charged Q-balls could have been detected, with reduced sensitivity, by our scintillators and nuclear track detectors.

7 Neutrinos from Stellar Gravitational Collapses

A stellar gravitational collapse (GC) of the core of a massive star is expected to produce a large burst of all types of neutrinos and antineutrinos with energies of $7-30$ MeV and with a duration of $\sim 10\,$s. The $\bar{\nu}_e$'s reaching MACRO can be detected via the process $\bar{\nu}_e + p \rightarrow n + e^+$ in the liquid scintillator. About $100 \div 150$ $\bar{\nu}_e$ events should be detected in our 580 t scintillator for a stellar collapse at the center of our Galaxy.

We used two electronic systems for detecting $\bar{\nu}_e$'s from stellar gravitational collapses. The first system was based on the dedicated PHRASE trigger, the second one was based on the ERP trigger. Both systems had an energy threshold of $\sim 7\,$MeV and recorded pulse shape, charge and timing informations. Immediately after a $> 7\,$MeV trigger, the PHRASE system lowered its threshold to about 1 MeV, for a duration of $800\,\mu$s, in order to detect (with a $\simeq 25\,\%$ efficiency) the $2.2\,$MeV γ released in the reaction $n + p \rightarrow d + \gamma_{2.2\,\mathrm{MeV}}$ induced by the neutron produced in the primary process.

A redundant supernova alarm system was in operation, alerting immediately the physicists on shift. We defined a general procedure to alert the physics and astrophysics communities in case of an interesting alarm. Finally, a procedure to link the various supernova observatories around the world was set up [46].

MACRO was completed at the end of 1994; since then the active mass was ~ 580 t and the livetime fraction was $\simeq 97\,\%$. The first parts of the detector started operation in 1989 [12] [46]. No stellar gravitational collapses in our Galaxy were observed from the beginning of 1989 to the end of 2000.

8 Cosmic Ray Muons

The large area and acceptance of our detector allowed the study of many aspects of physics and astrophysics of cosmic rays (CR). We recorded $\sim 6 \times 10^7$ single muons and $\sim 3.7 \times 10^6$ multiple muons at the rate of $\sim 18,000$/day.

Muon vertical intensity. The underground muon vertical intensity vs. rock thickness provides information on the high energy ($E \gtrsim 1.3\,$TeV) atmospheric muon flux and on the all-particle primary CR spectrum. The results can be used to constrain the models of cosmic ray production and interaction. The analysis performed in 1995 covered the overburden range $2200 \div 7000\,\mathrm{hg/\,cm^2}$ [47].

Analysis of high multiplicity muon bundles. The study of the **multiplicity distribution** of muon bundles provides informations on the primary CR composition model. The study of the **decoherence** function (the distribution of the distance between two muons in a muon bundle) provides mainly informations on the hadronic interaction features at high energies; this study was performed using a large sample of data and improved Monte Carlo methods, [48] [49]. We used different hadronic interaction models (DPMJET, QGSJET, SIBYLL, HEMAS, HDPM) interfaced to the HEMAS and CORSIKA shower propagation codes.

We also studied *muon correlations inside a bundle* to search for correlations of dynamical origin in the bundles. Since the cascade development in atmosphere is mainly determined by the number of "steps" in the "tree formation", we expect a different behaviour for cascades originated by light and heavy CR primaries, and the analysis should be less sensitive to the hadronic interaction model adopted in the simulations. This analysis shows that, in the energy region above 1000 TeV, the composition model derived from the analysis of the muon multiplicity distribution is almost independent from the interaction model.

We also searched for *substructures ("clusters") inside muon bundles* using different software algorithms; the study is sensitive both to the hadronic interaction model and to the primary CR composition model.

The ratio double muons/single muons: The ratio N_2/N_1 of double muon events over single muon events is expected to decrease at increasing rock depths, unless some exotic phenomena occur. The LVD collaboration reported that the ratio of multiple-muons to all-muons increases for rock depths $h > 7000\ hg/cm^2$ [50].

We measured the ratio N_2/N_1 as a function of the rock depth, using also multiple muon events at large zenith angles: our measured ratios as a function of the rock depth, are in agreement with the expectation of a monotonic decrease of N_2/N_1 down to $h \sim 10000\ hg/cm^2$. Above this value, the low statistics does not allow to reach a firm conclusion on a possible increase of N_2/N_1.

Muon arrival time distribution. We checked that it is random [51].

Muon Astronomy. In the past, some experiments reported excesses of modulated muons from the direction of known astrophysical sources, f.e. Cyg X-3. Our data do not indicate significant excesses above background, both for steady dc fluxes and for modulated ac fluxes.

The pointing precision of our apparatus was checked via the shadow of the Moon and of the Sun on primary cosmic rays. The pointing resolution was checked with double muons: the angle containing 68% of the events in a $\Delta\theta$ bin is 0.8^o, which we take as our resolution.

All sky d.c. survey. The sky, in galactic coordinates, was divided into bins of equal solid angle, $\Delta\Omega = 2.1 \cdot 10^{-3} sr$, $\Delta\alpha = 3^o$, $\Delta sin\delta = 0.04$; they correspond to cones of 1.5^o half angles. In order to remove edge effects, three other surveys were done, by shifting the map by one-half-bin in α (map 2), by one-half bin in sinδ (map 3) and with both α and sinδ shifted (map 4). For each solid angle bin we computed the deviation from the average measured muon intensity, after background subtraction, in units of standard deviations. No deviation was found and for the majority of the bins we obtain flux upper limits at the level of ${\Phi_\mu}^{steady}(95\%) \leq 5 \times 10^{-13} cm^{-2} s^{-1}$ [4].

Specific point-like d.c. sources. For Cyg X-3, Mrk421, Mrk501 we searched in a narrower cone (1^o half angle) around the source direction. We obtain flux limits at the level of $(2-4) \cdot 10^{-13} cm^{-2} s^{-1}$. There is a small excess of 2.0 σ in the direction of Mrk501.

Modulated a.c. search from Cyg X-3 and Her X-1. No evidence for an excess was observed and the limits are $\Phi < 2 \times 10^{-13} cm^{-2} s^{-1}$.

Search for bursting episodes. We made a search for pulsed muon signals in a 1^o half angle cone around the location of possible sources of high energy photons. Bursting episodes of duration

of ~ 1 day were searched for with two different methods. In the first method we searched for daily excesses of muons above the background, also plotting cumulative excesses day by day. In the second method we computed day by day the quantity $-Log_{10}P$ where P is the probability to observe a burst at least as large as N_{obs}. We find some possible small excesses for Mrk421 on the days 7/1/93, 14/2/95, 27/8/97, 5/12/98 [4].
Seasonal variations. Underground muons are produced by mesons decaying in flight in the atmosphere. The muon flux depends on the ratio between the decay and interaction probabilities of the parent mesons, which are sensitive to the atmospheric density and to the average temperature. The flux decreases in the winters, when the temperature is lower and the atmosphere more dense, and increases in the summers [4] [52].
Solar daily variations. Because of variations in the day-night temperatures we expect solar daily variations similar to seasonal variations, but of considerably smaller amplitudes. Using the total MACRO data, we find these variations with an amplitude $A = (0.88 \pm 0.26) \cdot 10^{-3}$ with a significance of about 3.4 σ [9].
Sidereal anisotropies are due to the motion of the solar system through the "sea" of relativistic cosmic rays in our galaxy. They are expected to yield a small effect. After a correction due to the motion of the Earth around the Sun, we observe variations with an amplitude of $8.6 \cdot 10^{-4}$ and a phase $\phi_{max} = 22.7^{\circ}$ with a statistical significance of 3 σ [9].
Moon and sun Shadows of primary cosmic rays. The pointing capability of MACRO was demonstrated by the observed "shadows" of the Moon and of the Sun, which produce a "shield" to the cosmic rays. We used a sample of $50 \cdot 10^6$ muons, collected over 74073 hours of livetime; we looked at the bidimensional density distribution of the events around the directions of the Moon and of the Sun [10] [53]. In Fig. 10 we show two-dimensional plots of the muon deficits caused by the Moon and the Sun. For the Moon: we looked for events in a window $4.375^o \times 4.375^o$ centered on the Moon; the window was divided into 35×35 cells, each having dimensions of $0.125^o \times 0.125^o$ ($\Delta\Omega = 1.6 \cdot 10^{-2} deg^2$). In the bidimensional plot of Fig. 10a one observes a depletion of events with a statistical significance of 6.5σ. The observed slight displacement of the maximum deficit is consistent with the displacement of the primary protons due to the geomagnetic field. We repeated the same analysis for muons in the sun window, Fig. 10b. The difference between the apparent sun position and the observed muon density is due to the combined effect of the magnetic field of the Sun and of the Earth. The observed depletion has a statistical significance of 4.6 σ [10]. Notice in Fig. 10b that there is no depletion of events in the symmetrical position (with respect to the theorethical sun position). This allows to place a rough upper limit on the $\widetilde{p}/p$ ratio [10].

9 Muon energy measurement with the TRD detector

The underground differential energy spectrum of muons was measured with a three TRD module detector located in the Attico. We analyzed two types of events: "single muons", i.e. single events in MACRO crossing one TRD module, and "double muons", i.e. double events in MACRO with only one muon crossing the TRD detector.The measurements refer to muons with energies $0.1 < E_\mu < 1\,\mathrm{TeV}$ and for $E_\mu > 1\,\mathrm{TeV}$ [8] [54]. In order to evaluate the local muon energy spectrum, we must take into account the TRD response function, which induces some distortion of the "true" muon spectrum distribution. The "true" distribution was extracted from the measured one by an unfolding procedure. The average single muon energy at the Gran Sasso underground lab is 270 GeV; for double muons it is $\sim$ 380 GeV. Double muons are more energetic than single muons; this is in agreement with the predictions of interaction models of

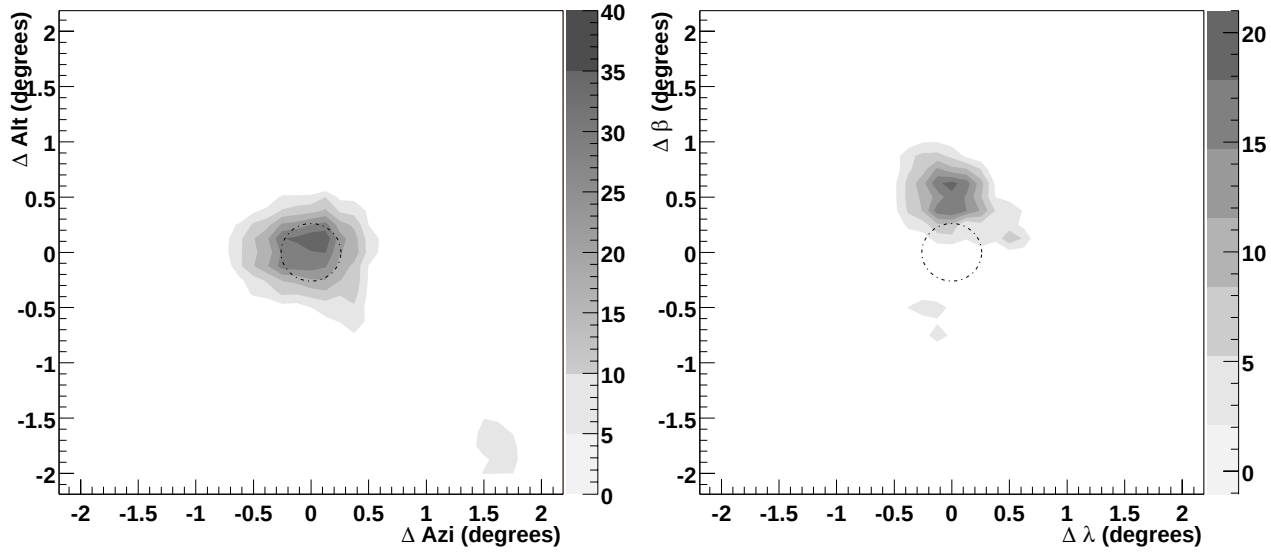

(a) (b)

Figure 10: Moon and sun shadows. (a) Two dimensional distributions of the muon event density around the moon direction. The various regions of increasing gray scale indicate various levels of deficit, in percent. The darkest one corresponds to the maximum deficit. (b) Same analysis in the sun direction. The theoretical centers of the Moon and Sun correspond to the centers of the dashed circles.

primary CRs in the atmosphere.

10 EAS-TOP/MACRO Coincidence Experiment

MACRO could detect events in coincidence with the EASTOP detector at Campo Imperatore. EASTOP measured the e.m. size of the showers above the surface, while MACRO measured penetrating muons underground [15][55]. The purpose was to study the primary cosmic ray composition versus energy, reducing the dependence on the interaction and propagation models. The two completed detectors operated in coincidence for a livetime of 960 days. The number of coincident events was 28160, of which 3752 had shower cores inside the edges of the EASTOP array ("internal events") and shower sizes $N_e > 2 \cdot 10^5$; 409 events had $N_e > 10^{5.92}$, i.e. above the CR knee. The data have been analyzed in terms of the QGSJET interaction model as implemented in CORSIKA [15] [55].

The e.m. detector of EASTOP was made of 35 scintillator modules, 10 m^2 each, covering an area of $\simeq 10^5\,m^2$. The array was fully efficient for $N_e > 10^5$. The reconstruction capabilities of the extensive air shower (EAS) parameters for internal events were: $\frac{\Delta N_e}{N_e} \simeq 10\%$ for $N_e \gtrsim 10^5$, and $\Delta\theta \sim 0.9^o$ for the EAS arrival direction.

We considered in MACRO muon tracks with at least 4 aligned hits in both views of the horizontal streamer tube planes. The muon energy threshold at the surface inside the effective area of EAS-TOP, for muons reaching the MACRO depth, ranges from 1.3 TeV to 1.8 TeV.

Event coincidence was made off-line, using the absolute time given by a GPS system: the

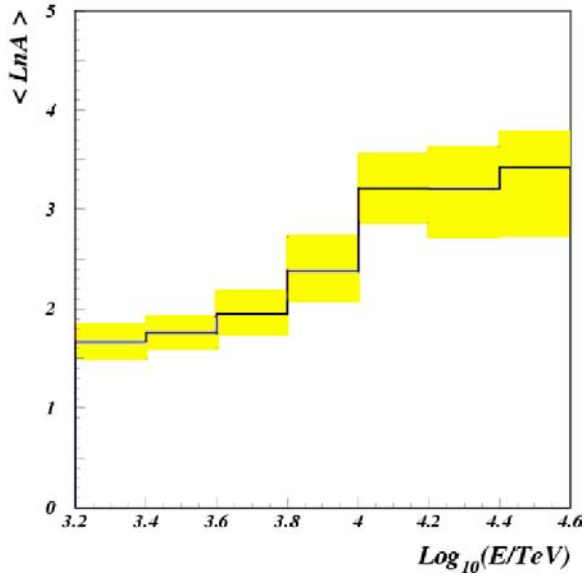

Figure 11: EASTOP-MACRO coincidences. $\langle log_{10}A \rangle$ vs primary energy; the histogram (black line) is obtained from the data, the shaded area includes the uncertainties discussed in the text (Preliminary).

accuracy was better than 1 μs.

Fig. 11 shows the result plotted as $\langle log_{10}A \rangle$ versus $log_{10}E$ (E in TeV); the data are consistent with an increase of $\langle log_{10}A \rangle$ with energy in the CR knee region. The results are in agreement with the measurements of EAS-TOP alone at the surface [56] and with the results of other experiments [17].

11 Search for Lightly Ionizing Particles

Fractionally charged particles could be expected in Grand Unified Theories as deconfined quarks; the expected charges range from Q=$e/5$ to Q=e 2/3. They should release a fraction $(Q/e)^2$ of the energy deposited by a muon traversing a medium. Lightly Ionizing Particles (LIPs) have been searched for in MACRO using a four-fold coincidence between three layers of scintillators and the streamer tube system [57]. The 90 % c.l. flux upper limits for LIPs with charges $2e/3$, $e/3$ and $e/5$ are at the level of $10^{-15} cm^{-2} s^{-1} sr^{-1}$ [13] [57]. One possible candidate events is being scrutinized.

12 Nuclear Track Detector Calibrations

We performed a number of calibrations of the nuclear track detector CR39 with both slow and fast ions. In all measurements we have seen no deviation of its response from the Restricted Energy Loss (REL) model. Stacks of nuclear track detectors (CR39 and Lexan) placed before and after various targets, were exposed to 158 A GeV Pb^{82+} ions at the CERN-SPS and to 1 A GeV Fe^{26+} ions at the BNL-AGS. In traversing the target, the beam ions produce nuclear

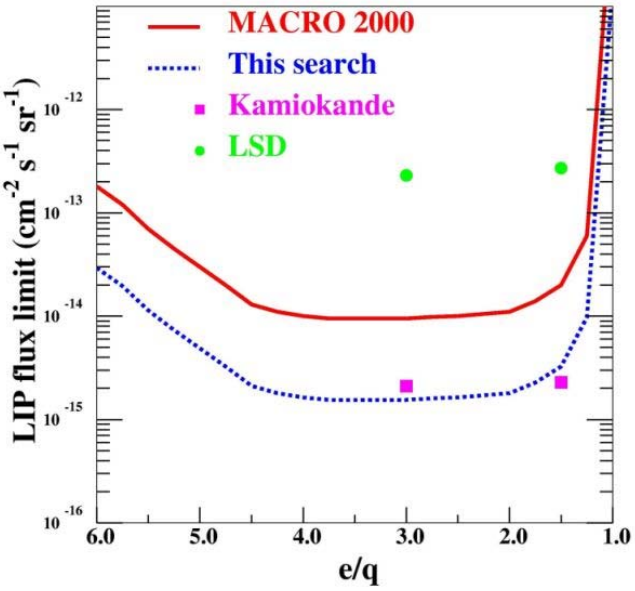

Figure 12: The 90% C.L. flux upper limits for LIPs (solid line) compared with the previous limits from MACRO (dashed line) and Kamiokande (black squares). (Preliminary).

fragments with $Z < 82e$ and $Z < 26e$ for the lead and iron beams, respectively; this allows a measurement of the response of the detectors in a Z region relevant to the detection of magnetic monopoles. Tests were made looking for a possible dependence of the CR39 response from its age, i.e. from the time elapsed between the date of production and the date of exposure ("aging effect"). No aging and no fading effects were observed [58]. The results of the MM search is best seen in Fig. 6.

13 Conclusions

The MACRO detector took data from 1989 to the end of year 2000. In 2002 we have extended and completed most of our analyses and searches. We would like to stress that we obtained important results in all the items listed in the proposal :

- GUT Magnetic Monopoles. We now have the best flux upper limit over the widest β range, thanks to the large acceptance and the redundancy of the different techniques employed. This limit is a unique result and it will stand for a long time.
- Atmospheric neutrino oscillations. In this field MACRO has had its major achievements. Analyses of different event topologies, different energies, the exploitation of Coulomb multiple scattering in the detector are all in agreement with the hypothesis of $\nu_\mu \rightarrow \nu_\tau$ oscillations, with maximal mixing and $\Delta m^2 = 2.5 \cdot 10^{-3}$ eV^2.
- High energy muon neutrino astronomy. We have been highly competitive with other underground experiments thanks to our good angular accuracy.
- Search for bursts of $\bar{\nu}_e$ from stellar gravitational collapses. MACRO was sensitive to supernova events in the Galaxy, it started the SN WATCH system, and for some time it was the only detector in operation.

- Cosmic ray downgoing muons. We observed the shadows of primary cosmic rays by the Moon and the Sun; this is also a test of the pointing capability. We observed seasonal variations over many years, and solar and sidereal variations with reasonable statistical significance, even if the amplitudes of the variations are small (0.08%). No excesses of secondary muons from astrophysical point sources (steady, modulated or bursting) were observed. The limits obtained are the best existing.
- Results have been obtained from coincidence events between MACRO and the EASTOP array. The data indicate an increase with increasing energy of the average Z of the primary CR nuclei.
- Sensitive searches have been carried out for possible Dark Matter candidates : (i) WIMPs, looking for upgoing muons from the center of the Earth and of the Sun; (ii) Nuclearites and Q-balls (obtained as byproducts of MM searches).
- Other limits concern possible Lightly Ionizing Particles with $\frac{e}{5} < q < \frac{2}{3}e$ [13].

The MACRO scientific and technical results have been or are being published in 50 papers in refereed journals.

Acknowledgments

We acknowledge the support of the Directors and of the staff of the Gran Sasso Laboratory and of the Institutions partecipating in the experiment. We thank the Istituto Nazionale di Fisica Nucleare (INFN), the US Department of Energy and the US National Science Foundation for their support. We acknowledge the strong cooperation of our technical staff, in particular of R. Assiro, E. Barbarito, A. Boiano, E. Bottazzi, P. Calligola, A. Candela, A. Ceres, D. Cosson, P. Creti, L. Degli Esposti, U. Denni, D. Di Ferdinando, R. Diotallevi, R. Farano, E. Favero, A. Frani, M. Gebhard, R. Giuliani, M. Goretti, H. Gran, A. Hawthorne, A. Leone, D. Margherita, V. Marrelli, F. Massera, S. Mengucci, M. Mongelli, L. Mossbarger, M.Orsini, S. Parlati, G. Pellizzoni, M. Perchiazzi, C. Pinto, A. Sacchetti, P. Saggese, S. Sondergaards, S. Stalio, M. Vakili, C. Valieri and N. Zaccheo. We thank INFN-FAI, ICTP (Trieste), NATO and WorldLab for providing fellowships and grants for non-Italian citizens.

References

[1] MACRO Collaboration, M.Ambrosio et al., "The MACRO detector at Gran Sasso", Nucl. Instr. Methods Phys. Res A486(2002)663.

[2] MACRO Collaboration, M.Ambrosio et al., "A combined analysis technique for the search for fast magnetic monopoles with the MACRO detector", hep-ex/0110083, Astropart. Phys. 18(2002)27.

[3] MACRO Collaboration, M.Ambrosio et al.,"Search for a diffuse neutrino flux from astrophysical sources with MACRO", astro-ph/0203181, Accepted for publication in Astropart. Phys.

[4] MACRO Collaboration, M.Ambrosio et al.,"Search for cosmic ray sources using muons detected by the MACRO experiment", hep-ex/0204188, Astropart. Phys. 18(2003)615.

[5] MACRO Collaboration, M.Ambrosio et al.,"Muon energy estimate through multiple scattering with the MACRO detector", physics/0203018, Nucl. Instr. Methods Phys. Res A492(2002)376.

[6] MACRO Collaboration, M.Ambrosio et al.,"Final results of magnetic monopole searches with the MACRO experiment", hep-ex/0207020, Eur. Phys. J. C25(2002)511.

[7] MACRO Collaboration, M.Ambrosio et al.,"Search for nucleon decays induced by GUT magnetic monopoles with the MACRO experiment", hep-ex/0207024, Eur. Phys. J. C26(2002)163.

[8] MACRO Collaboration, M.Ambrosio et al.,"Measurement of the residual energy of muons in the Gran Sasso laboratories", hep-ex/0207043, Accepted for publication in Astropart. Phys.

[9] MACRO Collaboration, M.Ambrosio et al.,"Search for the sidereal and solar diurnal modulations in the total MACRO muon data set", astro-ph/0211119, Accepted for publications in Phys. Rev. D.

[10] MACRO Collaboration, M.Ambrosio et al.,"Moon and Sun shadowing effect in the MACRO detector", Submitted to Astropart. Phys.

[11] MACRO Collaboration, M.Ambrosio et al.,"Study of atmospheric neutrino oscillations using upgoing muon multiple scattering", In preparation

[12] MACRO Collaboration, M.Ambrosio et al.,"Search for stellar gravitational collapses with the MACRO detector", Submitted to Eur. Phys. J. C

[13] MACRO Collaboration, M.Ambrosio et al.,"Search for lightly ionizing particles with the MACRO detector", In preparation

[14] MACRO Collaboration, M.Ambrosio et al.,"Atmospheric neutrino oscillations with MACRO", In preparation

[15] EASTOP-MACRO Collaborations, M.Aglietta et al.,"Primary cosmic ray composition between 10^{15} and 10^{16} eV from EAS electromagnetic and TeV muon data", In preparation

[16] MACRO Collaboration, M.Ambrosio et al.,"Status report of the MACRO experiment for the year 2001", LNGS-EXP-01-02 and hep-ex/0206027.

[17] G. Giacomelli and M. Sioli for the MACRO Collaboration, "Astroparticle Physics", 6th Constantine School on Weak and Strong Interactions Phenomenology, 6-12/4/2002, Mentouri University, Constantine, Algeria; hep-ex/0211035.

[18] M. Spurio for the MACRO Collaboration, "Measurement of the Atmospheric Muon Neutrino Flux: MACRO Final Results", 20th International Conference on Neutrino Physics and Astrophysics, 25-30/5/2002, Munich, Germany.

[19] M. Giorgini for the MACRO Collaboration, "Atmospheric neutrino oscillations with the MACRO experiment", Beyond the Desert, 2-7/06/2002, Oulu, Finland; hep-ex/0210008.

[20] S. Cecchini and A. Margiotta for the MACRO Collaboration, "Muons with the MACRO detector", 18th ECRS, 8-12/07/2002, Moscow, Russia.

[21] M. Sioli for the MACRO Collaboration, "Atmospheric neutrino oscillations with MACRO", 12th ISVHECRI, 15-20/07/2002, Geneve; hep-ex/0211030.

[22] G. Giacomelli for the MACRO Collaboration, "Search for GUT magnetic monopoles with the MACRO experiment at the Gran Sasso lab", 31st ICHEP, 24-31/07/2002, Amsterdam, The Netherlands; hep-ex/0210021.

[23] Y. Becherini for the MACRO Collaboration, "MACRO results on atmospheric neutrino oscillations", International School of Physics "Enrico Fermi", CLII course "Neutrino Physics", Varenna, Italy, 23/07-2/08/2002; hep-ph/0211172.

[24] G. Giacomelli for the MACRO Collaboration, "Neutrino physics and astrophysics with the MACRO experiment at the Gran Sasso lab", 25th meeting of the Nuclear Physics Division of the Brasilian Physical Society, 1-4/09/2002, S. Pedro, Brasil.

[25] I. De Mitri for the MACRO Collaboration, "Results of dark matter searches with the MACRO experiment", 4th Int. Workshop for the Identification of Dark Matter, September 2002, York (UK); hep-ex/0212055.

[26] M. Sioli for the MACRO Collaboration, "Studio dei neutrini atmosferici con l'esperimento MACRO", 88^o Congresso Nazionale della Società Italiana di Fisica, 26/09-01/10/2002, Alghero.

[27] L. Patrizii for the MACRO Collaboration, "Ricerca di monopoli magnetici e nucleariti con l'esperimento MACRO", 88^o Congresso Nazionale della Società Italiana di Fisica, 26/09-01/10/2002, Alghero.

[28] M. Giorgini for the MACRO Collaboration, "Ricerca di variazioni giornaliere (siderali e solari) e di variazioni stagionali nel flusso di muoni rivelati da MACRO", 88^o Congresso Nazionale della Società Italiana di Fisica, 26/09-01/10/2002, Alghero.

[29] M. Sitta for the MACRO Collaboration, "Ricerca di eventi di decadimento del nucleone indotto dal passaggio di un monopolo magnetico con l'esperimento MACRO", 88^o Congresso Nazionale della Società Italiana di Fisica, 26/09-01/10/2002, Alghero.

[30] A. Kumar for the MACRO Collaboration, "Magnetic monopoles in MACRO", 21st International Conference on Nuclear Track in Solids, 20-25/10/2002, New Delhi, India.

[31] V. Togo for the MACRO Collaboration, "Calibrations of CR39 and Makrofol nuclear track-detectors and search for exotic particles", 8th Topical seminar on innovative particle and radiation detectors, 21-24/10/2002, Siena, Italy.

[32] S.Ahlen et al., Nucl. Instr. Meth. Phys. Res. A324(1993)337.

[33] S.Ahlen et al., Phys. Lett. B357(1995)481.
M.Ambrosio et al., Phys. Lett. B434(1998)451; hep-ex/9807005.
M.Ambrosio et al., Phys. Lett. B478(2000)5; hep-ex/0001044.

[34] M.Ambrosio et al., Astropart. Phys. 9(1998)105; hep-ex/9807032.

[35] M.Ambrosio et al., Phys. Lett. B517(2001)59; hep-ex/0106049.

[36] Y.Fukuda et al., Phys. Rev. Lett. 81(1998)1562;
Phys. Lett. B433(1998)9;
Phys. Rev. Lett. 85(2000)3999;
Nucl. Phys. B Proc. Suppl. 91(2001)127.
T. Toshito, hep-ex/0105023 (2001).

[37] W.W.M. Allison et al., Phys. Lett. B391 (1997) 491;
Phys. Lett. B449 (1999) 137.
W. Anthony Mann, hep-ex/0007031 (2000);
T. Mann et al., Nucl. Phys. B Proc. Suppl. 91 (2001) 134.

[38] M. Ambrosio et al., Astrophys. J. 546(2001)1038; astro-ph/0002492.

[39] M.Ambrosio et al., Phys. Rev. D60(1999)082002, hep-ex/9812020.

[40] S.Ahlen et al., Phys. Rev. Lett. 72(1994)608.
M.Ambrosio et al., Astropart. Phys. 4(1995)33.
M.Ambrosio et al., Astropart. Phys. 6(1997)113.
M.Ambrosio et al., Phys. Lett. B406(1997)249.

[41] S. Orito et al., Phys. Rev. Lett. 66(1991)1951.

[42] G. Giacomelli et al., hep-ex/0005041.
D. Bakari et al., hep-ex/0004019; hep-ex/0003028.
G. Giacomelli and L. Patrizii, hep-ex/0302011.

[43] V. A. Rubakov, JETP Lett. B219(1981)644.
G.G. Callan, Phys. Rev. D26(1982)2058.

[44] S.Ahlen et al., Phys. Rev. Lett. 69(1992)1860.
M.Ambrosio et al., Eur. Phys. J. C13(2000)453; hep-ex/9904031.

[45] S. Coleman, Nucl. Phys. B262(1985)293;
A. Kusenko, Phys. Lett. B405(1997)108.

[46] S.Ahlen et al., Astropart. Phys. 1(1992)11.
R. Bellotti et al., Nucl. Phys. Proc. Suppl. 28A(1992)61.
M.Ambrosio et al., Astropart. Phys. 8(1998)123.

[47] M.Ambrosio et al., Phys. Rev. D52(1995)3793.

[48] M.Ambrosio et al., Phys. Rev. D56(1997)1407.
M.Ambrosio et al., Phys. Rev. D56(1997)1418.
S.Ahlen et al., Phys. Rev. D46(1992)895.
S.Ahlen et al., Phys. Lett. B249(1990)149.

[49] S.Ahlen et al., Phys. Rev. D46(1992)4836.
M.Ambrosio et al., Phys. Rev. D60(1999)032001; hep-ex/9901027.

[50] O. G. Ryazhskaya, Nucl. Phys. (Proc. Suppl.) B87(2000)423.

[51] S.Ahlen et al., Nucl. Phys. B370(1992)432.
R. Bellotti et al., Nucl. Phys. Proc. Suppl. 16(1990)486.

[52] M.Ambrosio et al., Astropart. Phys. 7(1997)109.

[53] M.Ambrosio et al., Phys. Rev. D 59(1999)012003; hep-ex/9807006.
M.Ambrosio et al., Nucl. Phys. Proc. Suppl. 61B(1998)180.

[54] M.Ambrosio et al., Astropart. Phys. 10(1999)11, hep-ex/9807009.
M.Ambrosio et al., Nucl. Phys. Proc. Suppl. 61B(1998)289.

[55] R.Bellotti et al., Phys. Rev. D42(1990)1396.
M. Aglietta et al., Nucl. Instr. & Meth. A336(1993)310.
M.Aglietta et al., Phys. Lett. B337(1994)376.

[56] M.Aglietta et al., Astropart. Phys., 10(1999)1.

[57] M. Ambrosio et al., Phys. Rev. D62(2000)052003; hep-ex/0002029.
S. Cecchini et al., Astropart. Phys. 1(1993)369.

[58] S. Cecchini et al., Radiat. Meas. 34(2001)55, hep-ex/0104022.
G. Giacomelli et al., Nucl. Tracks Radiat. Meas. 28(1997)217.
L. Patrizii et al., Nucl. Tracks Radiat. Meas. 19(1991)641.
G. Giacomelli et al., Nucl. Instrum. Meth. A486(2002)663.

MIBETA and CUORICINO. Neutrinoless Double Beta Decay Searches with Low Temperature Detectors

C. Arnaboldi[a], F. T. Avignone III[b], J. Beeman[c,d], M. Barucci[e], M. Balata[f], C. Brofferio[a], C. Bucci[f], S. Cebrian[g], R. J. Creswick[b], S. Capelli[a], L. Carbone[a], O. Cremonesi[a], A. de Ward[h], E. Fiorini[a], H. A. Farach[b], G. Frossati[h], A. Giuliani[i], P. Gorla[a], E. E. Haller[c,d], I. G. Irastorza[g], R. J. McDonald[c], A. Morales[g], E. B. Norman[c], A. Nucciotti[a], M. Pedretti[i], C. Pobes[g], V. Palmieri[j], M. Pavan[a], G. Pessina[a], S. Pirro[a], E. Previtali[a], C. Rosenfeld[b], A. R. Smith[c], M. Sisti[a], G. Ventura[e] and M. Vanzini[a]
(The CUORE COLLABORATION)

[a] Dipartimento di Fisica dell'Università di Milano-Bicocca
e Sezione di Milano dell'INFN, Milan I-20136, Italy
[b] University of South Carolina, Dept.of Physics and Astronomy
Columbia, South Carolina, USA 29208
[c] Lawrence Berkeley National Laboratory, Berkeley, California, 94720, USA
[d] Dept. of Materials Science and Mineral Engineering, University of California
Berkeley, California 94720, USA
[e] Dipartimento di Fisica dell'Università di Firenze
e Sezione di Firenze dell'INFN, Firenze I-50125, Italy
[f] Laboratori Nazionali del Gran Sasso, I-67010 Assergi (L'Aquila), Italy
[g] Laboratorio de Fisica Nuclear y Altas Energias Universidàd de Zaragoza
50009 Zaragoza, Spain
[h] Kamerling Onnes Laboratory, Leiden University, 2300 RAQ, Leiden, The Netherlands
[i] Dipartimento di Scienze Chimiche, Fisiche e Matematiche dell'Università dell'Insubria
e Sezione di Milano dell'INFN, Como I-22100, Italy
[j] Laboratori Nazionali di Legnaro, Via Romea 4, I-35020 Legnaro (Padova), Italy

Abstract

The progress achieved during 2002 by the MIBETA and CUORICINO experiments at Laboratori Nazionali del Gran Sasso is reported. The final results of the MIBETA experiment on DBD of Tellurium are discussed and details of the analysis of the dominant background contributions are given. The variuos stages of the installation of the CUORICINO detector are described.

1 Introduction

Double Beta Decay (DBD) consists in a rare transition from a nucleus (A,Z) to its isobar (A,Z+2) with the emission of two electrons. Three main channels can be recognized:

$$(A, Z) \rightarrow (A, Z + 2) + 2e^- + 2\overline{\nu}_e \tag{1}$$

$$(A, Z) \rightarrow (A, Z + 2) + 2e^- + (N)\chi \;\; [N = 1, 2, ...] \tag{2}$$

$$(A, Z) \rightarrow (A, Z + 2) + 2e^- \tag{3}$$

where χ is a massless Goldstone boson named Majoron. Decays to excited states of the daughter nucleus, characterized by a lower *effective* transition energy, are also possible. The lepton conserving process $\beta\beta(2\nu)$ (1) is allowed by the Standard Model and has been observed in various nuclei. On the contrary, both processes (2) and (3) violate the lepton number conservation and are forbidden by the Standard Model. Their observation would be therefore a clear sign of new phenomena beyond the Standard Model. No evidence has been claimed so far for these lepton number violating channels, with the only exception of a recently alleged evidence for $\beta\beta(0\nu)$ reported by Klapdor-Kleingrothaus et al. [1, 2] but criticized by other authors [3, 4]. Neutrinoless DBD ($\beta\beta(0\nu)$) is experimentally very appealing being characterized by a sharp peak at the transition energy in the electron sum spectrum (the nuclear recoiling energy is negligible).

Neutrinoless Double Beta Decay searches represent a unique tool to assess the Dirac/Majorana nature of neutrino and to check the Lepton Number Conservation law. Moreover, by directly measuring the *effective* neutrino mass ($| < m_\nu > |$), $\beta\beta(0\nu)$ experiments represent a powerful tool to set the absolute scale of the Majorana neutrino masses with sensitivities (1-100 meV) hardly reachable with competing techniques (e.g. direct measurements). Actually, a number of recent theoretical interpretations of the neutrino oscillations data [5, 6, 7, 8, 9, 10] imply that $| < m_\nu > |$ could be in the range 0.01 eV to the present bounds [11, 12], i.e. in a region accessible by the next generation experiments.

The experimental approach is usually based on the observation of a large number of nuclei, stable in normal beta decay but for which a double weak interaction process, changing the nuclear charge by two units, is allowed. Most sensitive experiments are presently based on the uniform approach in which the nuclei under observation (decay source) act at the same time as detector for the occurrence of a decay. The (1σ) sensitivity of such experiments

$$F_{0\nu} = \ln 2 \; N_{\beta\beta}\epsilon\frac{T}{n_B} = \ln 2\frac{x \; \eta \; \epsilon \; N_A}{A}\sqrt{\frac{M \; T}{B \; \Delta E}} \tag{4}$$

($N_{\beta\beta}$ is the number of $\beta\beta$ decaying nuclei under observation, η their isotopic abundance, N_A the Avogadro number, A the compound molecular mass, x the number of $\beta\beta$ atoms per molecule, ϵ the detection efficiency, M is the detector mass, T the measuring time, B the background counting rate per unit mass and ΔE the energy resolution) scales with the square root of their masses and the inverse of the observed background rate.

Because of their very good intrinsic energy resolution and the quite absolute absence of any limitation on the choice of the detector material, low temperature detectors (LTD)

represent an ideal experimental approach for such searches. Proposed almost 20 years ago [13] they are finally becoming a competitive approach also with respect to Germanium diodes. An important question is then if LTD's can actually represent the best technique for a possible discovery experiment. The CUORE experiment will address this question in an effort to demonstrate that an array of 1000, 760 g TeO_2 bolometers, will represent one of the best approaches presently available. It can be carried out without isotopic enrichment nor extensive Research and Development (R & D) , and it can achieve next generation sensitivity. The first step towards CUORE realization is the test of one of its 25 towers. Such an experiment, named CUORICINO, was approved by the LNGS Scientific Commission and its preparation and installation took most of our efforts during 2002.

2 Experimental setup

Two cryogenic setups have been installed in the eighties at LNGS by the Milano group. The first, used in the past for the MIBETA experiment on $\beta\beta(0\nu)$ of ^{130}Te (Hall A) is now hosting the CUORICINO detector. The second (Hall C) has been dedicated to the research and development activities for CUORICINO and, in the next future, for those of the larger, second generation experiment CUORE [14]. Both cryogenic setups consist of a dilution refrigerator having a power of 1000 μW and 200 μW at 100 mK respectively. A much larger experimental volume is moreover available in the Hall A cryogenic setup. The two refrigerators are realized with preliminarly tested low radiactive materials and are surrounded by heavy Lead shields and anti-Radon boxes. They are both equipped with an *embedded* Helium liquefier, providing a substantial recovery of the Helium and preventing Helium contamination of the tunnel atmosphere.

All the materials used for the setup construction were analysed to determine their radioactive contamination levels. These measurements are carried out by means of two large Ge detectors installed by the Milano group in the Gran Sasso underground Low Radioactivity Laboratory. The level of the radon contamination in the air of the Laboratory is continuously monitored. Both dilution refrigerators are equipped with heavy shields against environmental radioactivity. In particular, the Hall A dilution refrigerator is shielded with two layers of lead of 10 cm minimum thickness each. The outer layer is of commercial low radioactivity lead, while the internal one is made with special lead with a ^{210}Pb contamination of 16 $\pm$ 4 Bq/kg. The external lead shields are surrounded by an air-tight box fluxed with fresh nitrogen from a dedicated evaporator to avoid radon contamination of the gas close to the cryostat. The entire apparatus is hosted inside a Faraday cage to suppress electromagnetic interference. In order to shield the detectors against the unavoidable radioactive contamination of some fundamental components of the dilution refrigerator thick layers of Roman lead are placed inside the cryostat just above and below the detectors.

3 The MIBETA experiment

An array consisting of 20 crystals of TeO_2 of $3\times3\times6$ cm^3 each (MIBETA), for a total mass of 6.8 kg (by far the largest cryogenic mass operating underground), was operated in the Hall A dilution refrigerator until December 2001. Sixteen MIBETA crystals were made of natural TeO_2 . Of the remaining four, two were isotopically enriched at 82.3 % in ^{128}Te and other two at 75.0 % in ^{130}Te . By mass spectrometer measurements we found that, due to the crystallization process, these enrichment factors were lower than the original ones (94.7 % and 92.8 %, respectively). The array, held in a copper tower-like frame mounted inside the inner vacuum chamber (IVC) of the dilution refrigerator, was maintained at a constant temperature of about 10 mK. Each detector consisted of a $3 \times 3 \times 6$ cm^3 TeO_2 crystal of with a mass of 340 grams. A Neutron Transmutation Doped (NTD) thermistor and a Si doped resistor were glued on the surface of each crystal. The former was used to read-out the thermal signal while the latter acted as a heater to generate a reference heat pulse in the crystal in order to monitor continuously the gain of each bolometer. The electronic readout was accomplished with a room temperature low noise differential voltage-sensitive preamplifier, followed by an amplifier and an antialiasing Bessel filter. The MIBETA detector was shielded with an internal layer of Roman lead of 1 cm minimum thickness (Fig. 1). The big effort carried out during 2001 to check both the knowledge of the background sources and the performance of the new detector mounting system proposed for CUORICINO and CUORE, lead to a second run in which the detector structure was heavily modified (Fig. 1). The MIBETA tower was completely rebuilt with a structure very similar to the one of CUORICINO (i.e. of the proposed CUORE towers) in which all the surfaces of the TeO_2 crystals and of the mounting structure were subject to a dedicated etching process aiming to reduce radioactive contaminants. In this occasion, due to the more compact structure of the tower, an enlargement of the internal Roman lead shields was also realized. An external neutron shield (borated polyethylene) was added in June 2001. More details of the experimental setup can be found elsewhere [14].

All available data were analyzed during 2002 to extract the most relevant informations concerning both the physical processes (single and double beta decays) and the background origin.

3.1 Electron Capture of ^{123}Te

Contradictory experimental results have been reported [15, 16] in the past concerning the second forbidden unique electron capture (EC) of ^{123}Te to the ground state of ^{123}Sb [18, 19]. In particular, one of the claimed experimental evidences of the decay [15] is in contradiction with existing theoretical models predicting very low decay rates [20, 21]. A precise measurement of the ^{123}Te decay rate could therefore shed light on the experimental situation and represent a valid test of the theoretical nuclear models. EC processes, can be observed through the measurement of the inner bremsstrahlung (IB) photons accompanying a generally small fraction of decays, or through the atomic deexcitation cascade (X-rays and/or Auger electrons) following the decay. Individual atomic transitions (single X-rays or Auger electrons) can be observed using a detector in direct contact, but

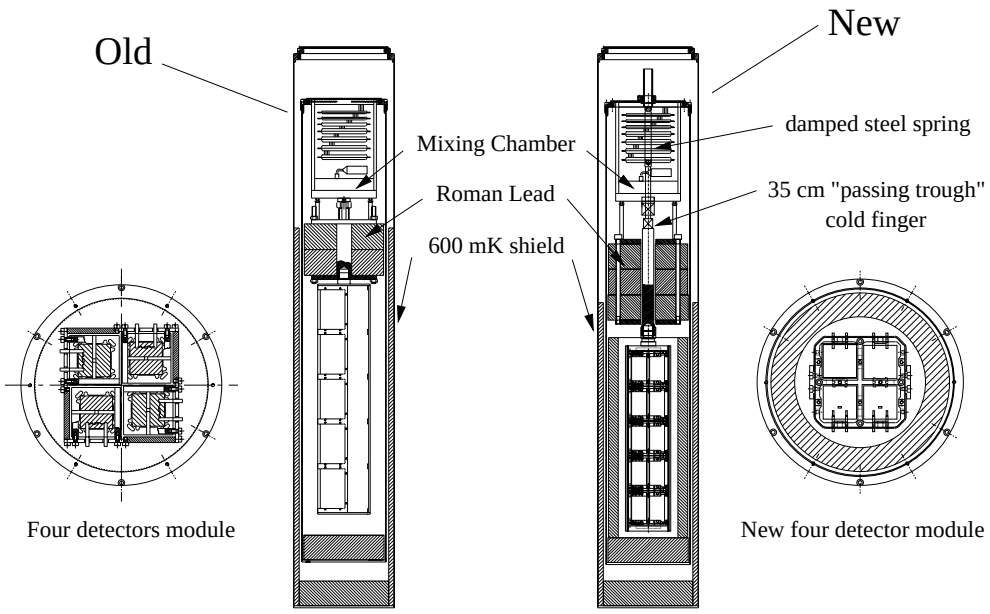

Figure 1: Scheme of the MIBETA detectors.

external to the decay source. A single line corresponding to the binding energy of the captured electron (sum of all atomic transition energies) is on the contrary expected for a pure calorimetric approach, in which the source is also the detector (as is the case for a low temperature thermal detector [23]). Unfortunately, atomic deexcitation cascades can be induced also by the interaction between the environmental radiation and the source (e.g. photoelectric or Compton effect). In this case, however, the involved atomic levels are those of the parent atom, while in a genuine EC decay they correspond to those of the daughter one. Background contributions can be therefore isolated by using calorimetric detectors characterized by very good energy resolutions. Since low temperature detectors accomplish both requirements, MIBETA detectors represented the ideal choice for such an analysis.

Evidence for the K EC decay of ^{123}Te was obtained by Watt and Glover [15] with a lifetime $t^K_{1/2} = (1.24 \pm 0.10) \times 10^{13}$ years, using a proportional counter.

This result was contradicted by a previous cryogenic experiment (Run 0) carried out underground by our group using four thermal 340 g TeO_2 detectors installed in the Hall A cryogenic setup [16]. Two separated peaks were observed in the spectrum recorded at low energy: a peak at 27.3 keV corresponding to the energy of Te K_α X-rays (produced by the interaction of radiation with nearby Te detectors), and a peak at 30.5 keV, corresponding to the total energy released by Te K EC to Sb. The different origin of the two peaks was moreover demonstrated by the comparison of the spectra collected requiring or not an anticoincidence between the four TeO_2 detectors [16]: the 27.3 keV line in fact disappeared in the anticoincidence spectra. By attributing the 30.5 keV peak to K EC of ^{123}Te we obtained an evidence for this process and quoted a lifetime $t^K_{1/2} = (2.4 \pm 0.9) \times 10^{19}$ years, six orders of magnitude higher than in the experiment by Watt and Glover. The main drawback of this measurement was the limited statistics. In addition the 30.5 keV signal could be also due to the activation of the ^{120}Te isotope (0.908 % abundance) by

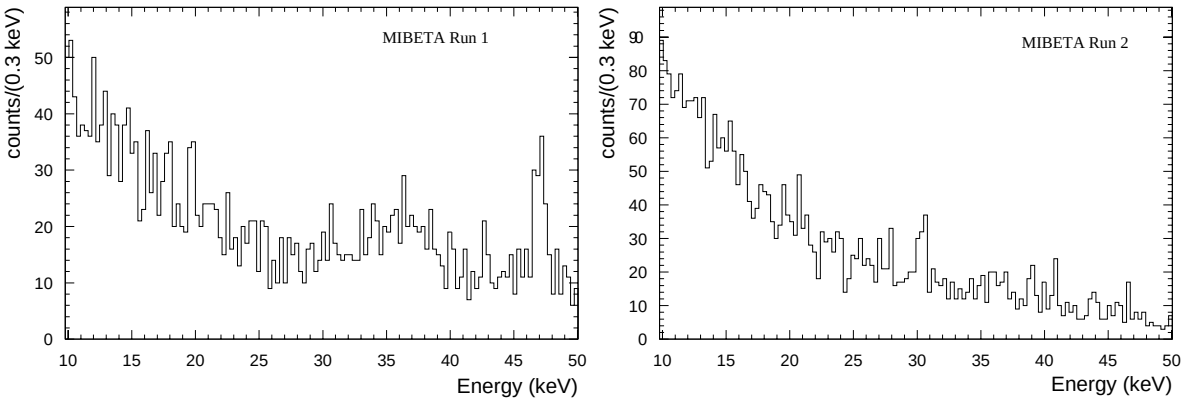

Figure 2: Low energy spectra obtained in the two MIBETA runs. The peak in the Run 1 spectrum, corresponding to the 46.6 line of ^{210}Pb has a width of 1 keV FWHM.

environmental neutrons. This isotope, despite its low abundance can in fact lead to a substantial production of ^{121}Te and ^{121m}Te with cross sections of 0.3 and 2 b respectively. These isomers decay by EC with lifetimes of 16.8 and 154 days, respectively, yielding the same signal in the detector as the one expected for the EC decay of ^{123}Te. The expected neutron activation in the underground laboratory is negligible, since thermal neutrons are suppressed by a factor of 10^4 with respect to sea level [17]. However, ^{121}Te and ^{121m}Te nuclei could have been produced when the detectors were outside the laboratory. They could have persisted in the detectors during the measurement, since the run started underground immediately after the crystal installation.

Following these consideration we carried out a similar analysis on the two MIBETA runs. Since the first MIBETA run (Run 1) started two years after the crystals were stored underground, most of the ^{121}Te and ^{121m}Te nuclei produced during their preparation should have been decayed. The spectrum corresponding to 724.88 hours $\times$ kg of effective running time is shown in Fig. 2. Due to a significant improvement in the background level the 27 keV X-ray peak (due to background excitation of Tellurium) and the peak at 39.9 keV (due to ^{212}Bi) are no more apparent. The peak at 46.5 keV is instead due to surface activity of ^{210}Pb. Unlike what indicated in the previous experiment, there is now no clear evidence of the peak at 30.5 keV, where the observed counts are 17 ± 12. By exploiting the fact that all crystals were brought outside the underground laboratory for a surface treatment between the first and the second MIBETA run, we tried to assess the origin of the observed disagreement. All crystals remained exposed to environmental neutrons for a period of about two months. After this operation they were again installed underground and the second MIBETA run (Run 2) totalling 259.59 hours $\times$ kg took place. The low energy spectrum reported in Fig.2 clearly shows a peak at 30.5 keV which could now be attributed to the K EC of ^{121}Te isomers produced by cosmic ray neutrons outside the tunnel and not to K EC of ^{123}Te.

Taking into account all these observations: i) the absence of a clear signal in Run 1; ii) the short period during which the TeO_2 crystals were stored underground before the start of Run 0; iii) the evidence for a neutron activation contribution to EC signals (30.5

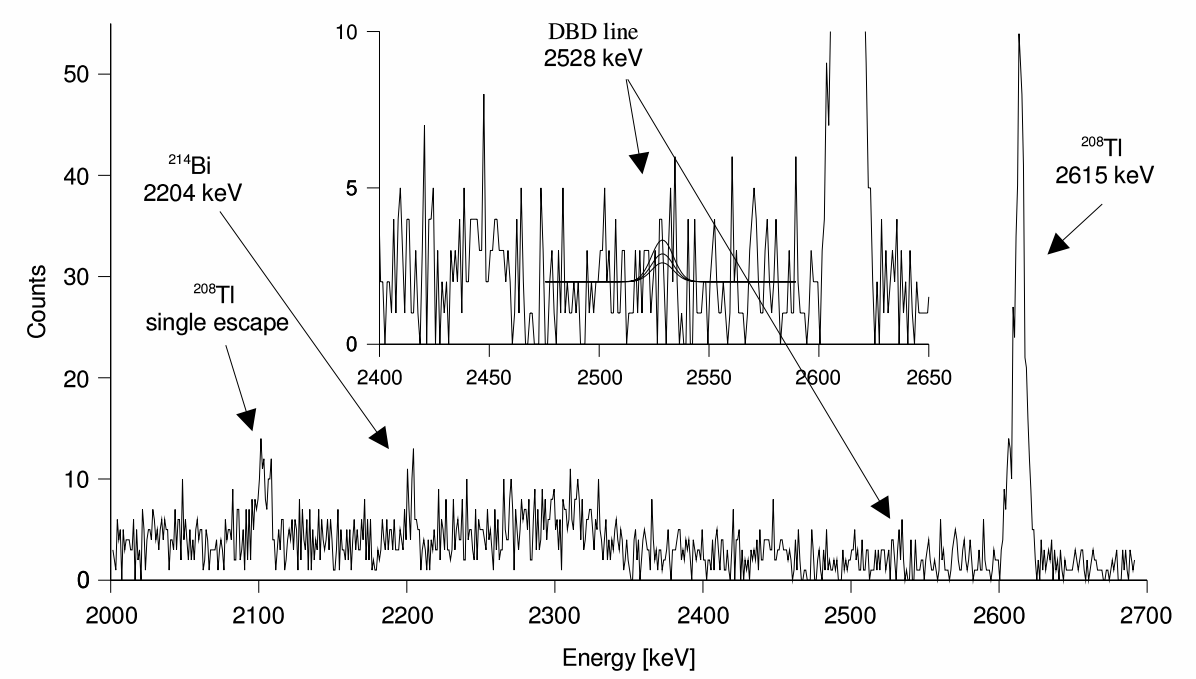

Figure 3: Total spectrum (in anticoincidence) in the region of neutrinoless DBD obtained with the twenty crystal array. The solid curves represent the best fit (lowest curve) and the 68 % and 90 % C.L. excluded signals.

keV line) in crystals exposed to sea level neutron flux before Run 2, we concluded that *it was not possible to report any evidence for K electron capture of* ^{123}*Te*. In particular, by applying a maximum likelihood analysis to the data collected during Run 1 we set a 90 % C.L. lower limit $t^K_{1/2} \equiv \frac{t_{1/2}}{BR^K} > 5 \times 10^{19}$ years on the half lifetime for K EC of ^{123}Te. By dividing this result for the branching ratio for K capture $BR^K = 1.83 \times 10^{-3}$ [20, 22], we obtained an inclusive limit for EC of ^{123}Te of $t_{1/2} > 9.2 \times 10^{16}$ years (90 % C.L.).

3.2 BDB results

The two MIBETA runs totalled ∼31,508 and ∼5,690 hours·kg of effective running time, respectively. Sum spectra were obtained both with no anticoincidence cut and by operating each detector in anticoincidence with all the others. In all these spectra the main lines due to the natural activity of the ^{232}Th and ^{238}U chains, of ^{40}K and the lines at 1173 and at 1332 keV due to cosmogenic ^{60}Co were observed. No peak appeared in the region of $\beta\beta(0\nu)$ of ^{130}Te, where the rates were, respectively, of 0.59 ± 0.06 and 0.33 ± 0.11 counts keV^{-1} kg^{-1} year^{-1}, when operated in anticoincidence. No peak also appeared at the energies corresponding to neutrinoless DBD of ^{130}Te to excited levels of ^{130}Xe, and at the energy of 867 keV corresponding to $\beta\beta(0\nu)$ of ^{128}Te.

The sum of the spectra obtained in anticoincidence in the two runs in the region above 2000 keV is shown in Fig. 3. It corresponds to ∼3.56 kg x year of TeO_2 and to ∼0.98 kg x year of ^{130}Te . The clear peaks corresponding to the lines at 2104 keV (single escape of the 2615 keV ^{208}Tl line), at 2204 keV (^{214}Bi) and at 2615 keV (^{208}Tl),

Table 1: Half lifetime limits (90 % C.L.) on lepton violating and conserving channels deduced from the MIBETA data analysis. E_0 is the energy at which $T_{1/2}$ was obtained while *a.c.* means anticoincidence between different detectors.

Isotope	Transition	Used Spectra	Cuts	E_0 (keV)	Efficiency (%)	$T_{1/2}$ (years)
^{130}Te	$0\nu : 0^+ \rightarrow 0^+$	All spectra	a.c.	2528.8	84.5	$> 2.1 \times 10^{23}$
^{130}Te	$0\nu : 0^{+*} \rightarrow 0^+$	All spectra	none	1992.8	7.9	$> 3.1 \times 10^{22}$
^{130}Te	$0\nu : 0^{+*} \rightarrow 2^+$	All spectra	none	1992.8	37.5	$> 1.4 \times 10^{23}$
^{130}Te	$2\nu : 0^+ \rightarrow 0^+$	^{130}Te crystals	a.c.			$> 3.8 \times 10^{20}$
^{130}Te	$1\chi : 0^+ \rightarrow 0^+$	^{130}Te crystals	a.c.			$> 2.2 \times 10^{21}$
^{130}Te	$2\chi : 0^+ \rightarrow 0^+$	^{130}Te crystals	a.c.			$> 0.9 \times 10^{21}$
^{128}Te	$0\nu : 0^+ \rightarrow 0^+$	All spectra	a.c.	867.2	97.9	$> 1.1 \times 10^{23}$

confirm the reproducibility of the array during both runs. It should be stressed that in the spectrum of the second run both the peaks and the continuum were decreased by a factor of about two with respect to the first run. Although very similar, these reduction factors are due to two different effects. According to the results of the background analysis, supported by the Monte Carlo simulation of the detector, the peaks contributions were due to sources outside the detector (substantially reduced by the increased shield of lead) while the continuum was mainly reduced by the surface treatment of the crystals and copper structures. This confirms that the origin of the background at the energy corresponding to neutrinoless DBD is mainly due to surface contamination.

Fit parameters and 90 % C.L. limits for the various decay processes (Tab. 1) were evaluated with a maximum likelihood procedure[24]. Similar results were however obtained following the approach proposed by G.J. Feldman and R.D. Cousins [25], suggested by the Particle data Group [26].

The constraints on the effective neutrino mass $\langle m_\nu \rangle$, on the right handed current parameters $\langle \lambda \rangle$ and $\langle \eta \rangle$ and on the coupling majoron parameter $\langle g_{\chi\nu} \rangle$ suffer from uncertainties in the calculation of the nuclear matrix elements [27, 28, 29, 30]. They are reported, for the various $\beta\beta(0\nu)$ channels in Table 2 on the basis of various QRPA calculations. Since shell model calculations do not seem appropriate for heavy nuclei [27] they were not included in the table. Taking into account theoretical uncertainties we obtained constraints in the ranges (1.1-2.6) eV; $(1.6 - 2.4) \times 10^{-6}$ and $(0.9 - 5.3) \times 10^{-8}$ for the values of effective neutrino mass, and the two right handed parameters λ and η respectively. The limit on $\langle m_\nu \rangle$ is presently the most restrictive one among those obtained with direct methods after those on ^{76}Ge (0.35-1.4 eV).

The 90 % C.L. limit for two neutrino DBD of ^{130}Te reported in Table 1 already excludes a relevant loss of the daughter isotope in geochemical experiments, which has been considered by O.K. Manuel [36]. We attempted also an evaluation of the rate for the lepton conserving process by analyzing the difference between the sum of the two spectra of the crystals isotopically enriched in ^{130}Te and the sum of those of the crystals enriched in ^{128}Te . (Fig. 4). These differences are positive in the region of two neutrino DBD with an excess of 269 ± 60 counts corresponding to $T_{1/2} = (6.1 \pm 1.4\, stat.) \times 10^{20}$ years. However a precise evaluation of the half life is not straightforward because the background

Table 2: Limits on the lepton non-conserving parameters from this experiment. For each parameter, limits are abtained assuming vanishing the others.

Ref.	$\langle m_\nu \rangle$	$\langle \lambda \rangle \times 10^{-6}$	$\langle \eta \rangle \times 10^{-8}$	$\langle g_{\chi\nu} \rangle \times 10^{-5}$
Engel et al. (1988)[31]	1.8			28
Engel et al. (1989)[32]	1.1			17
Muto et al. (1989)[33]	1.5	2.1	1.4	24
Suhonen et al. (1991)[34]	2.0	2.1	5.3	31
Tomoda et al. (1991)[35]	1.6	2.4	1.6	25
Faessler et al. (1998)[27]	2.1			33
Barbero et al. (1999)[28]	1.3	1.6	0.9	
Klapdor-Kleingrothaus and Stoica(2001)[29]	2.2-2.3			
Faessler and Simkovic (2001)[30]	2.6	2.4	1.8	

differs among the four enriched crystals. In particular different rates are observed for the 1460 keV gamma line of ^{40}K and for the alpha lines in the 4-6 MeV energy region. With the aid of a Monte Carlo simulation of the possible background contributions we were able to restrict the possible sources responsible of these lines. The 1460 keV gamma peak appears to be due to an accidental ^{40}K contamination localized on the bottom surface of the detector copper holder, while the alpha lines are clearly due to ^{238}U and ^{232}Th surface contaminations of the crystals. A similar - although lower - surface contamination is observed also for all the natural crystals.

Taking into account the different rates observed in the lines of our isotopically enriched detectors we extrapolated the contribution to the ^{130}Te - ^{128}Te spectra produced by such contaminations in the two neutrino DBD region. The maximum expected difference due to ^{238}U and ^{232}Th contaminations is negative and corresponds to 380 counts, which should therefore be added to the actually found signal. On the contrary the corresponding maximum expected difference due to background from ^{40}K (86 counts) is positive and should therefore be subtracted. Slightly different values are obtained by varying the contaminations location. In all the cases however negative values are obtained for the ^{238}U and ^{232}Th contribution (responsible of the differences in the alpha counting rates) and positive for the corresponding ^{40}K ones. We concluded that the difference in the crystal background rates could not account for the two neutrino DBD effect, but introduced a large systematics in the half life time evaluation. By assuming the above quoted background rates as

Table 3: Bulk contamination upper limits in picograms per gram.

Contaminant	^{232}Th	^{238}U	^{40}K	^{210}Pb	^{60}Co
TeO_2	0.5	0.1	1	10 μBq/kg	0.2 μBq/kg
copper	4	2	1	0	10 μBq/kg
Roman lead	2	1	1	4 mBq/kg	0
16 Bq/kg lead	2	1	1	16 Bq/kg	0

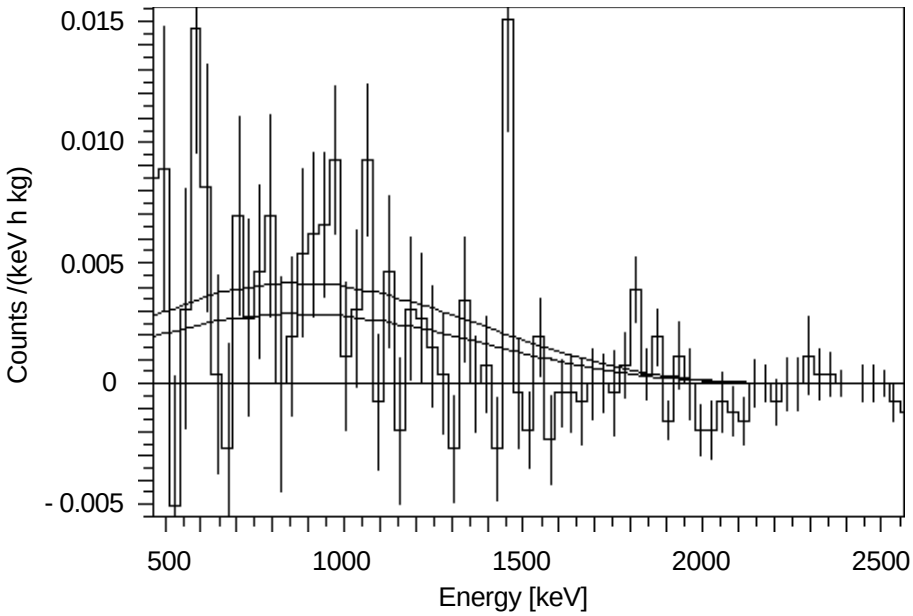

Figure 4: Total difference spectrum between ^{130}Te and ^{128}Te detectors (no background subtraction). The solid curves represent the best fit (lowest curve) and the 90 % C.L. excluded signal (Tab. 1)

the maximum possible contribution to the systematic error, we obtained the final result $T_{1/2} = (6.1 \pm 1.4\, stat.^{+2.9}_{-3.5}\, sys.) \times 10^{20}$ years. This value, while in agreement with most geochemically obtained results, looks somewhat higher than most of those predicted theoretically [37]. The already running NEMO 3 experiment [38], as well as the an improved search to be carried out with the larger CUORICINO array [39] being mounted in the Gran Sasso laboratory, will allow to reduce soon the present uncertainty.

3.3 Background analysis and CUORE/CUORICINO simulations

A big effort was carried out during 2002 to understand the origin of the background contributions and carefully describe the observed spectra. Radioactive contaminations of individual construction materials, as well as the contributions from the laboratory environment, were measured and the impact on detector performance determined by Monte Carlo computations. MIBETA data were used as a validation set. Through the identification of the dominant background contributions, the final goal of this analysis is the realization of effective procedures of material selection and detector structure design. When correctly validated it can moreover represent a powerful tool to estimate the experimental sensitivity of the future projects. The developed Monte Carlo code is based on the GEANT-4 package and models the shields, the cryostat, the detector structure and the detector array. It includes the propagation of photons, electrons, alpha particles and heavy ions (nuclear recoils from alpha emission) as well as neutrons and muons. For radioactive chains or radioactive isotopes alpha, beta and gamma/X rays emmissions are considered according to their branching ratios. The time structure of the decay chains is taken into account and the transport of nuclear recoils from alpha emissions is included.

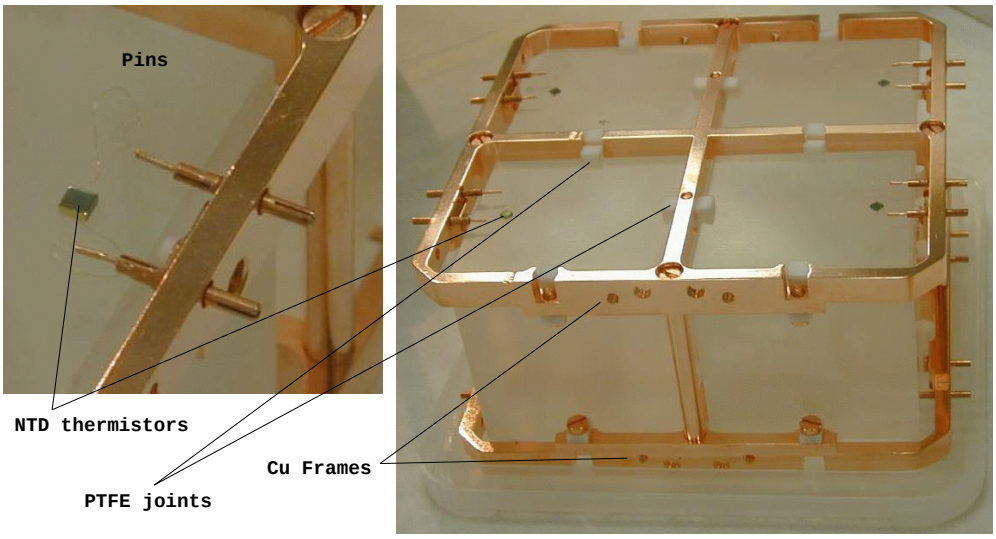

Figure 5: A CUORICINO 4 detectors basic unit.

The background sources considered are: i) bulk and surface contamination of the construction materials in^{238}U , ^{232}Th chains and ^{40}K and ^{210}Pb isotopes; ii) bulk contamination of construction materials due to cosmogenic activation; iii) neutron and muon flux in the Gran Sasso Laboratory; iv) gamma ray flux from natural radioactivity in the Gran Sasso Laboratory; v) background from the $\beta\beta(2\nu)$ decay.

For what concerns bulk contaminations the main contributions are found to originate from the heavy structures close to the detectors (the copper mounting structure of the array, the Roman lead box and the two lead disks on the top of the array) and from the detectors themselves (the TeO_2 crystals). The ^{232}Th , ^{238}U , ^{40}K and ^{210}Pb contamination levels of TeO_2, copper and lead as well as the ^{60}Co cosmogenic contamination of copper are deduced from the 90% C.L. upper limits obtained in the code validation process (quantitative comparison with MIBETA data) or measured with low activity *Ge* spectrometry [40]. They are summarized in Table 3 and were later used in the CUORE and CUORICINO sensitivity computations (Table 4). The ^{60}Co cosmogenic contamination of TeO_2 was evaluated according to the crystals history (i.e. their exposition to cosmic rays during the preparation phase, followed by the storing period underground).

Surface contaminations are relevant only when localized on the crystals or on the copper mounting structure directely faced to them. MIBETA background analysis showed that these contaminations give a relevant contribution in the ^{130}Te $\beta\beta(0\nu)$ energy region. The best fit configuration corresponded to U and Th contaminations with an exponential density profile and a $\sim 1\ \mu m$ depth. Dedicated procedures to strongly reduce such contaminations are under investigation and will probably represent one of the strongest efforts needed to reach the required CUORE sensitivity. Actually, the results of a similar effort performed between MIBETA runs 1 and 2 (surface treatment of the TeO_2 crystals and of the mounting structure copper) show that these procedures can be very effective. On the other hand, polishing powders with a radioactive content 1000 times lower then the ones used for MIBETA crystals are commercially available [41] and have already been used for CUORICINO preparation. An improvement of the surface contamination by one

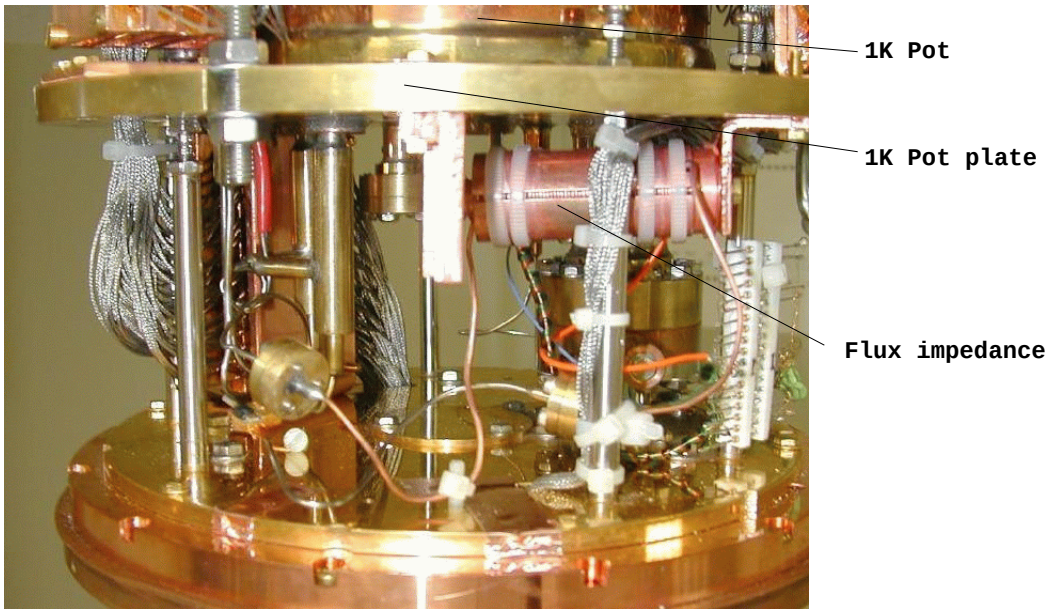

Figure 6: Details of the 1K pot impedance.

or two orders of magnitude is therefore not out of the reach. A similar situation holds for copper whose surface quality was effectively improved by means of an etching procedure [42] performed before MIBETA run 2. Improvements of this procedure (e.g. use of low contaminated liquids in a low background environment) are under investigation and should be tested in the near future.

4 CUORICINO

The CUORICINO detector represents the natural evolution of the MIBETA array and consists of a single CUORE tower modified to include 18 of the 20 MIBETA TeO_2 crystals. Its structure has been studied in order to assure a filling as complete as possible

Table 4: Computed CUORE background in the $0\nu\beta\beta$ decay and in the low energy regions for bulk contaminations in the different elements, the Cu structure accounts for the detector mounting structure and the 50 mK shield. With the already available materials background lower than $\sim 4 \times 10^{-3}$ $counts/(keV\ kg\ y)$ in the $0\nu\beta\beta$ decay region and $\sim 3 \times 10^{-2}$ $counts/(keV\ kg\ d)$ in the low energy (10-50 keV) region can be predicted

Simulated element	TeO_2 crystals	Cu structure	Pb shields	TOTAL
$0\nu\beta\beta$ decay region $counts/(keV\ kg\ y)$	1.6×10^{-3}	1.5×10^{-3}	7.0×10^{-4}	3.8×10^{-3}
dark matter region $counts/(keV\ kg\ d)$	2.3×10^{-2}	9.6×10^{-4}	5.0×10^{-5}	2.4×10^{-2}

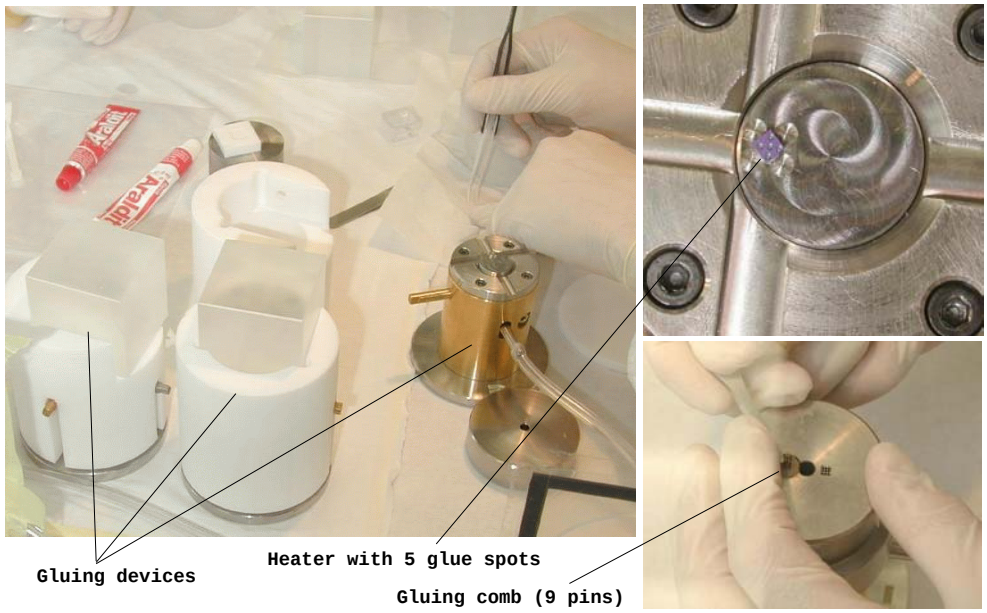

Figure 7: The CUORICINO thermistors and heaters gluing device.

of the experimental space available in the dilution refrigerator presently operating for the Mibeta experiment in Hall A. CUORICINO is therefore the most massive cryogenic detector for searches on rare events compatible with the sizes of the existing cryogenic facilities operating in the Gran Sasso Laboratories. After proper modifications of the thermal shields, it is now hosted in the same dilution refrigerator (Hall A) used for MIBETA. CUORICINO consists of an array of 44 cubic crystals of natural TeO_2 of $5 \times 5 \times 5$ cm^3, plus 18 $3 \times 3 \times 6$ cm^3 crystals (arranged in two planes of 9 crystals each) for a total mass of about 40 kg. Held in a copper tower-like frame, the detector is suspended inside the inner vacuum chamber (IVC) of the dilution refrigerator by means of a single steel spring and a copper bar fastened to the tower structure and thermally linked (copper strips) to the coldest point of the refrigerator. The structure of the single bolometers is very similar to that of the MIBETA detectors even if a new set of NTD thermistors and Si heaters was expressely designed for an optimal matching with the new detector features. A completely new and more compact wiring system was realized to allow the readout of the larger number of detectors. Twenty-four readout channels were endowed with a cold ($\sim$100 K) electronics stage. A completely new (fully programmable) front-end electronics has been installed. The VXI-based acquisition system has been improved to manage the larger number of channels. Besides being a crucial test for the CUORE project feasibility, this setup will make possible not only an improved search for neutrinoless double beta decay, but also a more sensitive search for direct interactions of WIMPs allowing also the observation of possible subdiurnal modulations of the signal induced by electromagnetic interactions of axions coming from the sun.
The CUORICINO installation phase started in January 2002, immediately after the completion of the last MIBETA run. After a number of small delays, mainly due to continuous modifications of the mechanical structure of the detector and to difficulties in the realization of the modified cryostat thermal shields, CUORICINO installation was definitely

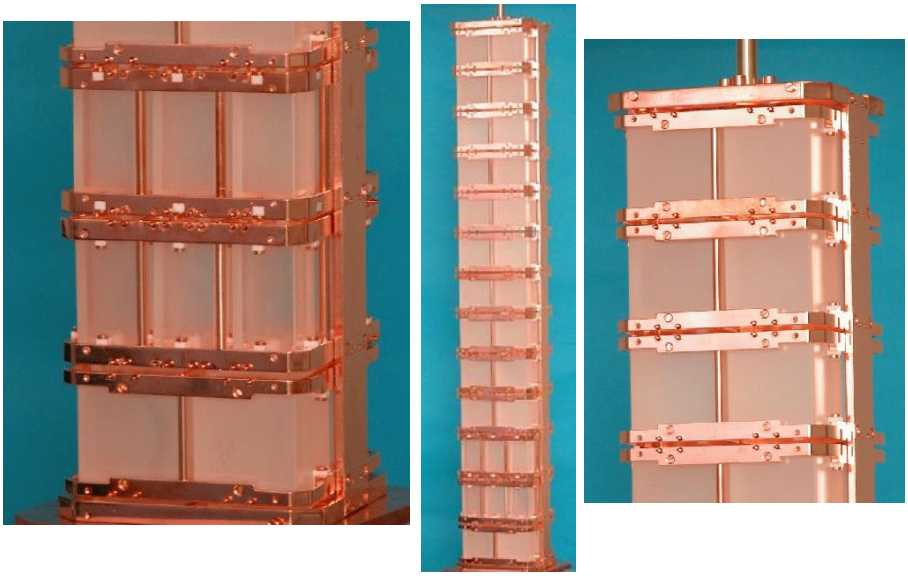

Figure 8: Details of the CUORICINO tower.

concluded only in December 2002. The detector has presently (17/01/2003) reached its base temperature (∼10 mK) and should start the first background measurement by February 2003.

4.1 CUORICINO R&D

The CUORICINO R&D activity with the Hall C cryogenic setup continued also in 2002 (in parallel with the detector construction), mainly to fix some of the detector design problems appeared in the last MIBETA run and to improve the cryogenic setup stability. In particular, a series of test measurements was dedicated to check the performance of a new PTFE joint design (Fig. 5). Besides improving the detector performance and reduce the detector sensitivity to vibrations (thus reducing the noise contributions) the new joints didn't require any modification of the copper frames and were therefore implemented in the final CUORICINO design. The thermal link between the detector and the refrigerator structure was optimized during the same runs. Dedicated measurements of the thermal conductivity of various samples of copper strips allowed the definition of the optimum link structure (materials and geometry). Special care was also dedicated to the optimization of the cryogenic setup performance. In particular a strong effort was made to reduce all possible noise contributions originating from vibrations of the cryostat setup. A series of different mechanical decouplers were mounted along the pumping pipes and on the pumps basements to avoid the vibration transmission through the tubes or the laboratory floor respectively. A new flux impedance (Fig. 6) thermally linked to the refrigerator *1K pot* was inserted between the *1K pot* itself and the Helium main bath to avoid vibrations originating from the turbulent behaviour of the incoming liquid Helium (due to the temperature gradient). In all cases the best perfoming solutions were also installed in the Hall A cryostat. A series of test measurements were also dedicated to the *cold electronics* stage and to the new wiring (and wire thermalization elements) design. In

particular, all the 24 CUORICINO *cold electronics* channels (4.2) were previously tested in the Hall C cryostat.

4.2 The CUORICINO detector

As stated above, the CUORICINO installation started in January 2002 and was completed in December 2002. Actually the TeO_2 crystals preparation was started previously (October 2001-March 2002), followed by the installation of the new wiring system and of the *cold electronics* elements (February-March 2002), the single detectors (April-June 2002) and 4 detector units (June-September 2002) assembly, the new inner Roman Lead shield realization and the cryogenic setup upgrade (June-September 2002), the front-end electronics realization, test and installation (July 2002, January 2003), the cryogenic setup test run (September-October 2002), the cryostat thermal shields realization (May-August 2002) and finally the Tower assembly and installation (September-November 2002).

4.2.1 The Cuoricino tower

The CUORICINO tower consists of a set of 44 cubic tellurite crystals of 5 cm side and 790 g mass, stacked in 11 units of four crystals each (*plane*). Two additional *planes*, similar in structure but containing 9 detectors each, host 18 of the 20 MIBETA crystals (Fig. 8). Each *plane* consists of two copper frames (Fig. 5) held in position by 4 cylindrical copper bars. Small PTFE supports hold tightly the crystals; their contraction at low temperature increases mechanical crystal stability. The gap between crystals is of 0.6 cm, assuring a very compact structure. The temperature sensors are Neutron Transmutation Doped (NTD) Ge thermistors. The crystals are thermally coupled to the heat sink by means of the already mentioned PTFE joints, while the connection between crystal and the thermistor lattice is provided by means of 9 glue spots (Fig. 7). The thermistor lattice is also connected to the heat sink by means of the readout gold wires. A set of copper pins glued to each *plane* copper frames realize the feed-through for signals readout (Fig. 5). A special heater, consisting of a silicon chip on which a narrow conductive meander is realized by implantation doping is glued onto the crystal and is used to deliver fixed amounts of energy through Joule power dissipation. The corresponding thermal pulses are used off-line for system instability corrections.
In order to avoid surface contaminations originating from the bad quality of the polishing powders used by the supplying factory (SICCAS Al_2O_3 and Cerium Oxide powders were found hardly contaminated from a radioactive point of view) all CUORICINO TeO_2 crystals were ordered withouth the usual optical surface treatment. SICCAS (Shanghai Institute of Ceramics) should take care of the crystals growth, cut and rough surface treatment using a radiopure powder (certified Sumitomo 7 μm Al_2O_3 powder) supplied by the CUORE Collaboration. All CUORICINO crystals were available and stocked underground in a Rn free atmosphere since the beginning of Summer 2001. The optical treatment of the crystal surfaces (necessary to avoid bad thermal conductances with the NTD thermistors) began in October 2001 in charge of the CUORE Collaboration, after a careful and long selection of the polishing powders (0.7 μm Al_2O_3) and pads (nylon). After the first unsuccessfull efforts, due to the extremely poor quality of the crystal surfaces

(characterized by the presence of defects and deep scratches), the situation improved only with the help of SICCAS: qualified staff came to Italy in December 2001 expressely to carry out a second surface treatment using polishing powders of better (with respect to Sumitomo powders) mechanical quality. The surface treatment procedure continued then successfully until March 2002. With the help of a new designed gluing system (Fig. 7), detectors preparation (NTD thermistors and Si heaters fastening) continued until June 2002. Due to a delay in the copper frames preparation and polishing, CUORICINO detectors were stored underground in an air tight, radon free environment until September 2002. Then the CUORICINO tower was finally assembled (Fig. 8). All detectors were assembled in a Rn free environment (a box fluxed with clean Nitrogen from an evaporator, Fig. 7) installed inside the CUORE clean room (Hall A). Similar devices were realized also for the planes and the tower assembly in order to minimize any possible exposition of the CUORICINO detectors to environmental Radon.
The modified cryostat thermal shields were ready by the end of September 2002, while the tower was finally suspended to the cryostat structure in December 2002. Cool down procedures began on 2^{nd} of January 2003.

4.2.2 The Cryogenic setup

Even if withouth principle difficulties, the installation of the CUORICINO detector inside the Hall A dilution refrigerator implied a huge amount of work. In fact, due to the increased number of detectors a completely new wiring system was required. Designed and tested during fall 2001, the new wiring system was realized in Milano in February and installed in Gran Sasso in March 2002. In the same period the installation of the *cold electronics* readout was completed. An extensive cryostat maintenance operation (including a complete check of the pumping system and of the Helium liquefier and the installation of the above cited *1K pot* flux impedance and mechanical decouplers) was then carried out between June and September 2002. A test run aiming at veryfing the full cryogenic system performance after all changes carried out since the MIBETA experiment stop (but using the original thermal shields and two 4 detector *units*) was carried out successfully in September 2002. After the delivery of the modified thermal shields, the CUORICINO tower cool down finally began on the 2^{nd} of January 2003.

4.2.3 The Front-End Electronics

Because of the different individual behaviour of each detector, the front-end readout of an array of large mass bolometers is a complex system which must be able to suite a large ranges of gains, detector biasing and offset compensation. A very precise analog triggering system is moreover needed for each channel and a very precise and stable (remotely selectable and triggerable) pulse generator is required for the continuous calibration of the array. All these features were taken in consideration in the CUORICINO implementation. Its main characteristics are: i) a low noise bias system for each bolometer; ii) a very small series and parallel noise and very small thermal drift of the very front-end; iii) a very precise analog trigger for each channel and a very stable pulse calibrating instrument with multi-outputs. Any needed parameter is completely remotely programmable. In addition, a very accurate and precise power supply system has been developed in order

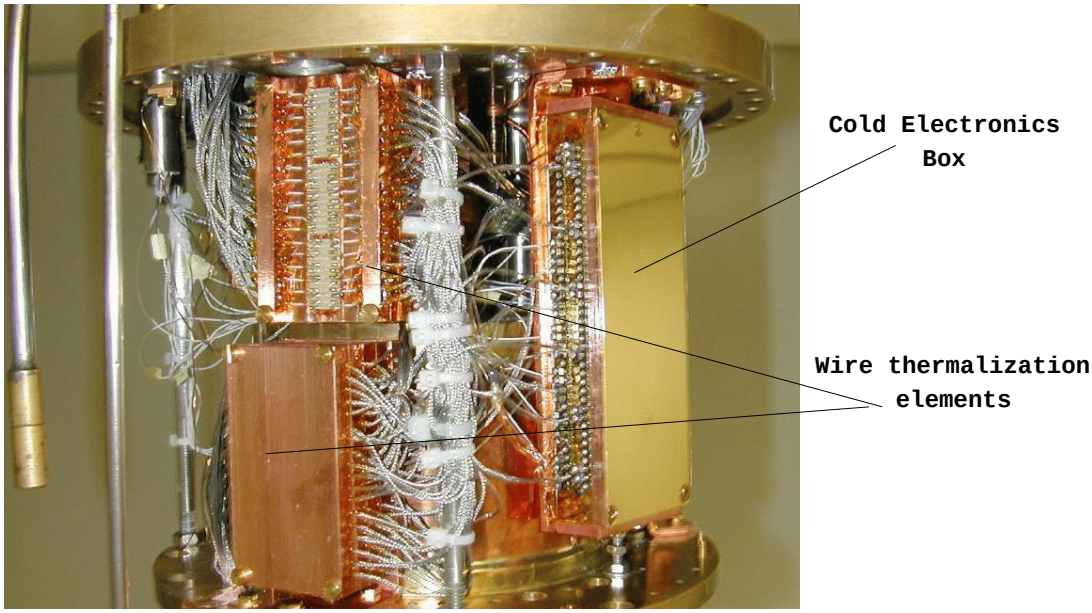

Figure 9: Deatils of the CUORICINO cold electronics box and of the wire thermalization elements.

to minimize drift effects. An accurate description of the front-end performance can be found in [43, 44, 45, 46, 47]. The complete front-end has been designed and realized within the collaboration of CUORICINO. The groups of Milano-Bicocca and Columbia University has been involved in the project. In particular the group of Milano-Bicocca has taken the responsibility of the design (2001), the test and the final installation of the electronics (July 2002 to January 2003), while the Columbia group has been responsible for the production of all the front-end channels (first half of 2002).
As mentioned above, 24 CUORICINO detectors are readout by a cold ($\sim$100 K) electronics stage located close to the CUORICINO tower (Fig.9) in order to lower the integration effects of the stray capacitances and improve the detectors performance. Fully designed and realized by the Milano-Bicocca group and previously tested in the Hall C cryogenic setup, this electronic stage was finally installed in the Hall A cryostat in March 2002. Due to its better noise figure of merit, notable improvements are expected especially near threshold (i.e. in the energy region of interest for dark matter searches).

5 Conclusions

The CUORICINO detector installation has finally concluded. The first DBD run will start in February 2003. According to the results obtained with MIBETA and CUORICINO R&D we are confident to reach with the CUORICINO detector the expected background level of 0.1 conts/keV/kg/yr in the $0\nu\beta\beta$ region.
The analysis of the full MIBETA data set has been concluded. Competing results on $\beta\beta(0\nu)$ of ^{130}Te have been obtained together with an indication for $\beta\beta(2\nu)$ of the same isotope. New limits on the ^{123}Te EC decay have been set. The results of the MIBETA background analysis show that, while bulk radioactive contaminations of the construction

materials are already under control, surface and cosmogenic contaminations will be the actual challenge for the CUORE project successfull realization.
We would like to acknowledge the continuous and constructive help of G. Ceruti, R. Gaigher and S. Parmeggiano and of our student F. Capozzi in various stages of the experiment. Special thanks are due to M. Perego for assembling the wiring system and the electronic read-out and to L. Tatananni, B. Romualdi and A. Rotilio for the realization of mechanical parts and the irreplaceable help in the construction of the Roman lead internal shield.

6 List of Publications

- C. Arnaboldi, C. Brofferio, C. Bucci, S. Capelli, O. Cremonesi, E. Fiorini, A. Giuliani, A. Nucciotti, M. Pavan, M. Pedretti, G. Pessina, S. Pirro, C. Pobes, E. Previtali, M. Sisti and M. Vanzini, *A calorimetric search on double beta decay of* ^{130}*Te*, Physics Letters B (in the press)

- A. Alessandrello, C. Arnaboldi, C. Brofferio, C. Bucci, S. Capelli, O. Cremonesi, E. Fiorini, A. Giuliani, A. Nucciotti, M. Pavan, M. Pedretti, G. Pessina, S. Pirro, C. Pobes, E. Previtali, M. Sisti, M. Vanzini and L. Zanotti, *New limits on naturally occurring electron capture of* ^{123}*Te*, Physical Review C (in the press)

- C. Arnaboldi et al. (the CUORE Collaboration), *CUORE: A cryogenic underground observatory for rare events*, Nuclear Instruments and Methods in Physics Research (in the press)

- O.Cremonesi, *Neutrinoless Double Beta Decay: Present and Future*, "XXth International Conference on Neutrino Physics and Astrophysics, May 25 - 30, 2002, Munich, Germany

- C.Brofferio, *World status of double beta decay*, 4^{th} International Workshop on the Identification of Dark Matter (IDM2002), York, Gran Bretagna, 2-6 September 2002 (in the press).

- E.Previtali et al., *CUORE*, 4^{th} International Workshop on the Identification of Dark Matter (IDM2002), York, Gran Bretagna, 2-6 September 2002 (in the press).

- C. Arnaboldi et al., *CUORE: low temperature techniques for neutrino physics*, The 23^{rd} International Conference on Low Temperature Physics, August 20-27, 2002,Hiroshima, Japan.

- C.Arnaboldi, C.Bucci, J.W.Campbell, A.Nucciotti, M.Pavan, G.Pessina, S.Pirro, E.Previtali, C.Rosenfeld, M.Sisti, *The programmable front-end system for CUORICINO, an array of large-mass*, IEEE Transactions on Nuclear Science, USA. (in the press)

References

[1] H.V. Klapdor-Kleingrothaus, A. Dietz, H.L. Harney and I.V. Krivosheina: Modern Phys. Lett. A, Vol.16 (2001) 2409-2420 ; H.V. Klapdor-Kleinghthaus Reply to comment of article "Evidence for Neutrinoless Double Beta Decay" arXiv:hep-ph/0205228

[2] L. Harney: Reply to the comment on "Evidence for neutrinoless double beta decay"- arXiv:hep-ph/0205293

[3] F. Feruglio, A. Strumia and F. Vissani, Nuclear Phys. B 637 (2002) 345

[4] C.E Aalseth et al, Modern Phys. A 17 (2202) 1475 hep-ex/0202018.

[5] S. Pascoli, S. T. Petcov, and L. Wolfenstein, Phys.Lett. **B524**, (2002) 319-331.

[6] F. Feruglio, A. Strumia and F. Vissani, hep-ph/0201291; Nucl.Phys. **B637**, 345 (2002).

[7] S. M. Bilenky, S. Pascoli and S. T. Petcov, arXiv: hep-ph/0105144 v1 15 May 2001; Phys. Rev. **D64**, 053010 (2001).

[8] S. Pascoli and S. T. Petcov, arXiv: hep-ph/0205022.

[9] H. V. Klapdor-Kleingrothaus, H. Ps, A. Yu. Smirnov, Phys. Rev. **D 63**, 073005 (2001).

[10] S. M. Bilenky, C. Guinti, W. Grimus, B. Kayser, and S. T. Petcov, Phys. Lett. **B 465**, 193 (1999); Y. Farzan, O. L. G. Peres and Y. Smirnov, Nucl. Phys. **B612**, 59 (2001).

[11] L. Baudis *et al.*, Phys. Rev. Lett. **83**, 41 (1999).

[12] C. E. Aalseth *et al.*, Phys. Rev. **D65**, 092007 (2002).

[13] E. Fiorini and T. Niinikoski, Nucl.Instrum. and Meth. In Phys.Res. 224 (1984) 83.

[14] C.Arnaboldi et al: CUORE: Cryogenic Underground Observatory for Rare Events, letter of intent to the Gran Sasso Scientific Committee and to the *Commissione Scientifica Nazionale II dell'INFN*, March 2001. C.Arnaboldi et al.: CUORE: a cryogenic underground observatory for rare events, hep-ex:0212053.

[15] D. N. Watt and R. N. Glover, Phyl. Mag. **7** (1962) 105.

[16] A. Alessandrello et al., Phys.Rev.Lett. **77** (1996) 3319.

[17] A. Bettini, Nucl. Phys. B (Proc.Suppl.) **100** (2001) 332.

[18] S. Ohya and T. Tamura, Nucl.Data Sheets **70** (1993) 531.

[19] R. B. Firestone, C. M. Baglin, and S. F. Chu, Tables of Isotopes (eighth edition), 1998 CD-ROM update.

[20] M. Bianchetti et al., Phys. Rev. C **56** (1997) R1675.

[21] O. Civitarese and J. Suhonen, Phys. Rev. C **64** (2001) 064312.

[22] W. Bambynek, Rev. Mod. Phys. **49** (1977) 77.

[23] N. Booth, B. Cabrera and E. Fiorini, Ann. Rev. Nucl. Part. Sci. **46** (1996) 471.

[24] S. Baker and P.D. Cousins., Nucl. Instrum. and Meth. 221 (1984) 437

[25] G.J. Feldman and R.D. Cousins, Phys. Rev. D57 (1998) 3873

[26] D.E. Groom et al., Europ. Phys. Journ. C15 (2000) 1

[27] A. Faessler et al., Journ. of Phys. G 24 (1998) 2139

[28] C. Barbero, J.M. Krmpotic, and D. Tadic, Nucl. Phys. A 650 (1999) 485

[29] S. Stoica and H.V. Klapdor-Kleingrothaus, Phys. Rev. C 63 (2001) 064304

[30] A. Faessler and F. Simkovic, Prog. in Part. and Nucl.Phys. 46 (2001) 233; F. Simkovic, P. Domin, and A. Faessler: Neutrinoless double beta decay of ^{134}Xe, arXiv:hep-ph/0204278 24 april 2002 , and references therein

[31] J. Engel, P. Vogel,and M.R. Zirnbauer, Phys.Rev.C 37 (1988) 731

[32] J. Engel, P. Vogel,X.D. Ji and S. Pittel, Phys.Lett.B 225 (1989) 5

[33] K. Muto, E. Bender, and H.V. Klapdor-Kleingrothaus, Z.Phys. A 334 (1989) 187

[34] J. Suhonen, J.D. Khadkikar, and A. Faessler , Phys.Lett.B 237 (1991) 8

[35] T. Tomoda, Rep.Prog. 54 (1991) 53

[36] O.K. Manuel, Proc. of the Int. Symp. on Nuclear Beta Decay and Neutrino, Osaka, Japan, World Scientific, Singapore,1986, p. 71; O.K. Manuel, J. Phys. G: Nucl. Part. Phys. 17, S221 (1991); J.T. Lee, O.K. Manuel and R.I. Thorpe, Nucl. Phys. A 529 (1991) 29 , and private communication by O.K. Manuel

[37] V.I. Tretyak and Yu.G. Zdesenko, Atomic Data and Nuclear Data Tables, 80 (2002) 83

[38] F. Piquemal et al: Start-up of the NEMO 3 experiment , hep-ph/0107005

[39] A. Alessandrello et al., Nucl. Phys. B (Proc. Suppl.) 87 (2000) 78

[40] G. Heusser, private communication.

[41] Admatechs Co. Ltd., Japan.

[42] V. Palmieri *et al.* "Electropolishing of seamless 1.5 GHZ OFHC copper cavities", Proceed. of the 7^{th} workshop on RF Superconductivity, Gif Sur Yvette, France 1995, B. Bonin ed., DIST CEA/SACLAY 96 080/1,**2**, 605. "Besides the standard Niobium bath chemical polishing"; Proceedings of the 10^{th} workshop on RF Superconductivity, Sept. 6-11 2001, Tsukuba, Japan, (2002) on press

[43] G.Pessina, A low noise, low drift, high precision linear bipolar (+/-10v) voltage supply reference for cryogenic front-end apparatus, The Review of Scientific Instruments,

[44] C.Arnaboldi, C.Bucci, O.Cremonesi, A.Fascilla, A.Nucciotti, M.Pavan, G.Pessina, S.Pirro, E.Previtali, M.Sisti, Low frequency noise characterization of very large value resistors, IEEE Transactioon Nuclear Science, vol.49, pp. 1808-1813, 2002.

[45] C.Arnaboldi, C.Bucci, J.W.Campbell, A.Nucciotti, M.Pavan, G.Pessina, S.Pirro, E.Previtali, C.Rosenfeld, M.Sisti, The programmable front-end system for cuoricino, an array of large-mass bolometers, IEEE Transaction Nuclear Science, vol.49, pp. 2440-2447, 2002.

[46] C. Arnaboldi and G. Pessina, A very simple base line restorer for nuclear applications, submitted to NIM A, July 2002.

[47] C. Arnaboldi and G. Pessina, A programmable calibrating pulse generator with multi-outputs and very high stability, submitted to the IEEE Nuclear Science. December 2002.

OPERA

METU, Ankara, Turkey
M. Guler, M. Serin-Zeyrek, P. Tolun, M.T. Zeyrek

LAPP, IN2P3-CNRS and Universit de Savoie, Annecy, France
A. Degre, D. Duchesneau, J. Favier, M. Lavy, H. Pessard

LAQUILA University and INFN, LAquila, Italy
P. Monacelli

Bari University and INFN, Bari, Italy
M. Ieva, M.T. Muciaccia, M. De Serio, S. Simone

IHEP, Beijing, China PR
S.L. Lu, J. Ren, S.J. Zhou

Humboldt University, Berlin, Germany
K. Winter

Bern University, Bern, Switzerland
K. Borer, J. Damet, M. Hess, U. Moser, K. Pretzl, T. Waelchli, M. Weber

Bologna University and INFN, Bologna, Italy
G. Giacomelli, G. Mandrioli, L. Patrizii, P. Serra, M. Sioli, G. Sirri

IIHE (ULB-VUB), Brussels, Belgium
G. Van Beek, P. Vilain, G. Wilquet

JINR, Dubna, Russia
D. Bardin, I. Boudagov, G. Chelkov, Y. Gornouchkine, Z. Kroumchtein, A. Nozdrin, A. Olchevski, A. Sadovski.

LNF, Frascati, Italy
F. Bersani Greggio, B. Dulach, A. Franceschi, F. Grianti, A. Paoloni, M. Spinetti, F. Terranova, L. Votano

LNGS, Assergi, Italy
C. Gustavino

Toho University, Funabashi, Japan
S. Ogawa, H. Shibuya

Mrkische Fachhochschule FB Elektrotechnik, Hagen, Germany
K. Schauties, H. Sohlbach, H. Woltersdorf

Israeli group c/o Technion, Haifa, Israel
J. Goldberg

Hamburg University, Hamburg, Germany
C. Ballhausen, F.-W. Buesser, J. Ebert, B. Koppitz, B. Naroska, W. Schmidt-Parzefall, R. van Staa, R. Zimmermann

Shandong University, Jinan, Shandong, China PR
C.F. Feng, Y. Fu, M. He, J.Y. Li, L. Xue

Aichi Educational University, Kariya, Japan
K. Kodama, N. Ushida

Kobe University, Kobe, Japan
S. Aoki, T. Hara

IPNL, IN2P3-CNRS and Universit C. Bernard Lyon I, Villeurbanne, France
L. Chaussard, Y. Dclais, C. Heritier, S. Katsanevas, I. Laktineh, J. Marteau, G. Moret

INR, Institute for Nuclear Research of the Russian Academy of Sciences, Moscow, Russia
S. Gninenko, N. Golubev, M. Kirsanov, V. Matveev, A. Toropine

ITEP, Moscow, Russia
A. Artamonov, P. Gorbounov, V. Khovansky, I. Tikhomirov, Y. Zaitsev

Mnster University, Mnster, Germany
P. Boschan, N. Bruski, D. Frekers

Nagoya University, Nagoya, Japan
K. Hoshino, M. Komatsu, M. Miyanishi, M. Nakamura, T. Nakano, K. Niwa, O. Sato, T. Toshito

"Federico II" University and INFN, Naples, Italy
M. Ambrosio, S. Buontempo, N. D'Ambrosio, G. De Lellis, G. De Rosa, F. Di Capua, P. Migliozzi, C. Pistillo, L. Scotto Lavina, G. Sorrentino, P. Strolin, V. Tioukov

Neuchatel University, Neuchatel, Switzerland
J. Busto, M. Hauger, J. Janiscko, F. Juget, J-L. Vuilleumier, J-M. Vuilleumier

Institute of Nuclear Power Engineering, Obninsk, Russia
S. Aplin, V. Galkine, V. Saveliev, M. Zaboudko

LAL, IN2P3-CNRS and Universit Paris-Sud, Orsay, France
J. Boucrot, J.E. Campagne, A. Cazes, A. Lucotte, J.P. Repellin

Padova University and INFN, Padova, Italy
R. Brugnera, F. Dal Corso, S. Dusini, C. Fanin, A. Garfagnini, L. Stanco

"La Sapienza" University and INFN, Rome, Italy
P. Righini, G. Rosa

Fachbereich Physik der Universitaet Rostock, Rostock, Germany
M. Beyer, H. Schroeder, R. Waldi, R. Zimmermann

Salerno University and INFN, Salerno, Italy
E. Barbuto, C. Bozza, G. Grella, G. Romano, S. Sorrentino

Sofia University, Sofia, Bulgaria
D. Kolev, R.Tsenov

IRES, IN2P3-CNRS and Universit Louis Pasteur, Strasbourg, France
R. Arnold, E. Baussan, M. Dracos, J.L. Guyonnet, J.P. Engel, B. Dorion

Utsunomiya University, Utsunomiya, Japan
Y. Sato, I. Tezuka

Rudjer Boskovic Institute (IRB), Zagreb, Croatia
K. Jakovcic, A. Ljubicic, M. Stipcevic

Abstract

The OPERA experiment has been designed for an appearance search of $\nu_\mu \leftarrow \nu_\tau$ oscillations in the parameter region indicated by Super-Kamiokande as the explanation of the zenith dependence of the atmospheric neutrino deficit. OPERA is a long baseline experiment being constructed at the Gran Sasso LAboratory in the CNGS neutrino beam from the CERN SPS. The detector design is based on a massive lead/nuclear emulsion target. Nuclear emulsion are used as high resolution tracking devices, fort the direct observation of the decay of the τ leptons produced in ν_τ charged-current interactions. Electronic detectors located the event in the emulsions. Magnetized iron spectrometers measure charge and momentum of muons. The discovery potential of OPERA originates from the observation of a ν_τ signal with very low background level. The direct observation of $\nu_\mu \leftarrow \nu_\tau$ app earance will constitute a milestone in the study of neutrino oscillations. The OPERA experiment will also search for $\nu_\mu \leftarrow \nu_e$ with a sensitivity a factor two better than current limits from CHOOZ.

1 Design principles

The OPERA experiment is designed for the direct observation of ν_τ appearance from $\nu_\mu \leftrightarrow \nu_\tau$ oscillations in the CNGS long baseline beam from the CERN SPS to the Gran Sasso Laboratory. The measurements of neutrino fluxes performed by the Super-Kamiokande experiment indicate a deficit of muon neutrinos and an anomaly in their zenith angle distribution, consistent with $\nu_\mu \leftrightarrow \nu_\tau$ oscillations with $\Delta m^2 \approx 1.8 \div 4 \times 10^{-3}$ eV^2 (90% C.L.) and full mixing. The MACRO and Soudan2 experiments made observations compatible with this result. Recently the K2K experiment obtained, by using a ν_μ beam produced at KEK and direct toward the 250 km far Super-Kamiokande detector, indications of neutrino oscillations: a reduction of ν_μ flux together with a distortion of the energy spectrum. Therefore, the primary goal of OPERA is to obtain direct evidence for ν_τ appearance, which would confirm the oscillation hypothesis.

Although the detector has been not optimized to search for $\nu_\mu \leftrightarrow \nu_e$, OPERA is also sensitive in searching for such sub-leading oscillations thanks to the very good electron identification of the ECC technique. In case of null observation, the sensitivity correspond to a limit $\sin^2 2\theta_{13} < 0.06$ at 90% C.L.

A long baseline (732 km) between the neutrino source (the CERN beam line) and the detector (located in the underground Gran Sasso Laboratory) allows to be sensitive to the oscillation parameters indicated by the Super-Kamiokande data. The CNGS neutrino beam has been optimized for the detection of ν_τ charged-current (CC) interactions and provides an average ν_μ energy of about 20 GeV. For the evaluation of the experiment an integrated fluency of 2.25×10^{-3} protons on target is assumed, corresponding to a 5 years SPS operation in a shared mode.

The main principle of the ν_τ search in OPERA is the "direct" detection of the decay of the τ lepton produced by CC interactions. This is achieved by a massive (about 1.8 Kton) neutrino target based on the ECC design which combines, in a sandwich-like cell, the high precision tracking capabilities of nuclear emulsion (giving a space resolution of a fraction of micron) and the large target mass provided by lead plates (1 mm thick). This technique has been recently demonstrated to be effective for τ detection by the DONUT Collaboration.

The basic element of the target structure is the "brick", composed by a consecutive series of individual cells with transverse dimensions of 10.2×12.7 cm^2. Bricks are arranged into planar structures ("walls"), which are interleaved with electronic tracker planes (see Figure 1). These planes are built from vertical and horizontal strips of plastic scintillator, 2.6 cm wide. The main purpose of the electronic target tracker is to localize the particular brick in which the neutrino interaction occurred, once an interaction trigger is recorded. In the past year a new emulsion detector, the so-called Changeable Sheet (CS), has been proposed and included in the final design of the experiment. It has a twofold purpose: to help in the identification of the brick where the neutrino interaction occurred and to reduce the emulsion scanning load. After the CS has been removed and scanned, the appropriate brick is extracted for the emulsion development and scanning in a quasi-online sequence. Large emulsion areas can be scanned with automatic microscopes equipped with fast track recognition processors. Charged particle momenta are measured from their multiple scattering in the brick and electron and gamma energies from shower development.

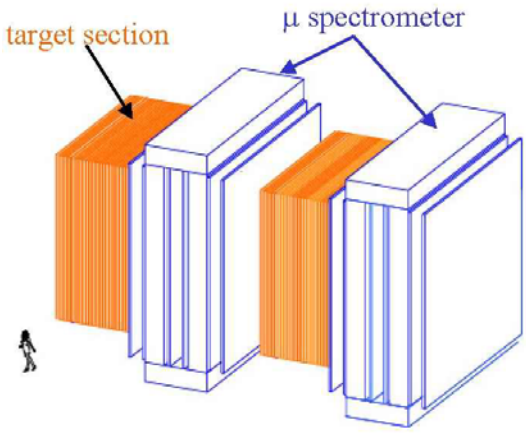

Figure 1: View of the OPERA detector composed of 2 super modules, each consisting of a target section and of a muon spectrometer.

The target and the tracker sections are further arranged into two independent super-modules (see Figure 1). Each super-module is followed by a downstream muon spectrometer. A spectrometer consists of a dipolar magnet made of two iron walls, and is equipped with vertical drift tube plane trackers. Planes of RPC's are inserted in gaps between the magnet iron plates, to allow a coarse tracking inside the magnet and a measurement of the stopping particles.

The OPERA design is optimized to achieve a very low background levels for the τ appearance search. The experiment aims at the analysis of all single-prong τ decay modes (e, μ, h). Signal events are classified as "long" or "short" decays depending whether the τ track traverses an emulsion sheet or not. The main background sources are charm production in CC interactions, hadronic interactions in lead and large angle muon scatterings. These events are rejected by the identification of the primary lepton in CC interactions and either by requiring the presence of a τ-like kink topology (long decays) or by an impact parameter method (short decays). In addition, a kinematic analysis is used to enhance the signal to background ratio. Overall, a total background of about 0.5 events is expected in five years run. If $\nu_\mu \leftrightarrow \nu_\tau$ oscillations occur, the average number of detected events ranges from 6 at $\Delta m^2 = 1.8 \times 10^{-3}$ eV^2 to 30 at $\Delta m^2 = 4 \times 10^{-3}$ eV^2. The achieved sensitivity at 90% C.L. covers the region of parameter space allowed by the Super-Kamiokande data. Within this region, the probability to obtain a statistical significance on the detected signal of at least 4σ (gaussian equivalent) is larger 90% after 5 year run.

Since the submission of the Status Report in 2001 the sensitivity has been improved and further studies are still in progress and we expect to finalize these calculations by the end of 2003.

2 Activity at the LNGS

2.1 Emulsion laboratories and tests at Gran Sasso

During the year 2002 the activity at the Gran Sasso has been focused on two major items: the set-up of emulsion handling facilities, which are expected to be operational in the near future during the installation and later on during the data taking, and the measurements both of the background in the sites which will be devoted to the emulsion storage and of the flux and the angular distribution of the cosmic rays. Furthermore, small laboratories for emulsion tests inside and outside the cavern, already set-up and operational, were upgraded.

The planned activities at the Gran Sasso, listed as a function of the scheduled implementation time, are:

1. the storage of emulsion plates under shielding. This activity will start soon after the emulsion film production at the Fuji Company (early in 2003) and the "refreshing procedure" (i. e. high humidity/temperature treatment) performed at the Tono Mine in Japan;

2. the installation and tuning of the Brick Assembly Machine (BAM);

3. the preparation of a clean area and a small development laboratory in the cavern, devoted to the detachment and processing of Changeable Sheets. We expect a rate of about 50 CS removed per day in the steady stage of data taking;

4. the construction of a cosmic-ray exposure pit, hosted in the surface Lab, to expose extracted bricks to cosmics in order to collect straight tracks useful for the emulsion film alignment inside the brick. A suitable Fe shielding is applied in order to suppress the electromagnetic, hadronic and the soft muon components;

5. the preparation of a large laboratory at the surface Lab, devoted to the dismantling and the development of about 50 bricks per day.

Results achieved in 2002 on the above items are reported below, including the corresponding test activities when appropriate.

2.1.1 Emulsion storage

During the past year, with the substantial help and advice from LNGS staff, the area assigned to the emulsion storage under shielding has been located at the entrance of the Hall B, where the gas system for the MACRO experiment was previously located. This area will be soon fully evacuated and rearranged.

The presence of gamma background in the cavern has been studied by setting-up on site radioactivity counters, with and without a 5 cm Fe shielding (courtesy of Dr. M. Laubenstein and Dr. M. De Deo, LNGS). It turned out that such a moderate shielding was already suitable for a substantial reduction (up to a factor of about 20) of the low-energy tail of the gamma/Compton activity, while for the high-energy peaks of the various Rn daughters it was strongly advised to apply fresh air recirculation.

Following these results, the storage area was designed as a stand-alone single room, of about 60 m^2, 2.80 m high, shielded with 5 cm Fe all around, with a shielded double entrance, to allow very compact storage and any first-in first-out handling of the emulsion boxes. Indeed, the expected monthly delivery rate is in the range of a few cubic meters, and compact pile-up will go on in the years 2003-2005, until the starting of the BAM operation, that will progressively evacuate the area. The same storage place will be used during the neutrino run to keep in stand-by the bricks selected by the trigger and not yet confirmed by the CS scanning.

Shielding is needed to limit to the minimum extent the pile-up of background. The latter will be also mitigated by some fading of the recorded latent image. A high temperature would be beneficial for that. On the other hand, it is much more important to keep it lower in order to avoid exceeding growth of the so-called fog, that is the diffused uncorrelated random grain noise. A value of the temperature in the range of 10 to 15 deg was selected for storage. There is no need for special air conditioning given the position of the storage site and the fresh air inlet.

The setting up of the area for the storage of the emulsion plates will be finalized in 2003.

2.1.2 Preparation of the BAM site

The BAM complex will be located in the by-pass corridor between the Hall B and the Hall A. A detailed project for area cleaning and reshaping, and of the housing of instrumentation inside separate sectors with specific clean- class and dark-room was designed in 2002, with the close cooperation of OPERA members and LNGS staff. The area will be cleaned up and made available early in 2003.

2.1.3 Emulsion processing in the cavern

The CS detector was added to the OPERA design in the year 2002, bringing improvements in the expected performances. A dedicated processing line in the cavern, much smaller size compared to the several (automatized) lines devoted to the brick processing at the surface Lab (see Section 2.1.5), has to be arranged to deal with CS. It turned out that, if conveniently upgraded, the existing test facility will be suitable for this purpose. Thus, such a test laboratory, fully operational also in 2002, is actually playing a multi-purposes role, as a vital infrastructure for the cosmic ray and radioactivity tests, as a prototype line to define and tune the future full-scale operation, and as a laboratory that will smoothly evolve into the CS processing station.

The present equipment, as assembled and upgraded during the last months, consists of a complete set of tanks, racks and tools to deal with the whole spectrum of safe-light dark-room operations with nuclear research emulsion plates.

An important step, still in progress, has been to bring and set-up at LNGS also a small refreshing facility, similar to the one successfully exploited for test-beams at CERN. It will be also soon possible to prepare full-size bricks manually assembled.

2.1.4 Cosmic ray pit and test exposures

A facility for cosmic ray exposures, featuring a reversed-telescope Fe structure allowing to host either emulsion packages or scintillators, was prepared at the surface Lab during 2002. The modular Fe slabs allowed to collect data after various Fe shielding thickness, ranging from 25 to 100 cm.

Both counting rates and angular distributions were made available by test exposures performed during 2002. Preliminary data were compared with a full Monte Carlo code developed within the MACRO Collaboration. Consequently, the design of the cosmic-ray pit has been fully defined, with about 50 cm Fe thickness at a depth of 8 m below ground, and a diameter of about 2 m. Under these conditions, we expect to collect a few penetrating tracks/mm^2 in a 1-2 day exposure within 300 mrad from the vertical direction. The analysis of the emulsion films exposed is in progress and will be finalized by this year. The tuning of the optimized integral flux and of the complete alignment procedure with full-size bricks will be further explored as soon as the pit will be built in the year 2003.

2.1.5 Emulsion handling on the surface

The executive design of the new building was defined in the 2002, with the very good co-operation between OPERA members and LNGS staff Engineers. As a result, the project, to be realized in the years 2003-2004, incorporates since the very beginning optimized functions and logistics for the part assigned to the OPERA project. The new building will host, mainly at the below-ground floor, the large-scale emulsion development laboratory. A dedicated access to the cosmic-ray pit, to be excavated at a few meter distance from the building, is foreseen.

2.2 RPC handling and tests at the LNGS

During the year 2002 the RPC (Resistive Plate Chamber) project for the OPERA experiment underwent a fundamental development inside the laboratories. The major result was the setting up of a full test facility in the Lab2 building, which is by now fully dedicated to the mass test of the roughly 1000 RPC detectors to be eventually installed in OPERA.

At the beginning of January the mechanical structure of the two vertical trigger walls (4×4 m^2 each) has been built under the supervision of the LNGS mechanical workshop. The two walls have been equipped with 128 glass RPC. This will correspond to quite a large amount of this new kind of detectors whose setup, use and study are intrinsically interesting.

The mechanical workshop of the laboratories have been also involved in the construction of a special table (1.25×3.00 m^2), which is used to test the reliability of the RPC detectors (the "pushing" test). The table is fully automated and checks the gluing of the detectors on a 10 cm basis. Other minor works have also been committed to the mechanical workshop related to the system test facility.

The electronics workshop dedicated a large amount of time to the system test. Their people adapted electronics cards from Macro experiment and new one for timing read-

out. The trigger walls with glass RPC correspond to roughly 1000 channels with digital and timing read-out for both the vertical coordinates. The Bakelite RPC for OPERA under test amounts to 36 detectors at a time, corresponding to roughly other 2000 digital channels. The latter electronics has also been developed at Gran Sasso.

The arrangements of the Lab2 building include a completely new distribution gas system with 4 distribution points, safety control alarms. Several services from the laboratories have been obviously involved. The gas system is now ready to be used for the starting of the test which is foreseen in February 2003.

The involvement of the Gran Sasso Laboratories corresponds to the nomination of a people from them as Test Coordinator, to be responsible of the whole test facility together with a Test Supervisor.

Concerning the RPC production the laboratories have been a key location for the provisional storage of the Bakelite planes. Bakelite planes have been first transported in Gran Sasso, visually inspected and then delivered to the assembling company. Storage of Bakelite is very important to keep humidity and temperature under control for the stability of the RPC response. The Gran Sasso laboratories finally housed one of the long term tests of the RPC for OPERA. People from Frascati and Padova contributed to these tests together with Gran Sasso physicists. Important results were obtained concerning aging and response stability.

THEORY GROUP

R.Aloisio, Z.Berezhiani, V.Berezinsky, G. Di Carlo, A.F.Grillo, A.Galante, M.Narayan, F.Vissani.

The activity of the group in year 2001 has concerned research in three fields: Astroparticle Physics, Particle Phenomenology and Computer simulations of Lattice Gauge Theory. The activities are more specifically reported below.

1 Astroparticle Physics

The Astroparticle group of LNGS in 2002 included R.Aloisio, V.Berezinsky, M.Narayan, F.Vissani and visitors V.Dokuchaev (Institute for Nuclear Research, Moscow), B.Hnatyk (Lviv University, Ukraine), S.Grigorieva (Institute for Nuclear Research, Moscow) and O.Petruk (Lviv University, Ukraine). The group worked in close collaboration with A.Vilenkin (Tufts University, USA), M.Kachelriess (CERN), P.Blasi (Firenze), G.Senjanovich (ICTP), A.Strumia (Pisa University) and others.

Scientific work

The main field of the work is astroparticle physics, including solar neutrinos, physics in underground detectors, massive neutrinos, ultra high energy cosmic rays, topological defects, and relativistic astrophysics. From several works finished in 2002 two following results can be mentioned.

V.Berezinsky, M.Kachelriess and S.Ostapchenko have demonstrated that similar to QCD cascade, the electroweak cascade can develop if initial energy is larger than $\sqrt{s} > 10^6$ GeV. Electroweak cascade is studied in the broken SU(2) model of weak interaction. The results can be generalized to an arbitrary spontanrously broken gauge group. The smallness of electroweak coupling constant is compensated by large logarithms for soft and collinear emission. The results are applied to superheavy ($m_X > 10^6$ GeV) particle decay. An interesting application to UHECR is related to the case when at tree level superheavy particle is coupled only to neutrinos. Due to EW cascading all partons appear in the cascade, and thus this mode of the decay produces the normal e-m cascade on CMB radiation.

F.Feruglio, A.Strumia and F.Vissani (hep-ph/0201291) using the oscillation data and techniques of statistical analysis have obtained prediction for the parameter of neutrinoless double beta decay m_{ee}. If neutrinos have 'normal hierarchy', the 90 % CL range is $m_{ee} = 1.1 - 4.1$ meV; if they have 'inverted hierarchy', $m_{ee} = 14 - 57$ meV. The existing bound implies that neutrinos must be lighter than 1.0 eV at 90 % CL: such a bound is competitive with the one from direct search for neutrino mass (tritium endpoint).

Conferences

F.Vissani works (together with O.Palamara) as the organizer of the LNGS seminar, he was one of organizers of the Summer Institute in LNGS and Summer school on astroparticle physics at ICTP, convener of the theory session on Double beta decay meeting in LNGS.

V.Berezinsky and F.Vissani as editors prepared the Proceedings of 5th Topical LNGS workshop "Solar neutrinos: where are the oscillations?"

R.Aloisio gave an invited talk at Aspen winter meeting on ultra high energy particles.

V.Berezinsky participated as invited speaker in European Cosmic Ray Symposium (Moscow), Texas Symposium (Florence), Dark Matter 2002 (Cape Town), Sakharov Conference (Moscow), High Energy Neutrino School (Les Houches), Astroparticle Physics School (Les Houches), INFN Neutrino School (Varenna).

F.Vissani presented invited talks at Congresso di Fisica Teorica di Cortona, at Neutrino workshop in Padova, at Workshop on neutrino news in Fermilab and at the Summer school on astroparticle physics at ICTP.

Journal and Proceedings publications of 2002

1.R.Aloisio and P. Blasi "Theory of synchrotron radiation. 1. Coherent emission from ensembles of particles" Astrop. Physics 18, (2002) 183

2.R.Aloisio and P. Blasi "Theory of synchrotron radiation. 2. Back reaction in ensembles of particles" Astrop. Physics 18, (2002) 195

3. V.Berezinsky, M.Kachelriess and S.Ostapchenko "Electroweak jet cascading in the decay of superheavy particles" Phys. Rev. Lett. 89 (2002) 171802

4. V.S.Berezinsky and V.I.Dokuchaev "High energy neutrinos from collapsing galactic nuclei" Nucl. Phys. Proc. Suppl. 110 (2002) 522

5.V.Berezinsky, M.Kachelriess and S.Ostapchenko "Extensive air showers from ultra high energy gluinos" Phys. Rev. D 65 (2002) 083004

6. V.Berezinsky "Exact analysis of the combined data of SNO and SuperKamiokande" Astrop. Physics 17 (2002) 509

7. A.Strumia and F.Vissani "Massive neutrinos and theoretical developments" Int. J. Mod. Phys. A17 (2002) 1755

8. A.Strumia, C.Cattadori, N,Ferrari and F.Vissani "Which solar neutrino data favor the LMA solution?" Phys. Lett. B 541 (2002) 327

9. F.Ferruglio, A.Strumia and F.Vissani "Neutrino oscillations and signals in beta and 0NU2beta experiments" Nucl. Phys. B 637 (2002)

10. F.Vissani (in LVD collaboration) "Effects of neutrino oscillations on the supernova

signal in LVD" Nucl. Phys. Proc. Suppl. 119 (2002) 410 11. F.Vissani "A coherent picture of massive neutrinos emerging?" Proc. of 9th Marcel Grossman meeting on general relativity (eds. R.Ruffini et al), World scientific 2425 (2002)

Preprints of 2002

1. R.Aloisio, P. Blasi, A. Galante, P.L.Ghia, A. F. Grillo "Detectability of space-time fluctuations in ultra figh energy cosmic ray experiments" astro-ph/0210402

2. R.Aloisio P. Blasi and A. Olinto "Gamma-ray constraints on neutralino dark matter clumps in the galactic halo" astro-ph/0206036

3. R.Aloisio, P. Blasi, A. Galante, P.L. Ghia and A. F. Grillo "Space time fluctuations and ultra high energy cosmic ray interactions." astro-ph/0205271

4. V.Berezinsky, M.Narayan and F.Vissani "Mirror model for sterile neutrinos." hep-ph/0210204

5. V.Berezinsky, A,Gazizov and S.Grigorieva "Signatures of AGN model for UHECR" astro-ph/0210095

6. V.Berezinsky (in LVD collaboration) "Study of single muons in LVD at Gan Sasso Laboratory" hep-ex/0202006

7. V.Berezinsky,A.Z.Gazizov, S.I.Grigorieva "On astrophysical solution to Ultra High Energy Cosmic Rays." hep-ph/0204357

8. B.Bajc, G.Senjanovic and F.Vissani "B-Tau unification and large atmospheric mixing: a case for noncanonical seesaw." hep-ph/0210207

The papers 1 and 3 of the preprint list refer to an ongoing activity concerning the search for effects of modifications of relativistic invariance (as those implied by many Quantum Gravity Theories) detectable in Ultra High Energy Cosmic Ray interactions. This activity involves theorists of the laboratory (R. Aloisio, A. F Grillo), of the L' Aquila University (A. Galante), of Firenze (P. Blasi) and of P.L. Ghia (experimentalist, Torino and LNGS).

2 Particle Phenomenology

The particle phenomenology group which included Z. Berezhiani, P. Ciarcellutti, L. Gianfagna and A. Galante, worked in close collaboration with A. Rossi (Padova), A. Drago, F. Frontera (Ferrara), R.S. Raghava (AT&T Bell Labs), I. Kogan (Oxford), L. Bento (Lisbon) and others.

Scientific work

The main field of the groups activity is the particle phenomenology, including neutrino physics, supersymmetry and grand unification, flavour problem and CP violation, and on particle astrophysics and cosmology. From works of 2002 the following results can be mentioned.

Z. Berezhiani and A. Rossi have analysed the present limits on the non-standard interactions of neutrinos to electrons and showed that reasonable limits on the electron and taon neutrino couplings can be obtained from the LEP limits on the $e^+e^- \to \nu\bar{\nu}\gamma$ reaction cross section. The same autrors, in collaboration with R.S. Raghavan, have studied the implications of the non-standard neutrino interactions for the solar neutrino signals, in particular, for Borexino detector, and have showed that the analysis of the recoil electron spectrum from the solar ^{7}Be neutrinos can provide limits on these interactions stronger than the present experimental limits from reactor and accelerator neutrinos.

Z. Berezhiani and L. Bento have suggested a new mechanism for primordial baryogenesis and dark matter production based on the concept of the hidden mirror sector of particles. Namely, non-zero lepton and thus B-L numbers in the Universe can be generated by out-of-equilibrium scattering processes which transform ordinary leptons and Higgses into their hidden partners, and B-L will be partially reprocessed into baryon asymmetry via the sphaleron effects. On the other hand, the same scatterings generate analogous asymmetry in mirror sector and thus mirror baryons can constitute dark matter, with implications for the large scale structures, CMB anisotropies, microlensing, etc.

Z. Berezhiani, A. Gorsky and I. Kogan have suggested that the time coordinate can emerge as a result of deconstruction, starting from Euclidean gauge field theory in 3 dimensions based on the chain product of the identical gauge groups $G_1 \times G_2 \times ...G_N$ with the Higgs in a mixed representations between the neighbour gauge factors.

Participation in conferences

Z. Berezhiani presented invited talks at
Les Houches Winter School on *High Energy Neutrino Astrophysics,* Les Houches, France, 25-26 Jan 2002
Int. Conf. *"Quarks 2002"*, Novgorod, Russia, 1-5 June 2002
XIV Rencontres de Blois *"Matter-Antimatter Asymmetry"*, Blois, France, 16-22 June 2002
"Channel Meeting on Theoretical Particle Physics", Plymouth, UK, 20-24 Oct 2002
Int. ISPM Workshop on *Gravitation and Cosmology*, Tbilisi, Georgia, 9-13 Sept. 2002
Int. Worskhop on High Energy Physics *"80 Anniversary of K.A. Ter-Martirosian"*, ITEP, Moscow, 1-2 Oct. 2002

Publications

[1] Zurab Berezhiani, Anna Rossi, "Limits on the nonstandard interactions of neutrinos from e^+e^- colliders." Phys. Lett. B535, pp. 207-218, 2002

[2] Zurab Berezhiani, R.S. Raghavan, Anna Rossi, "Probing nonstandard couplings of

neutrinos at the Borexino detector." Nucl. Phys. B638, pp. 62-80, 2002

[3] Luis Bento, Zurab Berezhiani, "Baryon asymmetry, dark matter and the hidden sector." Fortsch. Phys. 50, pp. 489-495, 2002

[4] Zurab Berezhiani, R.S. Raghavan, Anna Rossi, "Non-standard neutrinos interactions after SNO: the perspectives of Borexino." Proc. Int. Workshop "Neutrino oscillations" (Venice, 24-26 July 2001), Ed. M. Baldo-Ceolin, 2002, pp. 139-154

[5] Z. Berezhiani, A. Gorsky, I. Kogan, "On the deconstruction of time." JETP Lett. 75, pp. 530-533, 2002 [Pisma Zh. Eksp. Teor. Fiz. 75, pp. 646-650, 2002]

[6] Z. Berezhiani, I. Bombaci, A. Drago, F. Frontera, A. Lavagno, Gamma ray bursts from delayed quark deconfinement phase transition in neutron stars." Nucl. Phys. Proc. Suppl. 113, pp. 268-274, 2002; Proc Int. Conf. "Particle and fundamental physics in space" 14-19 May 2002, La Biodola, Italy

[7] Z. Berezhiani, I. Bombaci, A. Drago, F. Frontera, A. Lavagno, "Gamma-ray bursts from delayed collapse of neutron stars to quark matter stars" e-Print Archive: astro-ph/0209257, accepted in Astrophys. J. (in press)

3 Computer Simulations of Lattice Gauge theories

The activity of the group involved G. Di Carlo, A. Galante (L' Aquila) and V. Azcoiti and V. Laliena (University of Zaragoza, Spain).

The activity performed during 2002 is a continuation of earlier studies and concerned in particular a new method for simulations of actions with a topological term (θ term) and its application to two-dimensional models. This method, based on a new technique for the reconstruction of the probability distribution function for the topological order parameter, has been tested succesfully on analytically solvable models for which earlier attempts of simulation failed. A paper with the description of the method and the results obtained have been published in Phys. Rev. Lett. [1].

We have applied this method to the two-dimensional models CP^3 and CP^9 which shares with QCD many similarities (confinement, asymptotic freedom, possibility of 1/N expansion etc...): a letter with the results is in advanced writing. Two contributions on this subject have been presented to the Lattice 2002 Conference.

In parallel with the application of this method we have continued in the developing of new approaches to the problem; we believe that a multiple methods view have a great advantage in controlling systematical errors that can arise in a hard to estimate amounts from the fitting procedures that are intrinsic in the evaluation of the probability distribution function of the order parameter. A second way to look to the same problem has been already developped and his potentialities are currently under investigation.

Moreover we have extended the first method to cope with simulations of QCD at non zero barionic density. Some preliminar results for the SU(2) case have been obtained.

Finally we are performing a study of the chiral transition in QCD with dynamical fermions using the approach of the probability distribution function of the order parame-

ter. To this end a fairly large number of gauge field configuration has been generated on the APE machine, using a TAO code for dynamical fermions borrowed from the Pisa APE group. These configurations have been fully diagonalised on the PC cluster of LNGS-GrIV and the final analysis is under way.

Journal and Proceedings publications of 2002

[1] Vicente Azcoiti, Giuseppe Di Carlo, Angelo Galante, Victor Laliena; "New proposal for numerical simulations of theta-vacuum like systems". Phys.Rev.Lett. 89 (2002) 141601.

ERMES

Wolfango Plastino[a,b], Matthias Laubenstein[c],
Giuseppe Etiope[d], Paolo Favali[d]

[a] Department of Physics, University of Roma Tre,
via della Vasca Navale, 84, I-00146, Rome (Italy)
[b] National Institute for Nuclear Physics, Section Rome III,
via della Vasca Navale, 84, I-00146, Rome (Italy)
[c] National Institute for Nuclear Physics, Underground Laboratories of Gran Sasso,
S.S.17bis km 18+910, I-67010, Assergi (AQ) (Italy)
[d] National Institute for Geophysics and Volcanology, RIDGE unit
Roma 2 Department, via di Vigna Murata, 605, I-00143, Rome (Italy)

Abstract

The Environmental Radioactivity Monitoring for Earth Sciences (ERMES) research project has the following topics: a) correlations between the variations of radon with the strain processes of the rock [1],[2],[3] and transport properties related to the groundwater geochemistry [4]; b) radiocarbon and tritium high precision liquid scintillation spectrometry [5]; c) new devices development for nuclear spectrometry analyzing the light-yield properties of different scintillator crystals under extreme physical-chemical environmental conditions for geophysical prospecting and investigations for the volcanology, seismology and oceanography [6]. In this report we show the preliminary environmental radioactivity analysis on sea-water samples collected by GEOSTAR deep-sea observatory. The data seem to point out a mixing of water mass characterizing the dynamic interface between lithosphere (seabed) and ocean (sea-water).

1 Introduction

The Benthic Boundary Layer (BBL) is the dynamic interface between lithosphere (seabed) and ocean (sea-water) where many physical, geochemical and biological processes occur playing an important role in environmental global changes. Geohazards, carbon cycle, heat flow, life generation, climatic oceanography, are only some examples of local or global processes whose comprehension is today limited due to the lack of data related to the deep ocean floors. Lithospheric processes at the BBL impact the marine environment at different temporal and spatial scales. Earthquakes produce short-term effects (landslides and tsunamis) that threaten the lives and economy of coastal communities, while outgassing of greenhouse gases and mineral-rich fluids impact long-term global climates

and the formation of economically important mineral resources. The BBL has an important role on carbon cycle being either a potentially sinking or transition zone for carbon coming from shallower zones of from the lithosphere. Oil platforms are sited on the BBL, and cables and pipelines are lain across it. Delicate marine ecosystems have evolved in these extreme environment, yet it may be significantly affected by man's activities. The BBL dynamics however is not completely clear: it is not known how it is perturbed by energy and mass release from the seabed (seismicity, heat flow, gas diffusion, biological productivity, diagenetic reactions), what distances the particles and waves can be transported, what is the evolution and fate of bottom currents and storms. In this framework, the environmental radiocativity monitoring is a useful tool to better understand the BBL physical processes and its dynamics.

2 Experimental setup

GEOSTAR-2 (GEophysical and Oceanographic STation for Abyssal Research) is the first European deep-sea observatory for geophysical and environmental monitoring at seabed becoming operative in 2000. It was deployed in September 2000 from the Italian oceanographic ship Urania, in the southern Tyrrhenian Sea, between the Sicilian coast and the island of Ustica, at a depth of about 2000 m. This area was chosen as pilot test site being a key area for the Tyrrhenian seismicity and oceanography. After 206 days, in April 2001, the observatory was recovered. The sensors used for this mission (2 magnetometers, a prototype gravity meter, a hydrophone, a Doppler currentmeter, a single-point currentmeter, an automatic water sampler for laboratory geochemical analysis, a CTD and a transmissometer) were continuously controlled and managed by a data acquisition and control system able to transmit the data via surface buoy and radio or satellite link to onshore operators. This mission represented the longest lasting experiment using a complex module, with an intelligent unit, deployed at great depths. The environmental radioactivity measurements of the sea-water samples collected by GEOSTAR have been performed by High Purity Germanium (HPGe) coaxial detectors with characteristics summarized in Figures 1 and 2.

Each sea-water sample has been measured for about ten days using polyethylene box of 70 mm diameter and 30 mm height.

3 Results and Discussion

The spectrum of one sea-water sample is shown in Figure 3.

The environmental radioactivity analysis of the sea-water samples collected by GEOSTAR is shown in Figure 4.

In this preliminary step, the data seem to emphasize that GEOSTAR was able to observe environmental changes in the benthic boundary sea-water due to the interaction of lithosphere with a water mass moving vertically. This hypothesis may be confirmed by geochemical tracers as helium isotopes. These analyses are carring out and seem to justify this sea-water mixing also with the temperature and Doppler currentmeter data.

4 Conclusions

The physical properties of the BBL and its dynamics may be analyzed by multiparametric approach only. In this framework, the environmental radioactivity analysis of sea-water samples has a particular interst because it emphasizes, particularly, the mixing of water mass with different origin and better constrains the physical sources for the BBL dynamical processes. Then, the deep-sea observation and monitoring systems developed in the last decade, such as GEOSTAR, can contribute to cover a scientific gap on the oceanography physical of BBL.

Acknwoledgments The authors wish to dedicate this work to Dr. Giuseppe Smriglio unexpectedly died during this research activity. The authors are grateful to Prof. Alessandro Bettini for the his kind collaboration and Mr. Massimiliano De Deo of the LNGS for the useful and precious assistance.

References

[1] Plastino, W. et. al., Laboratori Nazionali del Gran Sasso, Annual Report from 1997 to 2001.

[2] Plastino, W. and Bella, F., 2001, *Radon groundwater monitoring at underground laboratories of Gran Sasso (Italy)*, Geophysical Research Letters, 28 (14), 2675-2678.

[3] Plastino, W., Bella, F., Catalano, P.G. and Di Giovambattista, R., 2002, *Radon groundwater anomalies related to the Umbria-Marche September 26, 1997 earthquakes*, Geofisica Internacional, 41(4), 369-375.

[4] Caputo, M. and Plastino, W., 2003, *Diffusion with space memory*, in "Geodesy, the challenge of the 3rd millenium", eds.: Grafarend, E., Krumm, F. and Schwarze, V., Springer Verlag, Berlin-Heidelberg, 429-435.

[5] Plastino, W., Kaihola, L., Bartolomei, P. and Bella, F., 2001, *Cosmic background reduction in the radiocarbon measurements by liquid scintillation spectrometry at the underground laboratory of Gran Sasso*, Radiocarbon, 43 (2A), 157-161.

[6] Plastino, W., De Felice, P. and de Notaristefani, F., 2002, *Radon gamma-ray spectrometry with YAP:Ce scintillator*, Nuclear Instruments and Methods in Physics Research, A, 486/1-2, 146-149.

Detector	volume [cm^3]	Relative efficiency	FWHM* [keV]
GePV p-type	225	56%	2.0
GeCris p-type	468	120%	2.0
GsOr p-type	414	96%	1.9

* FWHM of the *full energy peak* at 1332.47 keV for ^{60}Co.

Figure 1: Table. 1. Characteristics of the HPGe coaxial detectors.

Detector	Total background and for several radionuclides (counts/days)			
	(60–2700) keV	^{214}Bi (352 keV)	^{208}Tl (583 keV)	^{40}K (1461 keV)
GePV	951	5.3	4.1	6.3
GeCris	221	1.2	0.2	3.4
GsOr	980	5.1	1.7	8.4

Figure 2: Table. 2. Background of the HPGe coaxial detectors.

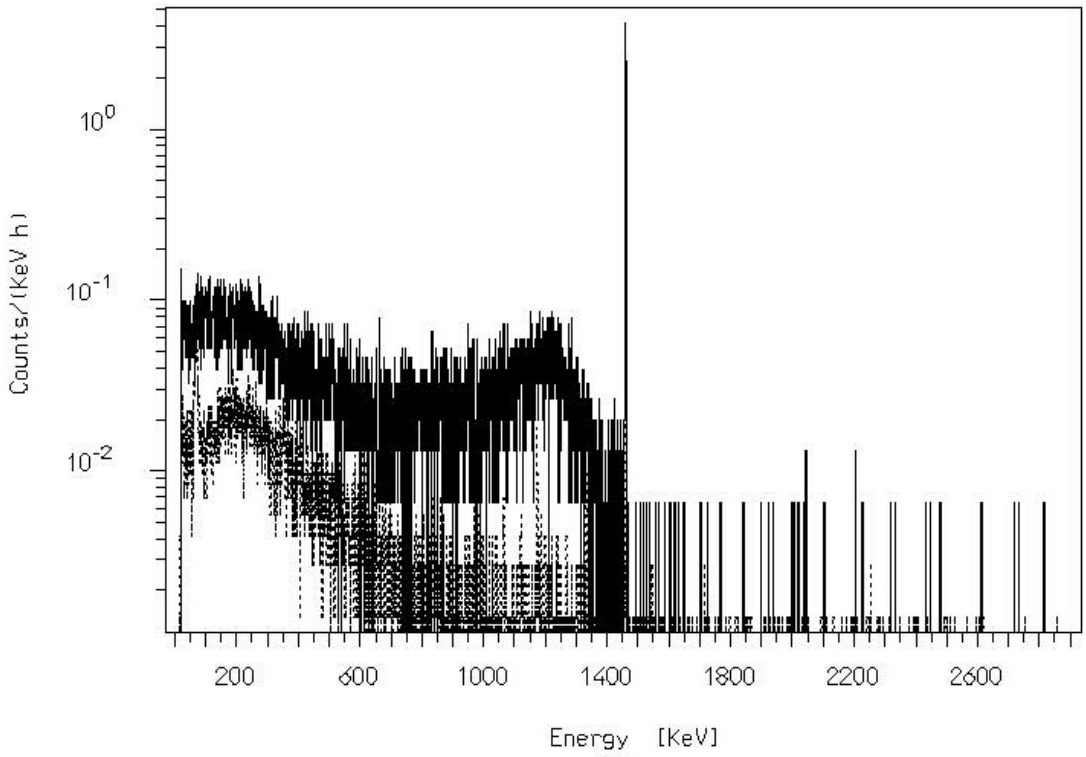

Figure 3: fig. 1. The spectrum of the sample n. 6 (solid line). The background of the HPGe (GeCris) detector is also showed (dashed line).

Sampl.	mass	^{226}Ra	^{234}Pa	^{235}U	^{228}Ra	^{228}Th	^{40}K	^{137}Cs	^{60}Co
	g	mBq/kg	mBq/kg	mBq/kg	mBq/kg	mBq/kg	Bq/kg	mBq/kg	mBq/kg
1	87,6	< 1,43E+1	< 1,07E+3	< 9,10E+0	< 2,15E+1	< 1,10E+1	12.8±1.3	8.1±4.1	< 9,40E+0
2	86,5	< 1,54E+1	< 1,09E+3	< 9,60E+0	< 2,43E+1	< 1,12E+1	13.2±1.3	< 6,50E+0	< 6,60E+0
3	62,5	< 3,05E+1	< 1,44E+3	< 2,01E+1	< 4,08E+1	< 3,57E+1	9.3±1.4	< 9,80E+0	< 1,12E+1
4	62,6	< 1,38E+1	< 8,94E+2	< 9,20E+0	< 2,21E+1	< 1,12E+1	12.7±1.3	9.6±3.9	< 6,20E+0
5	88,1	< 2,23E+1	< 1,48E+3	< 1,68E+1	< 2,79E+1	< 2,65E+1	11.3±1.6	< 7,20E+0	< 8,10E+0
6	80,2	< 1,43E+1	< 1,10E+3	< 9,50E+0	< 2,39E+1	< 1,21E+1	12.6±1.3	< 6,30E+0	< 7,30E+0
7	80,2	< 2,81E+1	< 1,81E+3	< 1,90E+1	< 3,73E+1	< 3,45E+1	10.9±1.6	< 9,50E+0	< 1,09E+1
8	80,8	< 1,36E+1	< 1,11E+3	< 8,60E+0	< 2,23E+1	< 1,06E+1	12.5±1.3	< 5,80E+0	< 6,30E+0
9	80,5	< 2,82E+1	< 1,94E+3	< 1,99E+1	< 4,27E+1	< 3,53E+1	11.7±1.7	< 1,00E+1	< 1,08E+1
10	82,0	< 1,57E+1	< 1,24E+3	< 9,40E+0	< 2,42E+1	< 1,54E+1	12.7±1.3	< 7,00E+0	< 7,60E+0
11	80,9	< 2,41E+1	< 1,33E+3	< 1,38E+1	< 3,16E+1	< 2,66E+1	11.3±1.6	< 1,08E+1	< 8,80E+0
12	81,8	< 2,05E+1	< 1,05E+3	< 1,23E+1	< 2,59E+1	< 3,19E+1	10.8±1.5	< 9,10E+0	< 7,10E+0
13	82,5	< 2,56E+1	< 1,51E+3	< 1,62E+1	< 3,36E+1	< 2,93E+1	10.8±1.5	< 8,30E+0	< 9,00E+0
14	89,0	< 1,25E+1	< 9,55E+2	< 8,20E+0	< 1,96E+1	< 9,70E+0	12.5±1.3	8.0±3.6	< 5,70E+0
15	89,3	< 2,15E+1	< 1,48E+3	< 1,53E+1	< 2,85E+1	< 2,76E+1	11.3±1.5	< 7,20E+0	< 8,60E+0
16	89,5	27.3±19.9	< 7,00E+2	< 9,40E+0	< 1,64E+1	< 1,74E+1	11.5±1.6	< 6,40E+0	< 5,10E+0
17	60,9	< 3,19E+1	< 1,40E+3	< 1,97E+1	< 4,13E+1	< 3,74E+1	10.0±1.5	< 9,80E+0	< 1,13E+1
18	57,5	< 1,65E+1	< 1,24E+3	< 1,13E+1	< 2,89E+1	< 1,75E+1	13.2±1.4	< 7,40E+0	< 8,20E+0
19	60,9	< 2,90E+1	< 1,18E+3	< 1,84E+1	< 3,70E+1	< 3,55E+1	10.7±1.5	< 9,50E+0	< 1,07E+1
20	57,5	< 1,55E+1	< 1,18E+3	< 1,01E+1	< 2,57E+1	< 1,35E+1	13.2±1.4	< 6,40E+0	< 7,00E+0
21	65,8	< 2,37E+1	< 9,89E+2	< 1,38E+1	< 3,04E+1	< 2,91E+1	10.9±1.5	13.9±6.7	< 8,00E+0
22	62,5	< 2,11E+1	< 1,13E+3	< 1,38E+1	< 3,73E+1	< 2,17E+1	12.4±0.4	< 9,70E+0	< 1,18E+1
23	63,4	< 2,10E+1	< 1,19E+3	< 1,36E+1	< 3,20E+1	< 2,07E+1	12.7±0.4	< 1,01E+1	< 1,24E+1

GeCris
GePV
GsOr
GeMPI

Figure 4: Table. 3. Environmental Radioactivity analysis of the sea-water samples collected by GEOSTAR

GIGS. The Interferometric Station at LNGS

Antonella Amoruso[a,c], Luca Crescentini[b,d,e]

[a] Dip.to di Fisica Univ. dell'Aquila, L'Aquila - Italy
[b] Dip.to di Scienze della Terra Univ. di Camerino, Camerino (MC) - Italy
[c] INFN - Gruppo collegato dell'Aquila, L'Aquila - Italy
[d] INFN - LNGS, L'Aquila - Italy [e] Spokeperson

Abstract

During 2002 strain data have been recorded continuously and a very-broad-band seimometer has been installed inside the interferometric station in October. We have identified a very plausible source of the slow events recorded in 1997 in a well known fault, located a few kms South of LNGS, which did not show any strong historical seismic activity.

1 Introduction

The interferometric station at LNGS consists of two 90-m long laser interferometers designed for geophysical purposes. Their azimuth are N66E and N24W, i.e. approximately perpendicular and parallel to the local direction of the Apennines. Instrumental configuration has changed since their first start up in 1994. ¿From May 1994 to October 1995 we have monitored the extension of a 90-m long baseline (azimuth = N66E), using a 20-cm long reference baseline (unequal-arm configuration). Since laser frequency fluctuations can give spurious signals whose amplitude depends on the difference in length between the two baselines, in order to check for their effects from December 1995 to October 1998 both arms were 90-m long and one component of shear strain was measured (equal-arm configuration). Some instrumental changes in 1999 allowed to measure extensions of the two baselines independently, so that now also areal strain can be obtained. Sampling frequency is 5 Hz.

In what follows, extensions are expressed as dimensionless strain, $\Delta l/l$, where l is instrument length, and Δl is positive for an increase in length. We use the symbol nϵ, nanostrain, for $\Delta l/l = 10^{-9}$.

The instruments are characterized by very high sensitivity ($\approx 3 \times 10^{-3}$nϵ), wide frequency band (from d.c. up to hundreds of Hz), large dynamic range (unbounded in principle), and good reliability. During the transit of teleseismic waves it recorded signals as large as 600 nϵ and as fast as 100 nϵ/s without any nonlinearity or abnormal behavior.

The experiment has been planned for a better knowledge of crustal deformation processes, due to tectonic processes (strain accumulation and release, aseismic slips, coseismic steps and earthquakes - regular and slow) as well as to earth tides.

2 Slow earthquakes

Several clustered slow earthquakes have been recorded by the geodetic interferometer from March to October 1997 (see 1999 LNGS Annual Report and [1]).

The swarm was preceded by few events which occurred at the end of 1996 and was followed by other episodic events. As already mentioned in the Introduction, until 1999 the interferometer measured difference in strain between one baseline oriented N66E and another baseline oriented N24W, i. e. one shear-strain component. Sampling frequency was 0.5 Hz. Slow earthquakes appear as nearly-exponential strain changes with duration from tens to thousands of seconds and amplitudes of a few nanostrains. Three more slow earthquakes have been recorded in May 2001. The shear-strain component of the signals is very similar to that of the 1997 events, and sources are presumably on the same fault. All the 2001 signals give negative (compressive) areal strain.

Since full source inversion of available strain data is not possible, at first we have tested the possibility that the slow events occurred on a fault with strike 100 deg , dip 60 deg , and rake -90 deg , in agreement with the overall geological setup of the area. We have computed the static response at the interferometer (both shear and areal strain) in case of a homogeneous elastic half-space (v_P = 5150 m/s, v_S = 2710 m/s, density=2700 kg/m^3, rigidity=2×10^{10} N/m^2) [2] moving the source on a 3D regular grid. The number of observed events with positive sign is much higher (about 5 times) than the number of events with negative sign, and we record many more small-amplitude observed events than larger ones. Assuming that the sources of the slow events are clustered and located on a planar fault, the cluster has then to cross a surface of zero shear response and has to be located close to a surface of zero response in dilatation, in a small-gradient region. Only one source region, located few kms South of the interferometer, fully satisfies the constraints (Figure 1).

Fault location and parameters are consistent with the well-known Vallefredda fault (fault 1 in Figure 2).

We have also tested as possible sources all the faults, including minor ones, mapped on the neotectonic map in [3] and located within approximately 10 km from the interferometer (Figure 2).

Amplitudes of the recorded signals (and, therefore, of the seismic moment) scale with the square root of the rise time [1]. We have normalized amplitudes of recorded slow earthquakes to a reference τ = 100 s by multiplying them by $10/\sqrt{\tau}$ (where τ is the rise time of each slow earthquake in seconds) and we have compared the normalized-amplitude frequency distribution of the observed events with the amplitude distribution computed for equal-sized rectangular sources regularly distributed on each of the seven fault planes, using the same Earth model as above. Observed and synthetic signals with normalized amplitude smaller than 1.2×10^{-9}, representing a conservative detection threshold, are discarded.

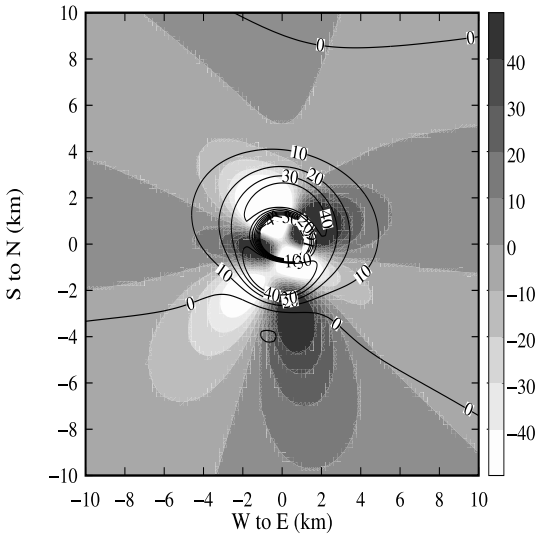

Figure 1: Shear (gray scale) and areal (contour lines) strain (in units of 10^{-9}) at the interferometer site for a point source (seismic moment 5×10^{14} Nm, dip 60 deg , rake -90 deg , strike 100 deg , depth 3 km) while varying its position around the interferometer. The only acceptable source region is located few kms South of the interferometer. The region located North of the interferometer must be rejected since the surface of zero areal strain dips toward North, i. e. in opposite direction with respect to the source.

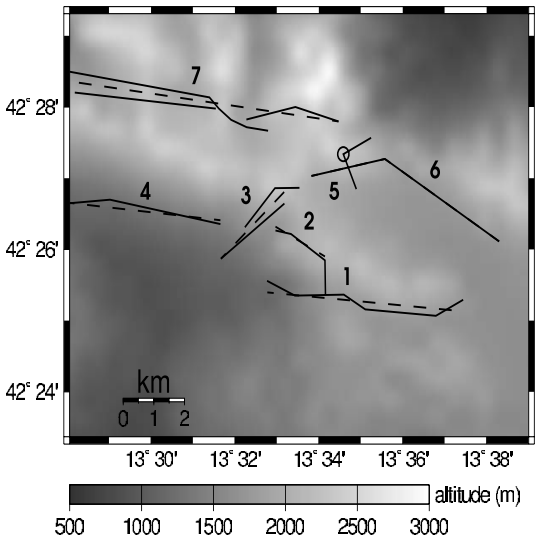

Figure 2: Map of the Gran Sasso region. Circle, location of the underground geodetic interferometer; solid lines starting from the circle, direction of the two interferometer arms; solid lines, surface trace of active faults [*Vezzani and Ghisetti,* 1998]; dashed lines, surface trace of tested planar faults.

For each of the faults, we have compared cumulative distributions of observed and synthetic amplitudes, by means of the Kolmogorov-Smirnov test [4]. The value of the seismic moment most appropriate for the sources of each tested fault is chosen by maximizing P. Several experiments have been performed, slightly moving and rotating each fault, testing different parts of it, and resizing rectangular sources. All the faults but number 1 strongly disagree with observations (Figure 3), while the agreement of fault 1 is extremely good, considering how crude the model is.

The significance level P is 0.96 for fault 1, 0.28 for fault 7, less than 0.03 for fault 5 and practically zero for the other faults. Best significance levels for fault 1 are reached when slip distribution is confined to depths greater than about 2.2 km. The seismic moment for each point source, and consequently for an event with rise time $\tau = 100$ s, is 4.9×10^{13} Nm, and dimensions of the rectangular sources are 263 m along strike and 217 m along dip. Of all patches covering the slipped area, 196 produce signals above our detection threshold, in good agreement with the number (161) of observed signals having normalized amplitude above the threshold. Sources deeper than about 4.5 km generate signals below the detection threshold, and we cannot exclude their existence. Additionally, sources on fault 1 give areal strain signals which are either detectable and compressive or undetectable, such as observed for the 2001 events.

3 Instrumentation developments

In October 2002, a three-component very-broad-band seismometer, flat in velocity down to 360 sec, has been installed inside the interferometric station by researchers of INGV (Istituto Nazionale di Geofisica e Vulcanologia). This installation is the deepest in Italy, measurements being consequently uninfluenced by the effects of the free (and weathered) surface. This feature would possibly let us study shear wave splitting changes during stress build-up [5]; the interesting topics are temporal changes of shear wave splitting in response to stress accumulation before earthquakes.

4 Conclusions

Although the role of slow earthquakes in the seismogenic process is still an open question, they seem to play an important part in reducing stress accumulation in the Gran Sasso area, and consequently mitigating the potential for strong earthquakes. Small slow earthquakes (such as those discussed here) produce neither surface deformations detectable by GPS or other current geodetic technique, nor seismic waves that can be detected by usual seismometers or easily recognized in seismograms. This area does not show significant instrumental or historical records of seismicity. The activity we recorded probably originated on a fault which very likely did not exhibit seismic activity in historic times. This is a significant difference with respect to other reported slow ruptures where slow earthquakes have generally occurred on faults which also show seismic activity. These suggest the existence of different modes of rupturing of the same structure and that deformation developed through slow fracturing represents an intermediate mode between seismic activity and creeping. In our case evidence suggests that the fault is currently

failing exclusively through slow fracturing. At least, it has done so during the sequence we documented. This fact may have important consequences on evaluating seismic hazard: a fault rated as active on geological grounds, may indeed be so. Yet its activity may be totally in the slow earthquake band, with no response in the seismic band of the spectrum. It is clear then that very-low frequency, high-sensitivity records of ground deformation contribute essential data to improve the real-time picture of seismic activity.

5 List of Publications

1. A. Amoruso, L. Crescentini, A. Morelli, and R. Scarpa, Slow Rupture of an Aseismic Fault in a Seismogenic Region of Central Italy, *Gephys. Res Lett.,*10.1029/2002GL016027, 2002.

References

[1] Crescentini, L., A. Amoruso, and R. Scarpa, Constraints on slow earthquake dynamics from a swarm in central Italy, *Science, 286,* 2132-2134, 1999.

[2] Okada, Y., Internal deformation due to shear and tensile faults in a half-space, *Bull. Seism. Soc. Am., 82,* 1018-1040, 1992.

[3] Vezzani, L., and F. Ghisetti, Carta geologica dell'Abruzzo, scale 1:100,000, *S.El.CA,* Firenze, 1998.

[4] Press, W. H., S. A. Teukolsky, W. T. Vetterling, B. P. Flannery, *Numerical Recipes in C. The Art of Scientific Computing. Second edition*, Cambridge Univ. Press, Cambridge, 1992.

[5] Crampin, S., Calculable fluid-rock interactions, *J. Geol. Soc.*, *156,*, 501-514, 1999.

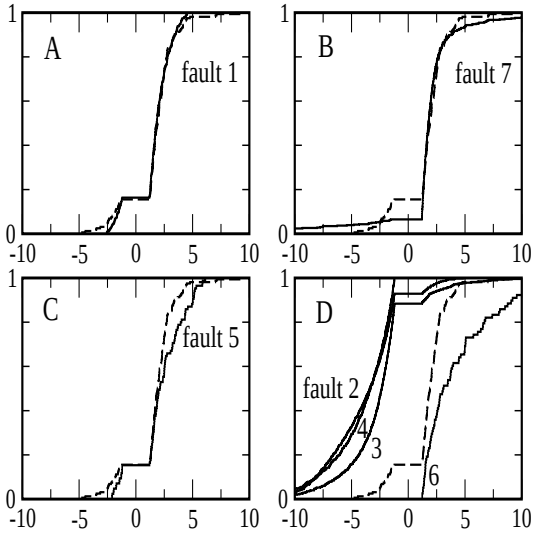

Figure 3: Cumulative distribution function (fraction of data points lower than a given value) versus amplitude of strain signals. Dashed lines in all plots represent the 161 observed normalized amplitudes larger than the threshold value. Solid lines represent synthetic signals from the different tested faults, after maximizing the significance level P. For faults in plot (D), retrieved P values are always zero and it is not possible to optimize parameters.

LNGS-EXP 20/99. Measurement of the Radon concentration in the water from the Gran Sasso fault

A. Bassignani[a], G. Colombo[a], M. De Deo[b], D. Di Ferdinando[c], L. Degli Esposti[c], R. Fresca Fantoni[a], G. Giacomelli[c], G. Mandrioli[c], F. Materazzi[a], D. Matteuzzi[c], L. Patrizii[c] and G. Sirri[c]

[a] Eni S.p.A. Agip Division, Radiation Protection Department, San Donato Milanese
[b] Laboratori Nazionali del Gran Sasso, Assergi (AQ)
[c] Dipartimento di Fisica dell'Università di Bologna and INFN, Bologna

Abstract

Since 1999 the Rn concentration in the groundwater from the fault in the interferometric tunnel of the underground Gran Sasso Laboratory has been monitored. The main goal of the experiment is the search for possible correlations between changes of the radon concentration in water and seismic activity.

Water is directly collected from the fractured rock and radon gas is extracted by nitrogen bubbling from samples of water. New data have been collected in 2002.

1 Introduction

Radon contents in groundwaters and in air are being monitored by several experiments with the aim of studying possible correlations between radon concentration variations and seismic phenomena [1-5].

We developed and implemented an automatic instrument for monitoring the radon concentration in the water coming from the Gran Sasso fault (in the middle of the interferometric tunnel). The fault is one of the most important features of the Gran Sasso Massif.

The apparatus may be considered to complement other instruments that are monitoring seismic activities in the underground laboratory: a geodetic interferometer [2], tiltmeters and the apparatus for groundwater analysis of the University of Roma Tre [3].

Since year 2000 we made measurements of the radon concentration in water with a sampling rate of 2 measurements per day [6].

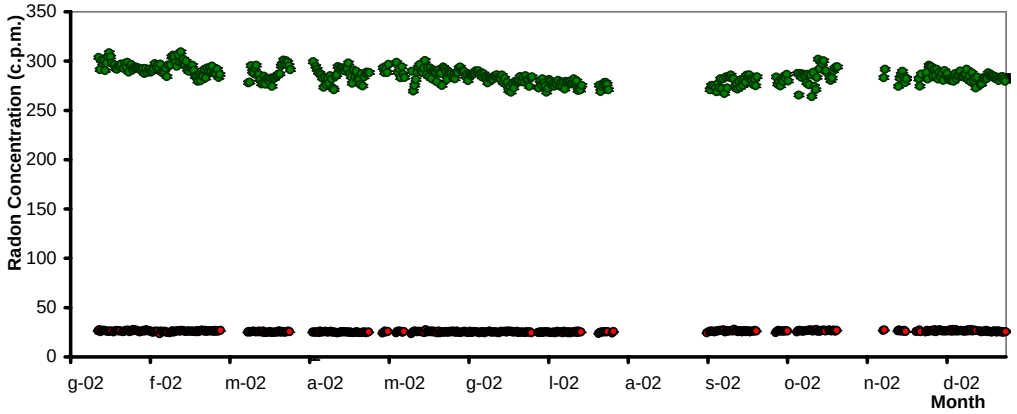

Figure 1: *Radon concentration in water and detector background (in counts per minute) during the year 2002.*

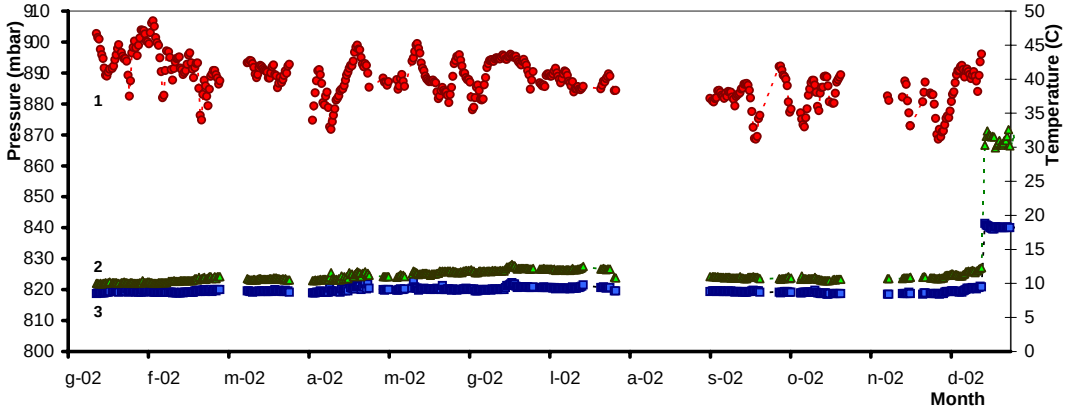

Figure 2: *Atmospheric pressure (1), detector temperature (2) and bubbling temperature (3) during the year 2002.*

2 Measurements

A plot of the radon concentration in water measured in the year 2002 is shown in Fig. 1. The data indicate some minor variations, which are being studied. We are also studying the possible correlations with seismic activity.

Atmospheric pressure and detector and bubbling temperatures are shown in Fig. 2.

3 Conclusions

An apparatus for monitoring radon concentration in the water from the Gran Sasso fault has been designed and implemented. The extraction technique and the detector system allow to have a good reproducibility and good signal to background ratio.

Data have been taken from June 2001 to December 2002; the 2002 data are shown in

Fig. 1. The time series of the data are under study.

Several improvements are under study. A new radon gas detector will be placed in series to the actual one; it will be used for cross-calibrations and for checking the stability of the system. In order to improve the continuity of data taking during black-outs, a new UPS system will be installed; it will have an automatic restart via computer network. A system for reducing the humidity inside the box containing the electronics will also be installed.

References

[1] M. Noguchi and H. Wakita, A method for Continous Measurement of Radon in Groundwater for Earthquake Prediction, Jou. Geoph. Res. 82 (1977) 1353.

[2] A. Amoruso et al., GIGS. The Interferometric Station at LNGS, LNGS Annual Report (2000) 177.

[3] F. Bella and W. Plastino, Radiocarbon and Radon analysis for geophysical monitoring of Gran Sasso acquifer, LNGS Annual Report (2000) 187.

[4] Dobrovolsky et al., Estimation of the size of earthquake preparation zones, Pure and Appl. Geophys. 117 (1979) 1025.

[5] M.M. Monnin and J.L. Seidel, Physical models related to radon emission in connection with dynamic manifestations in the upper terrestrial crust: a review, Radiation Measurements 28 (1997) 703.

[6] D. Barbaresi et al. , LNGS 20/99, LNGS Annual Report (2000) 195; LNGS Annual Report (2001) 243. See these reports for technical details.

TELLUS

V.Sgrigna[a], L.Conti[a], V.Malvezzi[a]

[a] Dipartimento di Fisica, Università degli Studi di Roma "Roma Tre", Italy

Abstract

To study local deformation processes associated with seismic activity a continuous monitoring of preseismic strains is carried out by tiltmeters located at three sites of LNGS. But during the earthquake preparation also electromagnetic emissions (EME) take place. Then, the study of preseismic EME waves and perturbation, instabilities, and particle precipitation they produce in the near Earth space is necessary for a better understanding of the earthquake generation mechanisms and occurrence. This study is performed by two specific space projects (ARINA and ESPERIA). The launch of the ARINA experiment is scheduled for end year 2003 on board of the RESURS-DK1 satellite, within the framework of the ARINA-PAMELA collaboration. A study, preliminary to this space experiment, is reported here on the basis of data collected by the SAMPEX-PET mission. It consists of a correlation carried out between earthquakes and burst of particles precipitating from the lower boundary of the inner radiation belt.

1 The aim of the TELLUS Experiment

The aim of the TELLUS experiment is the study of local ground strains related to earthquakes and associated electromagnetic emissions (EME). Continuous mechanical measurements are performed at three tilt sites of LNGS while EME wave investigations demand for specific space experiments to be carried out on board of LEO (Low Earth Orbit) satellites. Two space missions (ARINA and ESPERIA) are under study. They have been described in the previous LNGS Annual Report 2001. Then, the TELLUS experiment gives a contribution to a more general scientific project devoted to study ionospheric and magnetospheric perturbations caused by seismicity, and in particular, to develop a method to reveal short-term earthquake precursors.

2 Experimental Apparatus.

The experimental apparatus consists of three bi-axial tiltmeters, of the ARINA particle detector, and of the ESPERIA satellite configuration from a phase A study.

3 Tiltmeters

The two-component-horizontal-pendulum tiltmeters, with Zöllner bifilar suspension and relative analog detecting and digital acquisition systems, have been described in the LNGS Annual Report 2000.

3.1 ARINA particle detector and ESPERIA phase A study

The ARINA particle detector has been designed during 2001 and described in the LNGS Annual Report 2001 together with the ESPERIA phase A study. ARINA is an experiment devoted to particle measurements. Within the framework of the PAMELA-ARINA collaboration, the ARINA detector will be installed on board of the RESURS-DK1 satellite of the Russian Space Agency which launch is scheduled for end year 2003. The ESPERIA scientific project is planned with strong emphasis on coordinated ground-based and space observations. Past experience based on ground-based and space experiments and on theoretical studies strongly suggests that specific and dedicated space observations are necessary for a detailed modeling of the phenomena involved with natural and anthropogenic activities. ESPERIA will capitalize on past experience of its participant teams, and provide a flexible and easily manageable instrument for a state-of-art data acquisition and response to these new original geophysical and human-generated phenomena. The fundamental aspects concerning a specific space mission are synthesized in the following.

- *General requirements:*
  - Space and ground-based measurements.
  - Simultaneous and continuous measurements of the different parameters with an excellent capability in detecting particles over a broad energy range, as well as in revealing plasma instabilities and electromagnetic fluctuations.
  - Repeatability and maximum density of ground tracks over selected Earth's surface regions with high-accuracy and low-repetition time for a continuous ground monitoring of local and short-term time phenomena.
- *Specific Requirements:*

  a. Optimization of Orbital Parameters
  - Continuous monitoring without necessity to distinguish between survey and burst modes.
  - Efficiency and low costs of the ground segment operativeness including the optimization in the use of mass memory by frequent down-link procedures.
  - High-sensitivity measurements in zones with relatively minimum temporal and spatial field changes.
  - Maximum density of measurements and continuous EME monitoring over seismic areas.

- Necessity to detect particles affected by EME waves of terrestrial origin and generated by seismotectonic processes: particle detector must skim L-Shells just beneath the inner radiation belts with L $\simeq$ 1.2.

b. Model Payload

- Multi-instrument payload: ULF $\div$ HF electric and magnetic fields; ionospheric plasma temperature and density; particle fluxes, pitch angle, and energy.
- High instrumental sensitivity, signal-to-noise ratio, and dynamic range for all the parameters to be studied.
- Continuous data acquisition.
- No interaction and disturbances between the different instruments (sensors and related electronics).
- No differential phtoemission from the external surface of the platform and payload.
- No influence of electric field distortion in EME measurements caused by the satellite structure and geometry.

c. Ground-based measurements

- Seismic activity, continuous and simultaneous preseismic mechanical (tilt and strain) and electromagnetic fields in test areas.
- Comparison and integration of space observations with ground-based ones.

4 Results obtained with regards to year 2002

The results obtained with regards to year 2002 consist of a continuous ground tilt data collection at LNGS and of a correlation between earthquakes (EQs) and anomalous particle bursts (PBs) from PET (Proton Electron Telescope) SAMPEX satellite observations. The study of deformation processes related to earthquakes demands for a long time series of tilt data (a few years). For the period 1996-2000 results concerning aseismic creep strain episodes and their numerical modeling have been shown in the LNGS Annual Report 2001. Since then, a continuous tilt monitoring is in progress to perform a study on more recent seismo-associated phenomena. In the following the above-mentioned EQs-PBs correlation will be reported. It is based on the possible influence of seismicity in the ionosphere-magnetosphere transition region as suggested in recent times by a few space experiments. These revealed anomalous charged particle fluxes precipitating from the lower boundary of the inner Van Allen radiation belt caused by low-frequency seismo-electromagnetic emissions. Results seem to confirm previous observations. A marked short-term seismic precursor of $\simeq$ 4 hours is observed in the histogram of the time difference between the time occurrence of earthquakes and particle burst events. The two populations consist of continental earthquakes with $M \geq 5.0$ and anomalous particle bursts defined on the basis of a particle pitch angle and L-shell parameter background matrix. Several constrains and cuts have been applied to the data to take into account

of previous results and of measurements performed inside the SAA region or during ionospheric and magnetospheric perturbations. The best correlation is obtained only when considering high-energy electrons ($E \geq 4MeV$), which exhibit a relative long-term longitudinal drift, and during PET pointing modes when the detector yaw axis is substantially radial to the Earth, so the PET telescope may also detect particles with pitch angle in the loss cone (precipitating particles). Short-term preseismic particle bursts are important because may be also collected far from seismic areas and give complementary information with respect to that obtained from ground-based intermediate-term precursors. A brief description is reported below.

5 Introduction

In recent years, interest has been increasing in the so-called seismo-electromagnetic emissions (EME) consisting of broad band ($\simeq$ DC $\div$ a few MHz) EM waves generated and radiated by seismic sources into the near Earth's space before, during, and after an earthquake (EQ). Ground-based (Fraser-Smith et al., 1994; Hayakawa et al., 2000) and space observations as well as on laboratory measurements (Nitsan, 1977; Warwick et al., 1982; Yoshida et al., 1997) and related theoretical speculations gave information on the generation (Guo et al., 1994; Fenoglio et al., 1995; Molchanov et al., 1995; Teisseyre, 1997) and propagation (Molchanov et al., 1995; Grimalsky et al., 1999; Sorokin et al., 2001) mechanisms of such preseismic EME waves. (Fujinawa et al., 2002; Ogawa and Utada, 2000; Yoshida et al, 1997; Kopytenko et al., 1993; Parrot, 1993; Park et al., 1993; Warwick et al., 1982; Serebriakova et al., 1992.)

LEO (Low-Earth-Orbit) satellite observations mainly revealed preseismic changes of electric and magnetic fields and of ionospheric plasma temperature and density a few hours prior to EQs of moderate or strong magnitude (generally, greater than 5.0). Less frequent but interesting data have been collected in more recent times, concerning EME wave-particle interactions and related precipitation of radiation belt electrons and protons detected before EQs and characterized by an anomalous short-term and sharp increase of high-energy particle counting rates (CRs). In the following they are referred to as "particle bursts" (PBs). Most of PBs have been collected near the South Atlantic Anomaly (SAA) at altitudes generally between around 500 km and 1000 km, by several space experiments (Galper et al., 1989; Voronov et al., 1990; Galperin et al., 1992; Pustovetov and Malyshev, 1993; Aleshina et al., 1992). A.M. Galper and his co-workers of the Institute of Cosmic Physics of MEPhI first suggested the preseismic character of such PBs, by basing on PBs-EQs statistical correlations, while Molchanov, 1995; Aleshina et al., 1992 proposed a possible explanation for the PBs generation mechanism. The above-mentioned preseismic EME waves are thought to be produced in the earthquake focal area by several mechanisms (stress and strain field variations, rock dislocation and microfracturing, electrokinetic, piezomagnetic and piezoelectric effects, etc) (Slifkin, 1993; Johnston, 1997). Mainly the lower frequency content of such radiation (ULF/ELF EME waves from $\simeq$ DC to a few hundreds Hz) may propagate in the lithosphere (from the preparation hypocentral area to the Earth's surface) and penetrate, without any significant attenuation, into the near Earth space (atmosphere and ionosphere, up to the magnetosphere). At the

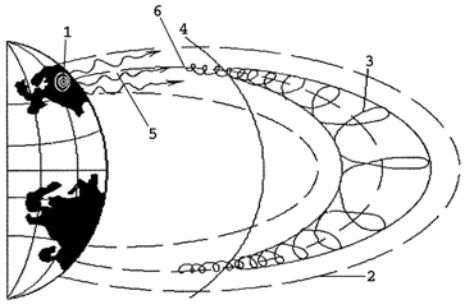

Figure 1: Trajectories of charged particles trapped by the geomagnetic field lines represented in a meridian plane. 1. earthquake hypocentral area where the EME waves are emitted during earthquake preparation; 2. geomagnetic field lines; 3. stationary trajectory of particles; 4. lower boundary of the radiation belt; 5. EME waves propagating from the preparation focal area to the ionosphere; 6. mirror points.

ionosphere-magnetosphere boundary these EM signals are transformed into Alfven waves which propagate along the geomagnetic field lines. At the radiation belt boundary, such waves resonantly interact with trapped particles (electrons and protons from a few MeV to several tens of MeV) causing particle precipitation as a result of pitch-angle diffusion (Aleshina et al., 1992; Abel and Thorn, 1998a,b). The wave-particle resonant interaction occurs since the frequency bouncing motion of particles lies in the same frequency range of ULF EME waves (Walt, 1994). A qualitative representation of this model is reported in figure 1.

Particle detectors installed on board of satellites may detect these preseismic PBs, since their lifetime is determined by the rate of particle loss during the interaction of particles with the residual atmosphere of the Earth, and a lifetime of the order of several tens of minutes is obtained for electrons and protons of several tens of MeV. During this time, particles (drifting longitudinally) may propagate several times around the Earth along the L-shell corresponding to the EME ground source location (Galper et al., 1989; Walt, 1994). The above-mentioned LEO observations seem to confirm the possibility to detect such PBs. Moreover, Intercosmos-24 satellite measurements also demonstrated (Molchanov et al.,1993) that ULF emissions of $\simeq 0.2$ nT can penetrate through the ionosphere and interact with energetic protons of $0.5 \div 5$ MeV near the equatorial plane of the magnetosphere. As a consequence of this cyclotron interaction, the proton distribution function becomes unstable after $\simeq 3 \div 6$ hours, for Cherenkov radiation of VLF waves in the frequency interval $0.1 \div 20 kHz$. Nevertheless, there is still an open debate whether the very-low amplitude of ULF EM waves may reach the inner Van Allen radiation belt and cause or not the above mentioned coupling phenomena, since the electric and magnetic components are estimated to be of some fraction of $mV/m(Hz)^{1/2}$ and of some fraction of $nT/(Hz)^{1/2}$, respectively (Parrot et al., 1993). On the other hand, experimental evidences from several space missions and the longitudinal drift character of precipitating PBs suggest a very exciting opportunity in EQ forecasting, consisting in the possibility to

Time duration:	from July 1992 to December 1999
Orbit altitude:	$520 \div 670$ km
Orbit inclination:	82°
PET Pointing modes:	ORR; MORR; 1 RPM (see text)

Table 1: Sampex-PET mission main characteristics

detect preseismic PBs not only over the seismic areas, where such events take place, but also at any longitude along the L-shell perturbed by the preseismic EME wave-particle interaction effect. For these reasons, we think that this opportunity demands for further investigations on the subject. The aim of the present study is only confined to give help in confirming or not the EQs-PBs correlation obtained by Galper and his co-workers. At this purpose, we have performed a correlation of similar quality making use of the same algorithms used by Russian colleagues and of data obtained by another space mission.

6 Selection of a Space Mission Suitable for the Study.

To obtain statistically significant results, long time series of data concerning particle fluxes, earthquake parameters and magnetospheric perturbations, caused by non-seismic sources, are requested. To detect PBs caused by preseismic EME waves the satellite orbit must "skim" L-shells just beneath the lower boundary of the inner radiation belt (average L-value $\simeq 1.2$). Previous results indicate an orbit between around 500 km and 1000 km of altitude as the most suitable for the study. Finally, high-energy particles are requested which exhibit a relative long-time longitudinal drift. Previous results and simple estimates (Walt, 1994), indicate a particle detector of electrons with $E_{e^-} > 5MeV$ and protons with $E_{p^+} > 50MeV$; energy resolution better than 5 MeV; time resolution less than 15s; angular acceptance as larger as possible; angular resolution better than $< 5^o$. A large angular acceptance is requested also to detect particles with pitch angle in the drift loss cone. No dedicated and suitable space missions have been found. Nevertheless, taking into account of all the above conditions, the SAMPEX (Solar Anomalous and Magnetospheric Particle EXplorer) NASA satellite, with on board the PET (Proton/Electron Telescope) detector, revealed to be the most suitable experiment for the study.

7 SAMPEX-PET Mission and Database

The main characteristics of the SAMPEX mission (Lennard et al., 2000) are reported in table 1.

The PET instrument is constituted by an array of silicon solid-state detectors that identifies electrons, protons and ions. PET channel level-2 data available for the study (Lennard et al., 2000) are reported in table 2.

It can be seen that in the PEN and RNG channels it is impossible to separate electrons from protons, PLE and PHI channels consist of very low energy protons, and EWG channel exhibit a poor statistic due to a low geometric factor. Then, only level-2 PET-data from

Particles	Energy (MeV)	Geometric factor (cm^2sr)	Channel
Protons	28÷60	1.5	PHI
Protons	19÷28	1.65	PLE
Electrons	2÷6	1.65	ELO
Electrons	4÷15	1.5	EHI
Electrons	4.30	–	EWG
Protons	> 60	0.4	RNG
Electrons	> 15		
Protons	> 85	0.25	PEN
Electrons	> 30		

Table 2: Characteristics of PET channel level 2 data

EHI and ELO channels can be considered. But, since EHI channel exhibit the best event statistics and has electrons with greater energy than those of ELO one, it must be expected that EHI electrons are the best set of data for our study Level-2 PET-data are constituted by 30s-averaged CRs. CRs of electron channels EHI and ELO are referred to as CREHI or CRELO, respectively. Unfortunately, the particle pitch angle is not present in the NASA database and only the α_{PET}-value (angle between the detector yaw axis and magnetic field) is given, so that the satellite PET-pointing modes influence the analysis (see, tab.1 and fig.2). As shown in table 1, SAMPEX-PET has operated with three different pointing programs: ORR (original Orbit Rate Rotation), MORR-1 and MORR-2 (Modified Orbit Rate Rotation), and 1 RPM (1 Rotation Per Minute). During the ORR pointing mode the detector yaw axis is substantially radial to the Earth. So, PET may also detect particles with pitch angle in the loss cone (precipitating particles). On the contrary, in the MORR mode the detector yaw axis is fundamentally perpendicular to the geomagnetic field lines, since it was implemented mainly to study particles with pitch angle near 90^o (trapped particles). Measurements with α_{PET} far from 90° are carried out during PET yaw axis changes from 90^o ($B < 0.3Gs$) to 0^o ($B > 0.3Gs$). Finally, in the 1 RPM mode the α_{PET} distribution is flat since the PET yaw axis rotates continuously at 1 RPM about pitch axis (solar direction). Then, it is evident that the ORR pointing mode is the most suitable to detect precipitating particles. As specified in table 1, CRs PET-data were divided in four time periods corresponding to the different pointing modes. In this table are reported daily data collected during optimal device working conditions (referred to as "good days") and events detected with good quality flag. The four panels in the first line of figure 2 show the geographic distribution of CRs measurements performed during each pointing time mode.

During the MORR (1) mode it is evident a non-homogeneous CRs geographical distribution due to scanty PET measurements performed in the longitude interval $[50^\circ \div 270^\circ]$. PET measurements are totally absent in this longitudinal interval during the 1 RPM and MORR (2) pointing programs. In correspondence with the latter two modes, an abrupt decrease is observed in the CRs distribution versus L, for L $\simeq 1.0 \div 1.3$ (second line of figure 2). The four panels in the third line of 2 clearly confirm that the α_{PET} distribution is pointing program dependent.

Pointing mode	Period	# good days	# CR	$\frac{\#days}{\#CR}$	# PBEHI	# PBELO
ORR	01/24/93 ÷ 05/26/94	247	211603	857	1734	1259
MORR (1)	05/27/94 ÷ 05/07/96	691	373976	541	3957	1848
1 RPM	05/08/96 ÷ 05/06/98	677	195187	288	1253	485
MORR (2)	05/07/98 ÷ 12/16/99	543	179457	330	1628	698

Table 3: PBEHI and PBELO catalogues in the different SAMPEX pointing time modes

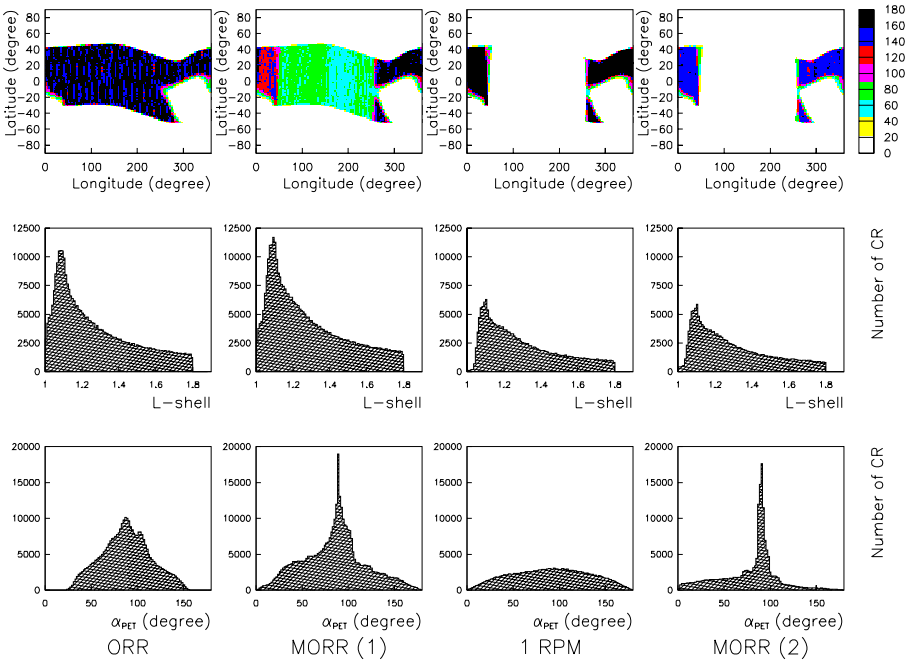

Figure 2: Distribution of PET measurements in the different pointing time modes. In the first line are reported the geographic distributions of CRs. In the second and third lines are shown the CRs distributions versus L-shell and α_{PET} ,respectively.

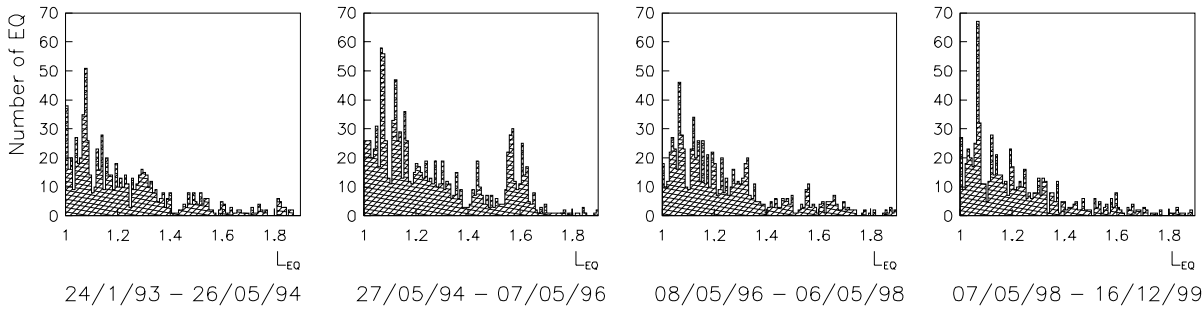

Figure 3: Distribution of earthquakes versus L_{EQ} calculated projecting the hypocenter at an altitude of $400km$. Only the seismic events setected according to the EQ analysis cuts are included (period 1992-1999).

EQ event definition	**PB event definition**
M $\geq$ 5.0	CRs: particle flux measurements integrated over 30s
Hypocentral depth $h \leq 100km$	CR daily background matrix $\{L, \alpha_{PET}\}$:
No oceanic crust EQs	$1.0 \leq L \leq 1.8$ (L-steps = 0.1)
Wave-particle interaction altitude (z):	$0^o \leq \alpha_{PET} \leq 180^o$($\alpha_{PET}$-steps = 15^o)
$100km \leq z \leq 1200km$	Poissonian cut: $p < 0.01$
L_{EQ} by IGRF 2000:	No measurements in the SAA region
$L_{EQ} \simeq L_z = 400km$	$Ap < 20$
$\downarrow$	SID = 0
$100km < z < 1200km \rightarrow \Delta L_z \simeq 0.1$	

EQ-PB correlation

$$\Delta L = L_{EQ} - L_{PB} < 0.1$$

$$\Delta T = T_{EQ} - T_{PB} \leq 6days \text{ (time window: 18 hours)}$$

Table 4: Selection criteria for the EQs and PBs populations to be correlated and related cuts applied to the data.

8 Selection Criteria and Related Cuts Applied to the EQs and PBs Populations to be Correlated

In table 4 are summarized selection criteria and related cuts applied to the data for the PBs-EQs time correlation. In the following sections we will give some details and clarify such conditions.

9 EQs Selection. EQ reference altitude and associated L-shell value.

Most of the seismic EME observations are associated with moderate and strong events ($M \geq 4.0 \div 5.0$), generally located in the Earth crust (Molchanov et al., 1993), then earthquakes with magnitude $M > 5.0$ and hypocentral depth $< 100km$ ($\simeq$ lithospheric depth) have been selected for the study. Oceanic crust earthquakes have been rejected for the possible absorption of EME waves in the oceanic water. Even if the seismic EME wave-particle interaction zone is not yet exactly predicted by the theory, according to Parrot et al (1993), we assume that it may extend at altitudes between $\simeq$100 km and $\simeq$1200 km, which approximately include all the belt boundary of interest for the study. Since, the L-shell value corresponding with a PB (L_{PB}) is known by PET measurements, an L-shell value must be associated to each EQ (L_{EQ}). It has been defined by projecting the hypocentral area at an altitude corresponding with the above-estimated EME wave-particle interaction zone. As a first attempt, we have considered the L_{EQ} value at a reference altitude z=400 km as a model dependent and tuneable parameter. Note that most of the EQs are located at $\pm 30^o$ of latitude, and that the variation of the projection altitude between 100km and 1200km results in a corresponding L_{EQ} uncertainty of about 0.1. Figure 3 shows the EQs vs L_{EQ} distribution, which profile is similar to that of

the SAMPEX CRs vs L-shell values associated to CRs (see the second line of figure 2). In the period 1992-1999 under study the number of earthquakes with $M > 5.0$ does not change substantially, excepted for some short time intervals when some strong seismic sequence occurs. But, the seismicity level in the period 1992-1994 was higher (b-parameter $\simeq 1.25 \div 1.12$) than normal ($b \simeq 1$), whereas in the period 1995-1999 it was lesser ($b \simeq 0.92 \div 0.87$). Therefore, during 1992-1994 a major probability exists to obtain a greater number of PBs and, then, a better PBs-EQs correlation.

10 PBs selection. Irregular CR events with respect to a background matrix.

The 30s temporal resolution of Level-2 PET-data does not allow the characteristic of a few seconds duration of a PB event to be observed. It is possible only to identify an anomalous deviation from the statistical distribution of the 30s integrated CRs. Since PBs are defined starting from charged particle CRs (table 2) which depend on the L-shell value corresponding with the measurement position and on the instrument pitch angle (α_{PET}), PBs have been defined with respect to a background $\{L, \alpha_{PET}\}$ matrix constructed as follows. L-shell and B values corresponding with the detection position of particles are calculated by the IGRF2000. Since, 99.5% of the L_{EQ} and L_{PB} distributions is included within L = 1.8 (figs. 2,3) and zones with $L_{EQ} < 2.0$ are mostly affected by ULF pre-seismic waves, we restrict our analysis to L-shell values $= 1.0 \div 1.8$. We divided the α_{PET} range ($0^o \div 180^o$) in steps of 15^o and the L-shell range ($1.0 \div 1.8$) in steps of 0.1. For each cell of the $\{L, \alpha_{PET}\}$ matrix, we evaluated the daily CR distribution in order to define a reference background value. The L and α_{PET} step widths are defined taking into account the particle fluxes variation and the exiguous number of measurements available per day. Statistical tests performed on daily CRs suggest a Poissonian distribution of CRs for each $\{L, \alpha_{PET}\}$ matrix cell. By basing on this result, we define a PB event as CRs that assume values greater than those of the relative $\{L, \alpha_{PET}\}$ background matrix and the probability (p) to be a Poissonian fluctuation is less than an assigned threshold value (we chose $p < 0.01$). Since the position of the lower limit of the inner radiation belt boundary varies with time, this belt boundary (and in particular the SAA region) was determined yearly by the IGRF 2000. The SAA region was excluded for the study as well as an attempt was also done to separate ionospheric and magnetospheric perturbations produced by external sources (sun and cosmic rays) from those caused by seismicity and Earth's environment. In particular, only data collected in periods of low-value geomagnetic indices ($Ap < 20$) or in absence of ionospheric disturbances (SID=0) are included in the analysis. The number of PBEHI and PBELO data are reported in table 3. Both PBEHI and PBELO distributions in the L=1.0 $\div$1.8 interval and for the four different α_{PET} modes (fig.4) agree with the CR's ones (fig.2). This indicates that the PB selection has not introduced evident systematic errors.

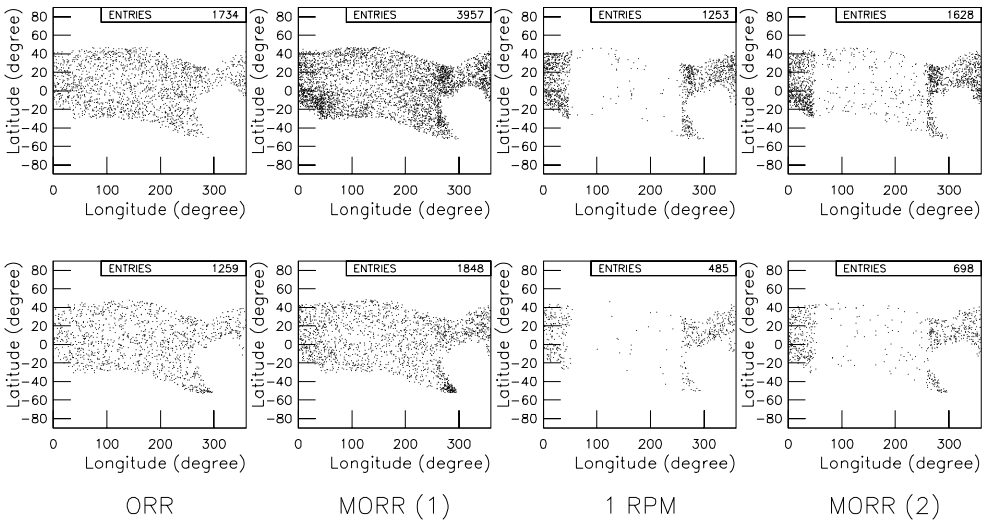

Figure 4: Geographic ditributions of PBEHI (first line) and PBELO (second line) in the $1.0 < L < 1.8$ interval vs the different pointing modes. Observations in the SAA region were excluded from the analysis.

11 PBs-EQs correlation

Contrary to the L_{EQ}-value (which is model dependent), the L_{PB}-value is model independent. In fact, the precipitating particles drift longitudinally around the Earth along a fixed L-shell, which is not modified by the EME interaction and directly known by the geomagnetic field value, measured on board a satellite. For the PBs-EQs correlation, we considered the L-shell difference $\Delta L = L_{EQ} - L_{PB}$ as a tuneable parameter. Due to the possibility that wave-particle interaction may take place within the maximum range of fluctuation of the inner boundary of the radiation belt (that is, between around 100km and 1200km), only data with $\Delta L = L_{EQ} - L_{PB} < 0.1$ have been included in the study (table 4). Since we use z = 400km as a reference altitude for the L_{EQ} definition, L_{PB} values range from -0.08 and +0.03 within the above-mentioned $\Delta L = 0.1$ interval. Then, we calculated the time differences $\Delta T = T_{EQ} - T_{PB}$, between the universal times of origin of the EQ (T_{EQ}) and PB (T_{PB}) events, respectively. We considered all such time differences $|\Delta T| \leq 3$ days, before and after each PB event (maximum time interval $|\Delta T| \leq 6$ days). Finally, a histogram of the ΔT frequency distribution has been performed for each PET pointing mode (fig.5) to look for the possible existence of a maximum peak in the $\Delta T > 0$ region (indicating that PBs statistically precede EQs). As shown in figure 5, significant results were obtained when considering PBEHI data obtained during the ORR mode. In fact, in this case a clear positive maximum peak appears evident near $\Delta T \simeq 4$ hours, indicating that high-energy electrons PBs statistically precede selected EQs. As expected, there is no other relevant peak at different ΔT values as well as when taking into account PBELO data and/or data collected during the other three pointing modes.To perform a reliable statistical analysis the PBs-EQs temporal correlation has been carried out in a time interval of ± 3 days with respect of each PB event, but for a better graphical

representation histograms are reported in figure 5 with a time window of ±18 hours.

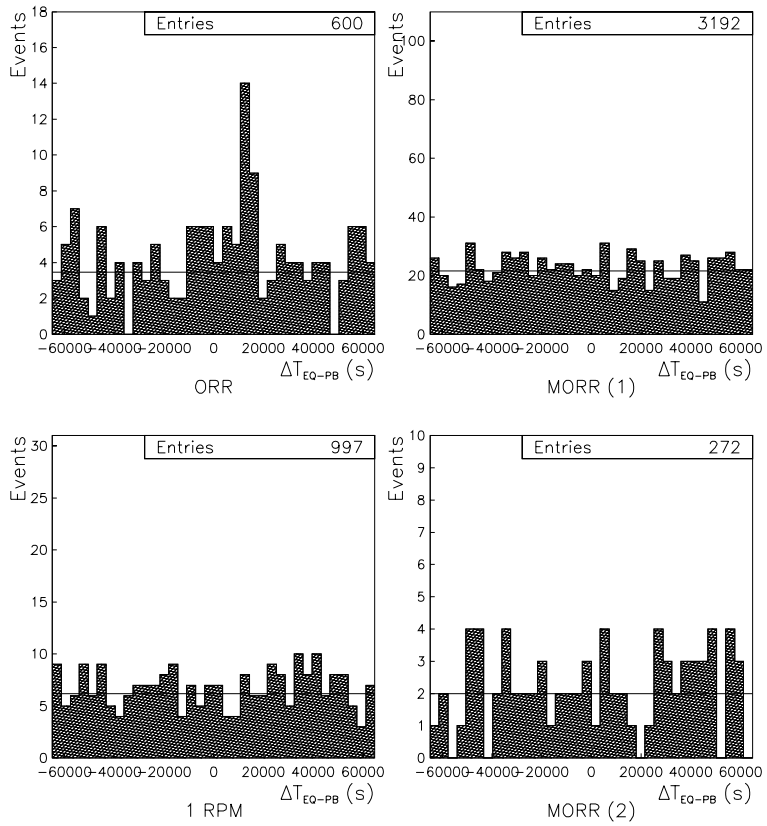

Figure 5: Histograms of the ΔT_{EQ-PB} temporal correlations between PBEHI and EQs in the four analysed periods. A clear peak is evident at $\Delta T = 4 \div 5h$ during the ORR pointing mode. This $\Delta T > 0$ maximum peak indicates that PBs statistically precede EQs. The bin step and time window are of 1h and of 18h, respectively. The horizontal line is the mean amplitude of the distribution.

12 Conclusions

Precipitating bursts of high-energy radiation belt electrons obtained from the SAMPEX level-2 PET-data have been statistically observed to precede of some hours the occurrence of moderate and strong earthquakes (M $\geq$ 5.0; depth $\leq$ 100 km). Such results agree with those (carried out with the same method) reported by Galper et al. (1989), Voronov et al. (1990), and concerning METEOR-3 data (Galper et al., 1989; 2000), but also add useful information on a few critical aspects about methods of investigation and data analysis. In fact, only high-energy particles, with a relatively long-term longitudinal drift, allowed the short-time earthquake precursor character of PBs to be observed. The best results were obtained from particles with pitch angle close to the loss cone, then indicating that detector pointing mode is critical for revealing preseismic PBs. Negative results were observed in the cases of not suitable satellite pointing programs, of low-energy particles,

and in presence of a poor statistics. No correlation was also found between PBs with other noise sources (solar and magnetospheric activity) that could, in principle, cause particle precipitation. The results of our study give useful information for a dedicated space mission devoted to identify short-term earthquake precursors. At this regard, a space mission (the ESPERIA space project) is under study by several teams leaded by Vittorio Sgrigna of the University "Roma Tre" (Italy).The relative Phase A report has been completed (Sgrigna et al, 2001) and includes a multi-instrument payload and a contemporary ground-based monitoring of several test areas.

13 List of Publications in 2002

- Sgrigna, V., D'Amgrosio, C., Yanovskaya, T.B., 2002. *Numerical modeling of preseismic slow movements of crustal blocks caused by quasi-horizontal tectonic forces*, Phys. Earth Planet. Int., 129, 313-324.

- Sgrigna, V., Console, R., Conti, L., Galper, A., Malvezzi, V., Parrot. M., Picozza, P., Scrimaglio, R., Spillantini, P., Zilpimiani, D., 2002. *Preseismic Natural Emissions from the Earth's Surface and their effects in the near Earth Space. A project for monitoring Earthquakes from Space*, EOS Trans., AGU, vol. 83, T22B-10, n.19, S356.

- Malvezzi, V., Sgrigna, V., Yanovskaya, T.B., 2002. *Observation and Modeling of Preseismic Fault Creep Events. Correlation with the 1997 Umbria-Marche earthquake Sequence (central Italy)*, EOS Trans., AGU, vol. 83, T31A-08, n.19, S358.

- Sgrigna, V., (Principal Investigator), 2001. ESPERIA: Earthquake investigation by Satellite and Physics of the Environment Related to the Ionosphere and Atmosphere, Phase A Report, Italian Space Agency (ASI), Program for Scientific Missions dedicated to Earth Sciences, Rome, July 2001, pp.194.

- Sgrigna V. et al, Correlations between Earthquakes and Anomalous Particle Bursts from SAMPEX Satellite Observations, Geophys. Res. Lett.,submitted.

References

[1] B.Abel and R.M.Thorne,1998. *Electron scattering loss in Earth's inner magnetosphere 1. Dominant physical processes*, JGR, **103**, pp.2385-2396.

[2] B.Abel and R.M.Thorne, 1998. *Electron scattering loss in Earth's inner magnetosphere 2. Sensitivity to model parameters*, JGR, **103**, pp.2397-2407.

[3] M.E.Aleshina, S.A.Voronov, A.M.Galper et al., 1992.*Correlation between Earthquake Epicenters and Regions of High-Energy Particle Precipitations from the Radiation Belt*, Cosmic Research, **30**, p.79.

[4] M.A. Fenoglio, M.J.S. Johnston, and J.D. Byerlee, 1995. *Magnetic and electric fields associated with changes in high pore pressure in fault zones: application to the Loma Prieta ULF emissions*, J Geophys. Res., **100**, pp. 12951-12958.

[5] A.C.Fraser-Smith, P.R. McGill, R.A. Helliwell, and O.G. Villard, Jr, 1994. *Ultra-low frequency magnetic field measurements in southern California during the Northridge earthquake of 17 January 1994*, Geophys. Res. Lett., **21**, pp. 2195-2198.

[6] Y. Fujinawa, K. Takahashi, and T. Matsumoto, 2002. *Modeling confined pressure changes inducing anomalous electromagnetic fields related with earthquakes*, J. Appl. Geophys., **49**, pp. 101-110.

[7] A.M.Galper, V.B.Dimitrenko et al., *Interrelation between High-Energy Charged Particle Fluxes in the Radiation Belt and Seismicity of the Earth*, Cosmic Research 27, n.5, p. 789, 1989.

[8] A.M.Galper, S.V.Koldashov, A.Murashov et al., *Study on the Possibility of Earthquake Forecasting*, int. report, 2000.

[9] Yu.I.Galperin, V.I.Larkina et al., *Precipitation of High-Energy Captured Particles in the Magnetosphere Above the Epicenter of an Incipient Earthquake*, 1992, Cosmic Research, V.30, n.1, p.89.

[10] Grimalsky V.V., I.A. Kremenetsky, and Yu.G. Rapoport. *Excitation of EMW in the Lithosphere and Propagation into Magnetosphere*, Ed. M.Hayakawa, TERRAPUB, pp. 777-787, 1999.

[11] Z. Guo, B. Liu, and Y. Wang. *Mechanism of electromagnetic emissions associated with microscopic cracking in rocks*, Ed M. Hayakawa TERRAPUB, pp. 523-529, 1994.

[12] M. Hayakwa, Yu. Kopytenko, N. Smirnova, V. Troyan and Th. Peterson, 2000. *Monitoring ULF Magnetic Disturbances and Schemes for Recognizing Earthquake Precursors*, Phys. Chem. Earth, **25**, pp. 263-269.

[13] M.J.S. Johnston, 1997. *Review of electric and magnetic fields accompanying seismic and volcanic activity*, Surv. Geophys., **18**, pp. 441-475.

[14] Yu.A.Kopytenko, T.G. Matiashvili, P.M. Voronov, and E.A. Kopytenko, and O.A. Molchanov, 1993. *Detection of ULF emission connected with the Spitak earthquake and its aftershock activity based on geomagnetic pulsations data at Dusheti and Vardziya observatories*, Phys. Earth Planet. Int., **77**, pp. 85-95, 1993.

[15] V.I.Larkina, A.V. Nalivayko, N.I. Gershenzon, M.B. Gokhberg et al., 1983. *Observations of VLF emission, related with seismic activity on the Interkosmos-19 satellite*, Geomagn. Aeron., **23**, pp. 684.

[16] M.H.Lennard, J.E.Mazur, and G.M.Mazon, 2000, *Level 2 Data Products NSSDC Submission Description*, Depth.of Phys., University of Maryland, Preprint $\#PP96-69$, version 1.0.

[17] O.A.Molchanov, O.A.Mazhaeva, A.N.Goliavin, M.Hayakawa, *Observation by the Intercosmos-24 satellite of ELF-VLF electromagnetic emissions associated with earthquakes*, Ann. Geophysicae, n.11, p.431-440, 1993.

[18] O.A.Molchanov et al., *Penetration Characteristics of Elettromagnetic Emissions from an Underground Seismic Source into the Atmosphere, Ionosphere and Magnetosphere*, 1995, J. Geophys. Res., n.100, p.1691-1712.

[19] U. Nitsan, 1977. *Electromagnetic emission accompanying fracture of quartz-bearing rocks*, Geophys. Res. Lett., **4**, pp. 333-336.

[20] T. Ogawa, and H. Utada, 2000. *Coseismic piezoelectric effects due to a dislocation. 1. An analytic far and early-time field solution in a homogeneous whole space*, Phys. Earth Planet. Int., **121**, pp. 273-288.

[21] K.Park, M.J.S.Johnston et al., *Electromagnetic precursor to earthquake in the ULF band: a review of observations and mechanisms*, rev. geophysics 31, 1993.

[22] M.Parrot, J. Achache, J.J. Berthelier, E. Blanc, A. Deschamps, F. Lefeuvre, 1993. *High Frequency seismo-electromagnetic effects*, Phys. Earth Planet. Int., **77**, pp. 65-83.

[23] Parrot M. *Electromagnetic Noise due to earthquakes. Handbook of Atmospheric electrodynamics* Vol.II, 95-116, Editor H.Volland (1995) CRC Press.

[24] V.P.Pustovetov, A.B.Malyshev, *Space-Time Correlation of Earthquake and High-Energy Particle Flux Variations in the Inner Radiation Belt*, Cosmic Research 31, n.5, p. 84, 1993.

[25] Serebryakova O.N., M. Parrot, et al., 1992. *Electromagnetic ELF radiation from earthquake regions as observed by low-altitude satellite*, Geophy. Res. Lett., **19**,pp. 91-94.

[26] L.Slifkin, 1993. *Seismic electric signals from displacement of charged dislocations*, Tectonophysics, **224**, pp. 149-152.

[27] Sorokin V.M., V.M. Chmyrev, and A.K. Yaschenko, 2001. *Electrodynamic model of the lower atmosphere and the ionosphere coupling*, J. Atm. Sol. Terr. Phys., **63**, pp. 1681-1691.

[28] Sgrigna, V., L. Conti, V. Malvezzi, 2001. *TELLUS.Ground deformations and their effects on the near-Earth Space, Laboratori Nazionali del Gran Sasso*, INFN, Annual Report 2001, pp. 247-264.

[29] Sgrigna, V., 2000. *Tectonic deformation events and local seismicity in the Gran Sasso Area of the Central Apennines*, Laboratori Nazionali del Gran Sasso, INFN, Annual Report 2000, pp. 181-185.

[30] R. Teisseyre, 1997. *Generation of electric field in an earthquake preparation zone*, Ann. Geofis., **XL**, pp. 297-304.

[31] P. Varotsos, and K. Alexopoulos, 1984. *Physical properties of the variations of the electric field of the Earth preceding earthquakes, I*, Tectonophysics, **110**, pp. 73-98.

[32] P. Varotsos, N. Sarlis, and M. Lazaridou, 1999. *Interconnection of defect parameters and stress-induced electric signals in ionic crystals*, Phys. Rev. B, **59**, pp.24-27.

[33] S.A.Voronov, A.M.Galper et al., *Increases in High Energy Charged Particle Fluxes near the South Atlantic Magnetic Anomaly and the Seismicity of the Earth*, Cosmic Research 28, n.5, p. 789, 1990.

[34] Warwick J.W., C. Stoker, and T.R. Meyer, 1982. *Radio emission associated with rock fracture: possible application to the great chilean earthquake of May 22, 1960*, J. Geophys. Res., **87**, pp. 2851-2859.

[35] Walt, 1994, *Introduction to Geomagnetically Trapped Particle*, Cambridge University Press, 1994.

[36] Yoshida S., M. Uyeshima, and M. Nakatani, 1997. *Electric potential changes associated with slip failure of granite: preseismic and coseismic signals*, J. Geophys. Res., **102**, pp. 14883-14897.

PULEX - II

F, Amicarelli[d], F. Antonelli[a], C. Ara[d], M. Balata[e], M. Belli[a,c], M. P. Cerú[d], S. Colafarina[d], L. Conti Devirgiliis[d], A. De Marco[d], A. Falgiani[e], S. Nisi[e], O. Sapora[b,c], L. Satta[f], G. Simone[a,c], E. Sorrentino[a,c], M. A. Tabocchini[a,c]

[a] Physics Laboratory, Istituto Superiore di Sanitá
[b] Comparative Toxicology and Ecotoxicology Laboratory, Istituto Superiore di Sanitá
[c] INFN Gr. Coll. Sanitá
[d] Department of Basic and Applied Biology, L' Aquila University
[e] Service of Chemistry, Cryogenic and Chemical Plants of the INFN Gran Sasso National Laboratory
[f] Energetics Department, Rome University "La Sapienza"

Abstract

PULEX II was designed as an experiment aimed at investigating the effects of background radiation environment on metabolism and responses to physical and chemical agents on cultured mammalian cells. The exploratory phase of the experiment has been concluded, and its feasibility has been demonstrated. The results are consistent with those of a preceding measurement performed a few years ago at the Gran Sasso Laboratory using yeast cells, and suggest that the background radiation can act as a priming dose capable of triggering an adaptive response in living cells.

PULEX II is an experiment aimed at comparing the effects of different background radiation environments on metabolism and responses to γ-rays and cycloheximide of cultured mammalian cells and, to our knowledge, it represents the first systematic study on this field. Chinese hamster V79 cells were cultured in parallel for up to nine months at the Istituto Superiore di Sanit (ISS) and at the INFN-Gran Sasso underground Laboratory (LNGS) where exposure due to γ-rays and to radon was reduced by factors of about 70 and 25, respectively. After 9 months, the cells grown at the LNGS (exposed to a cumulative dose of about 30 μGy of γ-rays, average radon concentration around 5 Bq/m3), compared to the cells grown at the ISS (cumulative dose of about 2 mGy of γ-rays, average radon concentration around 120 Bq/m3), exhibit: i) a significant increase of the cell density at; ii) a significantly higher capacity to scavenge organic and inorganic hydroperoxydes but a reduced scavenging capacity towards superoxide anions; iii) an increase in both the basal hprt mutation frequency and the sensitivity to the mutagenic effect of γ-rays; iv) a greater

apoptotic sensitivity, induced by cycloheximide a protein synthesis inhibitor, starting at the third month of culture, that is no longer detected after nine months.

For all the examined biological end points the differences found can be associated with differences in the radiation background, even though in most cases it is not possible to exclude a superimposed effect due to culture aging. For some endpoints this effect could be large enough to mask possible differences between the two cultures. These data could be interpreted by the occurrence of an adaptive response due to variations of the natural background radiation. It is plausible that permanence of cells for long time at reduced background can: i) down regulate expression of genes related to cell growth and repair, ii) modulate the antioxidant enzymatic pattern; iii) make cells more prone to misrepair the radiation-induced DNA lesions. However, the possibility cannot be excluded that, after many generations (9 months correspond to roughly 540 cell duplications), clones having different characteristics have been selected in the two cultures, independently of the different radiation background. Further experiments are needed to settle this issue. Nonetheless, the data are consistent with a role of environmental radiation in the response of a cell population to ionizing radiation, and suggest that this response may be more complex than that predicted by a linear relationship with the dose. This observation not only is important for a better understanding of the basic mechanisms in cell radiation biology, but also calls for further studies in order to ascertain possible implications for the estimation of risks to chronic exposures presently assumed for radiation protection purposes. The experiment here described represents to our knowledge the first systematic study concerning the effects on mammalian cells, and for a variety of biological end points, of different levels of chronic exposures to ionizing radiation, such as those related to natural background. It is worth noting that PULEX, a first biological experiment, performed a few years ago on yeast cells cultured at the Gran Sasso Laboratory, also indicated that cells grown in a low background environment are less protected from mutational damage induced by methyl-methane sulfonate than cells grown at the Genetic Laboratory of the Rome University "La Sapienza", in a "normal" background radiation environment [1]. The possibility to perform further experiments is being considered to get more insight on the mechanisms underlying the different biological responses observed in the different background conditions.

1 List of Publications

1. F.Antonelli, M.Belli, O.Sapora, G.Simone, E.Sorrentino, M.A.Tabocchini, F.Amicarelli, C.Ara, M.P.Cerú, S.Colafarina, L.Conti-Devirgiliis, A.De Marco, B.Pruiti, M.Balata, A.Falgian, S.Nisi, L.Satta. Radiation biophysics at the Gran Sasso Laboratory: influence of a low background radiation environment on the adaptive response of living cells. 6th International Workshop on Topics in Astroparticle and Underground Physics (TAUP), Paris, France, September 6-10, 1999. Nuclear Physics B 87 (2000) 508-509

2. F. Antonelli, M. Belli, G. Simone, E. Sorrentino, M.A. Tabocchini, O. Sapora, L. Conti Devirgiliis, M.P. Cerú, F. Amicarelli, C. Ara, B. Pruiti, M. Balata, A. Falgiani, S. Nisi, L. Satta. Influence of a low background radiation environment on the cell

response to physical and chemical agents: the Pulex-2 experiment at the LNGS. VII Congresso Annuale della Società Italiana di Mutagenesi Ambientale (SIMA), Cortona, 6 - 8 ottobre 1999

3. F. Antonelli, M. Belli, G. Simone, E. Sorrentino, M.A. Tabocchini, O. Sapora, L. Conti Devirgiliis, M.P. Ceru, F. Amicarelli, C. Ara, S.Colafarina, M. Balata, A. Falgiani, S. Nisi, L. Satta. Influenza del basso fondo di radiazione sulla risposta cellulare ad agenti fisici e chimici: la risposta adattativa delle cellule viventi. X Convegno Nazionale della Societa Italiana per le Ricerche sulle Radiazioni (SIRR), Frascati, 19-22 novembre 2000

4. L. Satta, F. Antonelli, M. Belli, O. Sapora, G. Simone, E. Sorrentino, M. A. Tabocchini, F. Amicarelli, C. Ara, M. P. Ceru, S. Colafarina, L. Conti Devirgiliis, A. De Marco, M. Balata, A. Falgiani, S. Nisi Influence of a low background radiation environment on biochemical and biological responses in V79 cells Radiat. Environ. Biophysics (2002) 41:217-224

References

[1] Satta L, Augusti-Tocco G, Ceccarelli R, Esposito A, Fiore M, Paggi P, Poggesi I, Ricordy R, Scarsella G, Cundari E (1995) Low environmental radiation background impairs biological defences of the yeast Saccaromyces cerevisiae to chemical radiomimetic agents. Mut Res 347: 129-133

TRANSNATIONAL ACCESS TO LNGS

1 The project

TARI ("Transnational Access to Research Infrastructures) is a support scheme of the EU research and technological development programme "Improving the Human Research Potential and Socio-Economic Knowledge Base" within the Fifth Framework Programme of the European Union.

The aim of the TARI scheme is to provide researchers from the European and Associated Countries with free access to the major research infrastructures in Europe. The TARI scheme is implemented with contracts between the European Commission and major European research infrastructures.

In November 2001 INFN signed a contract with the EU for Transnational Access to the LNGS infrastructures (contract number HPRI-CT-2001-00149, duration 28 months).

1.1 The LNGS facilities

Several facilities are available for TARI users at LNGS. Here is a short description of each of them.

- LUNA accelerator facility
- Low background facilities
- Radon counters and geophysics instrumentation
- Computing facilities
- Cryogenic facilities

1.2 How to apply for TARI

The application form can be downloaded from the LNGS web site (http://www.lngs.infn.it, link European Community Fundings). Information on how to apply can also be asked at the e-mail address: tari@lngs.infn.it

2 The TARI projects in 2002

In total 11 TARI projects were accepted in 2002: 5 projects were accepted in the first call (March 15, 2002) 6 projects in the second call (September 15, 2002).

3 projects are completed, 2 are ongoing, and 6 are going to start their activity between February and March 2003.

Table 1 summarises the main features of the projects .

In the following subsections we discuss briefly the status of the completed and ongoing projects. Reports are provided by the group leaders.

Table 1: Status of TARI projects at LNGS. The columns contain data respectively relative to project number and title, status (31-Dec-2002), name and home institution of the group leader, number and nationality of home institution of TA users, total amount of access delivered in 2002 under TA. HU-Hungary, P-Portugal, PL-Poland, F-France, FI-Finland, D-Germany, RO-Romania

Project	Title	Status	Group leader	TA users	Tot access (days)
01/02	Study of proton induced gamma back in metallic backings	Completed	Z. Fulop ATOMKI Debrecen (HU)	3 HU	49
02/02	Study of Ta, Zr and Ti nitride films by NRA	Completed	A.Pedro de Jesus, C. Phys. Nuclear, Lisboa (P)	4 P	36
03/02	Elements of the reconstruction program for the ICARUS exp.	Completed	A. Zalewska Inst.Nucl.Phys. Krakow (PL)	5 PL	75
04/02	FADC400 Development and test of Flash ADC 400 MHz	Ongoing	H. DeKerret College de France, Paris (F)	5 F	205
05/02	Nitrogen purification from Rn	Ongoing	M. Wojcik Jagellonian Univ., Krakow (PL)	3 PL	59
06/02	Background characterization for liquid scint. spectrometry at Underground Lab. Gran Sasso	Approved	L. Kaihola Perkinelmer life sciences Turku, FI	1 FI	-
07/02	Groundwater monitoring through overthrust fault	Approved	J. Wiegand Univ. of Essen (D)	2 D	-
08/02	Ultra-low level detection of the Tritium groundwater samples for liquid scintillation spectrometry at Underground lab. Gran Sasso	Approved	S. Cuna Nat. Inst. of R&D for isotopic and molecular techn. Cluj-Napoca (RO)	3 RO	-
09/02	COBRA R&D on CdTe detectors	Approved	K. Zuber Univ. of Oxford (UK)	6 D 1 UK	-
10/02	Software development and mechanical calculations for the ICARUS detector	Approved	J. Kisiel Inst. of Phys., Univ. of Silesia Katowice (PL)	7 PL	-
11/02	Study of radioactive trace contaminations in metal loaded scintillators	Approved	S. Schoenert Max Planck Inst. Heidelberg (D)	6 D	-

2.1 Project LNGS-TARI P01/02

- Project title:
  Study of proton-induced gamma background in metalling backings

- Status:
  Completed; 49 man-days delivered in 4 visits.

- Name and home institution of TA users:
  Z. Fulop (group leader) , E. Somorjai, G. Gyurky, Hungarian Academy of Science (ATOMKI), Institute of Nuclear Research, Debrecen (HU)

- Description of the project
  The 400 kV LUNA2 accelerator facility installed at the Laboratori Nazionali del Gran Sasso provides a unique possibility to study nuclear reactions at very low energies. Due to the extremely low cosmic background, the high energy gamma-rays emerging from the astrophysically important 14N(p,γ)15O reaction can be measured here even at very low intensities. However, the presence of light element impurities in the targets can cause severe problems since the proton beam can induce high energy gamma-radiation on these impurities. The objective of this project is to study these impurities and to choose the way of target preparation where the beam induced background is minimized. Moreover, the low cross sections necessitate very long irradiations with high beam current. Hence the study of target density profile stability is also desirable.

- Scientific outputs
  Solid state N targets have been produced with three different procedures: implantation, evaporation and sputtering. The implanted ones were produced at the accelerator of the Universidade de Lisboa, Portugal, bombarding Ti, Cu and Ta backings with an isotopically pure 14N low energy beam. Evaporated targets were prepared in the ATOMKI in Debrecen, Hungary evaporating a thin layer of Ti on Ta backings and exposing the heated Ti layer to N gas with pressure of 50 torr. Sputtered (deposited) targets were obtained by the RF magnetron sputtering technique at the Laboratori Nazionali di Legnaro. In the investigated range of proton energies between 140keV and 400keV the most relevant reactions on possible contaminants are 11B(p,γ)12C, 19F(p,α,γ)16O and 18O(p,γ)19F. All these reactions emit gamma-rays of more than 4 MeV and show resonance structures in the relevant range of proton energies. We concluded that the sputtered and the evaporated TiN targets on Ta backings have the most uniform density profile and withstand many days of beam bombardment with several hundreds of uA without any significant deterioation. On the other hand, the sputtered targets had the lowest 11B contamination. On the base of the work presented in this project it has been possible to develop reliable targets which allow to measure the reaction 14N(p,γ)15O at proton energies as low as 140 keV. Future experiments at LUNA2 will also largely benefit from our achievements.

- Publications:

"Target Stability and Beam-induced background studies at the LUNA Underground Facility", submitted to Nuclear Physics A.

2.2 Project LNGS-TARI P02/02

- Project title:
  Study of Ta, Zr and Ti nitride films by NRA.

- Status:
  Completed; 36 man-days delivered in 4 visits

- Name of the TA participants:
  A. P. de Jesus (Group leader), J. Cruz, R. Parafita, J. P. Ribeiro
  Centro de Fisica Nuclear, Lisboa (P)

- Description of the project
  The objectives of this project are:

  1) Establish which of the following methods of TaN, TiN and ZrN film production, reactive magnetron sputtering and ion beam implantation, lead to more uniform and pure films with a correct 1:1 stoicheometry.

  2) Relate film thickness, uniformity and impurity content with the potential existence of micro-pores and small cracks that limit the capacity for corrosion protection.

  In order to achieve these goals, the work was pursued along the following lines:

  1) Production of TiN and ZrN films by reactive magnetron sputtering and production of TaN, TiN and ZrN surface films by ion implantation, using the ion implanter of the Ion Beam Laboratory of ITN - Portugal.

  2) Stoicheometry and film uniformity analysis by RBS (for samples with light substrates) and impurity content analysis by PIXE and PIGE, at the Ion Beam Laboratory of ITN - Portugal.

  3) Surface structure analysis by AFM (Atomic Force Microscopy) and chemical analysis by X-ray diffraction.

  4) Film uniformity analysis by NRA, profiling the 14N content by the 278 keV (p, γ) resonance, and impurity content analysis by PIGE, at the LNGS - LUNA (400 kV accelerator) facility.

- Scientific outputs
  Data analysis made so far, on deposited films, allow us to draw the following conclusions:

  a) Thin films with thickness around 20 mg/cm^2 do not form a stable and uniform nitride X-ray diffraction does not show the peaks corresponding to the nitrides, although RBS analysis indicate a correct 1:1 ratio between the metal and nitrogen.

  b) NRA analysis made at LNGS show a uniform depth profile of most of the samples and an impurity content of B, C and O at the ppm level, that can be assigned to

the original metal. Data analysis on implanted films is still going on. The results obtained so far suggest the need to search for the thickness at which deposited nitrogen-metal films become nitride films, which we plan to undertake in the near future.

- Publications:
"Comparison between thin films of metal nitrides produced by reactive magnetron sputtering and ion beam implantatios", submitted to Journal of Applied Physics.

2.3 Project LNGS-TARI P03/02

- Project title:
Elements of the reconstruction Program for the ICARUS experiment

- Status:
Completed; 75 man-days delivered in 4 visits.

- Name of the TA participants:
A. Zalewska (group leader), K. Cieslik, Institute of Nuclear Physics, Krakow (PL)
J. Stepaniak, J. Lagoda, Institite for Nuclear Studies, University of Warsaw (PL)
M. Markiewicz, University of mining and metallurgy Warsaw (PL)
J. Holeczek, Institute of Physics, University of Silesia (PL)

- Description of the project:
The Gran Sasso Laboratories offer unique opportunities for the neutrino physics, which is at present the most promising window of the new physics beyond the standard model. The European long baseline program in Gran Sasso will play a strong and competitive role compared with the Japanese K2K and american MINOS experiments devoted to the study of the neutrino oscillations. The aim of the project is to develop and implement new software using the computer infrastructures and the PC arrays available at LNGS. The work is focused on the following selected topics: i) Detector calibration based on muon tracks; ii) Momentum determination based on the measurements of multiple scattering in Liquid Argon; iii) Reconstruction of the interactions;

  The project timetable is as follows

  1) definition the best interface (or interfaces) between the ICARUS general software packages and contributions developed by individual physicists or groups.

  2) Preparation of the preliminary skeleton programs for our topic of interest

  3) Interface our skeleton programs with the ICARUS general software and test them.

  4) In contact with the collaborating groups establish methods of testing the software componenets being worked out

  5) Prepare the web documentation for the software developed

- Scientific output:
  The work was done mostly in collaboration with the ICARUS groups from Gran Sasso, Aquila and Pavia. Availability of the complete data set from the Pavia tests in the Gran Sasso laboratory was crucial for performing the work. The scheleton simulation program has been settled, based on the GEANT package for simulating particle interactions and on the ROOT package for presenting simulation results. More in detail, contributions to our three main lines of activity were as follows:

  1. The determination of the electron drift velocity and electron lifetime based on muon tracks - work performed in collaboration with physicists from Gran Sasso and Aquila, described in the internal note ICARUS - TM/02-08 and in the paper "Observation of long ionizing tracks with the ICARUS T600 first half-module", recently sent for publication in NIM.

  2. The dependence of the frequency of electromagnetic interactions of high energy muons with energy transfer greater than a given limit has been calculated in liquid Argon as a function of the muon energy. The observed number of delta electrons, proton-electron pairs and electromagnetic showers with energies larger than 15 MeV has been measured on seventy long muon tracks (longer than 5m) collected during the Pavia tests. The muon energy distribution has been established.

  3. The simulation program for determination of muon momenta based on multiple scattering in liquid Argon has been set up and the working contacts with the Pavia physicists have started.

  4. The simulation program for studies of electromagnetic cascades and π_0 decays in liquid Argon has been prepared and a set of electromagnetic cascades and π_0's has been selected from the test data.

- Publications :
  "Observation of long ionizing tracks with the ICARUS T600 first half-module", submitted to Nuclear Instruments and Methods

2.4 Project LNGS-TARI P04/02

- Project title:
  FADC400

- Status:
  ongoing since May 2002; Access delivered up to 31-Dec-2002: 221 man-days; Expected end of the project: April 2003.

- Name of the TA participants:
  H. de Kerret (Group leader), A. de Bellefon, D. Kryn, M. Obolensky, T.Beau, G.Mention, J.Lamblin, College de France, Paris (F)

- Description of the project:
  The project entitled FADC 400 has for goal to test in realistic conditions the 400

Mhz flash adc which is developped in cooperation between the CAEN company (Viareggio, Italy) and the laboratory Physique Corpusculaire et Cosmologie (college de france,Paris).

- Results obtained (31-Dec-2002) and plans for the future:
  Several flash adc boards have been installed on several general facilities of the Gran Sasso laboratory: the Counting Test Facility (CTF), Borexino, and the Low Level Background Facility (LLBF). Data have been taken systematically with CTF, and analyzed. The integration in the acquisition is ready for the 2 other facilities, and will be done in the next months. Some partial datas have been taken in stand alone mode, and are being analysed. The flash adc was shown to be very efficient to fully understand the CTF detector, and the other electronics calibration and systematics effect. The work on the shape variation of the pulse (epending on its location in the detector) is still to be completed. This work has already risen very important issues concerning the noise and the pedestals of the boards. This will be incorporated in a new design of this board, for other customers, which is to be decided in the Spring.

- Publications:
  A specific paper on the flash adc itself to be published on Nuclear Instruments and Methods is in preparation; a second paper paper describing all installations of the Borexino detector, in also in preparation.

2.5 Project LNGS-TARI P05/02

- Project title:
  Nitrogen purification from Rn-PURAZOT

- Status:
  ongoing since June 2002; Access delivered up to 31-Dec-2002: 59 man-days Expected end of the project: April 2003

- Name of the TA participants:
  M. Wojcik (group leader), G. Zuzel, M. Misiaszek, Institute of Physics Jagellonian University, Krakow (PL)

- Description of the project:
  The main goal is to develop a N_2 generator allowing to flush permanently chambers of ultra-low background detectors (gamma spectrometers, dark mater detectors, ...) with nitrogen gas containing less than 5 mBq/m^3 of ^{222}Rn at flow rate higher than 2 m^3/d. To avoid an influence of the high and variable in time Rn concentration in laboratory air these detectors are closed in sealed chambers. To reduce the Rn activity in the gas surrounding the low-background detectors the chambers are flushed with nitrogen. However, the Rn concentration in evaporated nitrogen or in nitrogen stored in steel bottles is not negligible and not constant in time.

- Results obtained (31-Dec-2002) and plans for the future:
  A special Rn trap with charcoal was developed for the N_2 purification. The trap

was placed inside the 100 L dewar with liquid nitrogen. The dewar produce about 0.2 m^3/h of N_2,due to not ideal thermal insulation, which is not sufficient in some applications. For that reason a special heater was placed on the bottom inside the dewar. This heater allows us to generate even more than 2 m^3/h of N_2. The compatibility of our N2 generator with the existing nitrogen monitoring system at LNGS was successfully tested. We have performed the tests in October/November 2002. In the near future we will measure the purification efficiency of our Rn trap immersed in LN_2 and cooled by N_2 vapors inside the dewar.

- Publications:
  The participants are preparing a publication to be published on Nuclear Instrument and Methods.

3 Conclusions

During 2002 11 TARI projects at LNGS have been accepted: 3 of them are completed, 2 are ongoing, and 6 are expected to start in Feb/March 2003.

In total 441 man/days of access were delivered to 19 TA users in 2002.

Other 26 TARI users are expected to start their access to LNGS with the approved projects starting in Feb/March 2003.

New projects are expected to be submitted in the 2003 LNGS-TARI call for proposals (deadlines 15-Mar-2003 and 15-Sep-2003)

Members of the LNGS User Selection Panel for
TARI-HPRI-CT-2001-00149

Member	**Home institution**
Prof. Eckart Lorenz (Chairman)	Max-Planck-Institut fur Physik Werner-Heisenberg-Institut
Prof. Till Kirsten	Max-Planck-Institut fur Kernphysik Heidelberg
Prof. Angel Morales	University of Zaragoza
Dr. Vincenzo Patera	Laboratori Nazionali di Frascati INFN and Dipartimento di Energetica Università di Roma "La Sapienza"
Dr. Eugenio Scapparone	INFN sez. Bologna - Dipartimento di Fisica

Inside The Big Black Box
Analysing Visits to Physics Laboratories

IN3B

The European Union IN3B project (Inside the Big Black Box) aims at analysing the impact of visits to important physics laboratories on the lay public. This project - consisting in a "thematic network" - is carried out in the framework of the specific research and technological development program "Improving the Human Research Potential and the Socio-Economic Knowledge Base".

The network is made up of seven partner institutions. Amongst them, 5 laboratories: CERN (European Laboratory for Particle Physics) in Switzerland, Demokritos National Centre for Scientific Research in Greece, LNGS (Gran Sasso National Laboratories), DESY (the German Electron Synchrotron) and the Research Centre Juelich in Germany. CERN is responsible for the co-ordination of the network .

The main objective of this two-yearly project is both to develop a common methodology for analysing visits to science laboratories and their public, and to identify, on the basis of the results obtained, common strategies to improve the design, management and evaluation of visits to science laboratories. Moreover, the project will allow to expand this network to other laboratories in member countries, with a view to proposing a “standard quality” of communication activities for science laboratories which takes into account the feedback obtained by monitoring the reactions of visitors.

The project entails submission of face to face questionnaires to 900 visitors before visit begins and immediately after; 60 in depth interviews on visitors after the visit; 6 sessions of ethnografic on-site observation during the visit; follow-up on the sample of visitors by means of computer assisted telephone interviews (sample of 500 visitors) and computer assisted telephone interviews on a sample of population as control group (500 non visitors). In order to monitor the reactions of visitors, sociologists, psychologists and anthropologists are involved in the project.

Marie Curie Felloships

Borexino experiment has advanced a claim for 6 training site fellowships for the activities related to low activity measures in gases and liquids, purification of fluids from a radioactive point of view, measures of discrimination between signal and low energy background, characterization of environmental backgrounds.
Having obtained all the 6 requested fellowships, the Borexino collaboration has issued a competition for 4 of them, annual, which have been assigned to Burkhard Freudiger (June 2002), Cristian Lendvai, Ludwig Niedermeier e Olivier Dadoun (July 2002).
The Collaboration intends to advertize other two annual fellowships within the triennial duration of the contract.

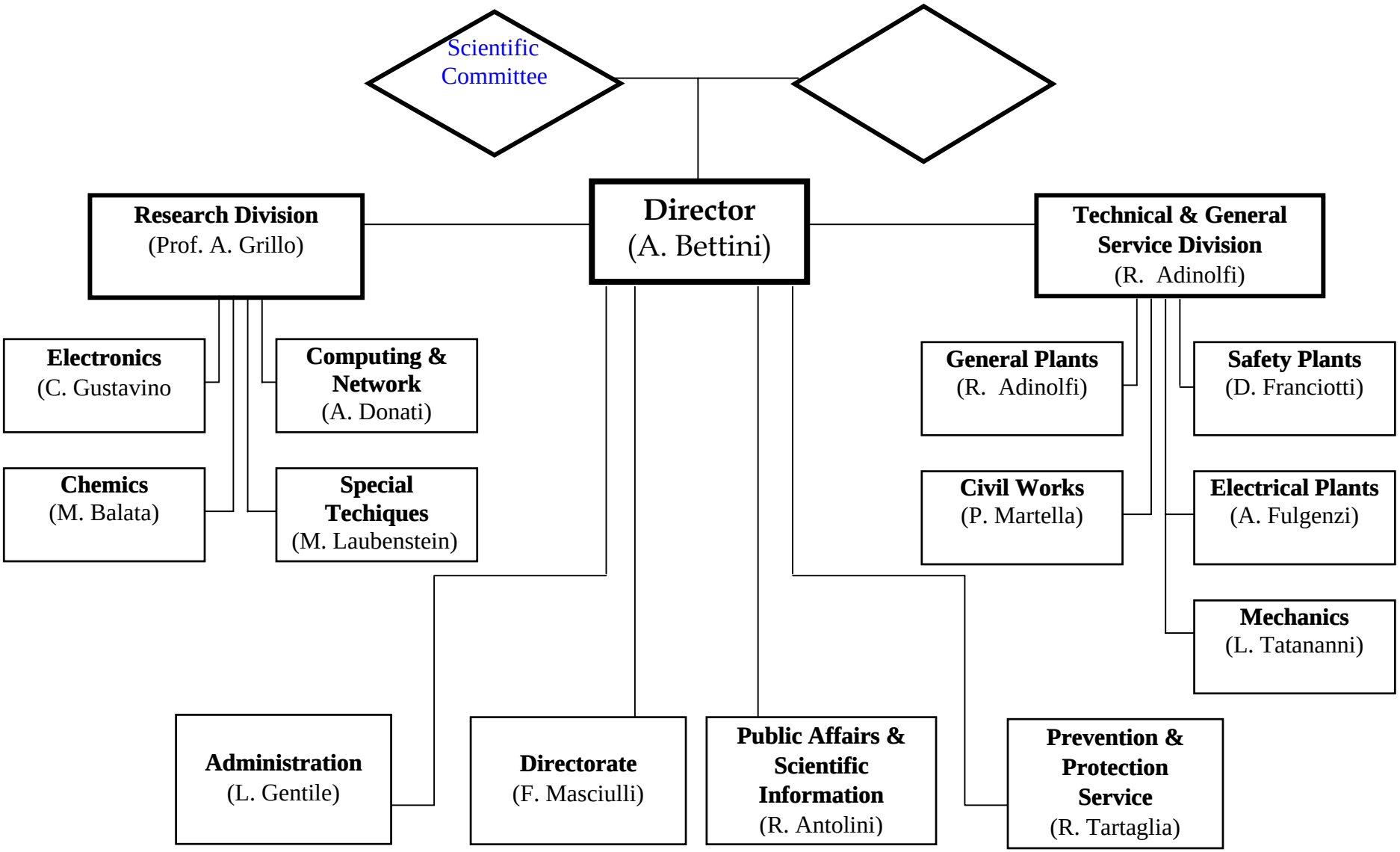
Scientific Committee
Director (A. Bettini)
Research Division (Prof. A. Grillo)
Technical & General Service Division (R. Adinolfi)
Electronics (C. Gustavino
Computing & Network (A. Donati)
Chemics (M. Balata)
Special Techiques (M. Laubenstein)
General Plants (R. Adinolfi)
Safety Plants (D. Franciotti)
Civil Works (P. Martella)
Electrical Plants (A. Fulgenzi)
Mechanics (L. Tatananni)
Administration (L. Gentile)
Directorate (F. Masciulli)
Public Affairs & Scientific Information (R. Antolini)
Prevention & Protection Service (R. Tartaglia)

Scientific Committee

Gran Sasso National Laboratory

Eckart Lorenz (Chairman)
Max-Planck-Institut fur Physik - Muenchen. Germany

Prof. Jacques Lefrancois
Laboratoire de l'Accélérateur Linéaire Orsey Cedex. France

Prof. Furio Bobisut
Dipartimento di Fisica G. Galilei dell'Università di Padova. Italy

Prof. Till Kirsten
Max-Planck-Institut fur Kernphysik – Heidelberg. Germany

Prof. Jaap Panman
CERN – PPE, Geneva. Switzerland

Prof. Fernando Ferroni
Dipartimento di Fisica Università "La Sapienza" - Roma. Italy

Prof. Antonio Masiero
Dipartimento di Fisica G. Galilei dell'Università di Padova. Italy

Prof. Vincenzo Patera
Laboratori Nazionali di Frascati - INFN and Dipartimento di Energetica
Universita' di Roma "La Sapienza". Italy

Prof. John F. Wilkerson
University of Washington - Department of Physics
Center for Expt. Nuclear Physics & Astrophysics - Seattle, Washington, USA

Laboratory Council

Gran Sasso National Laboratory

Prof. Alessandro Bettini (Director)
Eng. Alfredo Fulgenzi
Mrs. Luciana Gentile
Prof. Aurelio Grillo
Dr. Aldo Ianni
Prof. Piero Monacelli
Dr. Ornella Palamara
Dr. Libero Palladino
Mr. Antonello Rotilio

Gran Sasso National Laboratory – Personnel

Research Division

Grillo Aurelio (Head)

Arneodo Francesco
Besida Olivier
Di Carlo Giuseppe
Di Credico Alessandra
Di Pietro Giuseppe
Ferrari Nicola
Gazzana Stefano
Goretti Augusto
Ianni Aldo
Jamieson Andrea
Junker Matthias
Orsini Massimo
Palamara Ornella
Salvo Corrado
Vissani Francesco

Research Division Secretariat

Chiarizia Fausto
Fantozzi Vincenzo
Giusti Ersilia

Computing & Network

Donati Andrea (Head)

Giuliani Roberto
Parlati Sandra
Stalio Stefano
Taborgna Nazzareno

Electronics

Gustavino Carlo (Head)

Candela Attanasio
De Deo Massimiliano
D'Incecco Marco
Lindozzi Marco

Chemics

Balata Marco (Head)

Falgiani Antonella
Giusti Giuseppina
Ioannucci Luca
Nisi Stefano

Special Techniques

Laubenstein Matthias (Head)

Bucci Carlo

Technical Division

Adinolfi Falcone Raffaele (Head)

Technical Division Secretariat

Sartini Barbara

General Plants
Adinolfi Falcone Raffaele (Head)

Alessandri Gianni
Andreassi Massimo
Bonanni Achille
Dainese Nicola

Safety Plants
Franciotti Dino (Head)

Dionisio Mario
Panella Graziano

Electrical Plants
Fulgenzi Alfredo (Head)

Massimiani Nicola
Polidoro Nando
Torelli Fabrizio

Mechanics
Tatananni Ercolino (Head)

Romualdi Bruno
Rotilio Antonio

Civil Works
Martella Paolo (Head)

Lucente Alessandra
Marrelli Lorenzo

Administration
Gentile Luciana (Head)

Castorio Vincenzo
Di Credico Giovanna
Equizi Maria Pia
Gentile Antonella
Giusti Berardino
Giusti Maria Pia
Graziosi Cristina
Pezzini Margherita
Verzulli Dario

Directorate
Masciulli Franca (Head)

Cavalli Giovanni
Misticoni Consorti Maria Elena

Corrieri Franchina
Mancini Mara
Spagnoli Giovanna

Prevention & Protection Service

Tartaglia Roberto (Head)

Giampaoli Antonio
Mosca Giuseppina

Public Affairs & Scientific Information

Antolini Roberta (Head)

De Filippo Maria
Galeota Marco
Sebastiani Sonia

Associations -INFN-

Associated	Group/Experiment
Aloisio Roberto	Theory group
Aprili Piergiorgio	ICARUS
Berezinsky Veniamin	Theory group
Ciarcelluti Paolo	Theory physics
Costantini Maria Laura	ICARUS
Crescentini Luca	GIGS
D'angelo Davide	BOREXINO
Dadoun Olivier	BOREXINO
Di Vacri Assunta	LENS
Ferella Alfredo Davide	ICARUS
Formicola Alba	LUNA
Freudiger Burkhard	BOREXINO
Ghia Piera Luisa	LVD
Giuliani Gioacchino	LVD
Gorla Paolo	CUORICINO
Lendvai Christian	BOREXINO
Niedermeier Ludwig	BOREXINO
Pandola Luciano	GNO
Pirro Stefano	CUORICINO
Pyle Matt	CUORICINO
Ryazhaskaya Olga	LVD
Spadano Beatrice	GNO
Tomei Claudia	GENIUS

- Fellow -

Technologist	Bucciarelli Gabriele - Zarra Chiara
Undergraduate	Di Vacri Assunta
PHD	Kobychev Vladislav - Narayan Mohan
Marie Curie (EU contract)	Dadoun Olivier - Freudiger Burkhard
	Lendvai Christian - Niedermeier Ludwig

Meetings in 2002:

- **"Workshop in matter of safety in the working environment of the INFN"**
  20-21 February 2002

- **COPIT**
  11 May 2002

- "**Open Day"**
  12 May 2002

- **Meeting of the PRC of APPEC**
  June 24-25, 2002

- **Meeting Network TRM CEE**
  26 June 2002

- **Summer Institute "New Dimensions in Astroparticle Physics"**
  8-19 July 2002

- **Physics Teaching Association (A.I.F. school)**
  22 July-2 August 2002

- **"LVD The First Ten Years…"**
  28-29 October 2002

- **ßß Decay Meeting**
  11-12 November 2002

- **Pediatrics Conference**
  16 November 2002

- **Dentists Conference**
  30 November 2002

- **Physics Teaching Association (A.I.F. school)**
  2-6 December 2002

Seminars in 2002:

- L. BENTO **University of Lisbon** January 17, 2002
  Baryon Asymmetry, Dark Matter and the Hidden Sector

- S. BORGANI **INFN, Trieste** February 27, 2002
  Cosmology with clusters of galaxies

- P. BLASI **INAF/Osservatorio Astrofisico di Arcetri** March 21, 2002
  Observing Light from Galactic Dark Matter

- S. PARLATI/S. STALIO **LNGS** March 20, 2002
  New computing resources at LNGS: batch systems, transparent load balancing and pc clusters

- E. COCCIA **Univ. Tor Vergata (Roma)** April 4, 2002
  Physics with resonant-mass gravitational-wave detectors

- E. PANIZZI **Roma "La Sapienza"** April 11, 2002
  ApeMille: architettura, caratteristiche e utilizzo

- M. V. GARZELLI **Milano University** April 15, 2002
  A Bayesian view of Solar Neutrino Oscillations

- A. INCICCHITTI **INFN Roma 1** April 18, 2002
  Obtained results and perspectives on the WIMP investigation

- M. CHEN **Queen's University (Kingston, Canada)** April 24, 2002
  New Results from SNO

- S. COLAFRANCESCO **Osservatorio Astronomico di Roma** May 9, 2002
  Clusters of galaxies: the largest laboratories for astroparticle physics

- A. STRUMIA **CERN** May 6, 2002
  A review of NuTeV, LSND and solar neutrino anomalies

- E. BELLOTTI **Univ. di Milano** May 17, 2002
  GNO Results

- R. BATTISTON **Univ. di Perugia** May 30, 2002
  Astroparticle Physics in Space

- A. STUDENIKIN **Moscow University** June 11, 2002
  Effects of Matter Motion and Polarization in Neutrino Flavour and Spin Oscillations

- P. L. GHIA **CNR-IFSI (Torino)** June 19, 2002
  EAS-TOP, a Cosmic Ray Experiment at LNGS

- M.G. PIA/A. PFEIFFER **(INFN-Genova)/(CERN)** July 2, 2002
  Mini Workshop about Geant4 and Anaphe

- A. ZALEWSKA **Inst. of Nucl. Phys. (Krakow, Poland)** June 27, 2002
  Silicon detectors in high energy physics experiments

- G. GIACOMELLI **Univ. di Bologna** October 17, 2002
  Final results of the MACRO experiment at Gran Sasso

- C. SPIERING **DESY Zeuthen** October 24, 2002
  High Energy Neutrino Astronomy - a Promising Decade Ahead

- H.V. Klapdor-Kleingrothaus **MPI für Kernphysik, Heidelberg** Nov. 7, 2002
  First Evidence For Neutrinoless Double Beta Decay - And Future Of The Field

- M. MARTINI **INFM Milano-Bicocca** Novembre 21, 2002
  Thermoluminescence Dating: Recent Results And New Perspectives

- M. GOGBERASHVILI **Inst. of Physics of Tbilisi** December 4, 2002
  Preferred frame in brane world

- L. PASSALACQUA **I.N.F.N. (Frascati)** December 5, 2002
  Recent Results from DAFNE

- E. APRILE **Columbia Univ. (N.Y.)** December 12, 2002
  The Balloon-Borne Liquid Xenon Gamma-Ray Imaging Telescope